

DOCTOR OF PHILOSOPHY

The use of ultrasound on the extraction of microalgal lipids

King, Patrick Martin

Award date:
2014

Awarding institution:
Coventry University

[Link to publication](#)

General rights

Copyright and moral rights for the publications made accessible in the public portal are retained by the authors and/or other copyright owners and it is a condition of accessing publications that users recognise and abide by the legal requirements associated with these rights.

- Users may download and print one copy of this thesis for personal non-commercial research or study
- This thesis cannot be reproduced or quoted extensively from without first obtaining permission from the copyright holder(s)
- You may not further distribute the material or use it for any profit-making activity or commercial gain
- You may freely distribute the URL identifying the publication in the public portal

Take down policy

If you believe that this document breaches copyright please contact us providing details, and we will remove access to the work immediately and investigate your claim.

THE USE OF ULTRASOUND ON THE EXTRACTION OF MICROALGAL LIPIDS

By

PATRICK MARTIN KING

October 2014



THE USE OF ULTRASOUND ON THE EXTRACTION OF MICROALGAL LIPIDS

By

PATRICK MARTIN KING

October 2014

*A thesis submitted in partial fulfilment of the University's requirements for the
Degree of Doctor of Philosophy*

Acknowledgements

I would like to thank the Carbon Trust Algal Biofuel Challenge (ABC) for providing initial funding of this project and the Faculty of Health and Life Science at Coventry University for a continuation of this support.

I would like to express my thanks to Eadaoin Joyce, my director of studies, for her constant support, guidance and encouragement. I would also like to thank Krzysztof Noworarski and all members of Professor Tim Mason's Sonochemistry team for their additional support. Thank you to the technical staff in the Health and Life Science department in particular Dan Comeskey, for their practical guidance.

Special thanks to Rhianna and Ricky for your friendship and support during our studies, it would not have been the same without you. And thanks to everyone in JS217.

Finally I would like to give special thanks to my parents (Pat and Janette), brother Kieran and fiancée Amy for their never ending support and tea.

Data from this thesis was used in the following publications:

1. Nowotarski, K., King, P.M., Joyce, E.M., and Mason, T.J. (2013) *Ultrasonic disruption of algae cells*. American Institute of Physics. Conference proceedings. 1433. 237-240.
2. Joyce, E., King, P.M., and Mason, T.J. (2014) *The effect of ultrasound on the growth and viability of microalgae cells*. Journal of Applied Phycology. 26. 1741-1748.

Abstract

Microalgae synthesize and store large volumes of lipids (potentially over 25% of dry weight) which could provide a renewable source of biodiesel. Traditional extraction techniques often produce poor lipid yields particularly from microalgae with robust cell walls. This project investigated the role of power ultrasound as a cell disruption step in lipid extraction from four microalgal species. Nile Red staining was used to assess the time when ultrasound induced increased membrane permeability in each species and lipids were extracted using an ultrasound assisted Bligh and Dyer extraction method.

A 20 kHz probe system (40% amplitude, 0.086 W/cm^3) caused increased lipid recovery from dry biomass in all cases; *D. salina* (no cell wall) from 15 to 22.5% of dry biomass after 1 minute (26% when stressed with 35 g/L NaCl). *C. concordia* (thin cell wall) from 7.5 to 10.5% of dry biomass after 2 minutes (27% with 25% nitrogen reduction in growth media). *N. oculata* (thick cell wall) from 6.5 to 10% of dry biomass after 16 minutes (31.5% when stressed with 30 g/L NaCl). The stressed cultures yield could be improved to 35% when ultrasound was combined with S070 beating beads. *Chlorella sp.* (thick cell wall) from 6.3 to 8.7% of dry biomass, after 16 minutes (44% was achieved when harvested at day 9 instead of 15).

A Dual Frequency Reactor (16 and 20 kHz, 0.01 W/cm^3) flow system with S070 beads demonstrated that high lipid extraction yields could be achieved on a larger level with *N. oculata*. After 4:48 minutes sonication 24% lipid recovery was achieved. This system could theoretically increase daily microalgal oil production from 3.96 to 5.76 L per day when compared to conventional techniques, at an extra production cost of only 2.9 p/litre (1.5% increase).

D. salina, *N. oculata* and *C. concordia* resumed normal growth following sonication at 20 kHz after 1-20 days (8 minutes treatment for *D. salina*, 60 minutes treatment for *N. oculata* and 16 minutes treatment for *C. concordia*). It was found that the supernatant of sonicated *D. salina* and *C. concordia* when added to established cultures were able to boost their growth.

Introduction

Microalgae are known to produce high quantities of lipids (potentially over 25% of dry weight) which have shown great potential as a feedstock for biodiesel production. However, due to the strength of the cell walls of some microalgal species traditional lipid extraction techniques often produce poor recovery yields. Many, including Wijffels and Barbosa argue that a cellular disruption step needs to be incorporated into extraction techniques to increase lipid recovery yields. This project aims to investigate the use of ultrasound as a cellular disruption step to improve lipid recovery from microalgae.

1. Energy production and microalgal biofuels

1.1 Global energy supply and limitations

In recent years it has become increasingly obvious that alternatives to our current energy supply systems are needed. As of 2008 88% of the world's energy consumption came from fossil fuels, a total 35% from oil (Brennan and Owende, 2010). Currently the world is experiencing record high crude oil prices, increasing energy demand and consumption, along with depleting fossil fuel supply. Figure 1.1 shows a graph which depicts the trend in the amount of worldwide crude oil consumption over the last 30 years and the increase in use is clear. This greater consumption has led to a number of environmental implications associated with the use of fossil fuels (Wijffels and Barbosa, 2010). The main environmental threat associated with fossil fuel use is the emission of greenhouse gases caused by combustion, which has been linked to climate change (Maimoun *et al.* 2013). In 2006 29 GT of CO₂ was released into the atmosphere by fossil fuels. Estimations suggest

that 12 GT of this would be removed a year by natural processes such as photosynthesis, which leaves 17 GT of CO₂ to accumulate in the atmosphere annually (Brennan and Owende, 2010). As energy consumption and demand is increasing each year it is clear that fossil fuels are not a desirable option for energy supply and in the long term may prove unsustainable.

Figure 1.1 Worldwide crude oil consumption since 1980

This item has been removed due to third party copyright. The unabridged version of the thesis can be viewed at the Lanchester Library, Coventry University.

Figure 1.1 Increase in the worldwide crude oil consumption since 1980 (International Energy Outlook, 2013)

1.2 Traditional fossil fuels and their limitations

At this present time the world relies heavily on fossil fuels such as coal and crude oil for its energy needs. Crude oil is of particular importance as the world relies on it for its transport needs. Crude oil is easily refined into motor gasoline/petrol, diesel fuel and many other products including kerosene and heating oil (Borenstein *et al.*, 1997). This refinery process is known as cracking and employs heat to breakdown and separate complex molecules (Al-Humaiden *et al.*, 2013). Crude oil is often found underground, under the sea or in a number of other locations and large scale drilling operations are often needed to reach it. At the moment there are 90 oil producing countries worldwide but the majority of the oil produced and stored in reserves is in the Middle East (O'Rourke and Connolly, 2003). Table 1.1 shows the amount of oil produced, consumed and stored in reserves by some of the world's largest oil producing countries. This table clearly shows that currently the United States and China who are two of the world's largest and most powerful nations are consuming more oil than they are producing, while most other countries produce slightly more than they consume. Figure 1.1 shows a trend that American oil consumption is on the increase, this is also true for China, but as a rapidly developing country China may consume oil at a higher rate than the USA (Rapoza, 2013). Estimations based on the current trend in oil demand suggest that the world's oil supply will last for a further 70 years (The Economist, 2006). Considering this fact and the current trends in oil consumption mentioned it highlights the fact that alternative sources of fuel are needed.

Table 1.1 Oil consumption, demand and reserves of major oil producing nations

Country	Oil Consumption (million barrels per day)	Oil Production (million barrels per day)	Total oil reserves (billion barrels)
United States	18.69	8.45	20
Saudi Arabia	2.43	9.9	261.7
Russia	2.74	10.9	48.6
Iran	1.8	4.23	89.7
Mexico	2.07	2.93	28.3
Norway	0.2	2	9.4
China	8.2	4.07	24
Venezuela	0.74	3.02	76.9
Canada	2.15	3.59	6.6
UK	1.66	1.1	4.9
Iraq	0.68	3.4	112.5
UAE	0.43	3.09	97.8
Nigeria	0.28	2.53	22.5
Kuwait	0.32	2.68	96.5

Data regarding oil production and reserves taken from O'Rourke and Connolly, 2003 and World Key Energy Statistics, 2012 and data regarding oil consumption from <http://www.nationmaster.com>.

The negative issues affecting the current fossil fuel based energy supply system cannot be ignored; however, there are advantageous aspects to the current system. As mentioned previously the refinement of crude oil into a multitude of different transport fuels is a relatively quick and easy process in which advances are made on a yearly basis to improve yield and cost (Borenstein *et al.*, 1997). An argument in favour of retaining the current system is that any major upheaval in changing how the global energy needs are met would be a very costly and time consuming.

1.3 Biofuels

Biofuels are fuels that are derived from a biological source such as plants and microorganisms which employ carbon fixation as an energy source. The two most popular biofuels that are produced are biodiesel and bioethanol. Biodiesel is made by the transesterification of vegetable oils extracted from a biomass. It is commonly used as a fuel for road transportation as a diesel additive, also when employed with petroleum or diesel it can be used as an aviation fuel (Korres *et al.* 2008). Bioethanol is produced by the fermentation of glucose from biomass; its uses include road transportation fuel as a gasoline additive (Gong and Jiang, 2011). Biofuels are classified in terms of their historical development and referred to as generations.

1.3.1 First generation biofuels

First generation biofuels have shown rapid growth worldwide; in this generation vegetable oils are produced from crops and used in the transport fuel industry. Suitable crops, also known as oleaginous crops include rapeseed, wheat and maize. The two main outputs of first generation biofuels were bioethanol which is produced by the fermentation of glucose from crops and biodiesel which is produced by extracting oil from the crops followed by transesterification of the oil to Fatty Acid Methyl Esters (FAMES) (Brennan and Owende, 2010, Mohammadi *et al.*, 2011). Biofuels are able to reduce the effects of fossil fuels as it is suggested that any CO₂ released into the atmosphere from combustion subsequently will be removed from the atmosphere by the photosynthesis of the biofuel crops. This makes the biofuels “Carbon neutral”.

First generation biofuels have their limitations. A major drawback of biofuel crop production is that to meet the fuel demands of the transport industry it would be necessary to use the arable land currently used by the food industry. This along with the water and fertiliser demands for crop production, simply do not make this a totally viable option. As of 2010 1% of the world's available arable land is used for first generation biofuel crops, which provides 1% of the world's global transport needs (Brennan and Owende, 2010).

1.3.2 Second generation biofuels

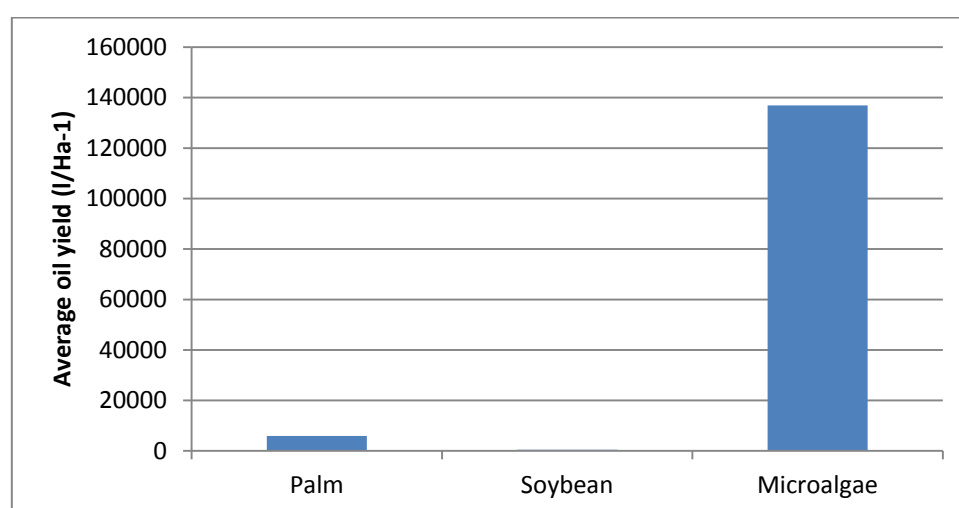
Second generation biofuels are produced to address the limitations of its predecessors. This generation differs from first generation biofuels which obtained oils from oleaginous crops by instead producing biofuels from biological waste products such as agricultural waste and forest residue. These are generally known as non-food based lignocellulosic biomass and in theory they should not interfere with arable land for food agriculture. Fuels produced by this technique include biodiesel and bioethanol (Mohammadi *et al.*, 2011).

Second generation biofuels are considered to be more advantageous than first generation biofuels as they use up agricultural waste products (Mohammadi *et al.*, 2011). However there is concern that withdrawal of agricultural biomass residue for increasing use in biofuel production could affect soil fertility and quality as there would be less available decomposing biomass or natural fertilizers to add nutrients to the soil (Mohammadi *et al.*, 2011). At the moment technology for fully realizing the potential of these biofuels is not available at the levels required for major commercial use (Brennan and Owende, 2010).

1.3.3 Third generation biofuels

The limitations of 1st and 2nd generation biofuels has revealed certain standards that any future biofuel must meet for it to be commercially and environmentally viable. It must be produced at a cost which is either less than or competitive with fossil fuels. It must require either zero or only a small amount of arable land use, minimum potable water use and ideally be carbon neutral in its rates of CO₂ production and consumption (Brennan and Owende, 2010). Third generation biofuels are believed to be the perfect candidates to do this by predominately employing algae and other microorganisms as a bio-feedstock. Kumar *et al.*, (2011) published a study which demonstrated that microalgae are capable of producing an average oil yield (136900 L/Ha⁻¹) which is which is considerably higher than first generation biofuel crops such palm (5950 L/Ha⁻¹) and soybean (446 L/Ha⁻¹).

Figure 1.2 Comparison of oil yield from Microalgae and Oleaginous crops



Microalgae (small unicellular microorganisms) and macroalgae (commonly known as sea weed) need only sunlight, CO₂, water, nitrogen and phosphorus to produce carbon rich lipids which when extracted can be transesterified to biodiesel (Wijffels and Barbosa, 2010). Although the main fuel derived presently derived from

microalgae is biodiesel, other fuels such as bioethanol can be produced by chemical and biochemical processing of biomass, alkanes produced from microalgal fatty acids (Radakovits, *et al.*, 2010) and butanol by acid hydrolysis and fermentation of microalgae biomass (Potts *et al.* 2011). Another advantage of microalgal biofuels is the additional by-products that can be extracted from microalgae which can be used in nutraceutical, pharmaceutical and cosmetic industries (Gong and Jiang, 2011). However, the current technology to extract oils is unable to meet production volumes for the energy needs of the transport industry. Another major limitation of third generation biofuels is that to produce enough fuel to support the transport industry considerable investment needs to be made into the development of large scale “algae farms” (Wijffels and Barbosa, 2010). It is also apparent that for microalgae biodiesel production to become commercially viable there needs to be significant support from national governments (Gallagher, 2011).

1.4 Summary of each fuel system

Table 1.2 compares each of the fuel systems discussed so far, including their sources, outputs, advantages and limitations.

Table 1.2 Comparison of fossil fuels with the three generations of biofuels

Fuel system	Fuel source	Fuel output	Advantages of this system	Disadvantages of this system
Traditional fossil fuels	<ul style="list-style-type: none"> • Crude oil • Coal 	<ul style="list-style-type: none"> • Gasoline/petrol • Diesel fuel • Jet fuel • Kerosene • Heating oil 	<ul style="list-style-type: none"> • System for refinement and distribution already in place. • Fossil fuels are very versatile in their uses. • There are political advantages for a nation that controls oil. 	<ul style="list-style-type: none"> • Burning fossil fuels has extremely hazardous effects on the environment. • Oils are being consumed more than they are being produced and reserves are believed to be running low. They are not an indefinite supply.
1 st generation Biofuels	<p>Oleaginous crops such as:</p> <ul style="list-style-type: none"> • Rapeseed • Maize • Wheat 	<ul style="list-style-type: none"> • Biodiesel • Bioethanol 	<ul style="list-style-type: none"> • Potentially a carbon neutral process. • Unlike crude oil, these can be produced almost anywhere worldwide. 	<ul style="list-style-type: none"> • Competes for freshwater supply intended for food agriculture. • Competes for arable land intended for food agriculture use. • Would simply not be able to meet the fuel demands of the transport industry.
2 nd generation Biofuels	<ul style="list-style-type: none"> • Agricultural waste products • Energy crops (e.g. switchgrass) 	<ul style="list-style-type: none"> • Biodiesel • Bioethanol 	<ul style="list-style-type: none"> • Potentially a carbon neutral process. • It will not compete with resources needed for food agriculture. 	<ul style="list-style-type: none"> • Technology to produce these oils is currently unable to meet the fuel needs of the transport industry. • May cause adverse effects on the fertility of soil.
3 rd generation Biofuels	<ul style="list-style-type: none"> • Microalgae • Macroalgae 	<ul style="list-style-type: none"> • Biodiesel • Bioethanol • Alkane fuels • Butanol fuels 	<ul style="list-style-type: none"> • Potentially a carbon neutral process. • It will not compete with resources needed for food agriculture. • Can potentially be produced at a cost less than or equal to fossil fuels. • Can produce other by-products which can be used in cosmetic and pharmaceutical industries. 	<ul style="list-style-type: none"> • Technology to produce these oils is currently unable to meet the fuel needs of the transport industry. • To produce enough fuel to support the transport industry considerable investment needs to be made into the development of large scale “algae farms”.

2. Algae and algal biofuels

As previously mentioned algae can be divided into two categories; microscopic unicellular or filamentous microalgae and multicellular macroalgae, more commonly known as seaweed. Due to their smaller size, good lipid content (of over 25% dry weight), convenience of growth and handling at a laboratory scale microalgae are often preferred for biofuel production over macroalgae (Wijffels and Barbosa, 2010, Wei *et al.*, 2013).

2.1 Microalgae

Microalgae are often single celled organisms but can also form simple colonies of cells or filaments. Like plant cells, they use light energy and carbon dioxide as their main energy and carbon sources respectively through photosynthesis (Converti *et al.*, 2009). This makes microalgae one of the largest contributors to atmospheric oxygen supplies. Microalgal cells can be motile with cell shapes varying from coccoid to rod shaped, size can vary between 1 - >100 μm and they are known to grow in clumps and to form filaments (Lee, 1999). Microalgae grow in both marine and freshwater ecosystems and can form algal blooms (Graham and Wilcox, 2000). Microalgae are versatile organisms that are used in a number of industries such as food where species such as *Chlorella* are useful for their high protein content, pharmaceutical industries where microalgal anti-oxidants can be employed, heavy metal removal and biofuels (Becker, 1994).

There are a large variety of microalgal species, but two basic cell types. The prokaryotic cyanobacteria, which are perhaps the most commonly known, on a cellular level have no membrane bound organelles and share a number of similarities with bacteria. The second algal cell type is the eukaryotic cell. These, like

mammalian cells have membrane bound organelles, and many have cell walls similar to that of their plant and bacterial cell counterparts. Eukaryotic *Chlorophyta* microalgal class or green microalgae are of most interest in the field of biofuel production (Brennan and Owende, 2010). See figure 2.1 for an example of a *Chlorophyta* cell.

Figure 2.1 *Chlorophyta* cell structure

This item has been removed due to third party copyright. The unabridged version of the thesis can be viewed at the Lanchester Library, Coventry University.

Figure 2.1a shows the internal structure of a typical *Chlorophyta* cell. Figure 2.1b shows the structure of *Chlorophyta* marine species *Dunaliella salina* using a microscope x40 objective. (Figure 2.1a is taken from www.algaeindustrymagazine.com, and figure 2.1b is from www.77ingredients.com)

Green microalgae are primarily found in a freshwater environment and it is estimated that roughly 10% of green microalgae species are from marine environments (Lee, 1999). Green algae need only water sunlight, carbon dioxide, nitrogen and phosphorus to grow, which makes them relatively simple to culture grow on a laboratory and industrial scale (Wijffels and Barbosa., 2010). They are known to have chloroplasts containing both chlorophyll a and b (Lee, 1999).

2.2 Microalgae production

There are a number of photoautotrophic production systems currently employed in industry for the large scale culturing of microalgae, the most common being open pond and closed photobioreactor systems. Open pond systems either use natural waters such as lakes or ponds, or artificial systems such as raceway ponds for microalgal growth. Raceway pond systems (see Figure 2.2) consist of a circular loop, usually about 0.5m deep which contains microalgae that are being constantly circulated around the loop (Li *et al.* 2013). They are usually located in an environment with a known sunny climate, CO₂ is provided either through natural absorbance of CO₂ from the atmosphere or by aeration and growth media is added on a regular basis (Brennan *et al.*, 2010).

Figure 2.2 Raceway pond algal growth system

This item has been removed due to third party copyright. The unabridged version of the thesis can be viewed at the Lanchester Library, Coventry University.

Figure 2.2 shows an example of a raceway pond system. This system is located in Imperial Valley California and can contain up to 40000 litres of algae (Image from <http://algae.ucsd.edu>).

The alternative to the open pond growth system is the closed photobioreactor system (Figure 2.3). These were designed to avoid some of the problems of the open pond system. For example open pond systems are often susceptible to bacterial contamination or environmental pollution, both of which can drastically affect microalgal growth, in a closed system this is not as large an issue. An additional drawback of open ponds is the evaporation of water, which again can affect growth. The two most common closed photobioreactors are tubular and column systems. Tubular systems (Figure 2.3a) are horizontal and consist of a series of tubes which are usually 0.1m wide. Microalgal cultures are pumped along the tube as it is aerated with CO₂. The flat horizontal design allows maximum exposure to sunlight. Column photobioreactors (Figure 2.3b) operate in the same way, except they are vertical and consist of 1 longer and wider tube, with a depth of about 0.1m. This space saving method also allows the microalgae to have maximum exposure to sunlight (Brennan *et al.*, 2010).

Figure 2.3 Closed photobioreactor algal growth system

a. Tubular photobioreactor

b. Column photobioreactor

This item has been removed due to third party copyright. The unabridged version of the thesis can be viewed at the Lanchester Library, Coventry University.

Figure 2.3a shows a laboratory scale tubular photobioreactor (Image from <http://sfsu.edu>). Figure 2.3b shows a laboratory scale column photobioreactor system (Image from <http://www.oilgae.com>).

2.3 Microalgal lipids

Microalgae are known to store high quantities of oil in the form of lipids, such as triacylglycerols (TAG) within internal organelles called lipid bodies. These molecules (Figure 2.4) are of great interest to the biofuels industry as they can be converted into fatty acid methyl esters (FAMES) by a simple process called transesterification. This is a reversible reaction in which a fat or oil reacts with an alcohol to form glycerol and more importantly FAMES (Vyas *et al.*, 2010). The FAMES formed can then be purified and used as biodiesel (Becker, 1994). The structure of common microalgal Fatty acids which forms FAMES is shown in Figure 2.5.

Figure 2.4 Triacylglycerol structure

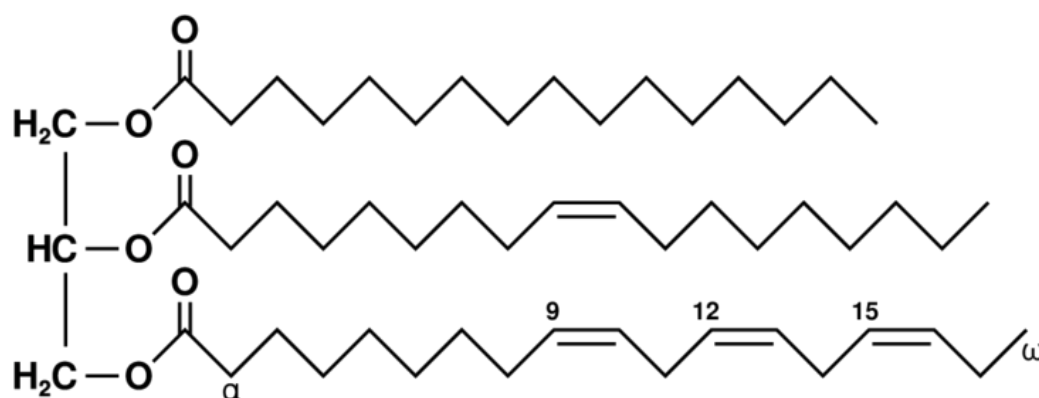


Figure 2.4 shows an example of a triacylglycerol, a type of lipid commonly found in microalgal cells (Figure 2.4 from <http://wikipedia.org>).

Figure 2.5 Structure of Fatty Acid

a. Linoleic acid ($C_{18}H_{32}O_2$) structure

This item has been removed due to third party copyright. The unabridged version of the thesis can be viewed at the Lanchester Library, Coventry University.

b. Palmitic acid ($C_{16}H_{32}O_2$) structure

This item has been removed due to third party copyright. The unabridged version of the thesis can be viewed at the Lanchester Library, Coventry University.

Figure 2.5 shows the structure of two fatty acids that are common to microalgal cells.

Figure 2.5a is Linoleic acid and 2.5b. is Palmitic acid. Both figures from <http://www.pherobase.com>)

Under normal conditions microalgae can produce a lipid content that is roughly 20-50% of their dry biomass (Araujo *et al.*, 2011); 25.5% on average (Hu *et al.*, 2008). Table 2.1 shows the documented lipid contents and environments of a number of microalgae that are commonly used in the biofuels industry.

Table 2.1 Comparison of the lipid content of several microalgal species commonly used in the biofuels industry

Species name	Natural environment	Average total lipid % dry weight
<i>Botryococcus braunii</i>	Freshwater	25-75
<i>Chaetoceros gracilis</i>	Marine	60
<i>Chaetoceros mulleri</i>	Marine	25
<i>Chlorella vulgaris</i>	Freshwater	52
<i>Dunaliella sp.</i>	Marine	30
<i>Dunaliella teriolecta</i>	Marine	36-42
<i>Isochrysis sp.</i>	Marine	21
<i>Neochloris oleoabundans</i>	Freshwater	35-54
<i>Nannochloropsis sp.</i>	Marine	31-68
<i>Nannochloropsis oculata</i>	Marine	28
<i>Tetraselmis sp.</i>	Marine	8
<i>Tetraselmis chui</i>	Marine	23
<i>Tetraselmis tetrahele</i>	Marine	30
<i>Thalassiosira weissflogii</i>	Marine	13

The above table shows total lipid content of several microalgal species that are commonly used in the biofuels industry. Data acquired from a study conducted by Araujo *et al.* (2011), Vyas *et al.* (2010) and from <http://www.oilgae.com>

The types of lipid produced by microalgae are various but include phospholipids which are employed in cell membranes, glycolipids which act as receptor sites and neutral lipids such as TAG which predominantly act as storage lipids. TAGs are of key importance to the biofuels industry (Williams and Laurens, 2010). TAG molecules are stored in lipid/oil bodies in the microalgal cytoplasm (Hu *et al.*, 2008). TAG molecules are synthesised by a series of enzymatic reactions in which fatty acids, which are produced in the cell chloroplasts are transformed into glycerol-3-phosphate (Hu *et al.*, 2008). This process is summarised in Figure 2.6.

Figure 2.6 Microalgal TAG synthesis pathway

This item has been removed due to third party copyright. The unabridged version of the thesis can be viewed at the Lanchester Library, Coventry University.

The above figure shows step by step the pathway of how TAG is formed. Each number refers to an enzyme. (1.) Cytosolic glycerol-3-phosphate transferase. (2.) Lyso-phosphatidic acid acyl transferase. (3.) Phosphatidic acid phosphatase. (4.) Diacylglycerol acyl transferase. (Adapted from Roessler *et al.*, 1994).

It has also been widely reported that when microalgal cells undergo various conditions of stress their lipid content can increase dramatically (Converti *et al.* 2009). This is due to a change in the type of lipid produced. When stress is detected by a microalgal cell the production of structural lipids ceases and TAG production for long term storage increases (Hu *et al.*, 2008). The process of storing lipids is brought about when cellular growth is limited but the metabolic energy supply reaching the cell is not, in the case of microalgae the energy supply is from photosynthesis (Ben-Amotz *et al.*, 2009). Conditions known to limit growth include variations in temperature, light intensity and concentrations of iron and phosphorus in the microalgal growth media (Converti *et al.*, 2009). However, many (Including Hu *et al.* 2008 and Converti *et al.* 2009) argue that variations in the nitrogen concentration of the microalgal growth media will bring about the most significant changes in lipid accumulation rates. All conditions mentioned can be easily manipulated at a laboratory scale to maximise the amount of microalgal lipid produced. For example,

microalgal growth media can easily be modified to mimic condition of nitrogen or iron deprivation. If this can be scaled up then it would be of great interest to the biofuels industry.

In comparison with other biofuel systems microalgae have a number of advantages. Where first and second generation biofuels compete with the food industry for arable land and potable water, microalgae can be grown in sea water and surface waters in a sunny climate, such as a raceway pond set up in a desert. In comparison with the limitations of fossil fuels which cause a number of environmental concerns such as increasing atmospheric CO₂ levels, the use of microalgal biofuels provides what could be a carbon neutral process. This is because any CO₂ released by combustion would be used up by microalgae during growth by photosynthesis. Currently there are limitations to the use of microalgal biofuels, as the production costs of large industrial scale microalgal growth are expensive. Production costs are around €250/kg of dry biomass, in comparison to a primary biofuel such as palm oil which costs €0.50/kg (Wijffells *et al.*, 2010). For this technology to advance, microalgae will need to be produced at a lower cost and on a larger scale. Another limitation is the efficiency of the methods employed to extract microalgal lipids from the biomass and this is the focus of this project.

3. Lipid extraction

3.1 Traditional lipid extraction techniques

Methods traditionally used for lipid extraction usually involve solvent extraction through diffusion. These methods however are not ideal as they either involve the use of dangerous and environmentally harmful solvents or are not capable of extracting substantial quantities of lipids from the biomass. Lipids (TAG) are non-polar so therefore non polar or low polar solvents such as chloroform or hexane are traditionally used in extraction (Aranda-Burgos *et al.*, 2014).

The Folch extraction method (Folch *et al.*, 1957) involves recovering lipids from a homogenised medium or dry biomass by adding 2:1 chloroform:methanol (v:v) solution, which acts as an extraction solvent. The suspension is thoroughly mixed and allowed to settle into phases. The lower organic layer is removed and evaporated to dryness. The lipids recovered are weighed gravimetrically and values expressed as a percentage lipid recovered from the biomass. This is a generic method employed on a variety of material including animal and plant tissues as well as microalgae. This technique is limited as it is quite time consuming and often has a poor lipid recovery rate. An additional limitation is that other organic materials, such as chlorophyll could be extracted unintentionally and measured as lipids.

The Bligh and Dyer lipid extraction technique involves a two step extraction by adding 1:2 chloroform:methanol (v:v) to a dry biomass (Bligh and Dyer, 1959). This is thoroughly mixed and chloroform and H₂O are then added to give a final concentration of 1:2:2 (H₂O:chloroform:methanol). The lower organic layer is removed and evaporated to dryness. The lipids recovered are weighed gravimetrically and values expressed as percentage lipid recovered from the total

biomass. This technique is less time consuming than the Folch method but both methods share the same limitations (Kumari *et al.*, 2011).

Finally the Soxhlet extraction (Soxhlet, 1879) involves bringing an appropriate solvent such as hexane to boiling point and percolating through the microalgal biomass. This then falls back into the evaporating flask and repeated until the solvent evaporates. The residue (oil) remaining is then weighed and expressed as percentage lipid in biomass. This method is very time consuming, quite costly in terms of the heat required to vaporise the hexane and less effective than the Bligh and Dyer method (Ranjan *et al.*, 2010).

Other extraction methods replace traditional solvents with supercritical liquids, one of the most common is supercritical CO₂. This treatment involves heating CO₂ to around 60°C and about 300 bar of pressure and using this as extracting agent of liquid and solid media (Cheng *et al.*, 2011). This method has proved to be more effective than traditional extraction methods at recovering a higher lipid yield. However this is not environmentally sustainable due to the energy requirements in terms of the temperatures and pressures needed.

It has been suggested by Wijffels and Barbosa (2010) that cells need to be physically ruptured and then treated with organic solvents to achieve total lipid recovery from the microalgal biomass, but because many microalgal species have thick rigid cell walls this is a difficult process and would require exposure to extreme mechanical, physical or chemical stress to disrupt cells (Wijffels and Barbosa, 2010). Extreme heating and pressure by autoclaving, bead beating, microwaves and osmotic shock treatment have all been suggested as physical methods to disrupt

microalgal cells (Lee *et al.*, 2010). However, one of the most promising methods for disrupting microalgal cells is ultrasonic treatment (Ranjan *et al.*, 2010).

3.2 Potential methods used for microalgal cell disruption

The process of the production of microalgal biodiesel with a cell disruption step included in illustrated in Figure 3.1. The microalgae biofuel production process can be summarised as follows; firstly the microalgae are grown, then when at a suitable cell concentration (dependent on species) the cultures are starved of nutrients to increase internal lipid content. Next, the cells would be broken open using one of the methods discussed in the current section and lipids would be extracted. The lipids would then be transesterified into fatty acid methyl esters, purified and employed as biodiesel. (Cooney *et al.* 2011)

Figure 3.1 The microalgal biodiesel production process

This item has been removed due to third party copyright. The unabridged version of the thesis can be viewed at the Lanchester Library, Coventry University.

The above figure summarises the microalgal biodiesel production pathway with a cellular disruption step included (Image from Solix Biofuels).

3.2.1 Microalgal cellular disruption by autoclave

Autoclaves employ extreme heat and pressure to disrupt microalgal cells (Prabakaran *et al.*, 2011). This method has multiple effects on microalgal cells, including cessation of cellular functions and growth, denaturing of enzymes and disruption of cell walls and membranes. The positive aspects of this approach are that it is very effective, as this technique is used commonly to destroy bacterial cells and sterilise laboratory and medical equipment. The main limitation of this method is the cost involved to generate the heat and pressure required. Most autoclaves have a fixed volume which means that any large scale lipid extraction would be batch type; also autoclave run times can be quite lengthy.

3.2.2 Microalgal cellular disruption by bead beating

This method involves adding a microalgal culture to a bead beater which contains beating beads in sizes ranging from 0.001 - 0.2 mm. These are then subjected to high speed rotary stirring which causes rapid bead movement throughout the culture and results in collisions with microalgal cells which would rupture the cells (Lee *et al.*, 2010). Studies have shown this method is quite effective and running costs are lower than autoclaving. However, after each run the beads and culture must be separated which can make this method very time consuming. In addition, as with using autoclaves, bead beaters have a limited volume within their reaction chambers, therefore only batch processing can take place unless a flow system can be developed.

3.2.3 Microalgal cellular disruption by microwave radiation

The microwave method involves exposing microalgae cultures to microwave radiation (usually around 2500 MHz) which will cause the cells to shatter (Lee *et al.*, 2010). This method which has been explored on a laboratory scale has low production costs due to low power inputs and is quite an efficient method as the exposure time needed to disrupt cells is generally quite short, around 5-10 minutes (microwaves are usually operated in a cycle mode, 21 seconds on 9 seconds off). Other research has shown that microwave radiation could also be employed to facilitate a direct transesterification method which could effectively avoid the extraction step of biofuel production (Koberg *et al.*, 2011). The main limitation of microwaves is that high temperatures (100°C) are required for extraction and a cooling step may be required (Iqbal and Theegala, 2013)

3.2.4 Microalgal cellular disruption by osmotic shock treatment

This method involves adding 10% NaCl to a microalgal culture and placing it in a vortex for 1 minute. The osmotic pressure brought about by this method is usually sufficient to burst most microalgal cells (Lee *et al.*, 2010). This method is advantageous as it is relatively rapid and simple to carry out. On the other hand the energy required for the vortex stage would simply not be sustainable at a large scale. Studies have also shown that this method is not effective against all types of microalgae. Species such as *Botryococcus braunii* and *Nannochloropsis oculata* have thick cell walls which are not easily disrupted using this method (Lee *et al.*, 2010).

3.2.5 Microalgal cellular disruption using ultrasound

When low frequency sound waves are applied to a liquid medium, areas of extreme heat and pressure are formed; this is as a result of the collapse of acoustic cavitation bubbles. When these bubbles collapse shear forces are created which are able to disrupt a range of cellular materials (Mason and Lorimer, 2002). This technology is advantageous as it requires low power inputs. In addition, this technology can be employed as a flow system which means there are no issues with a fixed treatment volume. A disadvantage of this technology is that it is not currently known if ultrasound can sufficiently disrupt microalgal species with extremely thick cell walls such as *Nannochloropsis* or *Scenedesmus*. Also it is possible that if ultrasound is applied for too long oil released from the microalgal cells could be emulsified which may make lipid recovery extremely difficult. Emulsification is the mixing 2 or more liquids that are usually immiscible; ultrasound is known to emulsify oil in water (Jambrak *et al.*, 2009). It is therefore important that microalgal cells are exposed to only the appropriate amount of ultrasound. It may also be worth exploring the effect of ultrasound on oil alone as prolonged exposure to ultrasound may cause degradation or emulsification (Behrend and Schubert, 2000).

3.2.6 Comparison of several microalgal membrane disruption methods

Table 3.1 displays a brief description and evaluation of several methods employed to disrupt microalgal cells. Despite having a few possible drawbacks, it is clear that ultrasound offers potentially advantageous technology for the disruption of microalgal cells. Arguably its main advantage is the low power input necessary for operation, which assists making microalgal biofuels a green and sustainable technology. The following sections will describe the application of power ultrasound in more detail and explore the options for its potential in the disruption of microalgal cells.

Table 3.1 Comparison of several methods used to disrupt microalgal cells

Cell disruption method	Brief description	Advantages of this method	Disadvantages of this method
Autoclaving	<ul style="list-style-type: none"> Employs extreme heat and pressure to disrupt cells 	<ul style="list-style-type: none"> Very efficient method of cellular disruption 	<ul style="list-style-type: none"> High cost of operation To run a complete cycle is time consuming Limited volume inside chamber
Bead beating	<ul style="list-style-type: none"> Employs high speed mixing of culture and beading beads to cause collisions to disrupt cells 	<ul style="list-style-type: none"> Very efficient method of cellular disruption More cost effective than the autoclave method 	<ul style="list-style-type: none"> Limited volume inside bead beater Removal of beads from culture may be a time consuming process
Microwave radiation	<ul style="list-style-type: none"> Uses high frequency microwaves to disrupt the microalgal cells 	<ul style="list-style-type: none"> Very efficient method Short reaction time needed Low operational cost Potential for a direct transesterification method 	<ul style="list-style-type: none"> High temperatures are often required for extraction, meaning a cooling step may be required
Osmotic shock	<ul style="list-style-type: none"> Involves vortexing a microalgal culture with a 10% NaCl solution to burst cells 	<ul style="list-style-type: none"> Very simple method to carry out Not time consuming 	<ul style="list-style-type: none"> Due to energy demands it may not be a sustainable method on a large scale Not effective against all microalgal cell walls
Ultrasound	<ul style="list-style-type: none"> Low frequency sound waves cause cavitation bubbles to form. When these collapse shear forces are formed to disrupt microalgal cells 	<ul style="list-style-type: none"> Low power input required Technology can be adapted to become part of microalgal photobioreactors 	<ul style="list-style-type: none"> It is not known how effective it would be against microalgal with thick cell walls If applied for too long ultrasound may potentially emulsify any potential oil released from microalgal cells

4. Ultrasound

4.1 Introduction to sonochemistry

Sonochemistry studies the effects of ultrasonic sound waves on chemical and physical reactions. Ultrasound is a sound which is at a frequency beyond the range of human hearing (>20 kHz). Ultrasonic devices use transducers which convert electrical energy to sound energy to produce an ultrasonic field. The use of ultrasound can be divided into two separate areas; diagnostic and power ultrasound (Mason, 1990).

Diagnostic ultrasound is the most commonly known form of ultrasound. This employs high frequency sound waves from 3-10 MHz as a diagnostic tool in the field of medical imaging (Figure 4.1). Sound waves at this level of low power and high frequency do not leave permanent effects to the medium that it is exposed to, making it ideal for non-invasive imaging (Mason and Peters, 2002). The most common known use is in foetal imaging; however it also has applications for detecting cancerous growth within the body (Phull and Mason, 1999). Ultrasound uses a pulse/echo technique to produce an image from within the body (Mason, 1990).

Figure 4.1 Range of sound frequencies

This item has been removed due to third party copyright. The unabridged version of the thesis can be viewed at the Lanchester Library, Coventry University.

Figure 4.1 shows the different sound frequencies in which ultrasonic effects can occur. As a comparison it also shows the range of human hearing (Image from Mason and Lorimer, 2002)

Power ultrasound employed for the disruption of microalgae, focuses on low frequency sound waves that range from 20-100 kHz, as shown in Figure 4.1 (Mason, 1991). The range of practical uses for power ultrasound is truly enormous. It is employed in many industries such as engineering and biological sciences for uses ranging from emulsification to impregnating dyes into leather (Sivakumar and Rao, 2003). Power ultrasound induces permanent changes in the medium they are exposed to due to a mechanism called acoustic cavitation (Mason, 1990).

4.2 Cavitation

When a liquid is exposed to low frequency sound waves (20-100 kHz) acoustic cavitation bubbles are produced. These are microscopic bubbles which in a matter of milliseconds form, grow and collapse, creating microscopic “hot spots” of extremely high pressures and heat upon their collapse (Mohalkar *et al.*, 1999). These “hot spots” are of great interest because of the range of their potential applications. The extreme conditions created by these “hot spots” lead to excited states, bond breakage and free radical production within the medium (Kuijpers *et al.*, 2002). The advantages of this from an industrial point of view is that these effects can lead to higher yields of output, shorter reaction times and less hazardous conditions needed for chemical reactions to take place (Bonrath, 2003).

Cavitation bubbles are formed by the rarefaction and compression phases of a sound wave that is exposed to a liquid medium (Mason, 1991). When the negative pressure of the rarefaction phase becomes large enough to stretch the molecular spacing of a liquid, a cavity will form (Kuijpers *et al.*, 2002). The negative pressure of the rarefaction stage will cause the distance between the molecules to exceed the critical molecular distance necessary to hold the liquid intact, the liquid will break and a cavity will be formed (Mason, 1991). The rarefaction and compression phases will cause the cavity to grow into a bubble. This bubble will grow until it reaches an unstable size, upon reaching this size a compression phase of the sound wave will cause the bubble to violently collapse resulting in large amounts of energy released in and around the bubble (Mason, 1991). Collapse of the bubble can generate temperatures of around 5000 K and pressure of 200 bar. This process is illustrated in Figure 4.2. These extreme conditions make power ultrasound a very useful tool (Kuijpers *et al.*, 2002).

Figure 4.2 Formation and collapse of a cavitation bubble

This item has been removed due to third party copyright. The unabridged version of the thesis can be viewed at the Lanchester Library, Coventry University.

The above image illustrates how through a series of rarefaction and compression cycles the cavitation bubble forms and collapses releasing extreme pressure and heat in the surrounding medium (Mason, 1991).

In addition to cavitation, mechanical forces associated with ultrasound have also been shown to disrupt cell walls and cause the release of compounds such as lipids (Cravotto *et al.*, 2008). Shock waves are an example of a physical mechanical force associated with ultrasound due to waves of extreme pressure created outside the cavitation bubble after collapse (Mason and Lorimer, 2002). When a cavitation bubble is formed near a solid surface, for an example the cell wall of a microalgal cell, the cavitation bubble will form and collapse in a non spherical shape. When collapsing in this shape the bubble will form a high pressured localised liquid jet against the solid surface (Figure 4.3). The combination of shock waves and liquid jet formation cause intense shear forces within the liquid media to break open microalgal cell walls.

Figure 4.3 Formation of liquid jet

This item has been removed due to third party copyright. The unabridged version of the thesis can be viewed at the Lanchester Library, Coventry University.

The above figure illustrates the collapse of a cavitation bubble and the formation of a liquid jet against the surface of a microalgal cell wall (Image from Mason and Lorimer, 2002).

4.3 Factors that affect acoustic cavitation

A number of factors need to be considered which can affect the formation of cavitation bubbles and these can be divided into the following categories; acoustic, external and solvent factors.

4.3.1 Acoustic factors

Acoustic factors are ones which are based on the formation of the cavitation bubbles themselves and include frequency, intensity and whether the energy is pulsed.

Frequency

Frequency is the number of sound waves that pass through a fixed unit in time. When frequency is increased the rarefaction phase of the sound wave shortens which means that the amplitude will have to be increased to maintain the same amount of cavitation. Other consequences of changing frequency include when employing a low frequency larger bubbles are formed and when using a high frequency, smaller bubbles are formed. Smaller bubbles produce a less violent collapse and therefore could potentially be less effective against microalgal cells (Mason and Peters, 2002).

Intensity

Acoustic intensity must pass a certain threshold for cavitation to occur. In general, a low frequency requires a low intensity and a high frequency requires a high intensity. An increase beyond this intensity threshold will usually cause an increase in sonochemical effects (Mason and Peters, 2002.)

Pulse

Pulsed ultrasound has been known to affect bubble formation and activity. The effect of this type of ultrasound depends on the ratio between pulse width and its repetition interval as well as the shape of the wave form and intervals between each pulse (Mason and Peters, 2002.)

4.3.2 Solvent factors

Solvent viscosity, surface tension and vapour pressure all influence cavitation bubbles. It is difficult for cavitation bubbles to form within viscous liquids, this is because negative pressure from the rarefaction cycle must overcome the liquids own natural cohesive forces. Solvents with low surface tension have been known to cause a reduction in the cavitation threshold. Solvents that have a low vapour pressure have been known to cause difficulty in the formation of cavitation bubbles, since the bubbles will contain less vapour than the solvent (Mason and Peters, 2002).

4.3.3 External factors

External factors which effect the formation of the cavitation bubbles may not be produced by the ultrasonic equipment but still need to be monitored due to their potentially adverse effects. These include temperature, pressure and bubbled gas (Mason and Peters, 2002).

External temperature

When the ambient temperature rises it will cause a decrease in surface tension and an increase in vapour pressure, lowering the cavitation threshold which means that lower intensities are required for cavitation to occur. On the other hand high temperatures approaching boiling point would form bubbles within the medium which act as barriers towards sound waves entering, resulting in less sonochemical effects (Mason and Peters, 2002).

Bubbled gas

Bubbled gas entering the medium lowers the cavitation threshold. Small gas bubbles entering a system act as nuclei for cavitation and as a result increased gas within the medium will cause enhanced cavitation along with a reduction in the intensity of the shock wave upon bubble collapse (Mason and Peters, 2002).

External pressure

When pressure is increased greater rarefaction pressure is required for cavitation to occur, hence higher acoustic intensity will be required to induce cavitation (Mason and Peters, 2002).

4.4 Ultrasonic equipment

4.4.1 Ultrasonic bath

This is perhaps the most commonly known type of ultrasonic device. Its structure usually consists of a stainless steel tank with one or more ultrasonic transducers attached beneath its base. Ultrasonic baths are usually operated at a frequency of around 40 kHz; some devices also have adjustable power and heating settings (Mason and Peters, 2002). An example of an ultrasonic bath is shown in Figure 4.4.

Figure 4.4 Ultrasonic bath

This item has been removed due to third party copyright. The unabridged version of the thesis can be viewed at the Lanchester Library, Coventry University.

The above figure displays an ultrasonic bath set up with a microalgal suspension (Mason, 1999).

4.4.2 Ultrasonic probe

The ultrasonic probe was developed to address problems associated with the ultrasonic cleaning bath, these being its inability to control energy input into a reaction and the systems general lack of power. Ultrasonic probes are generally operated at around 20 kHz and employ piezoelectric transducers attached to horns which are immersed into reactants. Probes are also equipped with an amplitude control and a pulse mode to control the actual power entering a system (Mason and Peters, 2002). Figure 4.5 displays a 20 kHz probe system.

Figure 4.5 Ultrasonic probe system

This item has been removed due to third party copyright. The unabridged version of the thesis can be viewed at the Lanchester Library, Coventry University.

The above figure displays a 20 kHz probe system set up with a microalgal suspension (Mason, 1999)

4.5 Calorimetry of ultrasonic equipment

Calorimetry is a form of thermal dosimetry. It is used to calculate both the power and intensity of ultrasonic equipment. As mentioned previously when ultrasound is applied to a system cavitation bubbles are formed, when they collapse large amounts of heat and pressure are produced. When an increasing amount of cavitation bubbles form and collapse, the temperature of the medium will increase (Berlan and Mason, 1996).

The calculation of power and intensity is done by measuring the increase in temperature over time while sonication is taking place. This increase in temperature over time is plotted into a graph. The gradient of the line of best fit of this plot can be used to calculate the power output of the ultrasonic equipment using the following equation (Berlan and Mason' 1996):

$$\text{Power} = (dT/dt)C_pM$$

In this equation dT/dt is the change in temperature over time, C_p is the heat capacity of the liquid medium and M is equal to the mass of the liquid medium (Berlan and Mason, 1996).

The reasons why calorimetry needs to be carried out are to make sure that power settings are compatible to other ultrasonic systems. A further reason is to ensure that the performance of the transducer has not been affected by aging and erosion, and finally to be able to get a rough estimation of the electronic intensity of the ultrasonic equipment.

4.6 Ultrasound and bacteria

Microalgae share numerous similarities with bacterial cells, which have been studied extensively in the field of sonochemistry. Ultrasound has been shown to inactivate bacterial cells by disrupting cell walls (Joyce *et al.* 2003). This was however found to be more effective on the thin cell walled gram negative bacteria, than on gram positive bacteria which have thick cell walls (Joyce, *et al.*, 2011). Some bacteria share a similar physiology to microalgae, therefore it is reasonable to assume that ultrasound may cause similar effects on microalgae.

4.7 Ultrasound assisted extraction (UAE)

The use of ultrasound in combination with solvents, also known as Ultrasound Assisted Extraction (UAE) to extract products from plant cells, which also share a number of similarities with microalgae, has been employed recently to extract numerous products from plant cells. UAE is often found to increase the efficiency of the extraction process. An example of this is the extraction of anti-oxidants from *Rosmarinus officinalis* in which UAE is more effective than traditional extraction and carried out at a lower temperature with less solvent (Paniwnyk, 2009). UAE has also been employed to extract oil from oleaginous crops such as soy bean, vegetables and seaweed. This technique resulted in an increase in extraction efficiency of up to 50% from each source by comparison to the soxhlet method (Cravotto *et al.*, 2008).

Some work has been carried by employing UAE to extract oil from microalgae but so far results have been inconclusive and lacked detail and depth. Ranjan *et al.*, (2010) developed a UAE Bligh and Dyer extraction method which saw the amount lipids recovered from the microalgae *Scenedesmus Sp.* increase from 2 - 6% of the total dry biomass when compared to the conventional Bligh and Dyer method. Though

these results are positive they are low lipid extraction yields, especially when considering that extractions from *Scenedesmus rubescens* (closely related to *Scenedesmus Sp.*) has been shown to be as high as 15% (Aravantinou *et al.* 2013). Cravotto *et al.*, (2008) developed a technique where they employed UAE on a marine microalgae species. This method showed very positive results, with lipid recovery increased from 4.8%, using the soxhlet extraction to 25.9% when UAE was employed. Though the results were positive this may be further optimised as tests were limited in terms of extraction time, ultrasonic equipment employed and microalgal species.

Considering the work carried out on similar species and limited research that has currently been conducted on UAE microalgae extraction methods there are indications that there is great potential for the use of ultrasound in lipid extraction from microalgae. The aim of this project is to research and develop methods to extract oils from microalgae using ultrasound technology.

5. Literature review

5.1 Algal biofuels

A broad description of the field of microalgal biofuels is given by Wijffels and Barbosa, (2010) who believes that this environmentally friendly alternative can be commercially available within the next 10-15 years. Wijffels and Barbosa suggest that due to increasingly high oil prices, energy demands and increases in atmospheric CO₂ levels, microalgal biofuel research must be given considerable attention as it may hold the answers to these problems. Photosynthetic microalgae need only sunlight, CO₂, water, nitrogen and phosphorus to produce carbon rich lipids. Micronutrients such as iron, cobalt, copper, manganese, and vitamins are also essential. When microalgae are stressed they store chemical energy in oil bodies which contain neutral lipids and triacylglycerols (TAG). This oil can be extracted and converted to fatty acid methyl esters and biodiesel by a process called transesterification.

In relation to this project a major issue that was raised is that commercial extraction of microalgal oils is still based on traditional techniques such as the Folch or Bligh and Dyer methods but so far applied and tested on very few microalgal strains (Wijffels and Barbosa, 2010). These techniques must be further developed and advanced. The use of ultrasound offers a potential way to develop sustainable and cost effective extraction methods. The majority of microalgae with high oil contents possess thick cell walls and extracting lipids at reasonable yields of around 25-50% of their dry weight is extremely difficult using conventional techniques. Organic solvents alone cannot be used to extract lipids from all microalgae. Some microalgae require exposure to harsh conditions to disrupt cells. Wijffels and Barbosa., suggests the use of mechanical, chemical or physical stresses. The shear forces produced by

ultrasound may have the potential to disrupt thick cell walls. Therefore it is advisable to test the UAE techniques on a number of microalgal species with variable cell wall strengths to optimise efficiency.

Another review by Brennan and Owende (2010) focused on the microalgal biofuels industry as a whole, covering a wide range of related issues and subject matter. This included the most suitable growth facilities, impact of strain selection, lipid production, extraction, purification and biofuel conversion technologies. Brennan and Owende provide a description of key factors that must be considered prior to selecting the correct microalgal strain for biofuel production. Algae must have high lipid production rates, ideally around 50% of the dry weight. When algae are produced on an industrial scale the selected species must be tough enough to survive stressful conditions that are commonly associated with large photobioreactors along with out-competing any wild microalgal or bacterial strains that may contaminate the system (Brennan and Owende, 2010). In addition it would be beneficial if they had low nutritional requirements, fast reproduction cycles and be tolerant to a wide range of temperatures.

Brennan and Owende also highlighted the dangers of increasing lipid production by altering the microalgal growth conditions, examples include limiting nitrogen and phosphorus in the growth media, altering temperature, light intensity and salinity. The authors stated that lipid accumulation due to nutritional starvation may not result in an increase in lipid productivity as lipid accumulation and biomass production may not be directly correlated in all microalgal species. Although nitrogen limitation is the most effective method of lipid accumulation in many microalgae species, the level of lipid accumulation must not adversely affect the growth of specific microalgae.

Brennan and Owende stress the importance of cell disruption in the recovery of oils from microalgae. Traditionally solvents such as hexane are used to remove oils from cells by altering the cell membrane which enables release of oil. Many microalgae, such as *Nannochloropsis* have extremely thick cell walls, which will adversely affect oil recovery by solvents as the cell membrane and solvent are not in direct contact. Brennan and Owende agree with Wijffels and Barbosa in that a physical stress must be used to disrupt the cell wall to achieve maximum oil extraction. Methods suggested include autoclaving, high pressure homogenisers and a combination of ultrasound and electromagnetic pulses.

5.2 Microalgal species

It is vital that the microalgae chosen as test species for a developing ultrasound assisted extraction (UAE) method are significantly different from each other. Species with different morphology, for example size and the presence of a cell wall are important factors to consider when developing an UAE method for use on microalgal species. It is also important to use species that have different lipid compositions to test the limits of extraction of methods developed. The four species chosen for this project are *Nannochloropsis oculata*, *Dunaliella salina*, *Chlamydomonas concordia* and *Chlorella Sp.* *Nannochloropsis oculata* is different from the other three species employed in this study in that it is a eustigmatophyte microalga, where the remaining three species are all the more commonly known “green algae” or chlorophyta (Fawley *et al.*, 2014). Eustigmatophyte and chlorophyta microalga are structurally very different which will be described in sections 5.2.1-4). The four diverse species chosen for this project should provide a basis to ensure that when the UAE method are employed for other microalgae with different cell wall structures this information can be interpreted to suggest optimum conditions of treatment.

5.2.1 *Nannochloropsis oculata*

Nannochloropsis oculata (*N. oculata*) is a small (1-2 μm length, 1-2 μm width), spherical, unicellular microalgae which is commonly found in salt water environments (Sukenik *et al.*, 1989). It is known to have an extremely thick and robust cell wall (Wijffels and Barbosa, 2010). This has both positive and negative attributes as this tough species should not be affected by harsh conditions associated with industrial scale raceway ponds or photobioreactors. Wijffels and Barbosa (2010) regard thick cell walls as a limiting factor and indicate *Nannochloropsis* as a problematic choice for biofuel production due to known difficulties disrupting the cell wall.

Converti *et al.* (2009) and Araujo *et al.* (2011) have stated *N. oculata* is a suitable candidate for biofuel production due to its high lipid content. Experiments undertaken by Converti *et al.* (2009) observed lipid contents as high as 24.3% however it has been found to be as high as 28.7% (Gouveia and Oliveira, 2009).

Nannochloropsis is considered an ideal test subject for ultrasonic lipid extraction techniques due to the high lipid content and to investigate the effects on its tough cell wall. If *N. oculata* cell walls can be disrupted by ultrasound then the technique could be optimised and employed on other tough species such as *Scenedesmus*.

5.2.2 *Dunaliella salina*

Dunaliella salina (*D. salina*) is a single cell marine microalgal species commonly found worldwide in sea salt fields. They are ovoid in shape and motile by use of twin flagella. It is commonly sized between 2-28 μm in length and 1-15 μm in width (Ben-Amotz *et al.*, 2009). *D. salina* does not have a true cell wall, hence it is easier to rupture than *N. oculata*. According to Gouveia and Oliveira, (2009) *D. salina* has a

dry weight lipid content of 16-20%. However according to a study by Araujo *et al.*, (2011) on *Dunaliella* sp. when stressed by increased salinity (from 25-35g/L) the lipid content can increase to 30.12%. This species is also a good test subject for UAE techniques as it offers a comparison to *N. oculata* which normally has higher lipid content and is much tougher to rupture.

5.2.3 *Chlamydomonas concordia*

Chlamydomonas concordia (*C. concordia*) is a unicellular marine microalga sized between 6-10 μM in length and 2.5 to 8 μM in width. They are ovoid in shape, motile by twin flagella and possess a thin cell wall. There are also spherical non-motile cells sized around 10 μM which contain lipid vesicles that are visible under a microscope (Green *et al.*, 1978). There is currently no record of the lipid content of *C. concordia* on record however Yoo *et al.* (2012) and Lv *et al.* (2013) have determined that *C. concordia*'s relative *Chlamydomonas reinhardtii* (*C. reinhardtii*) has a lipid content of between 25-35%. A study undertaken by James *et al.*, (2011) revealed that some mutant strains of *C. reinhardtii* can achieve lipid content of up to 65%. *C. concordia* is also considered a good test subject for ultrasonic extraction as it has a cell wall that is not as thick as *N. oculata* and so is considered a good intermediate between *N. oculata* and *D. salina*.

5.2.4 *Chlorella* Sp

Chlorella are traditionally a fresh water microalgal species, they are unicellular, non-motile and typically sized between 2-10 μM . They are also usually spherical with a visible thick cell wall. The lipid content of *Chlorella vulgaris* can vary from 16-52% of its dry mass (Araujo *et al.*, 2013). This species is considered a good candidate for

microalgal biofuel production because of its high biomass production rate and lipid content (Lui *et al.*, 2011).

5.3 Microalgal culturing techniques

Converti *et al.* (2009) cultured *N. oculata* using Guillard's F/2 medium (Guillard and Ryther, 1962), with a nitrogen concentration of 0.3g/L^{-1} at 20°C . Cultures were aerated using CO_2 from the air in an incubator equipped with artificial lighting at a photon flux density of $70\ \mu\text{Em}^{-2}\text{s}^{-1}$ for 14 days.

Tang *et al.* (2010) cultured *Dunaliella tertiolecta* (*D. tertiolecta*), which is a close relative of *D. salina* in Erdschreiber's medium, which was aerated with CO_2 and kept at a constant temperature of 23°C . This work illustrates the positive effects on growth rates of *D. tertiolecta*. Light intensities of 200 and $350\ \mu\text{E}/(\text{m}^2\ \text{s})$ were the most effective for promoting growth. CO_2 concentrations of 2, 4 and 6% and photoperiods of 24 hours light, 0 hours darkness were also shown to promote *D. tertiolecta*'s growth.

Green *et al.* (1978) described two methods for culturing *C. concordia*. Firstly, in Erdschreiber's medium using a photoperiod of 14 hours light, 10 hours darkness and secondly using Antia and Watts medium using a photoperiod of 12 hours light and 12 hours darkness. Both culturing techniques maintained *C. concordia* cultures at 15°C . Results indicated that culturing with Erdschreiber's encouraged higher growth rates. Converti *et al.* (2009) carried out an experiment showing that *Chlorella vulgaris* demonstrated growth when using Bold's Basal Medium and at a temperature of around 25°C . A study from Zhang *et al.* (2011) reiterates this and concluded a temperature ranging between $20\text{--}35^{\circ}\text{C}$ is optimum for growth rates and lipid production in *Chlorella*.

In general for growth of the microalgae in this project F/2 media should be employed for the marine species (*N. oculata*, *D. salina* and *C. concordia*) and Bolds Basel Medium with 3 fold Nitrogen and Vitamins (3N-BBM+V) was employed for *Chlorella* Sp. (as this was recommend by the supplier). The temperature should be set between 20-25°C.

5.4 Microalgal stressing

Triacylglycerols (TAG) produced by microalgae have the potential to produce energy rich biodiesel which could in theory work alongside and eventually replace the use of fossil fuels. A problem faced by the biofuel industry is that although large quantities of microalgae can be produced quite quickly, they usually produce poor lipid yields (Sharma *et al.*, 2012). Large scale rapid microalgal growth is at the expense of high TAG production. Lipids produced by microalgae can be placed into two groups; structural lipids such as phospholipids, which are polar and make up cellular membranes around the cell and its organelles and non-polar storage lipids such as TAG. Under growth conditions TAG are mainly synthesised during the light stage of growth and are later converted into structural lipids in the dark stage. Therefore under ideal conditions TAG are not stored for long periods and are quickly metabolised (Sharma *et al.*, 2012).

Under environmental stress such as nutrient depletion many microalgal species alter their lipid production pathway increasing the production of storage lipids, which enables cells to endure prolonged periods of adverse conditions for survival in extreme environments (Schuhmann *et al.*, 2012). Studies have shown that microalgae can be manipulated into producing and storing more TAG by mimicking environmental stresses which may cause microalgae to increase lipid induction. Stresses include changes in temperature or light conditions and varying nutrient levels (Converti *et al.*, 2009).

Converti *et al.* (2009) investigated the effect of temperature and nitrogen concentrations on the lipid content of *Nannochloropsis oculata* and *Chlorella vulgaris*. This was undertaken by culturing both species under optimum condition for 14 days. After this time microalgal cells were transferred to new media and grown

under conditions where the temperature and nitrogen concentration of the growth media was altered to differing degrees around the optimum. Cultures were allowed to grow for 14 days and the lipid content was monitored.

The data gathered by Converti *et al.* in their 2009 study illustrates that both temperature and nitrogen concentrations play a role in lipid induction for both species. When the temperature was increased from 20 to 25°C with *N. oculata* the lipid content rose from 7.9 to 14.92% and for *C. vulgaris* when the temperature was raised from 25 to 30°C the lipid content dropped from 14.71 to 5.9%. This indicates a good temperature for lipid production from both species is 25°C. With regards to nitrogen concentration both species showed a rise in lipid content when nitrogen concentration was reduced. The lipid content of *N. oculata* rose from 7.88 to 15.86% when the nitrogen concentration was lowered from 0.3 to 0.075g L⁻¹ and *C. vulgaris*' lipid content rose from 5.9 to 15.31% when the nitrogen concentration was lowered from 1.5 to 0.375g L⁻¹. This study concluded that nitrogen depletion results in a rise in microalgal lipid content.

The effect of nitrogen concentration on lipid accumulation was also investigated by Siaut *et al.* (2011) on *C. reinhardtii*. An established culture of *C. reinhardtii* was transferred to nitrogen depleted TAP media and allowed to grow under normal conditions. The lipid concentration was monitored daily using Nile Red staining. Results demonstrate the lipid concentration of *C. reinhardtii* increased on a daily basis until day 5 when it began to plateau at which point the lipid concentration had rose from ~1 to ~40 ug/10⁶ cells. Results from Converti *et al.* and Siaut *et al.* demonstrate that nitrogen starvation is an effective method to increase microalgal lipid content.

Araujo *et al.* (2011) investigated the effect of salinity on the lipid content of several microalgal species including *C. vulgaris*, *Dunaliella sp.* and *N. oculata*. All cultures were grown in media containing salt concentrations of 25 or 35 g/L. Results showed that for the majority of species grown in higher salt concentrations resulted in a higher lipid content. The lipid content of *N. oculata* rose from 22.75 to 23%, for *C. vulgaris* it increased from 16.6 to 52.49% and for *Dunaliella sp.* it increased from 12 to 30.12%. This study concluded that higher salinity can increase the lipid content of a number of algal species. These results were also noted in a study carried out by Liu *et al.* (2003) and Su *et al.* (2008).

A review by Sharma *et al.* (2012) stated that members of the *Dunaliella* family are the best example of a microalgae that are able to tolerate high salinity and therefore salinity may not be as an effective factor in the lipid accumulations of other microalgae species. This may be the reason that only small increases were observed in the lipid content of *N. oculata* in the tests carried out by Araujo *et al.* (2011) under the same conditions.

Tang *et al.* (2010) investigated the effect of both light source and light intensity on the FAME accumulation in *D. tertiolecta*. Cultures were prepared in Erdschreiber's medium which was kept at a constant temperature of 23°C. To investigate the effect of light three different light sources were employed, red LEDs, white LEDs and fluorescent lights. To investigate the effect of light intensity, cultures were grown as previously described but at light intensities of 100, 200 and 350 $\mu\text{E}/(\text{m}^2\text{s})$ using fluorescent lighting. Results showed that fluorescent lighting produced the highest FAME concentration which was 23.6% of its dry weight and that FAME content

increased as light intensity was increased. Ranging from 21.7% for 100 $\mu\text{E}/(\text{m}^2\text{s})$ to 23.4% at 300 $\mu\text{E}/(\text{m}^2\text{s})$.

These studies demonstrated that the manipulation of temperature, nitrogen concentration, salinity, light source and light intensity are all valid methods to stress microalgal cultures into producing and storing more internal lipids. The stressing methods employed in this project were varying the salinity, nitrogen and trace metal concentration of the growth media.

5.5. Microalgal growth measurement methods

Measurement of microalgal growth rates must be a rapid and simple process that identifies the stage of growth in microalgal cultures. It should also ideally be a non invasive process to prevent contamination of cultures.

5.5.1 Haemocytometer (HAE)

Haemocytometer counts involve visible enumeration of numbers in a microalgae population by counting the number of cells in a haemocytometer grid under a microscope and converting the counts to the number of cells/mL (Tang *et al.*, 2010).

5.5.2 Optical density (OD)

Optical density is a technique to measure microalgal growth rates by reading the optical density of a culture at 663-686nm. This method estimates the amount of biomass/ cell number present (Converti *et al.*, 2009, Tang *et al.*, 2010)

All methods outlined above can be used to measure the growth rates of microalgal cultures along with monitoring their physical condition and viability after treatment with ultrasound. These methods are the first step in monitoring the physical effect of ultrasound on microalgal cells

5.6. Lipid determination methods

5.6.1 Thin Layer Chromatography (TLC)

Thin layer chromatography (TLC) is a relatively quick and simple method used to determine the lipid content of a sample (Vieler *et al.*, 2007). It is primarily used as a qualitative technique however results can be quantified by lipid band analysis using computer software packages. The technique works by exposing samples to a solvent, which is known as the mobile phase. The solvent moves molecules from the sample along the TLC plate and since lipids have differing molecular weights separation will occur and molecules can be identified by comparison with commercial standards.

Vieler *et al.*, (2007) employed TLC to investigate the lipid content of *Chlamydomonas reinhardtii*. Lipids were extracted using the Folch method and concentrated tenfold. 2.5 and 5 µl samples were spotted onto HPTLC silica gel plates (Merck). The TLC plate was placed in a TLC chamber containing the first eluent which was methyl acetate:isopropanol:chloroform:methanol:KCL (25%) at a ratio of 25:25:25:10:4 (v:v:v:v:v) and allowed to run to a height of 13 cm on the TLC plate. The plate was then dried and placed back in a TLC tank containing the second eluent which was hexane:diethylether:acetic acid at a ratio of 70:30:2 (v:v:v) and allowed to run to a height of 18 cm on the TLC plate. Lipids were visualised by spraying the plate with primuline solution (Direct Yellow 59). When the plate was exposed to UV light at 366 nm lipids were visible as yellow spots. The intensity of each spot was then quantified using a digital image system with the program Argus X1 (Vieler *et al.*, 2007). This method is capable of detecting a variety of lipid molecules.

5.6.2 Gas Chromatography Mass Spectrometry (GC-MS)

HPLC can be used to detect and quantify microalgal lipids (Rombaut *et al.*, 2009) however Gas Chromatography Mass Spectrometry (GC-MS) is more commonly used to detect and quantify transesterified microalgal FAMES. GC-MS combines the methods of gas-liquid chromatography and mass spectroscopy to identify a vast number of substances from within a sample. This method cannot be applied to lipids and therefore any microalgal lipid samples must first be transesterified and the FAMES analysed.

A method for the analysis of microalgal FAMES was developed by Kamari *et al.* (2010). In this method lipids were extracted from microalgal biomass and analysed gravimetrically. The extracted lipid mass was then converted to FAMES by transesterification. FAME analysis was carried out by a QP2010 gas chromatography mass spectrometer (GC-2010 with a GC-MS QP-2010) equipped with a AOC-5000 autosampler (Shimadzu, Japan) using a SHIM-5MS column (30 mm x 0.25 mm x 0.25 μ m). The carrier gas employed was helium (99.9% purity) with a pre-column pressure of 49.7 kPa and a column flow rate set to 1 mL/min. The temperature program of the column was as follows; 40°C for 3 minutes, after which a 5°C/min increase until 230 °C, where this temperature is maintained for 40 minutes. The injection volume was 0.1 μ L, the injection temperature was 240°C and the split ratio was 1:30. The ion source temperature and the interface temperature were set to 240°C. FAME peaks were identified by comparisons with the retention times of FAME standards (Sigma).

This method (Kameri *et al.*, 2010) successfully enabled the detection and enumeration of FAMES from 27 different microalgal species from three different

phyla. This shows the versatility of this method in terms of different species. This technique was also efficient in detecting a variety of FAMES ranging from C12- C22, a variety of saturated fatty acids (SFA), monounsaturated fatty acids (MUFA) and polyunsaturated fatty acids (PUFA) were also detected. Kameri *et al.* state that this method is versatile in both the range of species that it can be applied to and the variety of FAMES it is able to detect and is ideally suited to the project in this thesis.

5.6.3 Nile Red analysis

Chen *et al.*, (2009) further developed the Nile Red staining method of Cooksey *et al.*, (1987), which was a relatively quick way to evaluate the lipid content of microorganisms using the lipid soluble fluorescent dye, Nile Red. When Nile Red dye is taken up by cells it binds to internal neutral lipids causing them to fluoresce enabling detection by a Spectro-fluorophotometer or fluorescent microscope. The problems with the Cooksey technique identified by Chen *et al.* were two fold; as it was not quantifiable and a number of microalgal strains were unable to take up the dye due to the cell wall thickness. Therefore, Chen *et al.*, aimed to improve the methods efficiency so that it could be used on a number of microalgal strains and further developed this technique to produce quantifiable results.

Various aspects of the Nile Red staining method were investigated by Chen *et al.* on *C. vulgaris* to identify optimum staining conditions for microalgae with thicker cell walls. These include: Dimethyl sulfoxide (DMSO) concentration, Nile Red concentration, staining time, staining temperature and microalgal cell concentration. It was determined that the optimum Nile Red staining technique was to introduce 5 μ L of subject algae at a cell concentration of $3 \times 10^5 \text{ mL}^{-1}$ to each of the individual wells of a 96 well microplate that contained 3 μ L of $0.5 \mu\text{g mL}^{-1}$ Nile Red solution. 292 μ L of 25% DMSO aqueous solution was then added to each well. The plate was mixed

using a vortex at 120 RPM and incubated at 40°C for 10 minutes. Fluorescence was then recorded at excitation and emission wavelengths of 530 and 575 nm using a Varian 96 well plate spectrofluorometer.

The method developed by Chen *et al.* was compared with the Cooksey method of staining using several microalgal strains and found that although results varied, this method always improved staining producing higher fluorescent intensities for all species. To quantify results a correlation coefficient between internal lipid content and Nile Red derived fluorescence intensity was developed. This was based on a standard curve of the Nile Red fluorescent intensities of concentrations varying from 2 - 20 $\mu\text{g mL}^{-1}$ of the neutral lipid triolein, which enabled lipid quantification by comparing fluorescence intensity with standard curves. Validation of this technique was tested by comparing the determination of lipid content of *C. vulgaris* with that of the traditional gravimetric method. No significant difference was found between the two techniques verifying this method as a competent way of quantifying microalgal lipid content.

5.7 Traditional lipid extraction techniques

5.7.1 Folch extraction method

Kamari *et al.*, (2011) employed the lipid extraction technique developed by Folch *et al.*, (1957) on the macroalgal species: *Ulva fasciata* (*U. fasciata*), *Gracilaria corticata* (*G. corticata*) and *Sargassum tenerrimum* (*S. tenerrimum*). 500 mg of dried macroalgal biomass was treated with 3 mL of chloroform:methanol (2:1 v:v) and vortexed for 1 minute and centrifuged at 2057 G for 15 minutes. The supernatant was removed and re-extracted with chloroform:methanol (1:1 v:v) and centrifuged as previously outlined. Supernatants were filtered through Whatman filter No. 1 and washed with 2 mL of Milli Q water and centrifuged again for 5 minutes at 2057 G. The lower phase of the sample was removed, evaporated and the remaining oil was measured gravimetrically. The amount of lipids extracted using this method ranged between 15 - 20% dry weight for all three species.

5.7.2 Bligh and Dyer extraction method

Kamari *et al.*, (2011) employed the lipid extraction technique developed by Bligh and Dyer (1959) on the macroalgal species: *U. fasciata*, *G. corticata* and *S. tenerrimum*. 500 mg of dried macroalgal biomass was treated with 3 mL of chloroform:methanol (1:2 v:v) vortexed for 1 minute and centrifuged at 2057 G for 15 minutes. The supernatant was removed and re-extracted with chloroform:methanol (1:1 v:v) and centrifuged as previously outlined. Supernatants were then filtered through Whatman filter No. 1 and washed with 2 mL of Milli Q water and centrifuged for 5 minutes at 2057 G. The lower phase of the sample was removed, evaporated and the remaining oil was measured gravimetrically. The amount of lipids extracted using this method ranged between 5 - 9% dry weight for all three species.

5.7.3 Ultrasound

A review of the relevant literature has shown that some studies have employed ultrasound to extract oil from microalgae, this is described in section 5.8. However, much more research has been undertaken in using ultrasound to extract oils from macroalgae and other oleaginous crops, this is described in section 5.8.1.

5.8 Ultrasound assisted extraction (UAE) of oils from microalgae

Ranjan *et al.*, (2010) conducted a study entitled “Mechanistic assessment of microalgal lipid extraction”. The project aims were as follows; firstly to compare the efficiency of three lipid extraction methods (Soxhlet, Bligh and Dyer and sonication), secondly, to assess the influence of solvents on lipid yield and thirdly using a sonication method with both chloroform:methanol (3:1) and *n*-Hexane.

The Soxhlet extraction method involved washing 5g of dried microalgal biomass with *n*-Hexane, filtering and evaporating the sample in a rotavapor leaving behind a lipid residue. In this case lipids extracted were 1% of the microalgal biomass. The modified Bligh and Dyer extraction method mixed 2g of dried microalgal biomass with sand and crushed with a pestle and mortar. Chloroform:methanol (3:1) solution was added and used to separate this mixture into 2 phases. The lower contained the lipids and the upper phase was discarded. The lower phase was vaporised in a rotavapor leaving behind the lipids. A lipid recovery of 2% of the total biomass was produced by this technique.

The sonication method employed chloroform:methanol (3:1) as solvent and 20 mL microalgal suspension was prepared in the same way as the Bligh and Dyer method which was sonicated for 30 minutes using a 20 kHz probe (Sonics and Materials, VCX 600) at a power of 500W set to 20% power output. Lipids were then extracted

using the Bligh and Dyer method. This produced a lipid recovery of 6% of the total biomass. Finally for sonication with *n*-Hexane, the Chloroform:methanol (3:1) solution was replaced with 20 mL *n*-Hexane, but other than this the method was identical. This produced a lipid recovery of 1% of the original biomass.

In conclusion in terms of lipid extraction, measured as a percentage of dry microalgal mass; sonication with chloroform:methanol (3:1) was the most efficient method followed by the traditional Bligh and Dyer technique. Results also indicate that the chloroform:methanol mix was the most efficient solvent for lipid extraction yields. Upon microscopic analysis of microalgal cells it was deduced that none of the extraction methods achieved complete cell disruption indicating that the majority of lipid extraction which had occurred was due to diffusion.

Further studies must consider a number of factors relating to ultrasonic lipid extraction from microalgal biomass for use in the biofuel industry. The results obtained by Ranjan *et al.*, further indicate that the ultrasound mediated Bligh and Dyer method may be an appropriate starting point for further research. Only one ultrasonic frequency was used in this study (20 kHz at 20% amplitude). Also employing different settings such as 30, 40 or 50% power output, along with different frequencies, or different ultrasonic equipment may produce very different results.

Unfortunately a number of problems are alluded to in the paper (Ranjan *et al.* 2010). It was claimed in the methods section that calorimetry of the ultrasound equipment was used to calculate the power of ultrasonic equipment. However the powers were not reported, making it impossible to replicate similar ultrasonic conditions. Also it was noted that a cooling jacket was used to maintain a constant temperature during ultrasonic treatment. However, it was not stated what the start temperature

was and this puts into question what role temperature played in the results. A final point must be made in respect of the microalgal species studied, *Scenedesmus Sp.* By analysing a different microalgal species which perhaps has a slightly weaker cell wall it is probable that cell wall disruption may occur under these conditions.

Converti *et al.*, (2009) carried out an investigation to determine which lipid extraction technique produced the most promising results using *N. oculata*. Classic lipid extraction methods using petroleum ether as a solvent for 4 hours produced a 7.2% lipid recovery from the biomass, Soxhlet extraction produced 8.2% while the Folch method employed a mixture of chloroform:methanol (2:1) for 1.5 hours achieving a 9% lipid recovery. The UAE Folch method produced a lipid recovery of 24.3% and was therefore used as the choice extraction method for all further studies. An ultrasonic treatment was applied to the Folch method by Krienitz and Wirth (2006). This involved transferring samples of *Nannochloropsis limnetica* to a tube containing 5 mL of chloroform:methanol (2:1) and samples were sonicated for 90 minutes in a 40 kHz bath. Converti *et al.*, employed the use of a 30 kHz Hielscher UP100H unit and sonicated for 6 hours instead of 90 minutes.

Results indicate the positive impact ultrasound had on lipid extraction. An increase in lipid extraction by 15.3% on a tough cell walled species like *N. oculata* is a very positive result because not all microalgal species are as hardy as *N. oculata*. Limitations of this technique include the length of the sonication time, as 6 hours would simply not be viable on an industrial scale as the energy cost entering this system would not be sustainable. Additionally operation of ultrasonic equipment for that length of time would require vast amounts of energy and the production price would be high, this would question if the method is carbon neutral. Calorimetry was

not carried out on the equipment which means that the energy required to cause cellular damage and bring about an increase in lipid recovery was not known.

Araujo *et al.*, (2011) investigated the oil content of 10 microalgal species including *N. oculata* and *Dunaliella sp.* using a combination of the Bligh and Dyer method and ultrasound. Microalgal samples were mixed with a chloroform:methanol solvent (2:1) in a 40 kHz ultrasonic bath (40 USC) for 20 minutes. The power entering this system was measured to be 80 W and the temperature maintained at 25°C. After sonication the chloroform layer was removed and evaporated and the remaining oils were measured gravimetrically. Of the ten microalgal species tested the amount of oil recovery in some cases, for example *Chaetoceros gracilis* was as high as 60% of the microalgal dry weight. The amount of lipids recovered was determined as 23% for *N. oculata* and 30.12% for *Dunaliella sp.*

Koberg *et al.*, (2011) attempted to use ultrasound to disrupt the cell wall of *N. oculata* and develop a direct transesterification technique from any TAG released. Although this project is not concerned with improving transesterification this method of ultrasonically disrupting *N. oculata* is of great interest. Koberg *et al.*, employed dried *N. oculata* which was added to a mixture of chloroform:methanol (2:1). The sample was then sonicated using a 20 kHz probe (Sonics and Materials, VC-600) for 5 minutes at 40% amplitude. After sonication the chloroform layer was removed and evaporated and the remaining oil was measured gravimetrically. Results showed that when the Bligh and Dyer method was used alone for lipid extraction the amount of lipids removed were less than 10% of the dry biomass. However when the ultrasound assisted method was employed the amount of lipids extracted from the dry biomass increased to 20%. Calorimetry was not carried out and so the power

entering the ultrasonic system is unknown, meaning that the energy input required to cause cellular damage and bring about an increase in lipid recovery was not known.

Lee *et al.*, (2010) compared a number of methods to extract microalgal lipids including a UAE method on *Botryococcus sp.*, *Chlorella vulgaris* (*C. vulgaris*) and *Scenedesmus sp.* This involved blending 0.5g of dry microalgal biomass with 100 mL distilled water and sonicating with a 10 kHz sonicator (Sonics and Materials) for 5 minutes. Lipids were extracted in a mixture of chloroform:methanol (1:1) and shaken in a separating funnel for 5 minutes. The lipid layer was removed and evaporated using a rotary evaporator and the weight of the remaining oil measured. Results obtained differed for each species; of *Botryococcus sp.* and *C. vulgaris* both resulted roughly a 1% increase in the amount of lipids recovered when ultrasound was applied and compared to solvent extraction alone. Whereas *Scenedesmus sp.* saw a 7% increase in the amount of lipids recovered. Calorimetry was not carried out which mean the power entering the system was not determined and the energy required to cause cellular damage and bring about an increase in lipid recovery was not known. Also measurements to control temperature were not documented. Hence, the slight increase in lipid extraction may be due to increased temperatures as well as ultrasound.

Neto *et al.* (2013) employed ultrasound to extract lipids from *C. minutissima*, *Thalassiosira. fluviatilis* and *T. pseudonana*. They employed 20 mL hexane and an ultrasonic bath for 20 minutes (intensity and power not stated by authors) to extract lipids from 100mg of dry microalgal biomass. The method resulted in 15.5% lipid recovery from *C. minutissima*, 40.3% from *T. fluviatilis* and 39.5% from *T. pseudonana*. The authors did not state lipid recovery values for when sonication was not employed, the effect that ultrasound has on lipid recovery from these species is

therefore not known. Other methods have shown that chloroform: methanol (various ratios) is a stronger solvent than hexane in terms of lipid recovery, employing UAE with these solvents instead may further increase lipid recovery yields.

It has also been reported that an ultrasound assisted Bligh and Dyer extraction method developed by Araujo *et al.* (2013) was able to achieve a 52% lipid recovery from the dry biomass of *Chlorella Sp.*, with a treatment time of 60 minutes compared with only 1.8 - 16% recovery from a range of other extraction techniques. This method employed a 40 kHz bath set at an intensity of 2.68 W/cm². Although this result is positive a 60 minute treatment time may not be a sustainable option for commercial scale lipid recovery. This data highlights the need for further investigation into UAE lipid methods with differing ultrasonic systems and treatment times to develop a method which obtains similar recovery rates but with shorter treatment times. Perhaps investigating lower frequencies (such as 20 kHz) that are known to produce more shear forces and a more aggressive reaction chamber would obtain similar recovery rates in a shorter treatment time.

A summary table of the UAE methods discussed in this section is highlighted in table 5.1.

Table 5.1: Summary table of ultrasound assisted extractions

Microalgal Species	Frequency (kHz)	Power & Intensity	Solvent Extraction Method	Lipid yield without ultrasound	Lipid yield with ultrasound	Reference
<i>Scenedesmus sp.</i>	20 (20% amplitude)	500 W	Chloroform:methanol (3:1) Hexane	2% N/A	6% 1%	Ranjan <i>et al.</i> (2010)
<i>N. oculata</i>	30	Not stated	Chloroform:methanol (2:1)	9%	24.3%	Converti <i>et al.</i> (2009)
<i>Chaetoceros gracilis</i> <i>N. oculata</i> <i>Dunaliella sp.</i> <i>Chaetoceros mulleri</i> <i>Chlorella Sp.</i> <i>Isochrysis sp.</i> <i>Tetraselmis sp.</i> <i>Tetraselmis chui</i> <i>Tetraselmis tetrathele</i> <i>Thalassiosira weissflogii</i>	40	80 W	Chloroform:methanol (2:1)	Not stated	60% 23% 30.12% 25.25% 52.49% 21.25% 8% 23.5% 30.25% 13.21%	Araujo <i>et al.</i> (2011)
<i>N. oculata</i>	20 (40% amplitude)	Not stated	Chloroform:methanol (2:1)	10%	20%	Koberg <i>et al.</i> (2011)
<i>Botryococcus sp.</i> <i>C. vulgaris</i> <i>Scenedesmus sp.</i>	10	Not stated	Chloroform:methanol (1:1)	8% 5% 1%	9% 6% 8%	Lee <i>et al.</i> (2010)
<i>Chlorella sp.</i> <i>Nostoc sp.</i> <i>Tolypothrix sp.</i>	50	Not stated	Chloroform:methanol (2:1)	0.08g 0.075g 0.03g	0.2g 0.18g 0.145g	Prabakaren <i>et al.</i> (2011)
<i>Chlorella Sp.</i>	40	2.68 W/m ²	Bligh and Dyer (1959) Chen <i>et al.</i> (1981) Folch <i>et al.</i> (1957) Hara & Radin (1978)	1.8% - Soxlet (1879) extraction	52.5% 10.9% 16.1% 2.2%	Araujo <i>et al.</i> (2013)

5.8.1 Ultrasound assisted extraction (UAE) of oils from macroalgae and other oleaginous crop

Cravotto *et al.*, (2008) developed a UAE method to extract oils from milled seaweed (SW), macroalgae and milled pure soybean germ (SG). Firstly, lipids were extracted from the two species using hexane in a separating funnel and by soxhlet extraction using hexane. The amount of lipid extracted from SW was 2% - dry biomass for the separating funnel method and 4.8% for the soxhlet extraction which took 4 hours. For SG, the separating funnel extracted a lipid content of 3.5% of the dry weight and the soxhlet extraction removed 8.6%, but this method took 8 hours.

Cravotto *et al.* employed a number of ultrasonic devices which were developed and produced in-house. The first was a 25 kHz immersion horn, which sonicated the sample for 1 hour in 50 mL hexane. The power entering this system was 80 W and the temperature maintained at 45°C. This technique recovered a lipid content of 18.7% for SW and 12.2% for SG. A second immersion horn employed was set at 40 kHz and the sample was sonicated for 1 hour in 50 mL hexane. The power entering this system was 80 W in 50 mL and the temperature maintained at 45°C. This method recovered a lipid content of 13.6% for SW and 8.9% for SG. A 300 kHz cup horn sonicated the sample in 40 mL of hexane for 1 hour. The power entering this system was 70 W and the temperature maintained at 45°C. This method recovered a lipid content of 12% for SW and 6.4% for SG. A 19 kHz cavitating tube sonicated the sample in 50 mL of hexane for 1 hour. The power entering this system was 80 W and the temperature maintained at 45°C. This method recovered a lipid yield of 24.7% for SW and 17.7% for SG.

The method that produced the most promising results was a combination of the 19 kHz cavitating tube (65 W) and a 25 kHz immersion horn (60 W). This dual frequency system sonicated the sample in 50 mL of hexane for 30 minutes and the temperature maintained at 45°C. This method recovered a lipid content of 25.9% for SW and 17.9% for SG. This method clearly increased the amount of lipids recovered in less time and with less energy entering the system. However other literature (for example Araujo *et al.* 2011) has demonstrated that when various ratios of chloroform:methanol are employed as the extraction solvent instead of hexane higher lipid recovery rates are usually achieved. This suggests that the soxhlet may not be suitable to be employed in UAE methods.

Kamari *et al.*, (2011) developed a UAE method to extract lipids from macroalgae and compared them with the traditional Folch and Bligh and Dyer methods using three test species: *U. fascianto*, *G. corticata* and *S. tenerrimum*. Kamari *et al.*, also developed an ultrasound assisted Bligh and Dyer and Folch method and compared the total amount of lipids extracted to conventional methods. In the UAE Bligh and Dyer method samples were first treated using the original Bligh and Dyer method. However, prior to centrifugation samples were sonicated in an ice bath for 2 minutes using a cup-horn sonicator (Branson, 2010). Results showed an increase of between 2 - 5% in the amount of lipids recovered for all three species when compared with the original method. The UAE Folch extraction method employed the Folch method, except prior to centrifugation samples were sonicated in an ice bath for 2 minutes using a cup-horn sonicator (Branson, 2010). Results show a decrease of between 1 and 7% for all three species when compared with conventional methods.

Data gathered by Kamari *et al.*, (2011) indicated that it would be favourable to further develop an ultrasound assisted Bligh and Dyer extraction method. However, reproducibility of results obtained is questionable as authors did not state the ultrasonic frequency employed or the power entering the ultrasonic system.

Lou *et al.*, (2010) developed a UAE method to extract oils from the chickpea plant. This involved mixing 1g of crushed chickpea powder with 8.5 mL of hexane:isopropanol (3:1) in a 50 mL beaker. The sample was immersed in a 40kHz ultrasonic cleaning bath (DL-360B, Shanghai Zhixin Instruments Co. Ltd.) and sonicated for 90 minutes at 50°C. The ultrasonic power entering this system was 230 W. After extraction the solvent was evaporated using a rotary evaporator and the remaining oil quantified. Results indicated that the amount of lipids extracted from the dry weight peaked at 80% after 30 minutes. This result was 35% higher than the amount of lipids extracted using the same method but without ultrasound.

Lou *et al.*, (2010) also developed a dynamic UAE system, which involved the exact set-up as previously described except the sample was placed in an extraction chamber and then immersed in an ultrasonic bath. The extraction solvent was pumped through the reaction chamber at a rate of 5 mL/min. This method produced a 2.06% higher lipid recovery than the static system and this was achieved in 20 minutes, 10 minutes faster than the static method.

5.8.2 Optimised ultrasonic extraction of microalgal oils

Although previous studies have indicated that treatment with ultrasound has a positive effect on the extraction of microalgal lipids compared to conventional methods, all developed methods require further optimisation. For example ultrasound may not produce complete cell disruption of *N. oculata* due to the rigid/hardy cell walls. To overcome this, ultrasound could be applied in conjunction with another physical method as described below.

Previous attempts have been made to combine ultrasound with other physical stresses to extract lipids from microalgae. An example of this was carried out by Pernet and Tremblay, (2003) where authors attempted to develop a technique which combined ultrasound with grinding to extract lipids from *Chaetoceros gracilis* (*C. gracilis*). This involved adding 15 µl of *C. gracilis* to 1.5 mL dichloromethane:methanol (2:1) and sonicating in an ultrasonic bath (HT50, VWR, Nepean) for 10 minutes at 5°C. The power entering this system was 50 W. After 10 minutes the sample was ground using a 7 mL Tenbroeck tissue grinder and the lipid layer of the sample was removed, evaporated and the lipid quantities determined using TLC. Results showed that the TAG quantities were significantly less when ultrasound and grinding were applied in conjunction than when employed alone. This indicates that further work needs to be carried out in the field of combined ultrasonic extraction. Employing physical techniques in unison with ultrasound may produce more promising results if different combination methods were tested.

Beating beads may offer a solution to this problem. Tang *et al.*, (2010) employed bead beating as part of a lipid extraction method. Concentrated microalgal biomass was mixed with glass beating beads in a vortex for 10 minutes. The physical stress was sufficient to disrupt the microalgae *D. tertiolecta*, which has no cell walls.

Lee *et al.*, (2010) investigated the efficiency of beating beads and several other extraction methods on three microalgal species: *Botryococcus sp.*, *C. vulgaris* and *Scenedesmus sp.* This method involved exposing microalgal cultures to 0.1 mm beating beads (Biospec Products Inc.) in a bead beater at a speed of 2800 RPM for 5 minutes. After this exposure time the Bligh and Dyer extraction method was used to separate lipids from the cellular material. The chloroform:methanol (1:1) solvent was evaporated using a rotary evaporator, the remaining oil weighed and the lipid content determined as a percentage of dry weight. Results indicated that bead beating induced a positive effect on lipid extraction for all three species. *Botryococcus sp.* resulted in lipid extraction increasing from 8 to 28%, *C. vulgaris* from 5 to 10% and *Scenedesmus sp.* from 2 to 11% using the Bligh and Dyer method and employing beating beads. Results indicate that bead beating can greatly increase lipid recovery.

Information gathered by Lee *et al.*, (2010) may prove vital for the optimisation of a UAE method. Employing spherical beads that are 150 - 350 µm in size with ultrasound will result in extreme conditions in the ultrasonic chamber, causing the beads to bounce. The beating beads are potentially 150 x the size of *C. vulgaris*. This method combines the shear forces of ultrasonic application with the collision based disruption of bead beating increasing the likelihood of cell disruption occurring.

5.9 Conclusions

A review of literature has shown there is great potential for employing ultrasound to extract microalgal lipids; with frequencies of 20 and 40 kHz shown to be the most promising. The uses of dual frequency and dynamic systems have also demonstrated improvements in lipid extraction rates when compared to conventional extraction techniques. The use of UAE methods in combination with the Bligh and Dyer method may also produce more promising results. For tough/hardy cell walled microalgae species the use of a secondary physical stress such as beating beads may provide further optimisation of lipid extraction rates.

6. Methods

6.1 Culture of microalgal species

N. oculata, *D. salina* and *C. concordia* were cultured in F/2 growth media in a growth room (Watford Refrigeration and Air Conditioning Ltd) (Figure 6.1) at a constant temperature of 20°C using a photo period of 12 hours light and 12 hours dark and at light intensities of 100% (70 $\mu\text{mol}/\text{m}^2\text{s}$). *Chlorella* Sp. was grown in the same conditions except the growth media employed was Bolds Basal Medium with 3 fold Nitrogen and vitamins (BBM + 3NV). Cultures were monitored every 3 days by haemocytometer (HAE) and optical density (OD) using a UV-Visible spectrophotometer to determine growth rates.

Figure 6.1 Microalgal growth room



6.1.1 Media preparation

6.1.1.1 F/2 media preparation

Natural sea water (NSW, Taymix Ltd) was pre-filtered through filter paper (Whatman No. 5, diameter 9 mm) and then through membrane filters (Osmotics Inc. 0.45 µm) using a Buchner funnel connected to a vacuum pump. Following filtration NSW was autoclaved at 121°C for 15 minutes. F/2 media components were then added to the sterile NSW as described in Table 6.1. Table 6.1 shows the composition for the preparation of 1L F/2 medium. pH of the medium was adjusted to 8.0 using 1M NaOH if too acidic or 1M HCl if too alkaline.

Table 6.1 Preparation of F/2 medium

Component	Stock solution	Quantity
NaNO ₃	75 g/L dH ₂ O	1 mL/L NSW
NaH ₂ PO ₄ H ₂ O	5 g/L dH ₂ O	1 mL/L NSW
Trace metal solution	See Table 6.2	1 mL/L NSW
Vitamin solution	See Table 6.3	1 mL/L NSW

Table 6.2 Preparation of trace metal solution

Component	Quantity
FeCl ₃ 6H ₂ O	3.15 g/L dH ₂ O
Na ₂ EDTA 2H ₂ O	4.36 g/L dH ₂ O
CuSO ₄ 5H ₂ O	0.01 g/L dH ₂ O
ZnSO ₄ 7H ₂ O	0.022 g/L dH ₂ O
CoCl ₂ 6H ₂ O	0.01 g/L dH ₂ O
MnCl ₂ 4H ₂ O	0.18 g/L dH ₂ O
Na ₂ MoO ₄ 2H ₂ O	0.006 g/L dH ₂ O

Table 6.3 Preparation of vitamin solution

This item has been removed due to third party copyright. The unabridged version of the thesis can be viewed at the Lanchester Library, Coventry University.

Tables 6.1-3 shows the components required to make up F/2 media recipe from Guillard and Ryther (1962).

6.1.1.2 Bolds Basal Medium with 3 fold nitrogen and vitamins preparation

A trace element solution was first prepared by adding the contents of Table 6.4 to 1000 mL of distilled water. This was then autoclaved at 15 Psi for 15 minutes. The next step was to prepare the vitamin B₁ stock solution, in which 0.12 g of Thiaminhydrochloride was added to 100 mL of distilled water. This was then filtered. The vitamin B₁₂ solution was prepared next by adding 0.1 g of cyanocobalamin to 100 mL of distilled water. 1 mL of this was added to 99 mL of distilled water to make the stock solution and filter sterilized. The instruction for the preparation of this media is taken from the Culture Collection of Algae and Protozoa website (<http://www.ccap.org>).

Table 6.4 Preparation of trace element solution

Component	Quantity
Na ₂ EDTA	0.75 g
FeCl ₃ 6H ₂ O	97 mg
MnCl ₂ .4H ₂ O	41 mg
ZnCl ₂	5 mg
CoCl ₂ 6H ₂ O	2 mg
Na ₂ MoO ₄ 2H ₂ O	4 mg

To prepare 1 L of BBM + 3NV the contents of Table 6.5 were added to 1 L of distilled water. This was then autoclaved at 15 psi for 15 minutes.

Table 6.5 Preparation of BBM+3NV

Component	Stock solution	Quantity
NaNO ₃	25 g/L dH ₂ O	30 mL/L dH ₂ O
CaCl ₂ 2H ₂ O	2.5 g/L dH ₂ O	10 mL/L dH ₂ O
MgSO ₄ 7H ₂ O	2.5 g/L dH ₂ O	10 mL/L dH ₂ O
K ₂ HPO ₄ 3H ₂ O	2.5 g/L dH ₂ O	10 mL/L dH ₂ O
KH ₂ PO ₄	2.5 g/L dH ₂ O	10 mL/L dH ₂ O
NaCl	2.5 g/L dH ₂ O	10 mL/L dH ₂ O
Trace element solution	See Table 6.4	6 mL/L dH ₂ O
Vitamin B ₁ solution	See section 6.1.1.2	1 mL/L dH ₂ O
Vitamin B ₁₂ solution	See section 6.1.1.2	1 mL/L dH ₂ O

6.1.2 Culture preparation

Microalgal cultures were prepared in a ratio of 1:4 microalgae: media. Master cultures and working cultures were prepared. Master cultures were used as a feedstock for all other cultures and were prepared in 600 mL tissue culture flasks (Nunc). Working cultures were primarily used for experiments and prepared in 10 and 20 L clear polypropylene carboys (Nalgene). Carboys were constantly aerated with air using air pumps (KOAIR KA65) operated at 65 l/min and a pressure of 0.04 MPA. Air flow was filtered using a 0.2 µm VentFilter Unit Millex-FG 50 (Millipore Co. USA).

6.1.3 Haemocytometer counts

Haemocytometer counts were employed to determine the number of cells within a microalgal population, both during growth and ultrasonic treatment. 10 µL of microalgal sample was transferred to a haemocytometer slide, covered with a cover slip and observed under a microscope using a 10X objective (*N. oculata* and *Chlorella Sp.* were observed using a 20X objective). Due to differences in cell size a different method was employed for each microalgal species.

To enumerate the number of *D. salina* and *C. concordia* microalgae cells, 8 of the 16 corner squares were counted. This was carried out in triplicate and the average taken. This figure was then divided by 8 to determine the number of cells in one square and the following equation employed to determine the number of cells/mL:

$$x \times 1.6 \times 10^5 = \text{Cells/mL}$$

To enumerate the number of *N. oculata* and *Chlorella Sp.* cells, 10 of the 25 central cells were counted. This was done in triplicate and the average taken. This figure was then divided by 10 and the following equation employed to determine

the number of cells/mL:

$$x \times 4 \times 10^6 = \text{Cells/mL}$$

6.1.4 Optical density (OD) measurements

Optical density measurements give an estimation of a microalgal population by measuring the amount of light absorbed by a microalgal suspension. Higher absorbance indicates a higher microalgal population. It is notable that cellular debris can cause considerable interference in optical density measurements, therefore it is not potentially the best method for analysis of cellular disruption and data from Haemocytometer (Section 6.1.3) and Spectro-fluorophotometer (Section 6.3.1) analysis should be relied upon. 1 mL of natural sea water was transferred to a plastic cuvette and placed in the reference cell of a UV-Visible spectrophotometer (UV-1700, Shimadzu) set to analyse 686 nm to measure chlorophyll A. The value for sea water was set to zero. 1mL of the microalgae sample was transferred to a plastic cuvette and placed in the active cell of the UV-Visible spectrophotometer for analysis.

6.1.5 Microalgal stressing methods

Each microalgal species was grown in their preferred media for 14 days; for *N. oculata*, *D. salina* and *C. concordia* this was F/2 media and for *Chlorella Sp.*, Bolds Basal Medium with triple nitrate and vitamins (3NBBM + V media). Samples were cultured in a growth room set to 20°C, 100% light intensity with a photoperiod of 12 hours light and 12 hours dark.

After 14 days 40 mL samples of each culture was transferred to 160 mL of media with the following variables applied; high salinity, nitrogen deprivation, and reduced trace metals. These variables are designed to induce lipid production and storage. Details of these variables and their concentrations for each species are listed in Table 6.6. Samples were grown in 200 mL conical flasks under the conditions outlined above for 14 days. Lipid content was monitored regularly by employing Nile Red staining and fluorescence analysis using a Spectro-photometer (RF-5301PC, Shimadzu).

Table 6.6 List of variables for the induction of lipids for each microalgal species

Condition	Species and variables			
	<i>N. oculata</i>	<i>D. salina</i>	<i>C. concordia</i>	<i>Chlorella Sp.</i>
Salinity Media + NaCl (g/L⁻¹)	+ 30 + 35	+ 30 + 35	+ 30 + 35	+ 30 + 35
Nitrogen Conc Media – N	- 25% -50%	- 25% -50%	- 25% -50%	- 25% -50%
Trace Metal solution (mL/L) Media – Trace metal solution	- 75% - 50%	- 75% - 50%	- 75% - 50%	- 75% - 50%

6.2 Ultrasonic treatment methods

After their required growth period (section 6.1) cultures of *D. salina*, *C. concordia*, *Chlorella Sp.* and *N. oculata* were subjected to ultrasonic treatment to assess the effect on the breakdown of cells and the subsequent release of lipids. Low and high density samples were assessed. Low density samples were taken straight from culture, but high density samples required concentration (section 6.2.1). The ultrasonic equipment employed in this work included a 20 kHz probe (with and without beads for *N. oculata*), 40 kHz bath, Dual Frequency Reactor (DFR) operating at 16 and 20 kHz and Hielscher Unit (20 kHz). All ultrasonic equipment was allowed to warm up for 30 minutes prior to use. After this time calorimetry was undertaken, this determines the initial rise in temperature due to sonication. This technique is used to determine the actual power entering each ultrasonic system and respective intensities and power densities.

6.2.1 Preparation of high density microalgal samples

High density microalgal samples were prepared using a centrifuge (Model number 5702, Eppendorf). Samples were centrifuged for 4 minutes at 1426 x G for *D. salina* and *C. concordia* and 1725 xG for *N. oculata* and *Chlorella Sp.* After centrifugation the majority of the supernatant was discarded (~90%). The remaining supernatant and pellet was mixed using a vortex for 30 seconds and transferred to a 1L flask. This process was repeated until the required volume was achieved.

6.2.2 Microalgal dry weight determination

10 mL microalgal sample was transferred to a pre-weighed 50 mL paper weighing bowl. The sample was dried in an oven set to 40°C for 48 hours and reweighed to determine the dry weight of 1 litre of each of the microalgal species.

6.2.3 Calorimetry of ultrasonic equipment

Calorimetry was carried out on the 20 kHz probe and 40 kHz bath to determine the power, intensity and density. Due to the construction, the reaction chambers of the DFR and the Hielscher unit were not easily accessible by a thermocouple. A power monitor plug (Make: Wilkinson's Model: H01569) was used to calculate the power and intensity instead

6.2.3.1 Calorimetry of 20 kHz probe

A 300mL beaker was filled with 200mL of Reverse Osmosis (RO) water. A probe was inserted into the beaker a third below the surface. A temperature probe was also inserted into the water at the same depth. The probe was set to 40% amplitude and the water was sonicated for three minutes. The temperature probe was used to record any change in the temperature at the following time intervals: 0, 5, 10, 15, 20, 25, 30, 40, 50, 60, 90, 120, 150 and 180 seconds. After the three minutes sonication the water was replaced with fresh of RO water. This process was carried out in triplicate and the probe was allowed to cool for 30 minutes in between each run.

6.2.3.2 Calorimetry of 40 kHz bath

A 300mL beaker was filled with 200mL RO water. A beaker was suspended in the sonication bath so that the water within the beaker was at a similar level to the water in the ultrasonic bath. A temperature probe was inserted into the water in the beaker and the water sample was sonicated for three minutes. The temperature probe was used to record any changes in temperature at the following time intervals: 0, 5, 10, 15, 20, 25, 30, 40, 50, 60, 90, 120, 150 and 180 seconds. After three minutes sonication the water was replaced with fresh RO water. This process was carried out in triplicate.

6.2.3.3 Determination of the ultrasonic power and intensity of the DFR and Hielscher unit

A Wilkinson's H01569 power monitor plug designed to monitor mains power used during operation of equipment was used to determine the power consumed by the DFR and Hielscher unit. The ultrasonic system was plugged into the mains via the power monitor. When the system was in operation its power would be displayed on the power monitor screen.

6.2.3.4 Calculation of ultrasonic power and intensity

The change in temperature over time was plotted on graphs for each run using each sonication device. The gradients of the graphs were then used to calculate the initial rate of change in temperature over time (dT/dt). The mass (M) of the RO water was 200 g (from 200 mL) in both cases and the heat capacity (C_P) was 4.1813. This information was then used to calculate the power (Watts) of the system using the following equation:

$$\text{Power} = (dT/dt)C_P M$$

Once the power was known it was then possible to calculate the intensity (W/cm^2) of the probe using the following equation:

$$\text{Power/Area} = \text{Intensity } (W/cm^2)$$

For the 20 kHz probe the area of the tip of the probe was measured and for the 40 kHz bath the area of the base of the beaker was measured as the area into which the sound energy was transferred from the sonicated water in the bath. Once the intensity is known it is then possible to calculate the power density (W/cm^3) using the following equation:

$$\text{Power density} = \text{Intensity/Volume}$$

6.2.4 20 kHz VCX 600 Probe (Sonics & Materials) treatment method (batch system)

A 20 kHz VCX 600 Probe (Sonics & Materials, Figure 6.2a) was set to 40% amplitude. Prior to treatment calorimetry was employed to determine the power and intensity of the ultrasonic system. For ultrasonic treatment, 200 mL of the microalgal suspension was sonicated for 16 minutes in a 300 mL beaker. The temperature was maintained below 30°C using an ice bath. See Figure 6.2b for a schematic diagram of the experimental set up. 10 mL samples were taken at intervals of 0, 1, 2, 4, 8 and 16 minutes sonication and transferred to 50 mL centrifuge tubes for further analysis.

This system was also employed with a variety of beating beads. 200 mL of sample was sonicated in a 250 mL glass round bottomed flask with either: 4.7g of glass beads (425 x 600 nm) purchased from Sigma (G-9143) or 1g of Guyson Turbobeats (S070 or S110), which were spherical shaped carbon steel beads. The S070 beads were sized between 180 - 350µM and the S110 bead were sized between 300 - 500µM. Both sampling times and volumes remained the same for each test with beads.

Figure 6.2a 20 kHz VCX 600 Probe (Sonics and Materials)



Figure 6.2b 20 kHz VCX 600 Probe set up diagram

This item has been removed due to third party copyright. The unabridged version of the thesis can be viewed at the Lanchester Library, Coventry University.

Figure 6.2a shows a 20 kHz VCX 600 Probe and 6.2b illustrates the experimental set up for the 20 kHz probe during microalgal treatment (Mason, 1999).

6.2.5 40 kHz 475TT Bath (Langford ultrasonics) treatment method (batch system)

A 40 kHz 475TT bath (Langford ultrasonics, Figure 6.3a) was used at a fixed frequency. Prior to treatment calorimetry was employed to determine the power, intensity and density of the ultrasonic system. For ultrasonic treatment, 200 mL microalgal sample was sonicated for 16 minutes in a 300 mL beaker. Temperature was maintained below 30°C by adding ice to the bath; see Figure 6.3b for the experimental set up for the 40 kHz bath. 10 mL aliquots were taken at intervals of 0, 1, 2, 4, 8 and 16 minutes sonication and transferred to 50 mL centrifuge tubes for further analysis.

Figure 6.3a 40 kHz 475TT bath (Langford ultrasonics)



Figure 6.3b 40 kHz bath experimental set up

This item has been removed due to third party copyright. The unabridged version of the thesis can be viewed at the Lanchester Library, Coventry University.

Figure 6.3a shows a 40 kHz Langford Ultrasonics 475TT bath and 6.3b illustrates the experimental set up for the 40 kHz bath during the microalgal treatment (Mason, 1999).

6.2.6 Dual Frequency Reactor (DFR - Advanced Sonics Processing Systems) treatment method (batch system)

A Dual Frequency Reactor (DFR - Advanced Sonics Processing Systems, USA), shown in Figure 6.4, consisted of two ultrasonic plates, both of which operated at different frequencies, 16 and 20 kHz respectively, set to a power setting of 50% amplitude. Ultrasonic treatment employed a volume of 1.1 L microalgal suspension sonicated for 16 minutes in the reaction chamber. Temperature was maintained below 30°C using the in-built water cooling system. 10 mL aliquots were taken at intervals of 0, 1, 2, 4, 8 and 16 minutes sonication and transferred to a 50 mL centrifuge tube for further analysis.

Figure 6.4 Dual Frequency Reactor (DFR - Advanced Sonics Processing Systems)



Figure 6.4 illustrates the Advanced Sonics Processing Systems Dual Frequency Reactor (DFR) used in the microalgal treatment.

6.2.7 Modified Dual Frequency Reactor (DFR - Advanced Sonics Processing Systems) treatment method (dynamic flow system)

Toward the end of this project the DFR system was returned to its manufacturers for modification to provide greater intensity. In the modified DFR (see figure 6.5) the space in between the two internal ultrasonic plates was reduced creating a more intense reaction chamber, this reduced the volume of the reaction chamber from 1.1L to 100 mL.

N. oculata was the only microalgal species tested using the modified DFR system. 800 mL samples of high density stressed *N. oculata* were subjected to the DFR flow system (50% amplitude, flow rate 0.5 L/minute) for 3 passes (triplicate). Samples were taken for analysis after each pass. A second test involved the investigation of the potential for further optimisation by passing the microalgae and S070 beads through the system to see if a further disruptive effect was observed.

Figure 6.5 Modified Dual Frequency Reactor (DFR - Advanced Sonics Processing Systems)

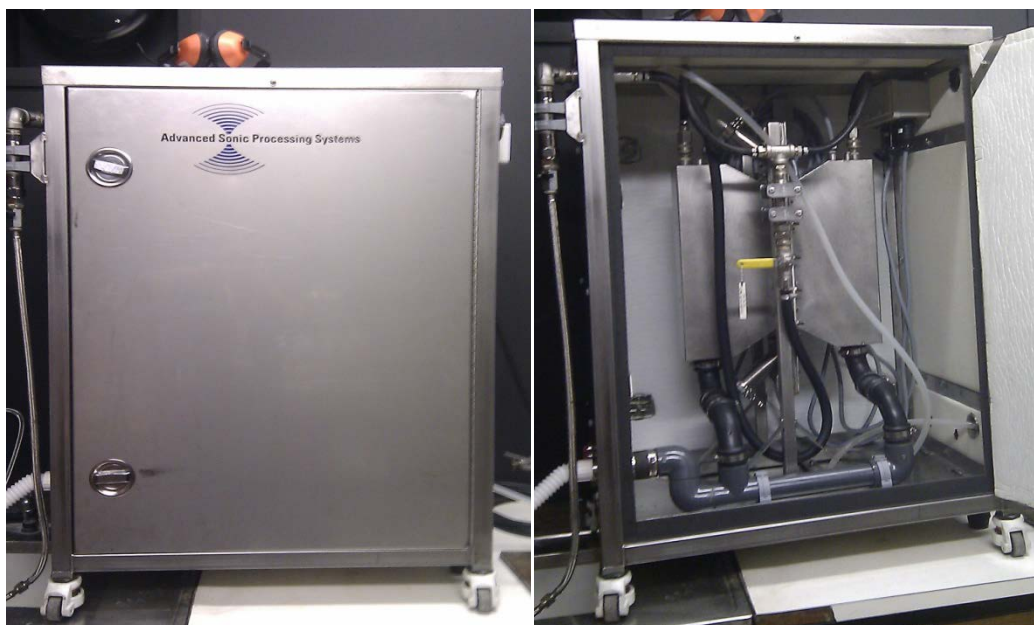


Figure 6.5 illustrates the Advanced Sonics Processing Systems modified Dual Frequency Reactor (DFR) used in this study.

6.2.8 Hielscher UIP100HD unit treatment method (dynamic flow system)

A Hielscher UIP100HD dynamic system was employed at a flow rate set to 0.925 L/min. Ultrasonic treatment employed a volume of 1.1 L microalgal suspension sonicated for 16 minutes. Figure 6.5 illustrates the experimental set up of the Hielscher unit. Temperature was maintained below 30°C using in-built water cooling system. 10 mL aliquots were taken at intervals of 0, 1, 2, 4, 8 and 16 minutes sonication and transferred to 50 mL centrifuge tubes for further analysis. It is important to note that since this is a dynamic (flow) system, the sample was not subjected to constant sonication. The total residence time in the ultrasonic reaction chamber was only 1.5 minutes over the 16 minutes circulating treatment.

Figure 6.6 Hielscher UIP100HD unit

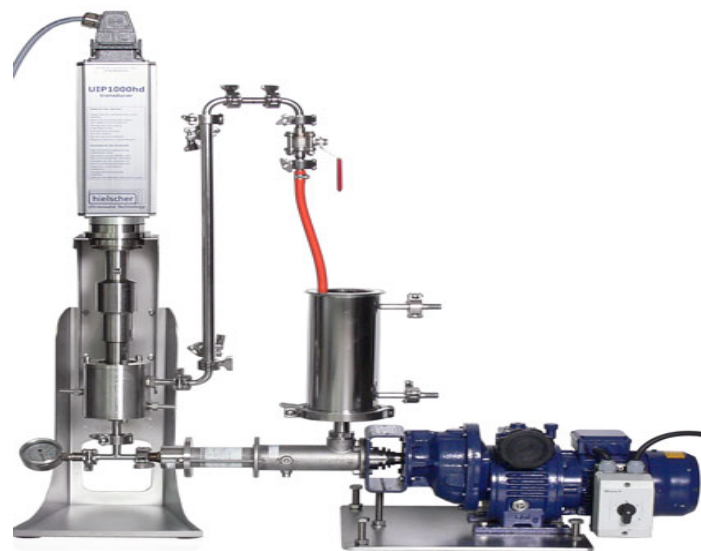


Figure 6.2.7 illustrates the Hielscher UIP100HD dynamic flow system used in the microalgal treatments.

6.3 Microalgal analysis methods

Following sonication, all samples were tested using the following methods; haemocytometer counts (section 6.1.3), optical density readings (section 6.1.4), Spectro-fluorophotometer, chlorophyll and carotenoid determination and fluorescent and confocal microscopy. These methods were employed to determine the concentration and condition of the microalgal cultures before and after sonication. Lipid analysis and determination was carried out on the samples using Thin Layer Chromatography (TLC), Nile Red Lipid analysis, Gravimetric measurement and GC-MS.

For all haemocytometer, OD, spectro-fluorophotometer and Nile Red lipid analysis data the Analysis of Variance (ANOVA) statistical test was employed. The ANOVA test was employed for these data sets because it is used to determine whether the means of several groups are equal, so it is suitable to determine if there is any difference between the means of samples taken at several time intervals. For all chlorophyll and carotenoid determinations, TLC, GC-MS and gravimetric lipid determination data a paired t test was employed. This test was employed as it directly determines if there is any difference between 2 sets of means, therefore it is suitable to determine if there was any difference between samples taken before and after ultrasonic treatment. Microsoft Excel was employed for all statistical analysis.

6.3.1 Spectro-fluorophotometer

1 mL sample of natural sea water was transferred to a glass cuvette and placed in the reference cell of the Spectro-fluorophotometer (RF-5301PC, Shimadzu) as a reference sample. 1mL of sonicated microalgae sample was transferred to a glass cuvette and placed in the sample cell of the Spectro-fluorophotometer for analysis. The Spectro-fluorophotometer was set to scan at an excitation wavelength of 465 nm along with a start and stop wavelength of 475 and 850 nm under PC control to record results.

6.3.2 Nile Red analysis

Nile Red is a fluorescent marker commonly used to detect intracellular lipids (Cooksey *et al.* 1987)

6.3.2.1 Nile Red staining

A stock solution of Nile Red (Sigma) was prepared in acetone at a volume of 250 $\mu\text{g/mL}^1$. This was added to samples so that the final Nile Red concentration was 0.04% (v:v). Samples were agitated in a vortex mixer for 30 seconds and then immediately transferred to an incubator set to 37°C and agitated at 100 RPM for 10 minutes (Thermo Scientific Max Q 8000). Analysis was carried out by fluorescent microscopy or Spectro-fluorophotometer.

6.3.2.2 Fluorescence microscopy

Fluorescence microscopy employed a Nikon DS-L2 camera control unit and microscope. This consisted of a DS-Fi1 camera head (Nikon) and HB-10101AF Super High Pressure Mercury lamp (Nikon). Fluorescence was detected using a 450-490 nm excitation filter. Under these conditions microalgal cells appeared red and internal lipids fluoresced in a yellow colour (Cooksey *et al.*, 1987).

6.3.2.3 Spectro-fluorophotometer

1 mL of natural sea water was transferred to a glass cuvette and placed in the cell of the Spectro-fluorophotometer (RF-5301PC, Shimadzu) as a reference sample. The Spectro-fluorophotometer was set to scan with an excitation wavelength of 525 nm along with a start and stop wavelength of 550 and 850 nm under PC control. 1mL of a Nile Red stained sonicated microalgae sample was transferred to a glass cuvette and placed in the cell of the spectro-fluorophotometer for analysis and the lipid peak was observed at ~560 nm. Nile Red analysis was employed to determine the time interval in which the Nile Red lipid peak was at its highest for each species when treated with each ultrasonic system. This information will determine when cell membranes and walls have been ruptured allowing increased entry of the Nile Red stain. This time interval will be employed as the sonication time for ultrasound assisted lipid extraction.

6.3.3 Extraction and gravimetric determination of lipid content

Two ultrasound assisted extraction methods were developed; an adapted Bligh and Dyer method (an adapted version of the method employed by Zimmerman *et al.*, 2011) using chloroform:methanol (1:2) as the extraction solvent and an ultrasound assisted hexane extraction.

The adapted Bligh and Dyer method is as follows. 10 g of dried biomass was transferred to 200 mL of chloroform:methanol (1:2). The sample was then sonicated using the 20 kHz probe (40% amplitude) for the amount of time indicated for that species by the Nile Red method (see 6.3.2.1). Immediately after this the sample was centrifuged at 802 x G. The supernatant was immediately transferred to a fresh pre-weighed large centrifuge tube and centrifuged (Rotina 420 Hettich Zentrifugen) again for 2 minutes at 802 x G. Samples were then immediately transferred to a fresh pre-weighed large centrifuge tube treated with 133 mL of chloroform:1% NaCl water (1:1), after separation the chloroform phase was removed and transferred to a fresh pre-weighed centrifuge tube. The centrifuge tube was then placed in a fume cupboard with an open top and allowed to dry. When dry the centrifuge tubes were re-weighed and the lipid weight was calculated and expressed as a percentage of microalgal biomass. This method was carried out in triplicate. The ultrasound assisted hexane extraction was identical to the previous method other than the choice of solvent.

6.3.4 Thin Layer Chromatography (TLC)

TLC plates consisted of silica gel on TLC aluminium foils with a fluorescence indicator at 254 nm, silica gel matrix; (L x W, 5 x 10 cm) from Sigma (60762). 5 µL of microalgal extract (dry lipid extract re-suspended in 1 mL hexane) were transferred to the TLC plate. Plates were placed in a 10% ethylacetate/hexane chamber for 5 minutes and then allowed to dry in a fume hood for 5 minutes. After this, plates were dipped in phosphomolybdic acid (20% solution in ethanol, Sigma catalogue number 319279) and heated in oven set to 110°C for 5 minutes. TAG bands were identified using 5 µl of glyceryl trilinoleate (T9517) as a standard. Semi-quantitative analysis was carried out using the ImageJ software to determine the intensity of TAG bands.

6.3.5 Transesterification of microalgal TAG

Lipid samples were converted to FAMES by firstly adding 1 mL of 1% NaOH in methanol to each gravimetric sample. These were then heated for 15 minutes at 55°C using a water bath. Following this period 2 mL of 5% methanolic HCL was added and samples were again heated for 15 minutes at 55°C using a water bath. This was followed by the addition of 1 mL of H₂O. FAMES were then extracted twice using 0.75 mL of hexane and the organic phases were then transferred to vials for GC/MS analysis.

6.3.6 Analysis of microalgal FAMES by GC-MS

A QP2010 gas chromatography mass spectrometer (GC-2010 with a GC-MS QP-2010) equipped with a AOC-5000 autosampler (Shimadzu, Japan) using a SHIM-5MS column (30 mm x 0.25 mm x 0.25 μ m) were employed for GC-MS analysis of FAME samples. The carrier gas employed was helium (99.9% purity) with a pre-column pressure of 49.7 kPa and a column flow rate set to 1 mL/min. The temperature program of the column was as follows; 40°C for 3 minutes, after which a 5°C/min increase until 250°C, this temperature was maintained for 38 minutes. The injection volume was 0.1 μ L, the injection temperature was 240°C, and the split ratio was 1:30. The ion source temperature and the interface temperature was set to 240°C. FAME peaks were identified and quantified by comparisons with the retention times of FAMES standards (Palmitic acid = P-0750, Linoleic acid = 62230-5ML-F, Sigma). These standards were chosen as they are commonly found in many microalgae (Demirbas and Demirbas, 2011).

6.3.7 Microscopy

6.3.7.1 Preparation of samples for microscopy

Microalgal samples in natural sea water were mixed thoroughly using a vortex. 10 μ L of each sample was transferred to a microscope slide, covered with a slip and sealed using clear nail polish.

6.3.7.2 Confocal microscopy

Images were acquired using Leica (UV-Vis-IR-M27) confocal microscope and a 63x 1.20W oil objective lens with aperture. The signal was captured using a laser

excitation at 543nm and 100% intensity. Auto-fluorescence was captured at a wavelength of 690 nm.

6.3.8 Chlorophyll A and carotenoid estimation

This method is adapted from a study carried out by Sukenik *et al.* (1989). 5 mL of microalgal sample was transferred to a 50 mL centrifuge tube and centrifuged at 802 x G for 5 minutes using an Eppendorf 5702 centrifuge. After 5 minutes the supernatant was discarded and 2 mL of RO water was added to the pellet and mixed thoroughly using a vortex. The sample was centrifuged again at 802 x G for 3 minutes. The supernatant was discarded and replaced by 9 mL of methanol and mixed thoroughly using a vortex. A further 1 mL of RO water was added and the sample was mixed again. The sample was centrifuged at 802 x G for 3 minutes. After this time if the pellet was still green, the sample required further centrifugation with 9 mL methanol and 1 mL water until the pellet was colourless. The supernatant was then analysed using a UV-Visible spectrophotometer (UV-1700, Shimadzu) reading at 480 and 663 nm. The following equation was used to determine the amount of Chlorophyll A (mg/L) in the sample:

$$\text{Chlorophyll A (mg/L)} = 13.5 \times \text{OD 663} \times 10/\text{sample volume}$$

(Sukenik *et al.*, 1989)

The following equation was used to determine the amount of total carotenoids in the sample:

$$\text{Total carotenoids (mg/L)} = 4.4 \times \text{OD 480} \times 10/\text{sample volume}$$

(Sukenik *et al.*, 1989)

6.4 Effect of sonication on the growth of microalgal species

The following methods involved treating each microalgal species with the 20 kHz probe (40% amplitude) for different time periods depending on the species (60 minutes for *N. oculata*, 8 minutes for *D. salina* and 16 minutes for *C. concordia*). Due to time constraints this was not carried out on *Chlorella Sp.* Samples were again taken at different time periods depending on the species (0, 15, 30, 45 and 60 minutes for *N. oculata*, 0, 1, 2, 4 and 8 minutes for *D. salina* and 0, 2, 4, 8 and 16 minutes for *C. concordia*). Samples were treated in different ways to explore the various effects that sonication may have on growth. Samples were analysed by haemocytometer counts (see 6.1.3) and OD measurements (see 6.1.4) on days 1, 3, 5, 10, 15, 20, 25, 30 and every 10 days thereafter.

6.4.1 Effect of sonication on the growth of microalgal species

200 mL of microalgae was sonicated in triplicate using the 20 kHz probe (40% amplitude) and 20 mL samples were taken at the allotted time periods (See Section 6.4). These samples were then allowed to grow under normal conditions for >100 days.

6.4.2 Effect of sonication on the growth of resuspended microalgal cultures

200 mL of microalgae was sonicated in triplicate using the 20 kHz probe (40% amplitude) and 20 mL samples were taken at the allotted time periods (See Section 6.4). These samples were then transferred to 80 mL of F/2 media and allowed to grow under normal conditions for >100 days.

6.4.3 Effect of sonicated microalgae on the growth of an established microalgal culture

200 mL of microalgae was sonicated in triplicate using the 20 kHz probe (40% amplitude) and 20 mL samples were taken at the allotted time periods (See Section 6.4). These samples were then transferred into 80 mL of an established culture of the same species and allowed to grow under normal conditions for >100 days.

6.4.4 Effect of the supernatant of sonicated microalgae on the growth of an established microalgal culture (1:4 ratio)

200 mL of microalgae was sonicated in triplicate using the 20 kHz probe (40% amplitude) and 30 mL samples were taken at the allotted time periods (See Section 6.4). These samples were centrifuged at 802 x G for 10 minutes and 20 mL of its supernatant was then transferred into 80 mL of an established culture of the same species and allowed to grow under normal conditions for >100 days.

6.4.5 Effect of the supernatant of sonicated microalgae on the growth of an established algal culture (4:1 ratio)

200 mL of microalgae was sonicated in triplicate using the 20 kHz probe (40% amplitude) and 100 mL samples were taken at the allotted time periods (See Section 6.4). These samples were centrifuged at 802 x G for 10 minutes and 80 mL of its supernatant was then transferred to 20 mL of an established culture of the same species and allowed to grow under normal conditions for >100 days.

7.0 Results and Discussion

7.1 Growth of microalgal cultures

D. salina, *N. oculata* and *C. concordia* cultures were grown using f/2 growth media, and *Chlorella Sp.* cultures in 3N-BBM + V media. All cultures were grown in 20L carboys in a growth room (Watford Refrigeration and Air Conditioning Ltd.) at a constant temperature of 20°C using a photo period of 12 hours light and 12 hours dark and at light intensities 100% (70 $\mu\text{mol}/\text{m}^2\text{s}$). All microalgal cultures were monitored during growth by haemocytometer and optical density readings and allowed to grow for 15 days.

7.2 Calorimetry of ultrasonic equipment

Calorimetry was carried out on each ultrasonic device before it was used each day. The next section will describe how the calorimetry of the 20 kHz probe set to 40% amplitude was carried out. For calorimetry of all other ultrasonic devices employed please consult Appendix 1.

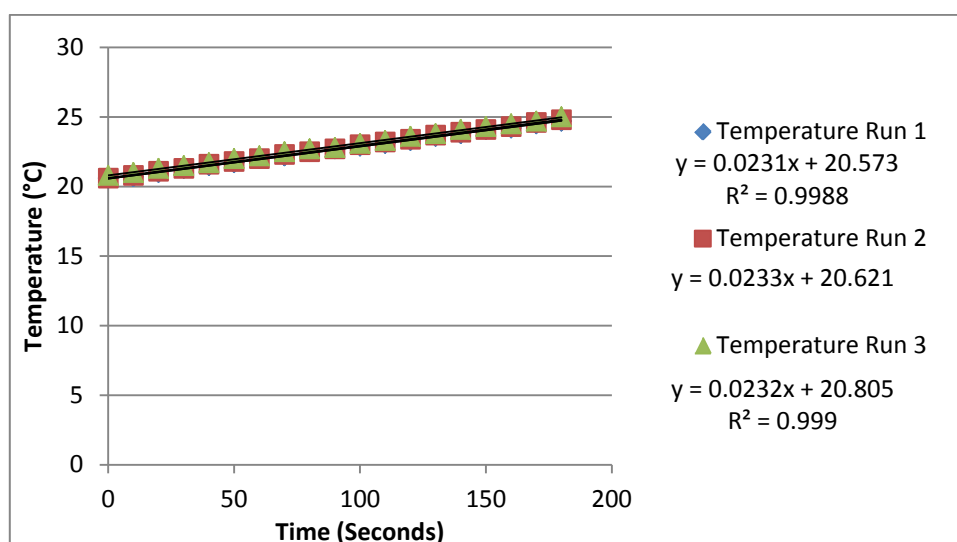
Table 7.1 shows the change in temperature over three minutes using a 20 kHz probe set to 40% amplitude applied to a media of RO water.

Table 7.1 Change in temperature over three minutes for the use of the 20 kHz probe set at 40% amplitude

Time (Seconds)	Temperature (°C)		
	Run 1	Run 2	Run 3
0	20.6	20.6	20.8
10	20.7	20.8	21
20	21	21.1	21.3
30	21.3	21.3	21.5
40	21.5	21.6	21.7
50	21.7	21.8	22
60	22	22	22.2
70	22.2	22.3	22.5
80	22.5	22.5	22.7
90	22.7	22.7	22.8
100	22.9	23	23.1
110	23.1	23.2	23.3
120	23.3	23.4	23.6
130	23.6	23.7	23.8
140	23.8	23.9	24.1
150	24.1	24.1	24.3
160	24.2	24.3	24.5
170	24.5	24.6	24.7
180	24.7	24.8	25

Figure 7.2.1 shows the information from Table 7.1 expressed in a temperature against time graph to obtain the gradient.

Figure 7.2.1 Temperature (°C) versus Time for 20 kHz probe set at 40% amplitude



From the information in Figure 7.2.1 it is possible to calculate both the power and intensity of the 20 kHz probe set at 40% amplitude. The gradient for each run is shown below:

$$\text{Run 1} = 0.0231$$

$$\text{Run 2} = 0.0233$$

$$\text{Run 3} = 0.0232$$

The liquid medium was RO water, mass was 200ml and its heat capacity was 4.1813J/ (g-K). Using this information it is possible to calculate the power for each run using the following equation:

$$\text{Power} = (dT/dt)C_pM$$

Therefore for:

$$\text{Run 1: Power} = 0.0231 \times 4.1813 \times 200 = 19.3 \text{ Watts}$$

$$\text{Run 2: Power} = 0.0233 \times 4.1813 \times 200 = 19.5 \text{ Watts}$$

$$\text{Run 3: Power} = 0.0232 \times 4.1813 \times 200 = 19.4 \text{ Watts}$$

Therefore the average power reading would be:

$$\frac{19.3 + 19.5 + 19.4}{3} = 19.4 \text{ Watts}$$

Knowing that the area of the probe was 1.13 cm^2 , it is now possible to calculate the intensity of the probe using the following formula:

$$\text{Intensity} = \text{Power/Area}$$

$$\text{Intensity} = 19.4/1.13$$

$$\text{Intensity} = 17.2 \text{ Watts/cm}^2$$

The power generated by the 20 kHz probe set at 40% amplitude is 19.4 Watts, and its intensity is 17.2 Watts/cm^2 .

Knowing that the intensity of the probe was 17.2 Watts/cm^2 it is now possible to calculate the power density of the 20 kHz probe using the following formula:

$$\text{Power density} = \text{Power/Volume}$$

$$\text{Power density} = 19.4/200$$

$$\text{Power density} = 0.097 \text{ Watts/cm}^3$$

A summary of the calorimetry results for all ultrasonic equipment employed is shown in Table 7.2.

Table 7.2 Summary of power measurements for each ultrasonic system employed

Ultrasonic system	Power (Watts)	Power intensity (W/cm²)	Power density (W/cm³)
20 kHz probe 40% amplitude 200 mL	19.4	17.2	0.097
40 kHz bath 200 mL	13.9	0.34	0.07
DFR 50% amplitude 1.1 L*	600	1	0.545
DFR 50% amplitude 100 mL*	600	1	6
Hielscher unit 200 mL*	137	20.448	0.685

* = measured using power monitor (Wilkinson's H01569)

The above table displays the ultrasonic power (Watts), intensity (Watts/cm²) and density (Watts/cm³) values determined by calorimetry for each ultrasonic system employed. Power values for the DFR and Hielscher unit were determined using a power monitor (Make: Wilkinson's, Model: H01569) as carrying out calorimetry was not practical due to it being extremely difficult to insert a thermocouple into their reaction chambers. It is important to note that the power measurements obtained from calorimetry and those from the power monitor cannot be directly compared. This is because the power measurements obtained from the power monitor are for the operation of the entire equipment, calorimetry determines the power within the ultrasonic system.

7.3 Effect of ultrasound on *D. salina*

Cultures of *D. salina* (200 mL) were sonicated in triplicate for 16 minutes using a 20 kHz probe (40% amplitude, 0.097 W/cm^3), 40 kHz bath (0.07 W/cm^3), Dual frequency reactor (0.545 W/cm^3) and the Hielscher unit (0.102 W/cm^3). 10 mL samples were taken at time intervals of 0, 1, 2, 4, 8, and 16 minutes for analysis. This was carried out on both low and high density samples of *D. salina*.

To determine any physiological effects which ultrasound may have on *D. salina*, samples were analysed by the following techniques:

- Haemocytometer counts to determine any changes in the microalgal population as sonication was applied.
- Optical density to detect changes in cell population. This method was found not to be suitable to detect changes in cell population after sonication. Please see page 76 for further details.
- Spectro-fluorophotometer to detect changes in cellular chlorophyll levels. This was only carried out on low density samples as high density samples were too dense/concentrated to obtain reliable readings.
- Carotenoid and chlorophyll recovery to detect cellular chlorophyll and carotenoid levels. This was only carried out on low density samples as high density samples were too dense and concentrated to obtain reliable readings with the Spectro-fluorophotometer.
- Confocal microscopy to visually compare the effects of ultrasound on the cellular morphology of *D. salina*.
- Nile Red staining analysed by spectro-fluorophotometer and the fluorescent microscope to detect changes in intracellular lipids. This was only carried out

on low density samples as high density samples were too dense/ concentrated to obtain reliable readings with the Spectro-fluorophotometer. This determines the time interval in which the Nile Red lipid peak was at its highest for *D. salina* when treated with each ultrasonic system. This information will indicate when cell membranes have been ruptured, allowing increased entry of the Nile Red stain

- Ultrasound assisted lipid extraction through the adapted Bligh and Dyer method and the Hexane extraction method to determine any increase in lipid recovery levels with ultrasound employed in the extraction technique. Results were measured gravimetrically and expressed as lipid percentage of dry weight.

7.3.1 Effect of ultrasound on the cellular population of *D. salina*

Haemocytometer measurements were employed to monitor changes in the cellular population of *D. salina* as ultrasound was applied. Figure 7.3.1 displays the reduction in the cellular population for low density *D. salina* cultures treated with each ultrasonic system.

Figure 7.3.1 Reduction in the cellular population of low density *D. salina* treated with each ultrasonic system at $25^{\circ}\text{C} \pm 0.5^{\circ}\text{C}$

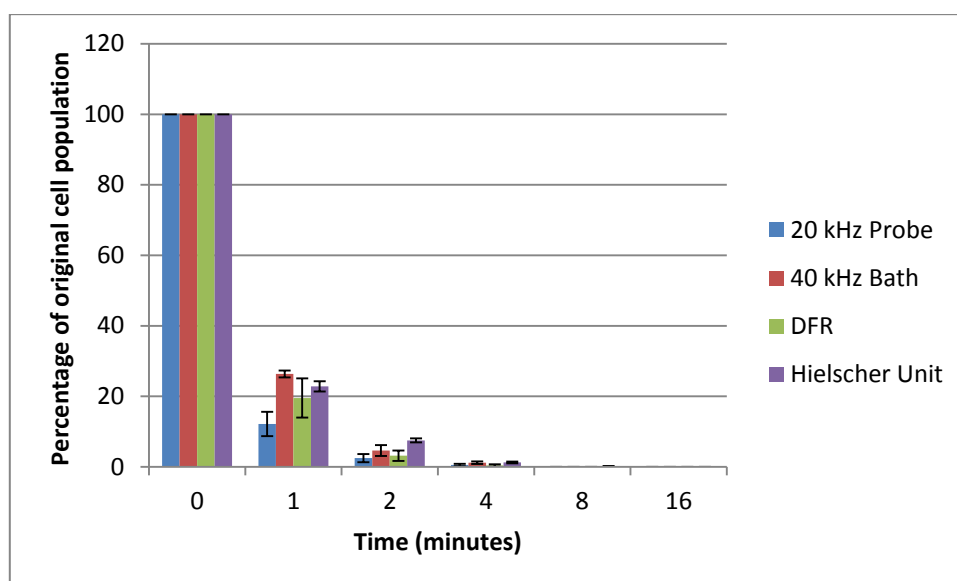
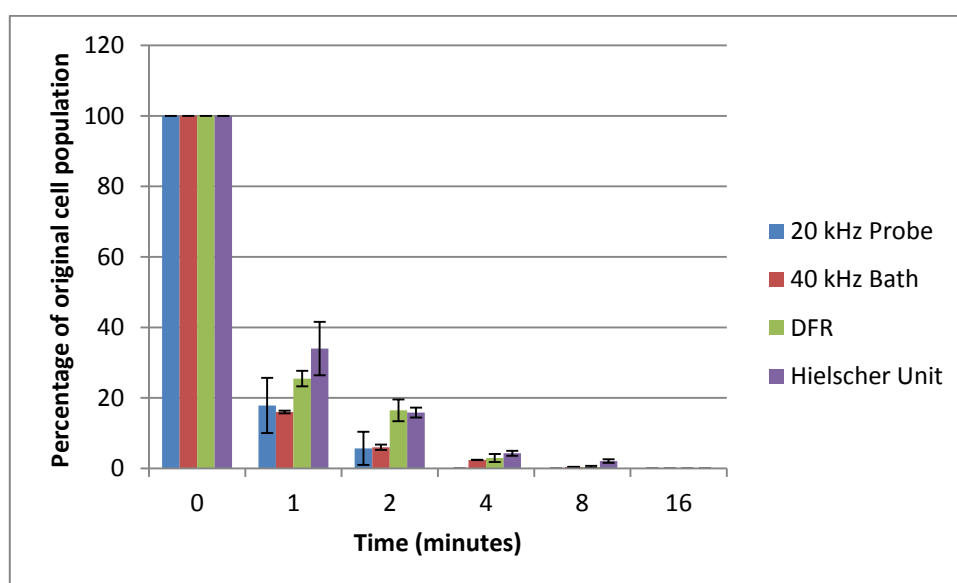


Figure 7.3.1 clearly shows that the 20 kHz probe (40% amplitude, 0.097 W/cm^3) system resulted in a significant reduction ($P = 5.04\text{E}^{-10}$) in the *D. salina* population as ultrasound was applied. After 4 minutes treatment the entire population of *D. salina* was destroyed with the 20 kHz probe. The 40 kHz bath (0.07 W/cm^3) decreased the population of *D. salina* as ultrasound was applied and after 8 minutes treatment the entire population of *D. salina* was destroyed ($P = 9.67\text{E}^{-8}$). Complete cellular destruction was achieved after 4 minutes ($P = 5.06\text{E}^{-8}$) using the DFR system (0.545 W/cm^3 by power monitor) and 8 minutes ($P = 2.12\text{E}^{-10}$) using the Hielscher system

(0.102W/cm³ by power monitor). The starting cell concentration was $\sim 1.6 \times 10^6$ cells/mL.

All ultrasonic systems were also employed on high density cultures of *D. salina* and results are displayed in figure 7.3.2.

Figure 7.3.2 Reduction in the cellular population for high density *D. salina* treated with each ultrasonic system at 25°C \pm 0.5°C

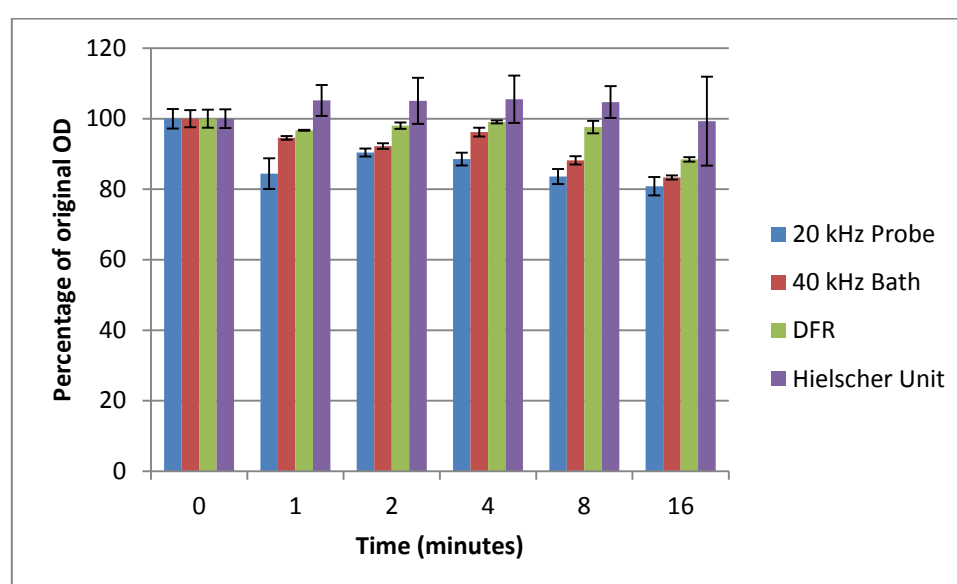


The above figure clearly shows that after 2 minute's sonication with the 20 kHz probe system (40 % amplitude, 0.097 W/cm³) the entire population of high density *D. salina* was significantly reduced ($P = 9.67E^{-8}$). After 8 minutes sonication using the 40 kHz bath system (0.07 W/cm³), DFR (0.545 W/cm³) and Hielscher (0.102 W/cm³) the entire population of high density *D. salina* was reduced. The starting cell concentration was $\sim 1.9 \times 10^7$ cells/mL.

7.3.2 Effect of ultrasound on the optical density of *D. salina*

Optical density measurements at 686 nm were taken to monitor changes in the cellular population. Figure 7.3.3 displays the optical density measurements for low density *D. salina* samples treated with the 20 kHz probe system.

Figure 7.3.3 Reduction in the optical density readings (686 nm) for low density *D. salina* treated with all ultrasonic systems

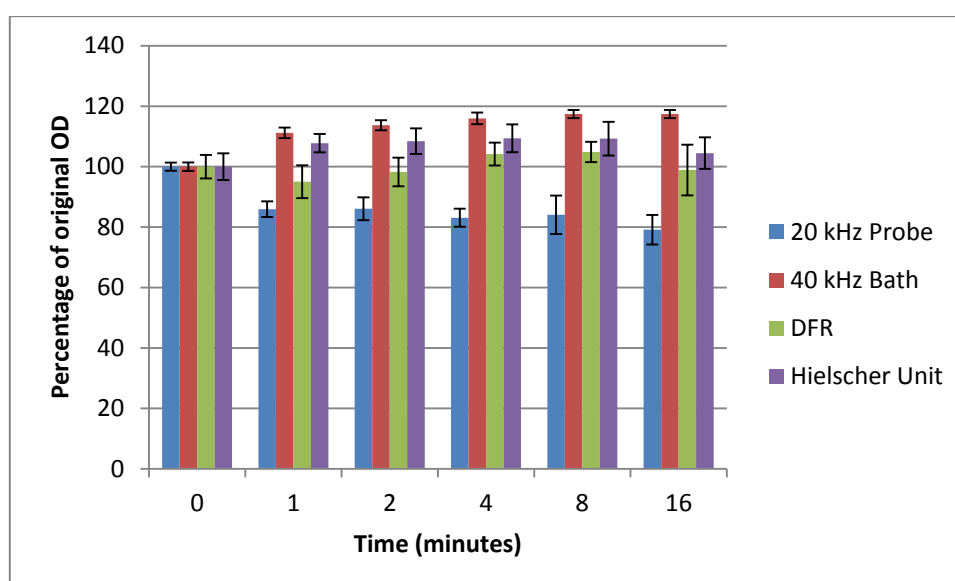


The above figure shows that the 20 kHz probe ($P = 0.028$), 40 kHz bath ($P = 3.6E^{-6}$) and DFR systems ($P = 3.46E^{-7}$) cause the optical density of *D. salina* to significantly decrease as ultrasound was applied. This indicates that cells have been destroyed and chlorophyll released into the surrounding media. The Hielscher system resulted in a small fluctuation and then decrease in the optical density of *D. salina* as ultrasound was applied, despite this haemocytometer data have shown cells to be disrupted. These fluctuations may be due to cellular debris caused by ultrasound interfering with the passage of light through the UV-Visible spectrophotometer and causing anomalous results. Similar fluctuations were reported by Wu (2010) who employed a similar technique to measure the OD of cyanobacteria treated with

ultrasound. It is important to note the OD measurements are not likely to reach 0 as there will always be some form of cellular debris present in the liquid. The starting OD was ~0.53.

All ultrasonic systems were also employed on high density cultures of *D. salina*. OD results are displayed in Figure 7.3.4.

Figure 7.3.4 Reduction in the optical density readings (686 nm) for high density *D. salina* treated with all ultrasonic systems



The above figure shows that the optical density of high density *D. salina* significantly decreases as ultrasound is applied with the 20 kHz probe ($P = 0.04$), this indicates cell disruption. The 40 kHz bath resulted in an increase in the optical density at 686 nm for high density *D. salina* suspensions as ultrasound is applied. Haemocytometer data revealed that cells have been disrupted. However, the increase may be due to the sample being too dense to obtain an accurate measurement. DFR treatments slightly decreased the optical density of high density *D. salina* suspensions as ultrasound is applied indicating cell disruption. When the Hielscher system was employed the optical density of high density *D. salina* increased as ultrasound was

applied. As previously explained these fluctuations are most likely due the cellular debris interfering with the passage of light through the UV-Vis. The starting OD was ~2.42.

7.3.3 Effect of ultrasound on spectro-fluorophotometer measurements of *D. salina*

The spectro-fluorophotometer was employed to detect changes in the level of intracellular chlorophyll as ultrasound was applied. Figure 7.3.5 displays the percentage reduction in the chlorophyll emission peak for low density *D. salina* cultures for each ultrasonic system as sonication was applied.

Figure 7.3.5 Effect of ultrasound on the chlorophyll emission peak of *D. salina*

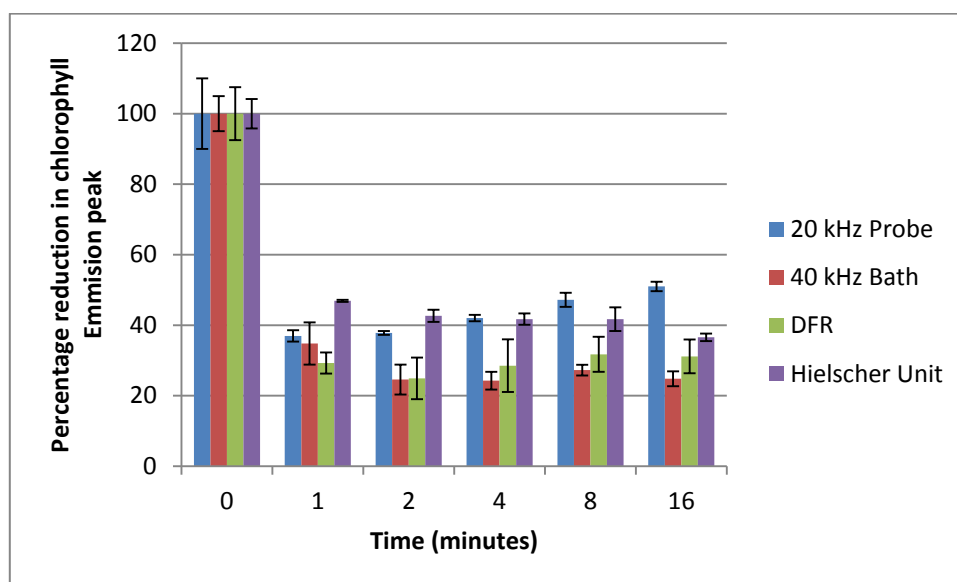


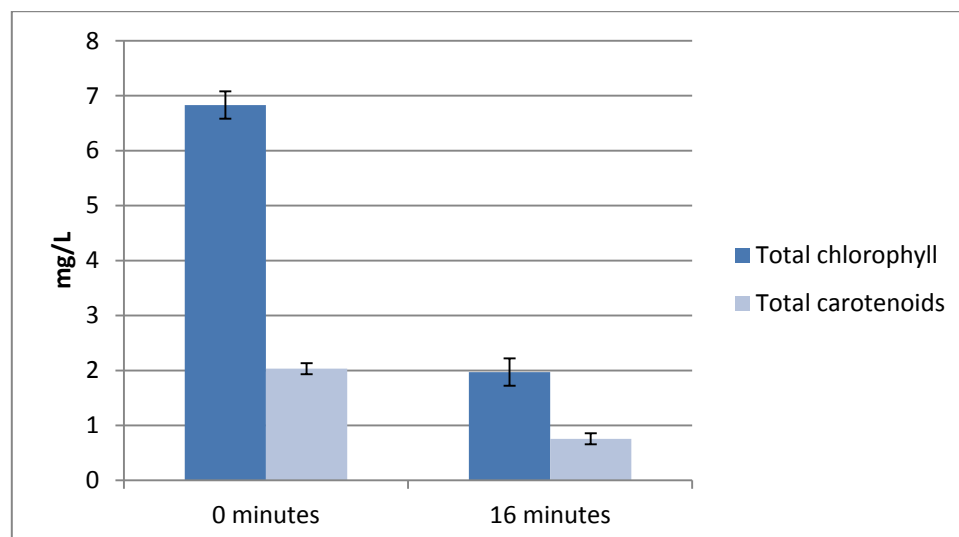
Figure 7.3.5 demonstrates a rapid reduction in the height of the chlorophyll peak as sonication is applied for each ultrasonic system. This indicates that the cells have been ruptured and chlorophyll has been released after 1 minute. The height of the starting emission peak was ~116.5 units.

7.3.4 Effect of ultrasound on chlorophyll a and carotenoid recovery from *D. salina*

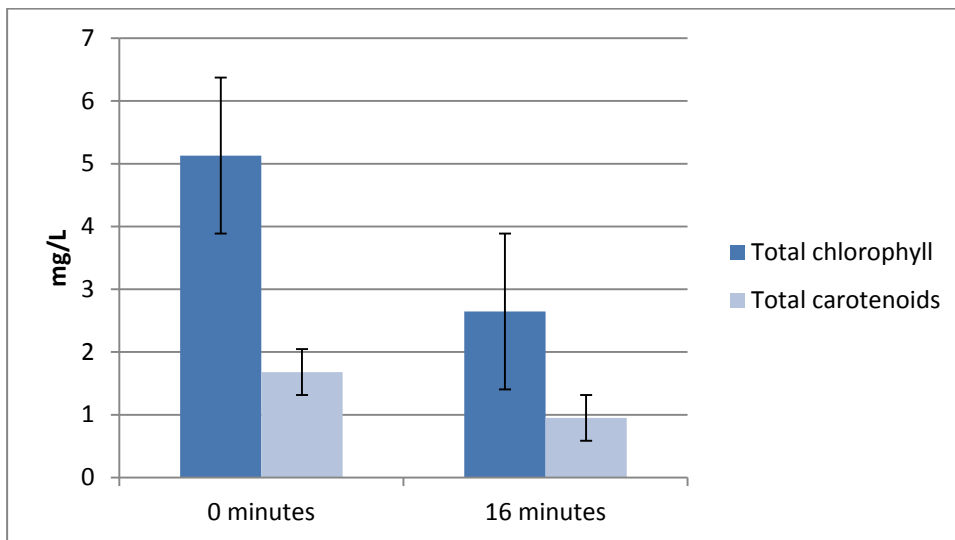
The chlorophyll a and carotenoid recovery procedure was carried out to determine the amount of chlorophyll a and carotenoids extracted with and without ultrasound. Figure 7.3.6 shows the amount of intracellular chlorophyll and carotenoids recovered from an untreated biomass and a biomass treated using each ultrasonic system for 16 minutes. 16 minutes treatment was employed to determine the effect of prolonged sonication on cells.

Figure 7.3.6 Chlorophyll a and carotenoid recovery from low density *D. salina* treated using each ultrasonic system

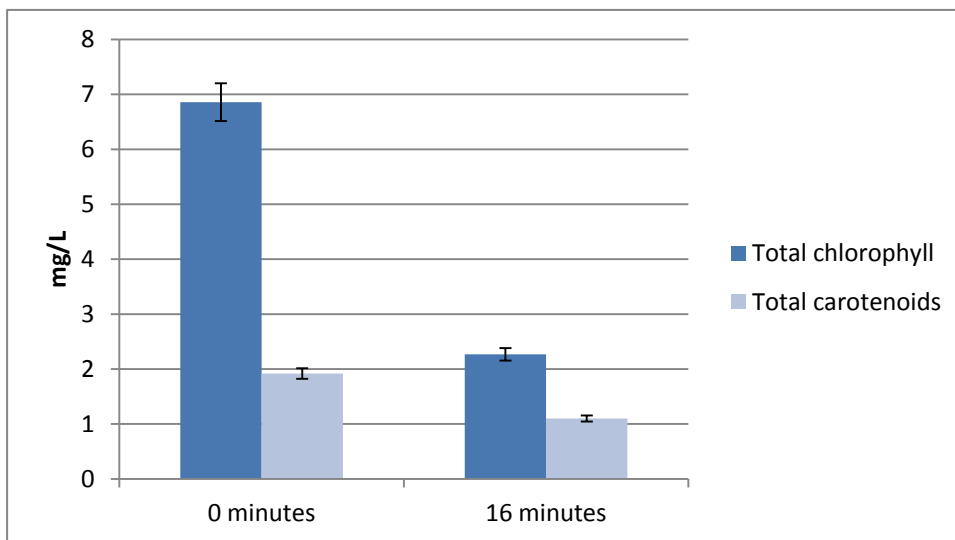
a. 20 kHz probe



b. 40 kHz bath



c. DFR system



d. Hielscher unit

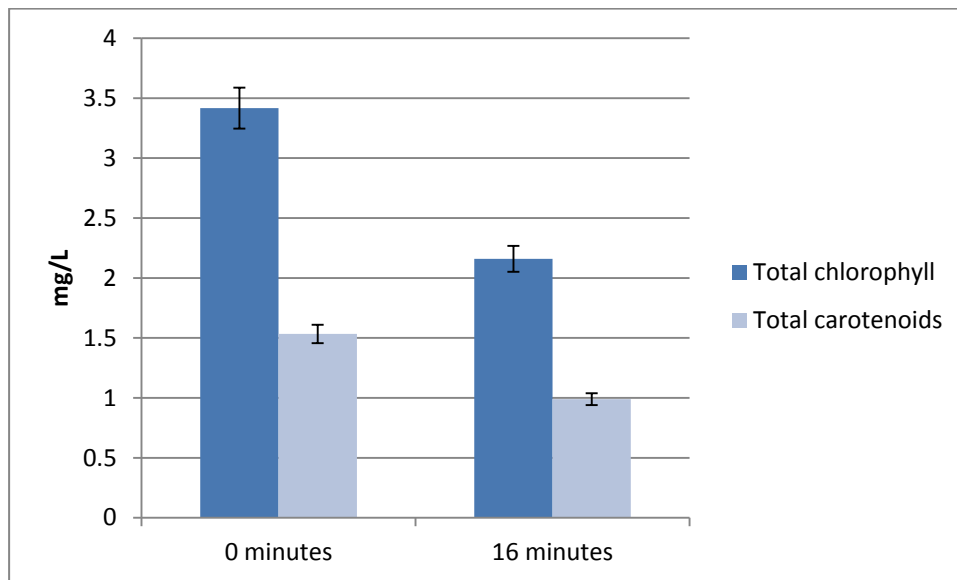
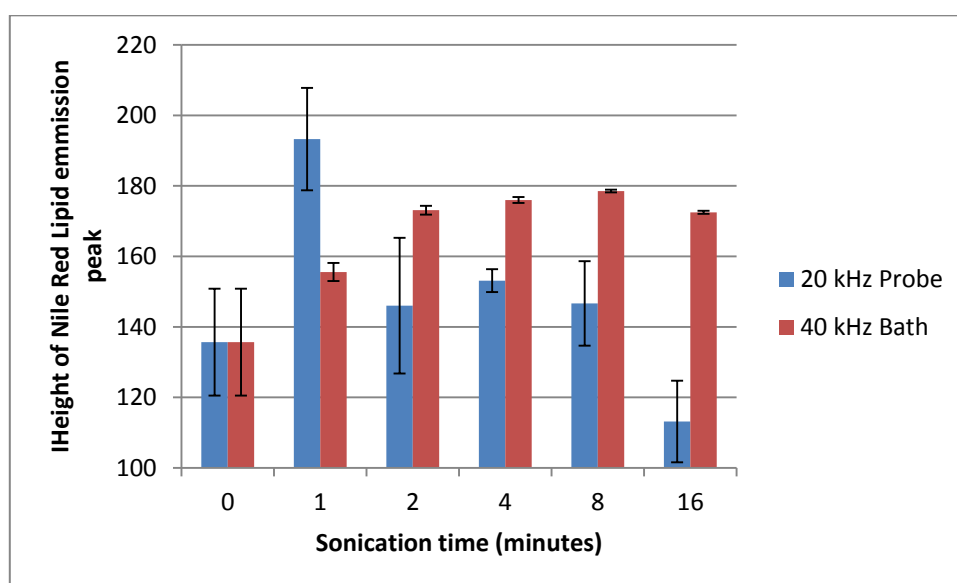


Figure 7.3.6 demonstrates that the amount of intracellular chlorophyll a and carotenoids dramatically decreased as ultrasound is applied. All systems appear to release the same amount of pigment after 16 minutes ultrasonic treatment; however haemocytometer data suggests that each system may have reached this level at different times. This indicates that all of the ultrasonic systems are capable of weakening the cell membrane of *D. salina* resulting in cell leakage.

7.3.5 Effect of ultrasound on the intracellular lipids of *D. salina* measured by Nile Red staining

Nile Red staining measured by spectro-fluorophotometry was employed to determine the amount of intracellular lipids detectable before and during sonication. This method determines the time interval in which the Nile Red lipid peak was at its highest for *D. salina* when treated with each ultrasonic system. This information will determine when cell membranes have been ruptured, allowing increased entry of the Nile Red stain. This time interval will be employed as the sonication time for ultrasound assisted lipid extraction. Figure 7.3.7 displays the increase in the Nile Red lipid peak as ultrasound was applied using each ultrasonic system. The DFR and Hielscher systems were not available for this procedure as they were returned to their manufacturers.

Figure 7.3.7 Lipid peak of low density *D. salina* treated with ultrasound measured by Nile Red staining



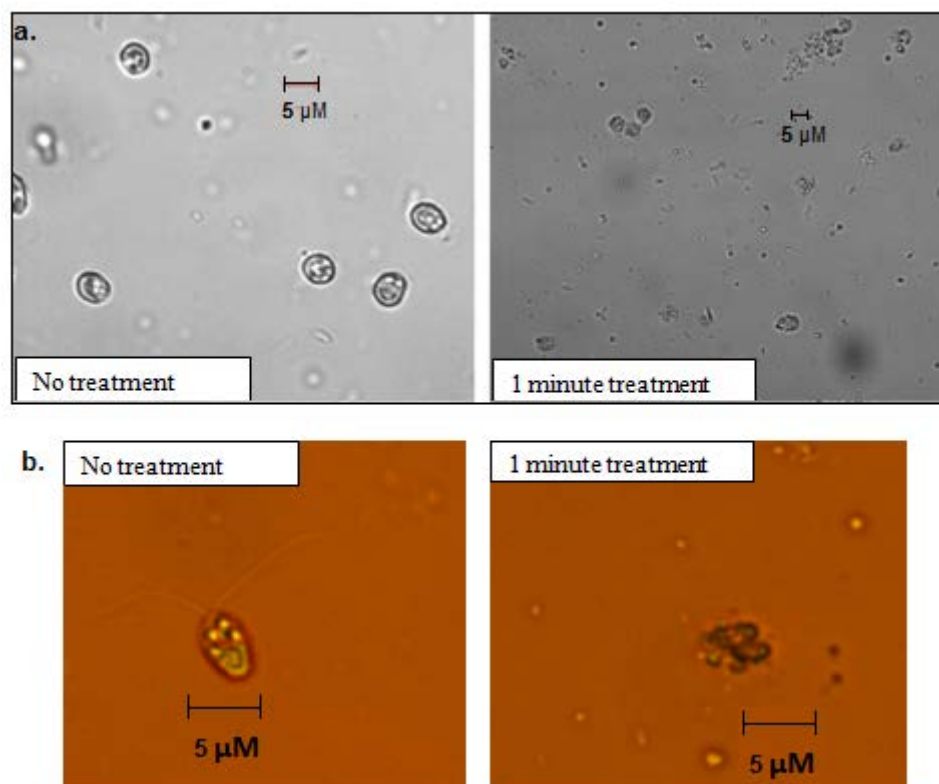
The above figure shows that the lipid peak significantly increases after 1 minute treatment ($P = 0.045$) using the 20 kHz probe (40% Amplitude, 0.097 W/cm^3). This

indicates that the cell membrane has been ruptured allowing increased uptake of Nile Red into the cell. Therefore only 1 minute sonication using the 20 kHz probe is needed to disrupt the cell membranes of *D. salina*. After 1 minute the Nile Red lipid peak decreases which may be due to the lipids being emulsified by sonication possibly making Nile Red unable to bind to them. The 40 kHz bath shows a steady increase in the Nile Red peak as ultrasound is applied; this then reaches a maximum after 8 minutes of treatment and then decreases. The 40 kHz probe is therefore not as efficient as the 20 kHz probe for increasing the membrane permeability of *D. salina*.

7.3.6 Effect of ultrasound on *D. salina* viewed by microscopy

Confocal microscopy (x63 magnification) and fluorescence microscopy (x100 magnification) were employed to observe the physiological condition of *D. salina* cells before and after sonication with the 20 kHz probe (40% Amplitude, 0.097 W/cm³). The physical state of 100 cells on a slide was observed to determine their state before and after ultrasonic treatment. These images are displayed in Figure 7.3.8.

Figure 7.3.8 Microscopy images of low density *D. salina* treated with the 20 kHz probe



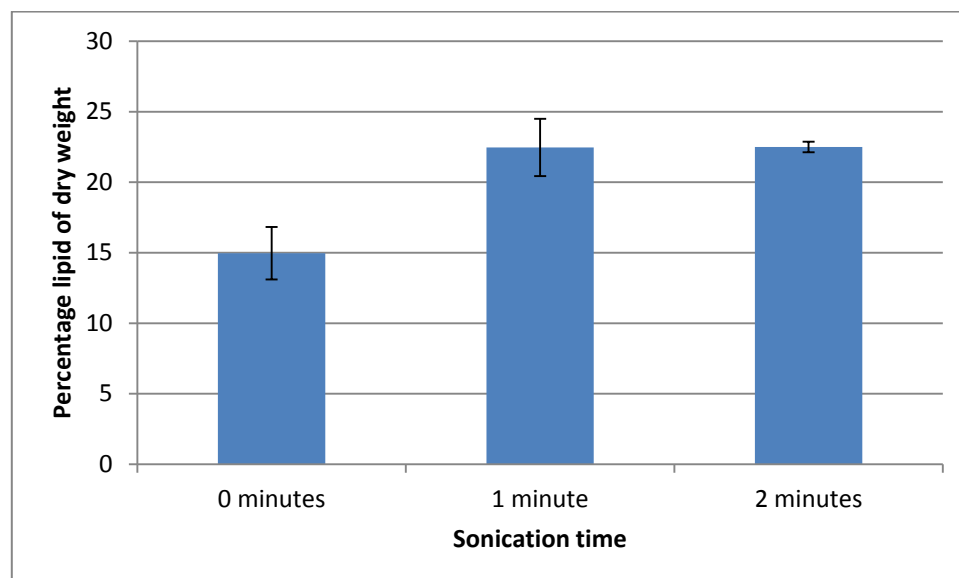
Figures 7.3.8a. (confocal microscope) and 7.3.8b. (fluorescent microscope) demonstrate the destructive power of one minute exposure with the 20 kHz probe (40% amplitude, 0.097 W/cm³) on *D. salina*. Before ultrasonic treatment the images

clearly show that the cells were intact. Before sonication 100% of the cells were intact and 76% were motile. After sonication 90% of the cells were disrupted as shown in Figure 7.3.8 a. and 7.3.8b, additionally none of the cells remained motile. After ultrasonic treatment the images show that the cells were no longer intact.

7.3.7 Effect of the 20 kHz probe (40% Amplitude, 0.097 W/cm³) on the lipid recovery of *D. salina* measured gravimetrically

Nile Red analysis showed that 1 minute treatment with the 20 kHz probe (40% amplitude, 0.097 W/cm³) was the best ultrasonic system for increasing the cell permeability of *D. salina* (see Section 7.3.5 for more details). UAE lipid extraction was carried and gravimetric lipid analysis was used to determine if ultrasound affected the amount of lipids recovered from *D. salina*. Figure 7.3.9 illustrates lipid recovery from *D. salina* using the adapted Bligh and Dyer method with and without sonication.

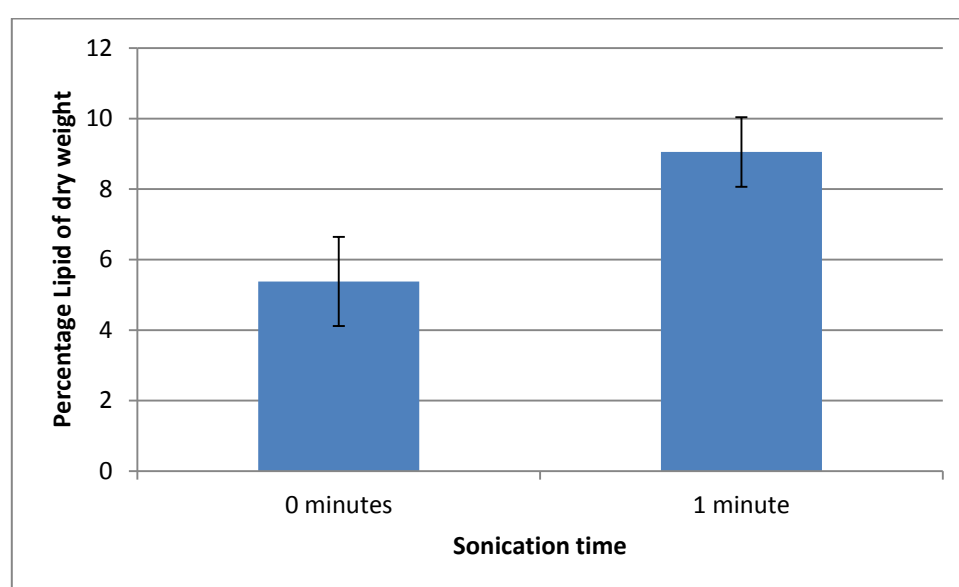
Figure 7.3.9 Lipid recovery from *D. salina* with and without sonication (Adapted Bligh and Dyer method)



The above figure clearly demonstrates that sonication significantly increased the amount of lipids recovered from *D. salina* from ~15 - ~22% dry biomass ($P = 0.07$). A sample treated with 2 minutes sonication was also included to demonstrate whether more than one minute of sonication time is needed to achieve an optimum lipid recovery. There is a very small increase (0.2%) in lipid recovery when sonicated for

2 minutes instead of 1; statistical analysis has shown that there is no significant difference between these 2 extraction times ($P = 0.495$). This means that 1 minute of sonication is optimum to maximise lipid recovery from *D. salina*. Figure 7.3.10 illustrates lipid recovery from *D. salina* using the hexane extraction method with and without sonication.

Figure 7.3.10 Figure 7.3.9 Lipid recovery from *D. salina* with and without sonication (Hexane method)



Results again indicate that sonication increase the amount of lipids recovered. When using hexane as the extraction solvent the amount of lipids recovered increases from ~4.5 - ~9% dry biomass. This is not as effective as using ultrasound with chloroform: methanol (1:2) which recovered ~22% lipids from dry biomass.

7.3.8 Summary of the effect of ultrasound on *D. salina* treated for 16 minutes

Table 7.3 summarises the effects of ultrasound on *D. salina* (200 mL) treated for 16 minutes with all 4 ultrasonic systems. Results are displayed in terms of percentage.

Table 7.3 Effect of ultrasound on *D. salina*

Test employed	20 kHz probe (0.097 W/cm ³)	40 kHz bath (0.07 W/cm ³)	DFR (0.545 W/cm ³)	Hielscher Unit (0.102 W/cm ³)
% Reduction in population (LD)	100	100	100	100
% Reduction in population (HD)	100	100	100	100
% Reduction in OD (LD)	20	18	16	2
% Reduction in OD (HD)	20	+18	5	+5
% Reduction in Chlorophyll peak	52	70	66	63
% Reduction in chlorophyll estimation	70	51	68	29
% Increase in Nile Red lipid peak	36 (after 1 minute treatment)	25 after 8 minutes	N/A	N/A
% Increase in lipids recovered from dry biomass using Bligh and Dyer	From 15- 22 %	N/A	N/A	N/A
% Increase in lipids recovered from dry biomass using hexane	From 4.5 to 9	N/A	N/A	N/A

LD = Low density

HD = High density

Table 7.3 shows that each ultrasonic system has a destructive effect on *D. salina*. It appears that the 20 kHz probe had the strongest effect; with the highest reduction in optical density, chlorophyll and after 1 minute of treatment the highest increase in Nile Red lipid peak. This data suggests that 1 minute of sonication is sufficient to

cause enough damage to *D. salina* to bring about an increase in lipid recovery. This was confirmed by both extraction techniques employed, lipid recovery increased from 15-22% dry biomass with chloroform:methanol (1:2) and from 4.5 to 9% dry biomass with hexane. The strong destructive ultrasonic effect on *D. salina* was expected as ultrasonic disruption of microalgal cells with the 20 kHz probe and 40 kHz bath has been previously observed by Wu *et al.* (2011). It is notable the cellular debris can cause considerable interference in optical density measurements (Wu, 2011). This questions the accuracy of using OD measurements for the work and highlights that haemocytometer counts and spectro-fluorophotometry measurements should be relied upon instead.

The adapted Bligh and Dyer extraction method produced greater lipid recovery levels than hexane extraction as highlighted in previous studies. Ranjan *et al.* (2010) investigated the effect of ultrasound on lipid recovery from *Scenedesmus Sp.* and conclude ultrasonic extraction with a 20 kHz probe and chloroform:methanol (3:1) produced a lipid recovery of 6% dry biomass, the same method but with hexane instead of chloroform:methanol (3:1) produced a 2% lipid recovery from dry biomass. For future studies it is advisable not to use hexane for lipid extractions from *D. salina*. The reason that these two lipid extraction techniques have different starting concentrations is because although both solvents are non polar and dissolve lipids it would seem that chloroform:methanol (1:2) appears to be a better solvent for lipid recovery than hexane (Grubauer *et al.* 1989).

The highest lipid recovery from *D. salina* was 22% dry biomass. Previous studies from Gouveia and Oliveira (2009) have stated that *D. salina* normally has a lipid content between 16 - 20% dry biomass, however Araujo *et al.* (2011) stated that when stressed the lipid content of *Dunaliella Sp.* (a close relative of *D. salina*) can

reach as high as 30.12% dry biomass. This indicates that a lipid recovery of 22% dry biomass could potentially be improved upon. Therefore in section 7.7.1 stressing techniques will be investigated in order to improve the lipid content of *D. salina*. The data from this chapter has led to the conclusion that the optimum lipid extraction technique is using the adapted Bligh and Dyer method coupled with 1 minute treatment with the 20 kHz probe (40% amplitude, 0.097 W/cm³). This should be the lipid extraction methodology employed for stressed *D. salina* in chapter 7.7.1 and for future lipid extraction.

7.4 Effect of ultrasound on *N. oculata*

Cultures of *N. oculata* (200 mL) were sonicated in triplicate for 16 minutes using a 20 kHz probe (40% amplitude, 0.097 W/cm^3), 40 kHz bath (0.07 W/cm^3), Dual Frequency Reactor (0.545 W/cm^3) and the Hielscher unit (0.102 W/cm^3). 10 mL samples were taken at time intervals of 0, 1, 2, 4, 8, and 16 minutes for analysis. This was carried out on both low and high density samples of *N. oculata*.

To determine any physiological effects which ultrasound may have on *N. oculata*, samples were analysed by the following techniques:

- Haemocytometer counts to determine any changes in the microalgal population as sonication was applied.
- Optical density to detect changes in cell population. This method was found not to be suitable to detect changes in cell population after sonication. Please see page 76 for further details.
- Spectro-fluorophotometer to detect changes in cellular chlorophyll levels. This was only carried out on low density samples as high density samples were too dense/concentrated to obtain reliable readings.
- Carotenoid and chlorophyll recovery to detect cellular chlorophyll and carotenoid levels. This was only carried out on low density samples as high density samples were too dense and concentrated to obtain reliable readings with the Spectro-fluorophotometer.
- Confocal microscopy to visually compare the effects of ultrasound on the cellular morphology of *N. oculata*.
- Nile Red staining analysed by spectro-fluorophotometer and the fluorescent microscope to detect changes in intracellular lipids. This was only carried out

on low density samples as high density samples were too dense/ concentrated to obtain reliable readings with the Spectro-fluorophotometer. This determines the time interval in which the Nile Red lipid peak was at its highest for *N. oculata* when treated with each ultrasonic system. This information will indicate when cell membranes and walls have been ruptured allowing increased entry of the Nile Red stain

- Ultrasound assisted lipid extraction through the adapted Bligh and Dyer method and the Hexane extraction method to determine any increase in lipid recovery levels with ultrasound employed in the extraction technique. Results were measured gravimetrically and expressed as lipid percentage of dry weight.

7.4.1 Effect of ultrasound on the cellular population of *N. oculata*

Haemocytometer measurements were employed to monitor changes in the cellular population of *N. oculata* as ultrasound was applied. Figure 7.4.1 displays the reduction in the cellular population for low density *N. oculata* cultures treated with each ultrasonic system.

Figure 7.4.1 Reduction in the cellular population of low density *N. oculata* treated with each ultrasonic system at $25^{\circ}\text{C} \pm 0.5^{\circ}\text{C}$

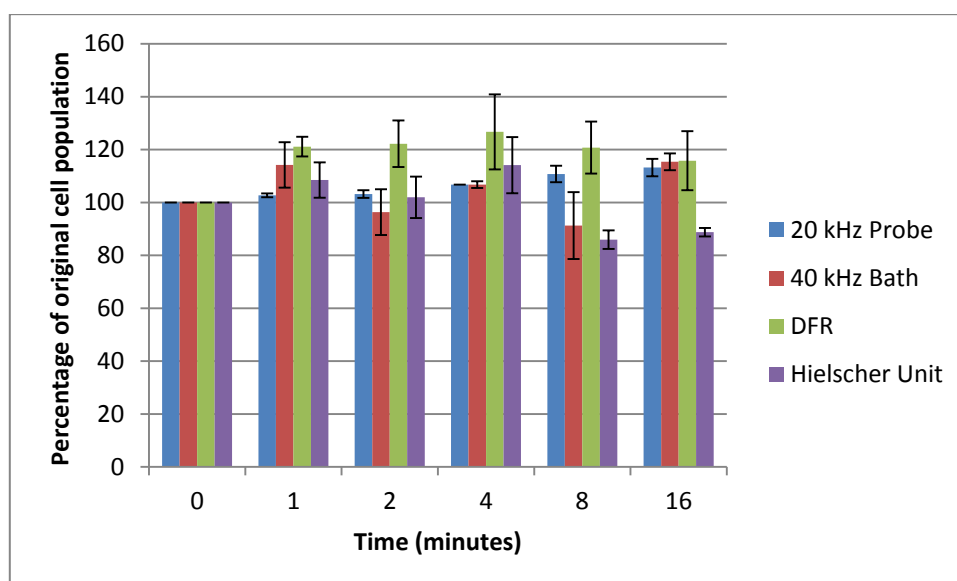
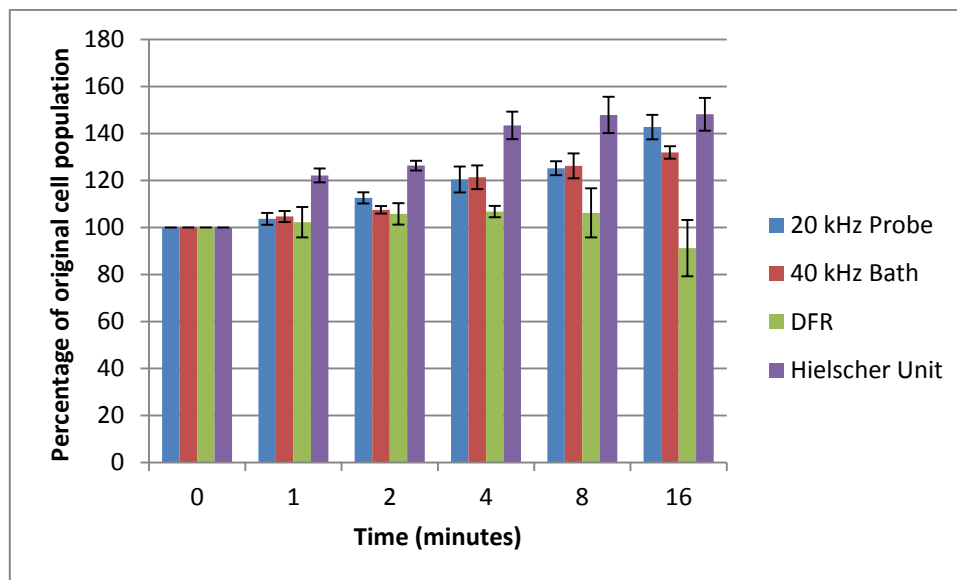


Figure 7.4.1 clearly shows that none of the ultrasonic systems have a strong effect in reducing the cellular population of *N. oculata* and only the Hielscher unit demonstrated a drop in the population of *N. oculata*. The 20 kHz probe (40% amplitude, 0.097 W/cm^3), 40 kHz bath (0.07 W/cm^3) and DFR system (0.545 W/cm^3) caused the observed population of *N. oculata* to increase as ultrasound was applied. This increase in cellular population induced by ultrasound is due to cells de-clumping. This phenomenon has been observed previously with both bacteria and microalgae in species which exist naturally in clumps (Joyce *et al.* 2003, 2011). The process of clumping together is also known as flocculation and under certain

conditions such as in the presence of specific trace metals in growth media *N. oculata* has been known to do this (Eldridge *et al.* 2012). All ultrasonic systems were also employed on high density cultures of *N. oculata*, results are displayed in figure 7.4.2. The starting cell concentration of *N. oculata* was $\sim 3.7 \times 10^7$ cells/mL.

Figure 7.4.2 Reduction in the cellular population for high density *N. oculata* treated with each ultrasonic system at $25^\circ\text{C} \pm 0.5^\circ\text{C}$

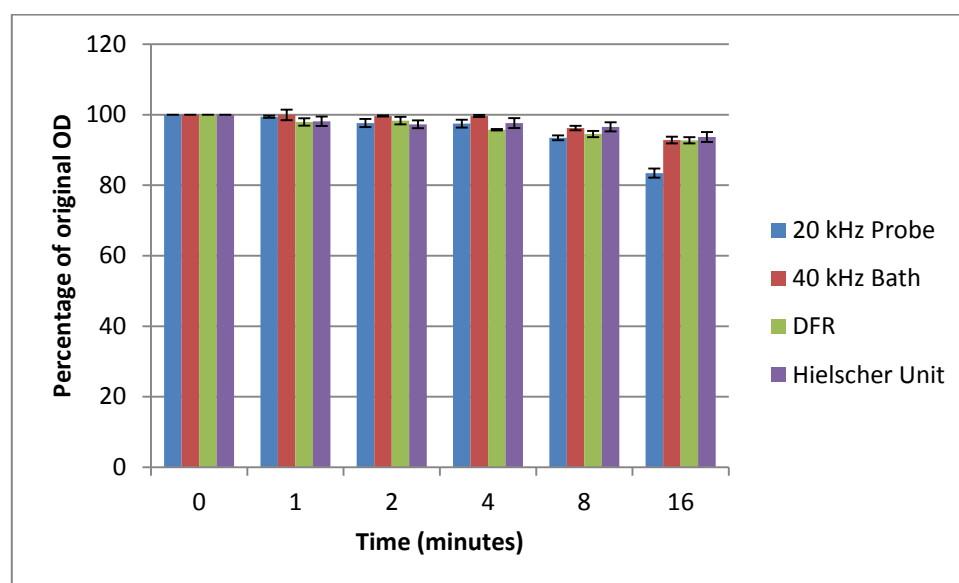


The above figure clearly shows an increase in the population of *N. oculata* for each system except the DFR, this is a similar de-clumping as displayed in Figure 7.4.1. The DFR system shows a very small drop in the population of *N. oculata* as ultrasound was applied, this indicates that the DFR system was able to disrupt a small amount of the *N. oculata* cells (10%). The starting cell concentration of high density *N. oculata* was $\sim 1.4 \times 10^8$ cells/mL.

7.4.2 Effect of ultrasound on the optical density of *N. oculata*

Optical density measurements at 686 nm were taken to monitor changes in the cellular population. Figure 7.4.3 displays the optical density measurements for low density *N. oculata* samples treated with each ultrasonic system.

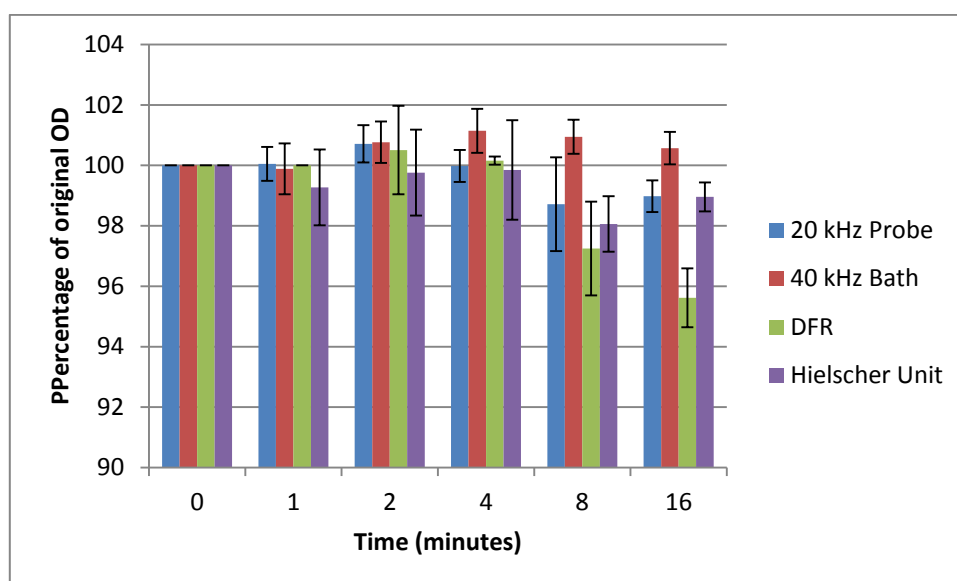
Figure 7.4.3 Percentage reduction in the optical density readings (686 nm) for low density *N. oculata* treated each ultrasonic system



The above figure shows that each of the ultrasonic systems cause the optical density of *N. oculata* to fluctuate and then slightly decrease as ultrasound is applied. This indicates that there may be a very small decrease in the cellular population of *N. oculata*; however this reduction may also be due to the previously reported de-clumping effects. The 20 kHz probe system showed the greatest drop in optical density over time ($P = 3.78E^{-6}$). The starting OD of *N. oculata* was ~ 0.5 .

All ultrasonic systems were also employed on high density cultures of *N. oculata* and results are displayed in Figure 7.4.4.

Figure 7.4.4 Optical density readings (686 nm) for high density *N. oculata* treated with all ultrasonic systems



The above figure shows that each ultrasonic systems causes the optical density of high density *N. oculata* to fluctuate as ultrasound is applied. The three most aggressive systems (20 kHz probe, DFR and Hielscher) also show a very small drop in the optical density after 16 minutes. This indicates that there may be a very small decrease in the cellular population of *N. oculata*, however it is more likely that this reduction may be due to the previously reported de-clumping effect. The large clumps of suspended cells are likely to cause interference to optical density measurements resulting in increased OD, after the disruption of the clumps it is likely a drop in OD would occur. The DFR shows the greatest drop in optical density over 16 minutes. The starting OD of high density *N. oculata* was ~2.7.

7.4.3 Effect of ultrasound on spectro-fluorophotometer measurements of *N. oculata*

The spectro-fluorophotometer was employed to detect changes in the level of intracellular chlorophyll as ultrasound was applied. Figure 7.4.5 displays the percentage reduction in the chlorophyll emission peak for low density *N. oculata* cultures for each ultrasonic system as sonication was applied.

Figure 7.4.5 Effect of ultrasound on the chlorophyll emission peak of *N. oculata*

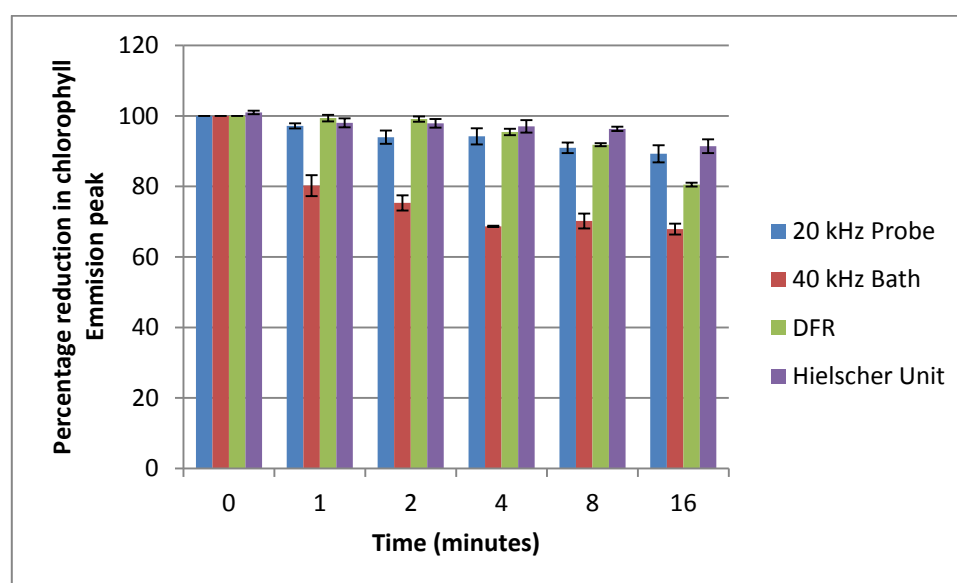


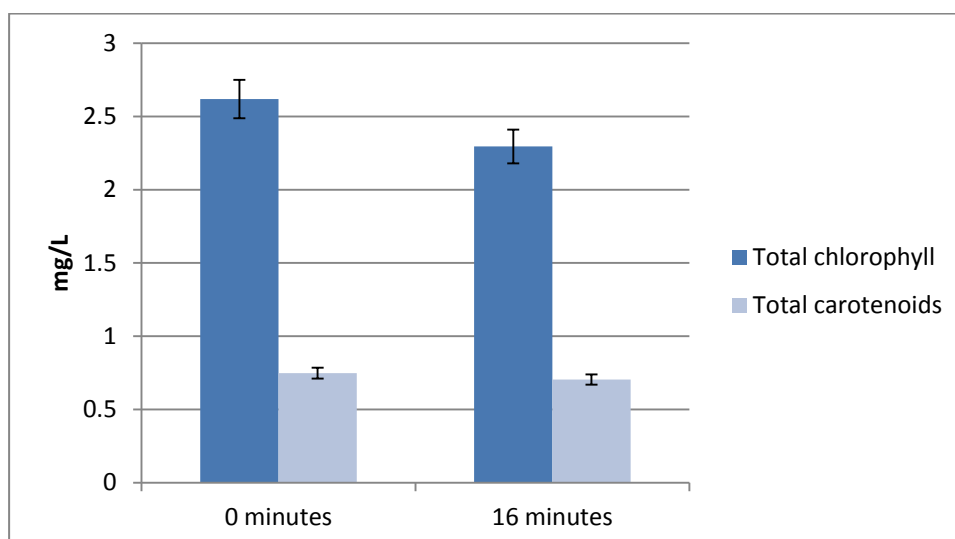
Figure 7.4.5 illustrates a rapid reduction in the height of the chlorophyll peak as sonication is applied for each of the ultrasonic systems. This indicates that despite previous haemocytometer data showing that there was no reduction in the cell population, the cells have been damaged and chlorophyll has been released. The 40 kHz bath shows the most rapid reduction of the chlorophyll peak ($P = 0.001$). The height of the starting emission peak was ~78.4 units.

7.4.4 Effect of ultrasound on chlorophyll a and carotenoid recovery from *N. oculata*

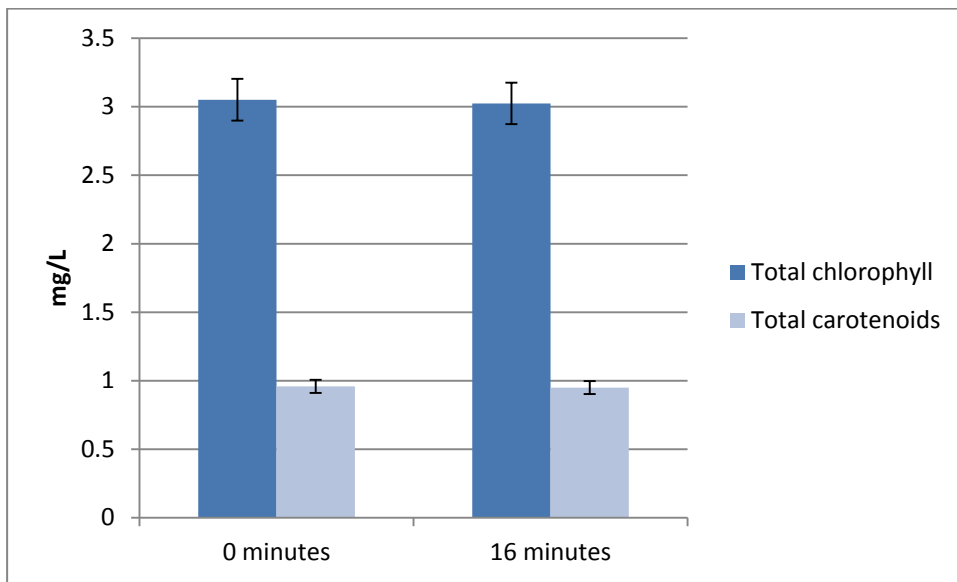
The chlorophyll A and carotenoid recovery procedure was carried out to determine the amount of chlorophyll a and carotenoids that can be extracted from the *N. oculata* biomass with and without ultrasound. Figure 7.4.6 shows the amount of intracellular chlorophyll and carotenoids recovered from an untreated sample and a sample treated using each ultrasonic system after 16 minutes. 16 minutes treatment was employed to determine the effect of prolonged sonication on cells.

Figure 7.4.6 Chlorophyll a and carotenoid recovery from low density *N. oculata* treated using each ultrasonic system

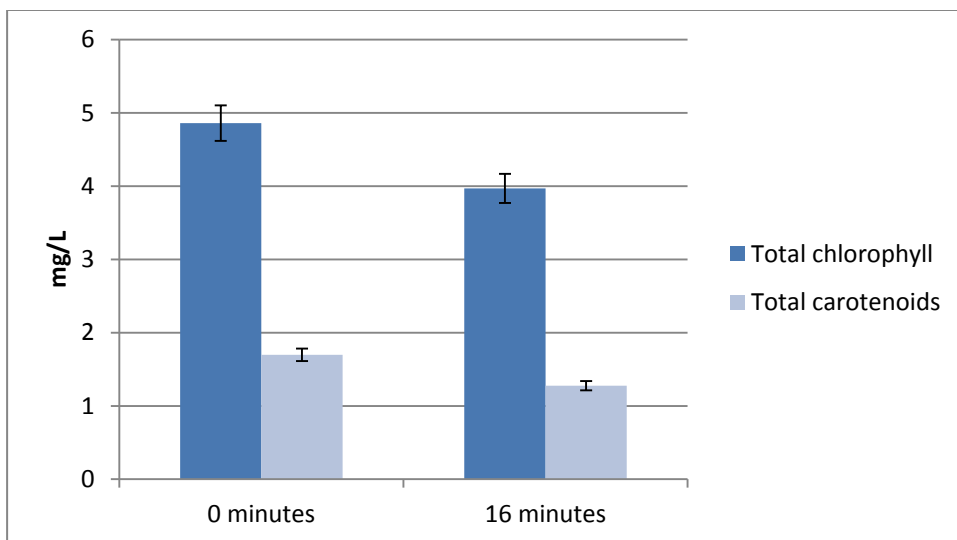
a. 20 kHz probe



b. 40 kHz bath



c. DFR



d. Hielscher unit

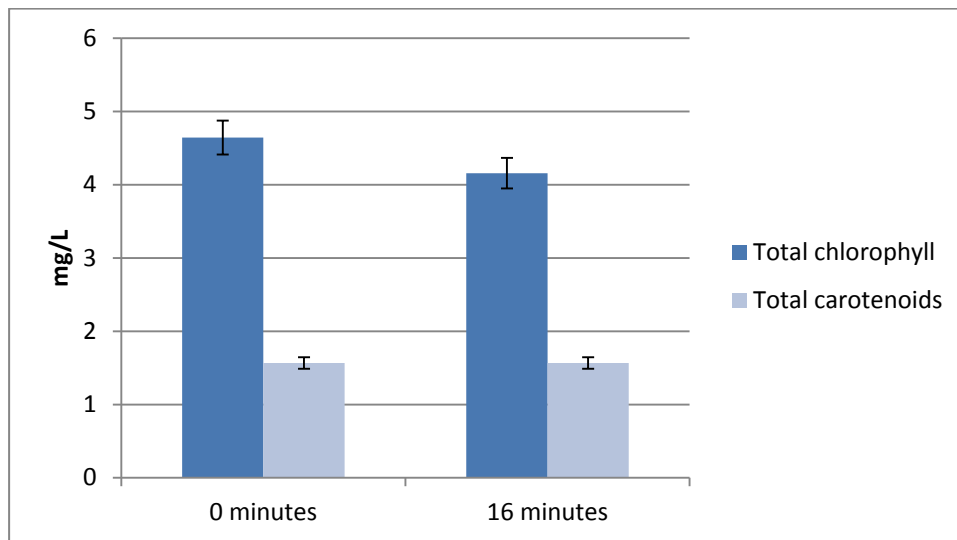
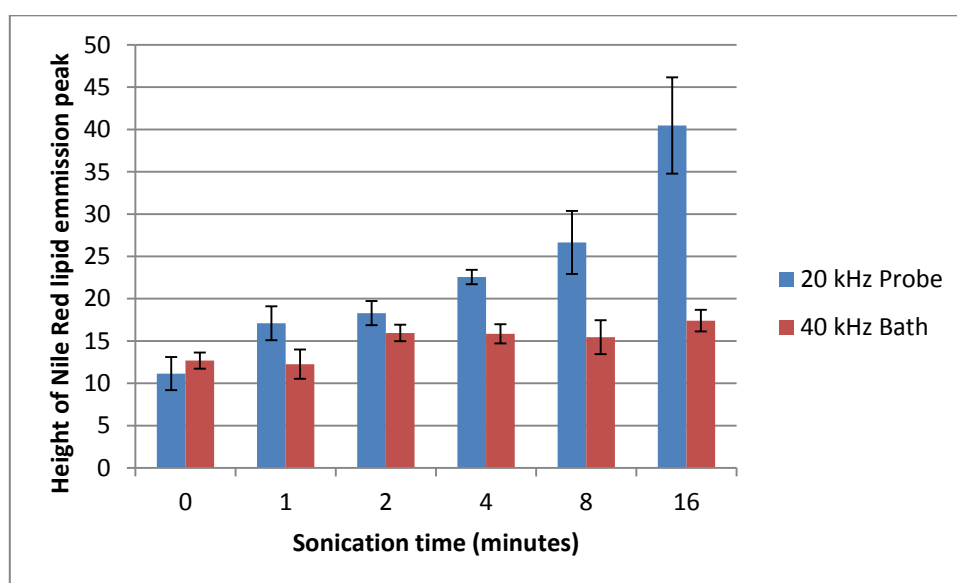


Figure 7.4.6 shows that the concentration of intracellular chlorophyll a and carotenoids slightly decreased as ultrasound is applied. The 20 kHz probe and DFR systems appear to cause a greatest reduction in the chlorophyll ($P = 0.014$) and carotenoids levels ($P = 0.01$) of *N. oculata*. This indicates that all of the ultrasonic systems are capable of weakening the cell wall of *N. oculata* resulting in cell leakage.

7.4.5 Effect of ultrasound on the intracellular lipids of *N. oculata* measured by Nile Red spectro-fluorophotometer measurement

Nile Red staining measured by spectro-fluorophotometry was employed to determine the amount of stained lipids present before, during and after sonication. This method determined the time interval in which the Nile Red lipid peak was at its highest for *N. oculata* when treated with each ultrasonic system. This information will determine when cell membranes and walls have been ruptured, allowing increased entry of the Nile Red stain. This time interval will be employed as the sonication time for ultrasound assisted lipid extraction. Figure 7.4.8 displays the increase in the Nile Red lipid peak as ultrasound is applied using each ultrasonic system. The DFR and Hielscher systems were not available for this procedure as they were returned to their manufacturers.

Figure 7.4.7 Lipid peak of low density *N. oculata* treated with ultrasound measured by spectro-fluorophotometry



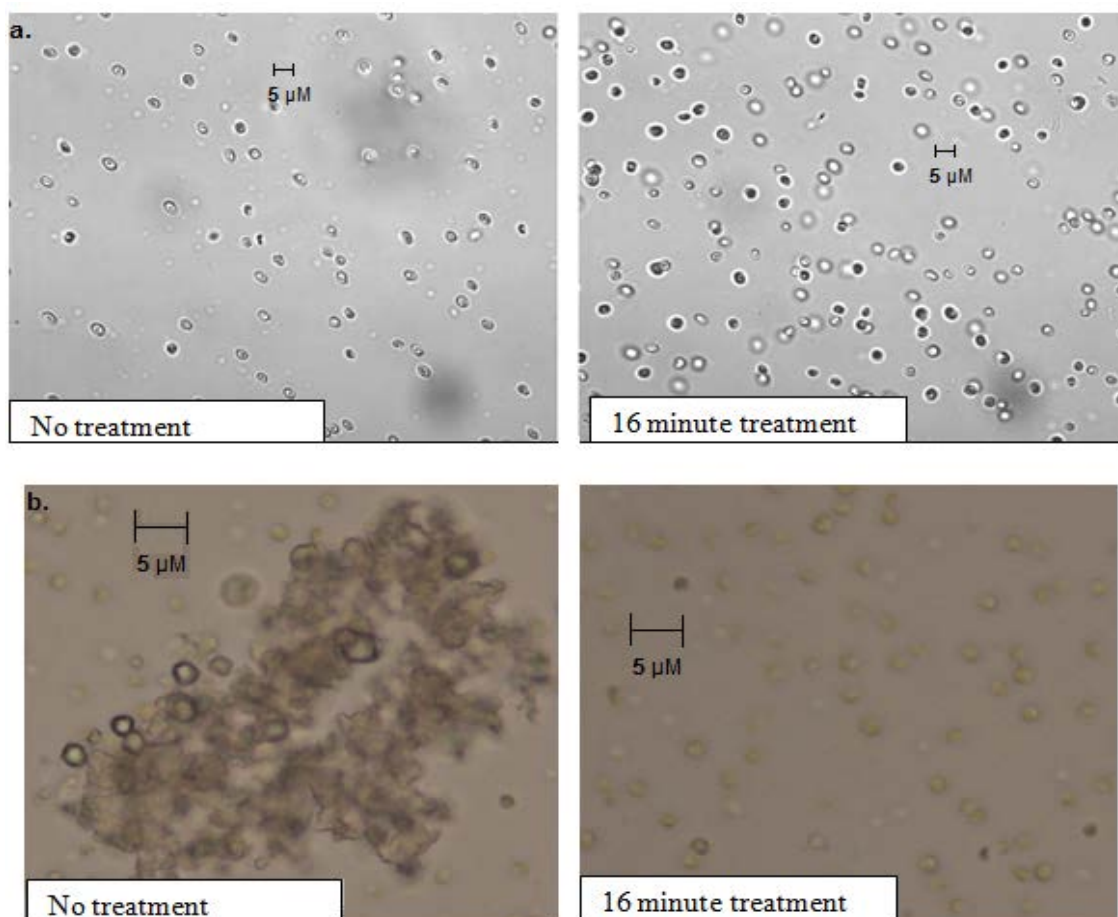
The above figure shows that the lipid peak significantly increases after 16 minute treatment ($P = 0.001$) using the 20 kHz probe (40% Amplitude, 0.097 W/cm^3). This

indicates that the cell walls and membrane has been ruptured allowing increased uptake of Nile Red into the cell and increased staining of lipids. This indicates that at least 16 minute sonication using the 20 kHz probe is needed to disrupt the cell walls of *N. oculata*, increasing membrane permeability. The 40 kHz bath shows a steady increase in the Nile Red peak as ultrasound is applied; however the peak does not reach the levels achieved with the 20 kHz probe. Therefore 16 minute treatment with the 20 kHz probe (40% amplitude, 0.097 W/cm³) will be employed for the extraction methods.

7.4.6 Effect of ultrasound on *N. oculata* viewed by microscopy

Confocal microscopy (x63 magnification) and fluorescence microscopy (x100 magnification) were employed to determine the physiological condition of *N. oculata* cells before and after sonication with the 20 kHz probe (40% Amplitude, 0.097 W/cm³) for 16 minutes. These images are displayed in Figure 7.4.8. The physical state of 100 cells on a slide was observed in order to determine their state before and after ultrasonic treatment.

Figure 7.4.8 Microscopy images of low density *N. oculata* treated with the 20 kHz probe



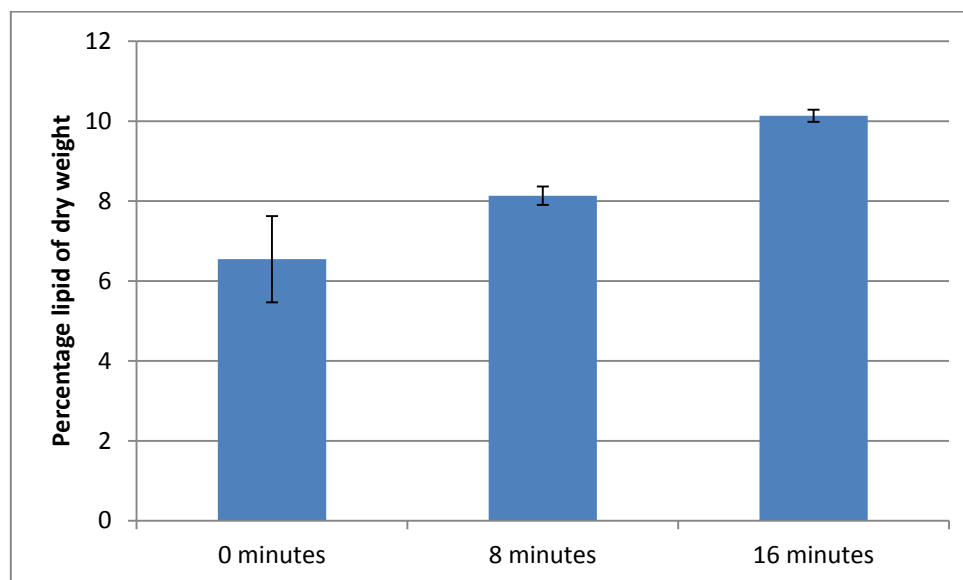
Both figures 7.4.8.a (confocal microscope) and 7.4.8.b (fluorescent microscope) demonstrate that the 20 kHz probe (40% amplitude, 0.097 W/cm³) does not seem to

cause any major cellular destruction to *N. oculata*. Before ultrasonic treatment was applied the images show that the cells were intact, and they seemed to remain intact after treatment. Fluorescence microscopy displays a clump of *N. oculata* cells, there were roughly 12500 of these large clumps/ mL of *N. oculata* cells before sonication. After sonication these clumps been broken up by the effects of the 20 kHz probe (after sonication there were no large clumps remaining, only 4166 smaller clumps/mL). Figure 7.4.8.a shows a higher number of cells after sonication due to the previously reported declumping effect. There does not appear to be any physical damage to *N. oculata* cells that is visible at this level of microscopy, even though previous spectro-fluorophotometry data suggests otherwise in Figure 7.4.5.

7.4.7 Effect of the 20 kHz probe (40% Amplitude 0.097 W/cm³) on the lipid recovery of *N. oculata* measured gravimetrically

Nile Red analysis determined that at out of the systems employed at least 16 minutes treatment with the 20 kHz probe (40% amplitude, 0.097 W/cm³) was the optimum ultrasonic system for increasing the cellular permeability of *N. oculata* (see section 7.4.5 for more details). UAE lipid extraction was carried and gravimetric lipid analysis was used to determine if ultrasound affected the amount of lipids recovered from *N. oculata*. Figure 7.4.9 illustrates lipid recovery from *N. oculata* using the adapted Bligh and Dyer method with and without sonication.

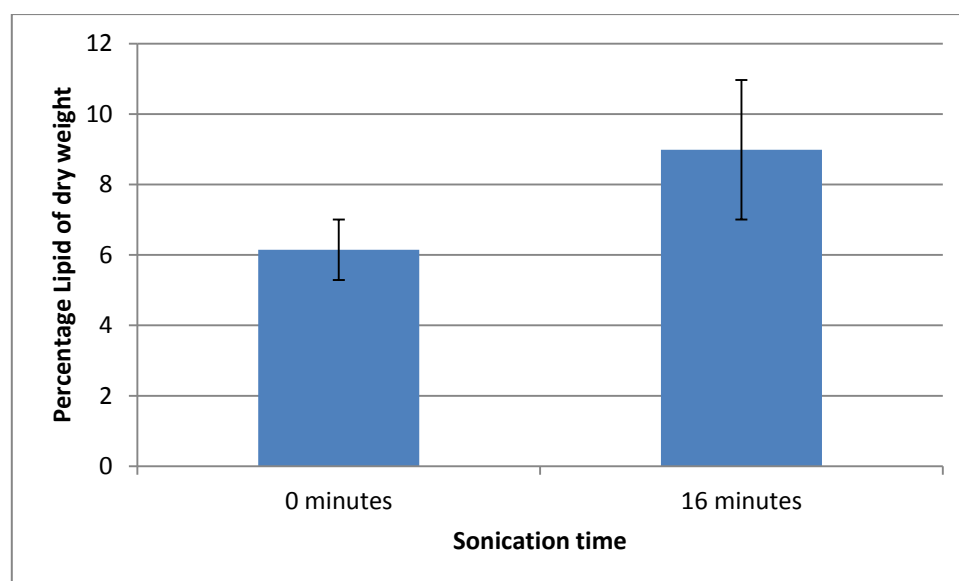
Figure 7.4.9 Lipid recovery from *N. oculata* with and without sonication (Adapted Bligh and Dyer method)



The above figure clearly demonstrates that sonication increases the amount of lipids recovered from *N. oculata*. Without sonication the lipid recovery achieved was ~6.5, this rose to 10% ($P = 0.039$) when ultrasound was applied. An 8 minute extraction time was included and this confirmed that at least 16 minutes treatment time was required to cause a large increase in lipid recovery as only a 8.05% lipid recovery

from dry biomass was achieved. This indicates that as previously stated in the Nile Red study at least 16 minutes of sonication is needed to improve lipid recovery. If any time interval higher than this was employed, the economical viability of this method will be brought into question because of the potential cost of prolonged use of ultrasonic equipment. Figure 7.4.10 illustrates lipid recovery from *N. oculata* using the hexane extraction method with and without sonication.

Figure 7.4.10 Lipid recovery from *N. oculata* with and without sonication (hexane)



As for the hexane extraction, results again indicate that sonication increases the amount of lipids recovered. When using hexane as the extraction solvent the amount of lipids recovered increases from ~6 - ~9% dry biomass. This is not as effective as using ultrasound with the adapted Bligh and Dyer method which achieved a 10% lipid recovery from dry biomass.

7.4.8 Summary of the effect of ultrasound on *N. oculata*

Table 7.4 summarises the effects of ultrasound on *N. oculata* (200 mL) treated for 16 minutes with all 4 ultrasonic systems. Results are expressed as a percentage.

Table 7.4 Effect of ultrasound on *N. oculata*

Test employed	20 kHz probe (0.097 W/cm ³)	40 kHz bath (0.07 W/cm ³)	DFR (0.545 W/cm ³)	Hielscher unit (0.102W/cm ³)
% Reduction in population (LD)	+17	+19	+19	10
% Reduction in population (HD)	+41	+35	10	+45
% Reduction in OD (LD)	18	5	5	5
% Reduction in OD (HD)	1	+1	5	1
% Reduction in Chlorophyll peak	10	35	20	10
% Reduction in chlorophyll estimation	10	0	19	11
% Increase in Nile Red lipid peak	260	30	N/A	N/A
% Increase in lipids recovered from dry biomass using Bligh and Dyer	From 6.5 to 10%	N/A	N/A	N/A
% Increase in lipids recovered from dry biomass using hexane	From ~6 to 9%.	N/A	N/A	N/A

LD = Low density

HD = High density

The table above shows that none of the ultrasonic systems have a strong destructive effect on *N. oculata*. The majority of systems caused a de-clumping effect previously discussed in this chapter. Haemocytometer and chlorophyll estimation data shown that the DFR system seemed to have the strongest destructive effect on *N. oculata*.

Due to the DFR system being unavailable the Nile Red lipid determination was not carried out using this system for *N. oculata*. The 20 kHz probe caused a 260% increase in the Nile Red lipid peak; this is a 9 fold increase to that of 40 kHz probe. The data suggests that 16 minutes treatment with the 20 kHz probe is sufficient to cause enough cell wall and membrane damage to *N. oculata* to bring about an increase in lipid recovery. This was confirmed by both of the extraction techniques employed, lipid recovery increased from 6.5 - 10% dry biomass with adapted Bligh and Dyer and from 6 - 9% dry biomass with hexane. As with *D. salina* the adapted Bligh and Dyer extraction method produced greater lipid recovery levels than the hexane extraction.

The highest lipid recovery from *N. oculata* was 10% dry biomass, previous studies from Gouveia and Oliveira (2009) have stated that *N. oculata* usually has a lipid content around 23% dry biomass, however Araujo *et al.* (2011) stated that when stressed lipid recovery from *N. oculata* can reach as high as 28.7% dry biomass. This suggests that a 10% lipid recovery from dry biomass can be greatly improved upon. Therefore section 7.7.2 will report on stressing techniques used to improve the lipid content of *N. oculata*. Since no ultrasonic system employed in this study caused a strong destructive effect on *N. oculata*, the effect of ultrasound combined with a range of beating beads will also be reported in this section. The data from this current section has suggested that the optimum lipid extraction technique is using the adapted Bligh and Dyer method coupled with 16 minutes treatment with the 20 kHz probe (40% amplitude, 0.097 W/cm³). This should be employed as the lipid extraction method for stressed *N. oculata* in chapter 7.7.2.

7.5 Effect of ultrasound on *C. concordia*

Cultures of *C. Concordia* (200 mL) were sonicated in triplicate for 16 minutes using a 20 kHz probe (40% amplitude, 0.097 W/cm^3), 40 kHz bath (0.07 W/cm^3), Dual Frequency Reactor (0.545 W/cm^3) and the Hielscher unit (0.102 W/cm^3). 10 mL samples were taken at time intervals of 0, 1, 2, 4, 8, and 16 minutes for analysis.

To determine any physiological effects which ultrasound may have on *C. concordia*, samples were analysed by the following techniques:

- Haemocytometer counts to determine any changes in the microalgal population as sonication was applied.
- Optical density to detect changes in cell population. This method was found not to be suitable to detect changes in cell population after sonication. Please see page 76 for further details.
- Spectro-fluorophotometer to detect changes in cellular chlorophyll levels. This was only carried out on low density samples as high density samples were too dense/concentrated to obtain reliable readings.
- Carotenoid and chlorophyll recovery to detect cellular chlorophyll and carotenoid levels. This was only carried out on low density samples as high density samples were too dense and concentrated to obtain reliable readings with the Spectro-fluorophotometer.
- Confocal microscopy to visually compare the effects of ultrasound on the cellular morphology of *C. concordia*.
- Nile Red staining analysed by spectro-fluorophotometer and the fluorescent microscope to detect changes in intracellular lipids. This was only carried out on low density samples as high density samples were too dense/

concentrated to obtain reliable readings with the Spectro-fluorophotometer. This determines the time interval in which the Nile Red lipid peak was at its highest for *C. concordia* when treated with each ultrasonic system. This information will indicate when cell membranes and walls have been ruptured allowing increased entry of the Nile Red stain

- Ultrasound assisted lipid extraction through the adapted Bligh and Dyer method and the Hexane extraction method to determine any increase in lipid recovery levels with ultrasound employed in the extraction technique. Results were measured gravimetrically and expressed as lipid percentage of dry weight.

7.5.1 Effect of ultrasound on the cellular population of *C. concordia*

Haemocytometer measurements were employed to monitor changes in the cellular population of *C. concordia* as ultrasound was applied. Figure 7.5.1 displays the reduction in the cellular population for low density *C. concordia* cultures treated with each ultrasonic system.

Figure 7.5.1 Reduction in the cellular population of *C. concordia* treated with each ultrasonic system at $25^{\circ}\text{C} \pm 0.5^{\circ}\text{C}$

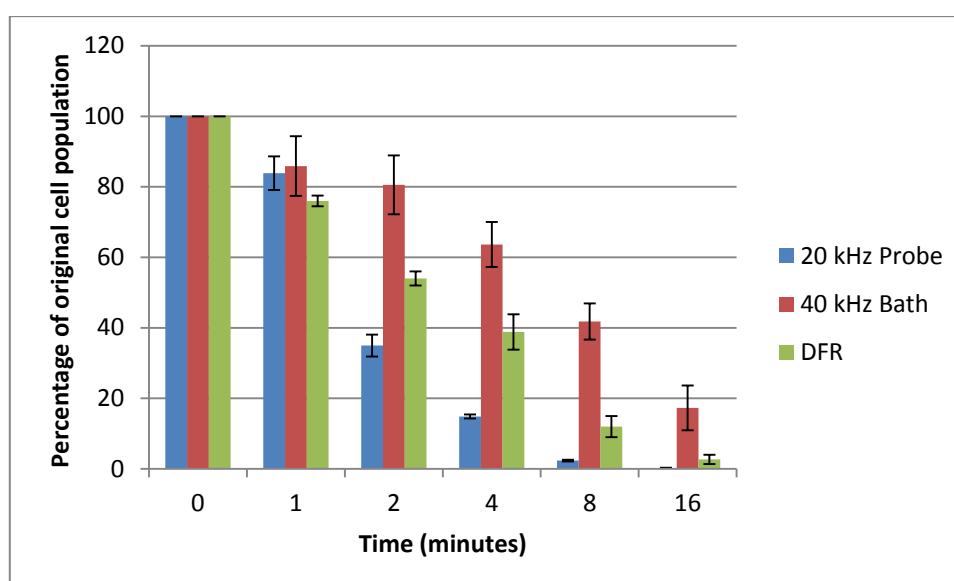
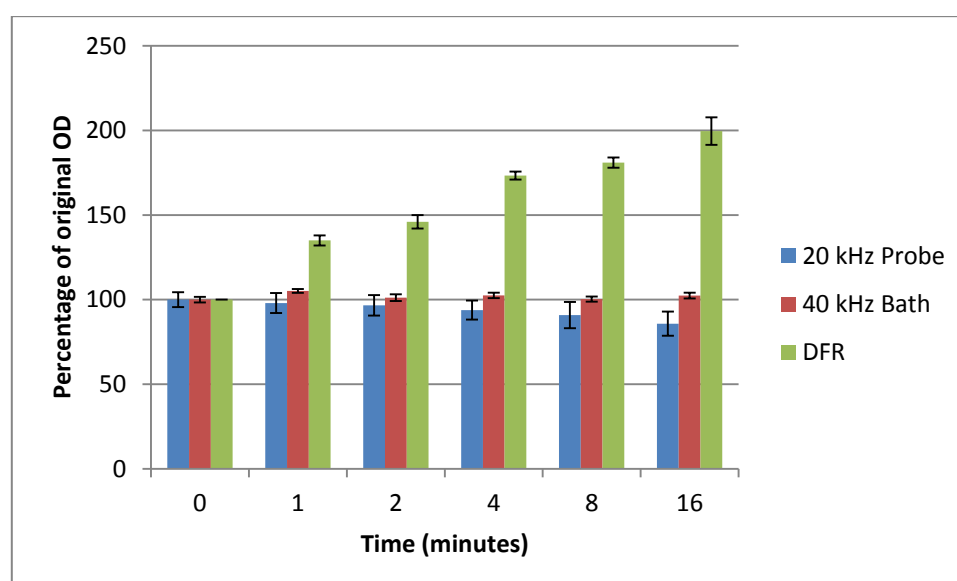


Figure 7.5.1 clearly shows that the 20 kHz probe (40% amplitude, 0.097 W/cm^3) system resulted in the greatest reduction in the *C. concordia* population ($P = 1.18\text{E}^{-12}$) and after 16 minutes treatment the entire population of *C. concordia* was destroyed. The 40 kHz bath (0.07 W/cm^3) and the DFR system (0.545 W/cm^3) decreased the population of *C. concordia* as ultrasound was applied but total cellular disruption was not achieved with either system after 16 minutes. The starting cell concentration of *C. concordia* was $\sim 1.2 \times 10^6$ cells/ml.

7.5.2 Effect of ultrasound on the optical density of *C. concordia*

Optical density measurements at 686 nm were taken to monitor changes in the cellular population. Figure 7.5.2 displays the optical density measurements for low density *C. concordia* samples treated with each ultrasonic system expressed as a percentage reduction.

Figure 7.5.2 Percentage reduction in the optical density readings (686 nm) for low density *C. concordia* treated with each ultrasonic system



The above figure clearly shows that the 20 kHz probe caused the optical density of *C. concordia* to decrease as ultrasound is applied. This indicates that there has been a reduction in the cellular population of *C. concordia*. The 40 kHz bath and the DFR system resulted in an increase in the optical density as ultrasound is applied. Although haemocytometer data has shown cellular disruption with both systems this optical density data has suggested that these systems are not as effective as the 20 kHz probe system. As previously explained these fluctuations in OD are most likely due the cell debris interfering with the passage of light through the UV-Visible spectrophotometer. The starting OD of *C. concordia* was ~0.3.

7.5.3 Effect of ultrasound on spectro-fluorophotometer measurements of *C. concordia*

The spectro-fluorophotometer was employed to detect changes in the level of intracellular chlorophyll as ultrasound was applied. Figure 7.5.3 displays percentage reduction in the chlorophyll emission peak for low density *C. concordia* cultures for each ultrasonic system as sonication was applied.

Figure 7.5.3 Effect of ultrasound on the chlorophyll emission peak of *C. concordia*

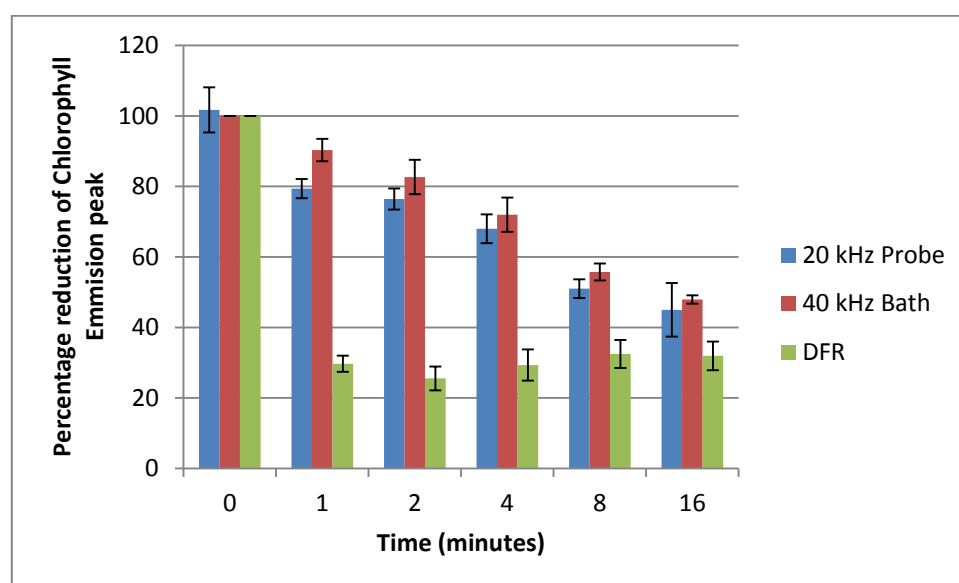


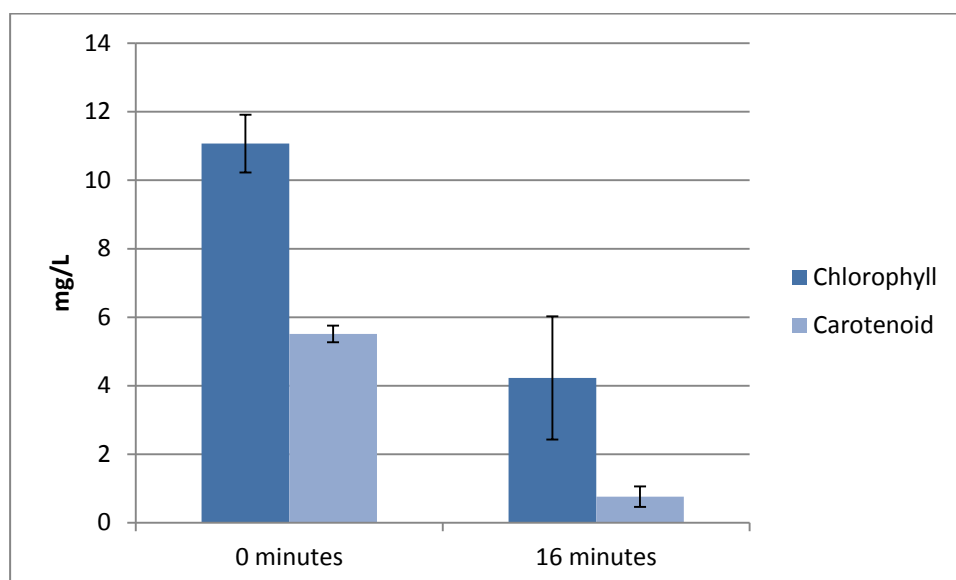
Figure 7.5.3 demonstrates a rapid reduction in the height of the chlorophyll peak as sonication is applied for each ultrasonic system. This indicates that cells have been ruptured and chlorophyll has been released. The largest reduction was observed by used of the DFR. The height of the starting emission peak was 117.7.

7.5.4 Effect of ultrasound on chlorophyll a and carotenoid recovery from *C. concordia*

The chlorophyll a and carotenoid recovery procedure was carried out to determine the amount of intracellular chlorophyll a and carotenoids within samples. Figure 7.5.4 shows the amount of chlorophyll a and carotenoids recovered from an untreated sample and a sample treated using each ultrasonic system after 16 minutes. 16 minutes treatment was employed to determine the effect of prolonged sonication on cells.

Figure 7.5.4 Chlorophyll a and carotenoid recovery from low density *C. concordia* treated using each ultrasonic system

a. 20 kHz probe



b. 40 kHz bath

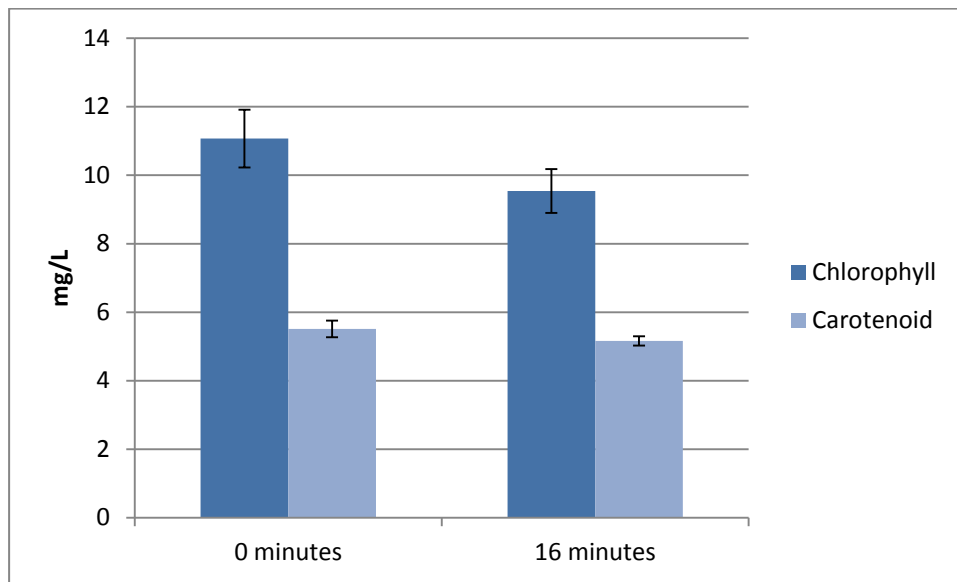
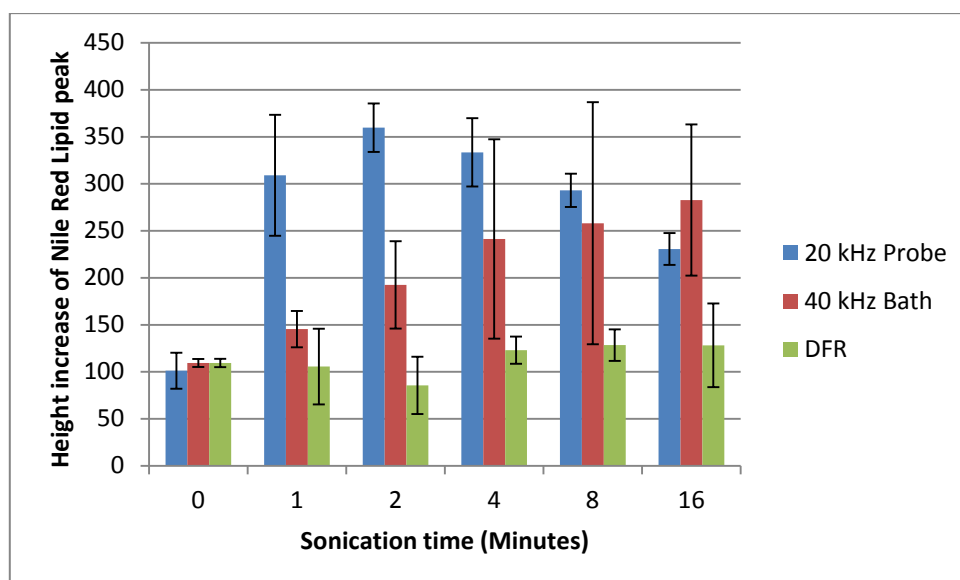


Figure 7.5.4 shows that sonication applied by both ultrasonic systems caused the chlorophyll and Carotenoid recovery levels of *C. concordia* to decrease. This again suggests that ultrasound caused damage to the cell walls of *C. concordia* and leakage of cell pigments and other materials occurred. The 20 kHz probe system caused a higher rate of reduction in pigment levels than the 40 kHz bath (chlorophyll $P = 0.07$, carotenoid $P = 0.004$). The DFR system was not available for this procedure as it had been returned to its manufacturer.

7.5.5 Effect of ultrasound on the intracellular lipids of *C. concordia* measured by Nile Red spectro-fluorophotometer measurement

Nile Red staining measured by spectro-fluorophotometry was employed to determine the amount of intracellular lipids present before and during sonication. This method determined the time interval in which the Nile Red lipid peak was at its highest for *C. concordia* when treated with each ultrasonic system. This information will determine when cell membranes and walls have been ruptured, allowing increased entry of the Nile Red stain. This time interval will be employed as the sonication time for ultrasound assisted lipid extraction. Figure 7.5.5 displays the increase in Nile Red lipid peak as ultrasound is applied using each system.

Figure 7.5.5 Lipid peak of low density *C. concordia* treated with ultrasound measured by spectro-fluorophotometry



The above figure shows that the lipid peak significantly increases after 2 minutes treatment ($P = 0.001$) using the 20 kHz probe (40% Amplitude, 0.097 W/cm^3). This indicates that the cell membrane has been ruptured allowing increased uptake of Nile Red into the cell. Therefore only 2 minute sonication using the 20 kHz probe is

needed to disrupt the cell membranes of *C. concordia* increasing membrane permeability. After 2 minutes the lipid peak decreases which may be due to the lipids being emulsified by sonication which possibly makes Nile Red unable to bind to them. The 40 kHz bath and DFR systems show a steady increase in the Nile Red peak as ultrasound is applied; neither system displayed as high an increase in the Nile Red peak as the 20 kHz probe. The 40 kHz bath and DFR are therefore not as efficient as the 20 kHz probe at increasing the membrane permeability of *C. concordia*.

7.5.6 Effect of ultrasound on *C. concordia* viewed by microscopy

Fluorescence microscopy (x100 magnification) was employed to visibly determine the state of the *C. concordia* cells before and after sonication with the 20 kHz probe (40 % amplitude, 0.097 W/cm^3) to detect any physiological effects ultrasound may cause. Figure 7.5.8 displays before and after images of a culture of *C. concordia* treated with the 20 kHz probe. Due to the poor visibility of the cells fluorescence microscopy was employed to visualise internal chlorophyll which appears red. The physical state of 100 cells on a slide was observed to determine their state before and after ultrasonic treatment. These images are displayed in Figure 7.5.6.

Figure 7.5.6 Microscopy images of low density *C. concordia* treated with the 20 kHz probe

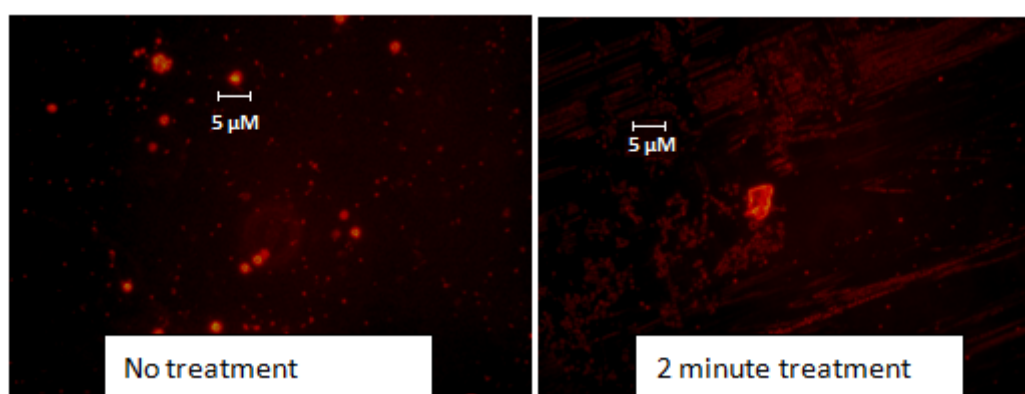


Figure 7.5.6 clearly shows less visible intact cells and more clumps of debris after sonication with the 20 kHz probe for 2 minutes. This indicates that 2 minutes treatment time is sufficient to cause cellular damage to *C. concordia*. Before sonication 100% of the cells were intact and after ultrasonic treatment approximately 90% of the cells were disrupted in the field of view investigated.

7.5.7 Effect of the 20 kHz probe (40% Amplitude, 0.097 W/cm³) on the lipid recovery of *C. concordia* measured gravimetrically

Nile Red analysis determined that 2 minutes treatment with the 20 kHz probe (40% amplitude, 0.097 W/cm³) was the optimum ultrasonic system for increasing the membrane permeability of *C. concordia* (see section 7.5.5 for more details). Gravimetric lipid determination was carried out to detect if ultrasound had an effect on the amount of lipids recovered from *C. concordia*. Figure 7.5.7 shows the lipid recovery from *C. concordia* using the adapted Bligh and Dyer method with and without sonication.

Figure 7.5.7 Lipid recovery from *C. concordia* with and without sonication (Adapted Bligh and Dyer method)

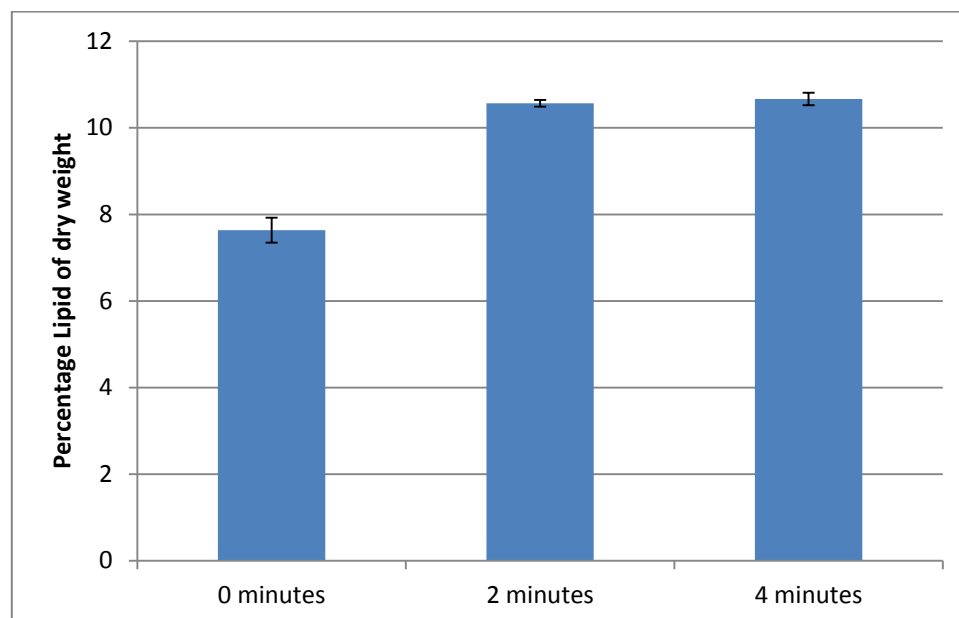
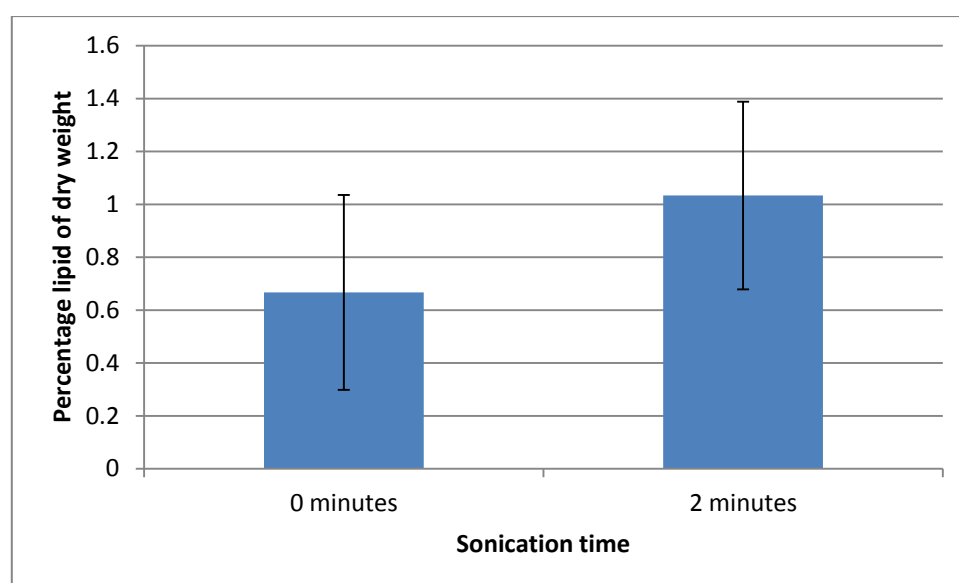


Figure 7.5.7 clearly demonstrates that sonication significantly increases the amount of lipids recovered from *C. concordia* from ~7.5 - ~10.5% dry biomass ($P = 0.01$). A sample sonicated for 4 minutes was also included to demonstrate whether more than 2 minutes of sonication time were needed to achieve higher lipid recovery. There is a

very small increase (0.26%) in lipid recovery when sonicated for 4 minutes instead of 2 minutes. Statistical analysis has shown that there is no significant difference between these 2 time points ($P = 0.311$). This means that 2 minutes of sonication is sufficient to maximise lipid recovery from *C. concordia*. Figure 7.5.8 illustrates lipid recovery from *C. concordia* using the hexane extraction method with and without sonication.

Figure 7.5.8 Lipid recovery from *C. concordia* with and without sonication (hexane)



Results again indicate that sonication increases the amount of lipids recovered. When using hexane as the extraction solvent the amount of lipids recovered increases from ~0.6 - ~1.1% dry biomass. This data confirms that hexane is not as effective as chloroform: methanol (1:2) as the extraction solvent, this was also reported by Ranjan *et al.* 2010.

7.5.8 Summary of the effect of ultrasound on *C. concordia*

Table 7.5 summarises the effects of ultrasound on *C. Concordia* (200 mL) treated for 16 minutes with the 3 ultrasonic systems employed. Results are expressed as a percentage.

Table 7.5 Effect of ultrasound on *C. concordia*

Test employed	20 kHz probe (0.097 W/cm ³)	40 kHz bath (0.07 W/cm ³)	DFR (0.545 W/cm ³)
% Reduction in population	100	82	95
% Reduction in OD	15	0	200
% Reduction in Chlorophyll peak	55	50	70
% Reduction in chlorophyll estimation	64	18	N/A
% Increase in Nile Red lipid peak	260 (after 2 minutes treatment)	160	50
% Increase in lipids recovered from dry biomass using Bligh and Dyer	From 7.5 to 10.5%.	N/A	N/A
% Increase in lipids recovered from dry biomass using Hexane	From 0.6 to 1.1%	N/A	N/A

LD = Low density

HD = High density

The table shows that each ultrasonic system has a destructive effect on *C. concordia*. It appears that the 20 kHz probe had the strongest effect as it brought about the highest reduction in cell population, chlorophyll estimation and after 2 minutes of treatment the highest increase in the Nile Red lipid peak. This data suggests that 2 minutes treatment is sufficient to cause enough damage to the cell wall and membrane of *C. concordia* to bring about an increase in lipid recovery. This

was confirmed by both extraction techniques employed, lipid recovery increased from 7.55 - 10.5% dry biomass with chloroform: methanol and from 0.6 - 1.1% dry biomass with hexane. As with *D. salina* and *N. oculata* the chloroform:methanol (1:2) extraction method produced greater lipid recovery levels than the hexane extraction technique. For future studies it is preferable to use chloroform:methanol (1:2) and advisable not to use hexane for lipid extractions from *C. concordia*.

The highest lipid recovery achieved from *C. concordia* was 10.5% dry biomass. Previous studies from Yoo *et al.* (2012) have stated that *C. reinhardtii* (a close relative of *C. concordia*) can have a lipid content of 25-35% dry biomass. Although this was not used in this study, this indicates that a lipid recovery of 10.5% dry biomass may be improved upon. Section 7.7.3 reports stressing techniques to improve lipid recovery from *C. concordia*. The data from this current section has determined that 2 minute treatments with the 20 kHz probe (40% amplitude, 0.097 W/cm³) with chloroform:methanol (1:2) as the extraction solvent should be employed as the lipid extraction method for stressed *C. concordia* in section 7.7.3.

7.6 Effect of ultrasound on *Chlorella Sp.*

Cultures of *Chlorella Sp.* (200 mL) were sonicated in triplicate for 16 minutes using a 20 kHz probe (40% amplitude, 0.097 W/cm³) and the 40 kHz bath (0.07 W/cm³). 10 mL samples were taken at time intervals of 0, 1, 2, 4, 8, and 16 minutes for analysis. This was carried out on low density samples of *Chlorella Sp.*

To determine any physiological effects which ultrasound may have on *Chlorella Sp.*, samples were analysed by the following techniques:

- Haemocytometer counts to determine any changes in the microalgal population as sonication was applied.
- Optical density to detect changes in cell population. This method was found not to be suitable to detect changes in cell population after sonication. Please see page 76 for further details.
- Spectro-fluorophotometer to detect changes in cellular chlorophyll levels.
- Carotenoid and chlorophyll recovery to detect cellular chlorophyll and carotenoid levels.
- Fluorescent microscopy to visually compare the effects of ultrasound on the cellular morphology of *Chlorella Sp.*
- Nile Red staining analysed by spectro-fluorophotometer to detect changes in intracellular lipids. This determines the time interval in which the Nile Red lipid peak was at its highest for *Chlorella Sp.* when treated with each ultrasonic system. This information will indicate when cell membranes and walls have been ruptured allowing increased entry of the Nile Red stain
- Ultrasound assisted lipid extraction through the adapted Bligh and Dyer method to determine any increase in lipid recovery levels with ultrasound

employed in the extraction technique. Results were measured gravimetrically and expressed as lipid percentage of dry weight.

7.6.1 Effect of ultrasound on the cellular population of *Chlorella Sp.*

Haemocytometer measurements were employed to monitor changes in the cellular population of *Chlorella Sp.* as ultrasound was applied. Figure 7.6.1 displays reductions in the cellular population for low density *Chlorella Sp.* cultures treated with each ultrasonic system.

Figure 7.6.1 Reduction in the cellular population of *Chlorella Sp.* treated with each ultrasonic system at $25^{\circ}\text{C} \pm 0.5^{\circ}\text{C}$

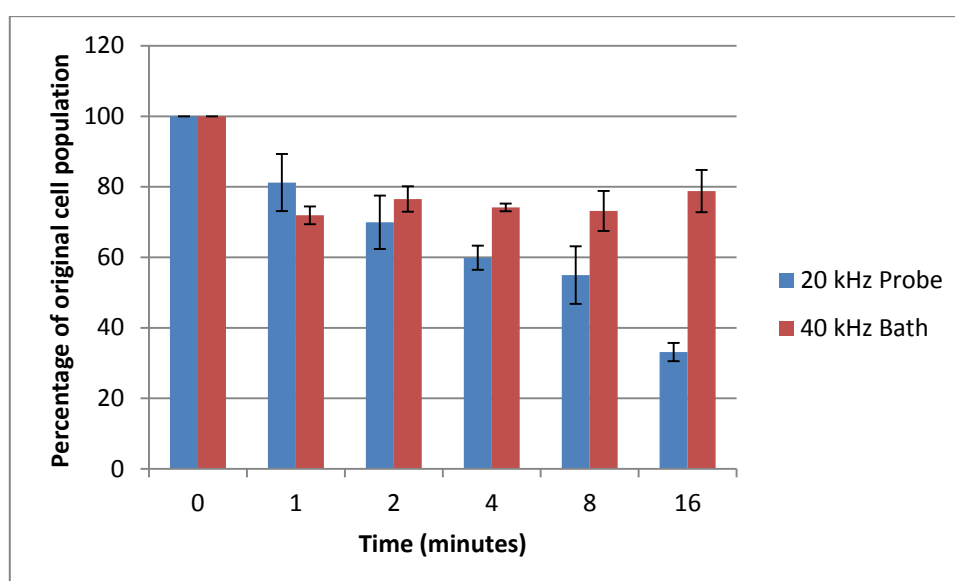
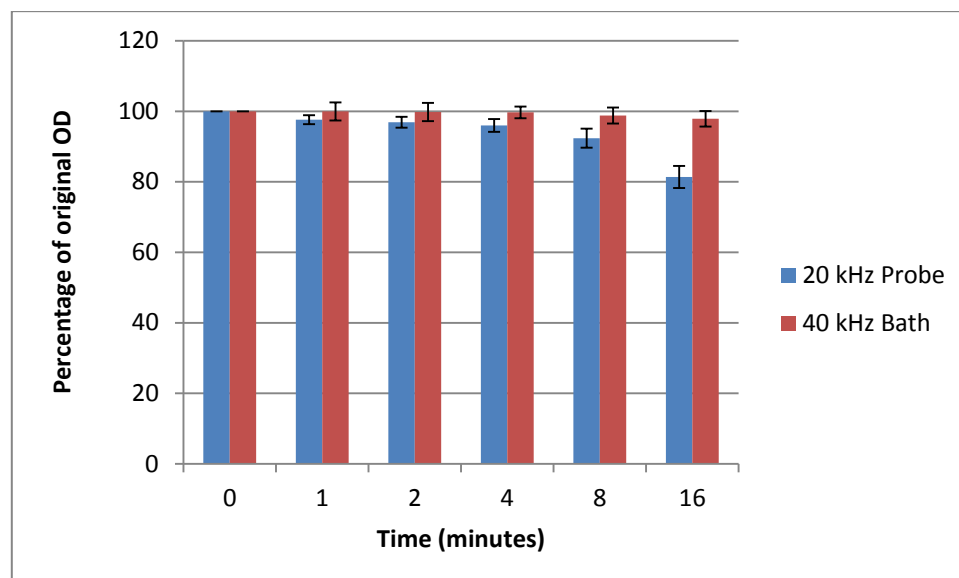


Figure 7.6.1 clearly shows that the 20 kHz probe (40% amplitude, 0.097 W/cm^3) system resulted in the greatest reduction in the *Chlorella Sp.* population of ~65% after 16 minutes treatment ($P = 4.73\text{E}^{-5}$). Although the population continually dropped over 16 minutes, there was not complete cellular reduction with the 20 kHz probe. The 40 kHz bath (0.07 W/cm^3) was less effective than the 20 kHz probe and caused a ~25% reduction in the cellular population of *Chlorella Sp.* ($P = 0.01$). The starting concentration of *Chlorella Sp.* was $\sim 4.6 \times 10^6$ cells/mL.

7.6.2 Effect of ultrasound on the optical density of *Chlorella Sp.*

Optical density measurements at 686 nm were taken to monitor changes in the cellular population of *Chlorella Sp.* as ultrasound was applied. Figure 7.6.2 displays the optical density measurements for low density *Chlorella Sp.* samples treated with both systems expressed as a percentage reduction.

Figure 7.6.2 Percentage reduction in the optical density readings (686 nm) for low density *Chlorella Sp.* treated with the 20 kHz probe system



The above figure shows that the 20 kHz probe and the 40 kHz bath systems cause the optical density of *Chlorella Sp.* to decrease as ultrasound is applied, indicating that ultrasound caused the population to decrease. These findings support the haemocytometer data which indicated that the cellular population decreased as ultrasound was applied. The 20 kHz probe ($P = 0.0003$) caused a greater reduction in OD than the 40 kHz system. The starting OD of *Chlorella Sp.* was ~ 0.44 .

7.6.3 Effect of ultrasound on spectro-fluorophotometer measurements of *Chlorella Sp.*

The spectro-fluorophotometer was employed to detect changes in the level of intracellular chlorophyll as ultrasound was applied. Figure 7.6.3 displays the percentage reduction in the chlorophyll emission peak for low density *Chlorella Sp.* cultures for each ultrasonic system as sonication was applied.

Figure 7.6.3 Effect of ultrasound on the chlorophyll emission peak of *Chlorella Sp.*

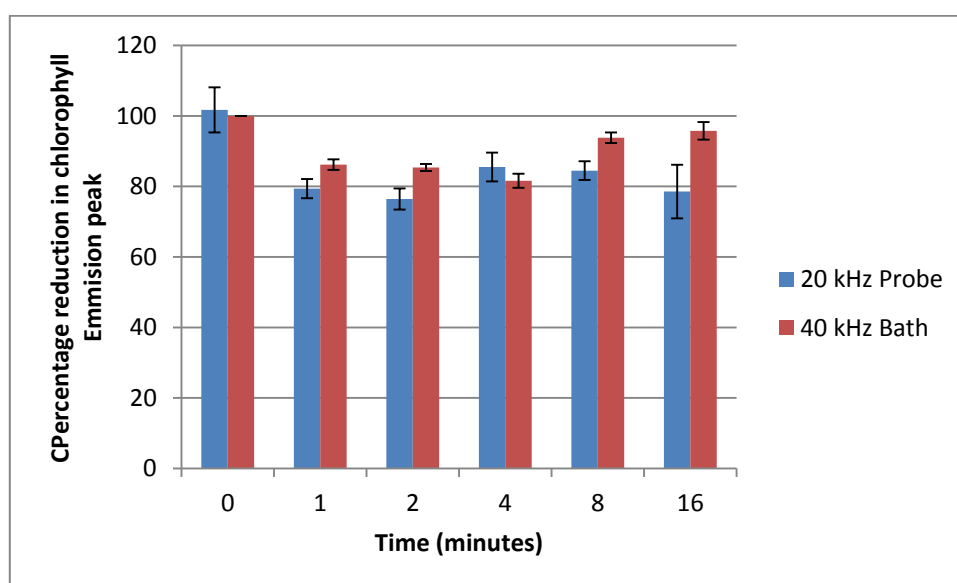


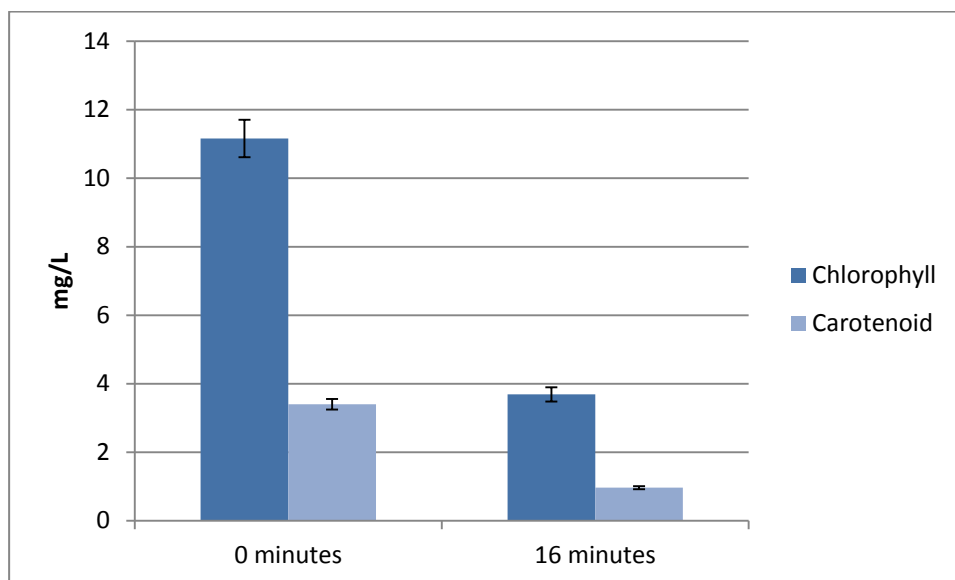
Figure 7.6.3 demonstrates a reduction in the height of the chlorophyll peak as sonication is applied for both of the ultrasonic systems. This indicates that the cells have been ruptured and chlorophyll has been released. There was a greater reduction in the chlorophyll peak when the 20 kHz probe system was employed indicating that this system causes more cellular damage than the 40 kHz bath. The starting height of the chlorophyll emission peak was ~70.3.

7.6.4 Effect of ultrasound on chlorophyll a and carotenoid recovery from *Chlorella Sp.*

The chlorophyll a and carotenoid recovery procedure was carried out to determine the amount of intracellular chlorophyll a and carotenoids within samples. Figure 7.6.4 shows the amount of chlorophyll and carotenoids recovered from an untreated sample and a sample treated using each ultrasonic system after 16 minutes. 16 minutes treatment was employed to determine the effect of prolonged sonication on cells.

Figure 7.6.4 Chlorophyll a and carotenoid recovery from low density *Chlorella Sp.* treated using each ultrasonic system

a. 20 kHz probe



b. 40 kHz bath

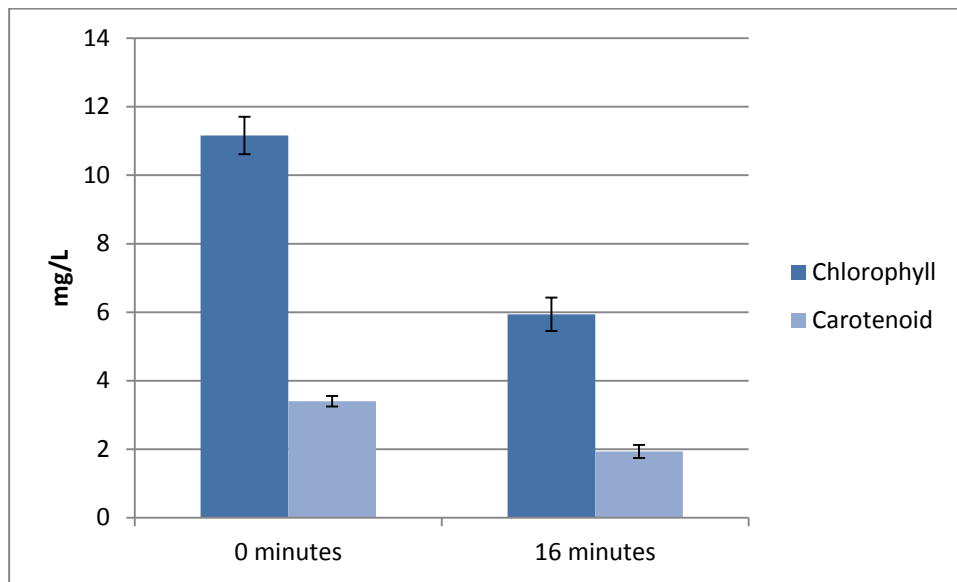
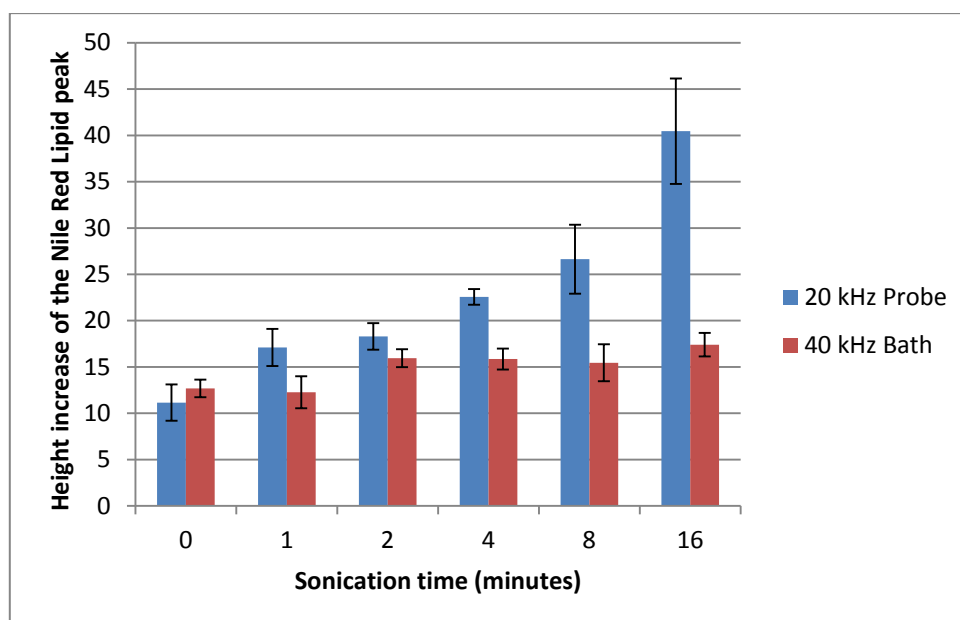


Figure 7.6.4 shows that sonication applied by both ultrasonic systems caused the intracellular chlorophyll and carotenoid levels of *Chlorella Sp.* to drop. This again suggests that ultrasound caused damage to the cell walls of *Chlorella Sp.* and leakage of cell pigments and other materials occurred. The 20 kHz probe system (Chlorophyll $P = 0.07$, carotenoid $P = 0.004$) caused a higher rate of reduction in pigment levels than the 40 kHz bath.

7.6.5 Effect of ultrasound on the intracellular lipids of *Chlorella Sp.* measured by Nile Red spectro-fluorophotometer measurement

Nile Red staining measured by spectro-fluorophotometry was employed to determine the amount of intracellular lipids present before, during and after sonication. This method determined the time interval in which the Nile Red lipid peak was at its highest for *Chlorella Sp.* when treated with each ultrasonic system. This information will indicate when cell membranes and walls have been ruptured allowing increased entry of the Nile Red stain. This time interval will be employed as the sonication time for ultrasound assisted lipid extraction. Figure 7.6.5 displays the increase in the Nile Red lipid peak as ultrasound is applied using both system.

Figure 7.6.5 Lipid peak of low density *Chlorella Sp.* treated with ultrasound measured by spectro-fluorophotometry



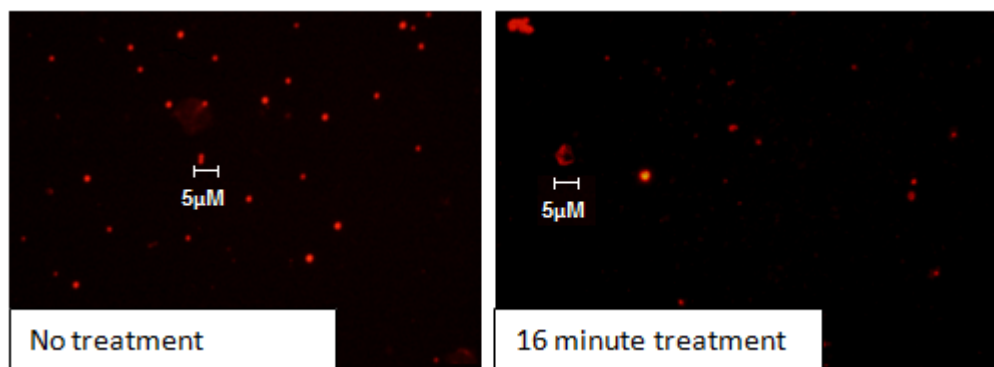
The above figure shows that the lipid peak significantly increases over 16 minutes treatment ($P = 6.67E^{-13}$) using the 20 kHz probe (40% Amplitude 0.097 W/cm^3). This indicates that the cell membrane has been ruptured allowing increased uptake of

Nile Red into the cell. At least 16 minutes sonication using the 20 kHz probe is needed to disrupt the cell membranes of *Chlorella Sp.* causing increased membrane permeability. The 40 kHz bath shows a steady increase in the Nile Red peak as ultrasound is applied, this rate of increase is lower than that of the 20 kHz probe. The 40 kHz bath is therefore not as capable as the 20 kHz probe at causing cellular disruption and increasing the membrane permeability of *Chlorella Sp.*

7.6.6 Effect of ultrasound on *Chlorella Sp.* viewed by microscopy

Fluorescent microscopy (x100 magnification) was employed to visibly determine the state of the *Chlorella Sp.* cells before and after sonication to detect any physiological effects ultrasound may have on the cells. Figure 7.6.6 displays before and after images of a culture of *Chlorella Sp.* treated with the 20 kHz probe. Due to the poor visibility of the cells fluorescent microscopy was employed in order to visualise internal chlorophyll which appears red. The physical state of 100 cells on a slide was observed to determine their condition before and after ultrasonic treatment. These images are displayed in Figure 7.6.6.

Figure 7.6.6 Microscopy images of low density *Chlorella Sp.* treated with the 20 kHz probe



The above figure clearly shows that there are less visible cells and more clumps of debris after sonication with the 20 kHz probe (40% amplitude, 0.097 W/cm^3) for 16 minutes. This indicates that 16 minutes treatment time causes damage to *Chlorella Sp.* Before sonication 100% of the cells were intact and after ultrasonic treatment roughly 65% of the cells were disrupted in the observed field of view.

7.6.7 Effect of the 20 kHz probe (40% Amplitude, 0.097 W/cm³) on the lipid recovery of *Chlorella Sp.* measured gravimetrically

Nile Red analysis determined that 16 minutes treatment with the 20 kHz probe (40% amplitude, 0.097 W/cm³) was the optimum ultrasonic system for increasing the cellular permeability of *Chlorella Sp.* (see section 7.6.5 for more details). Gravimetric lipid determination was carried to detect if ultrasound had an effect on the amount on lipids recovered from *Chlorella Sp.* Figure 7.6.7 shows the lipid recovery from *Chlorella Sp.* using the adapted Bligh and Dyer method with and without sonication.

Figure 7.6.7 Lipid recovery from *Chlorella Sp.* with and without sonication (Adapted Bligh and Dyer method)

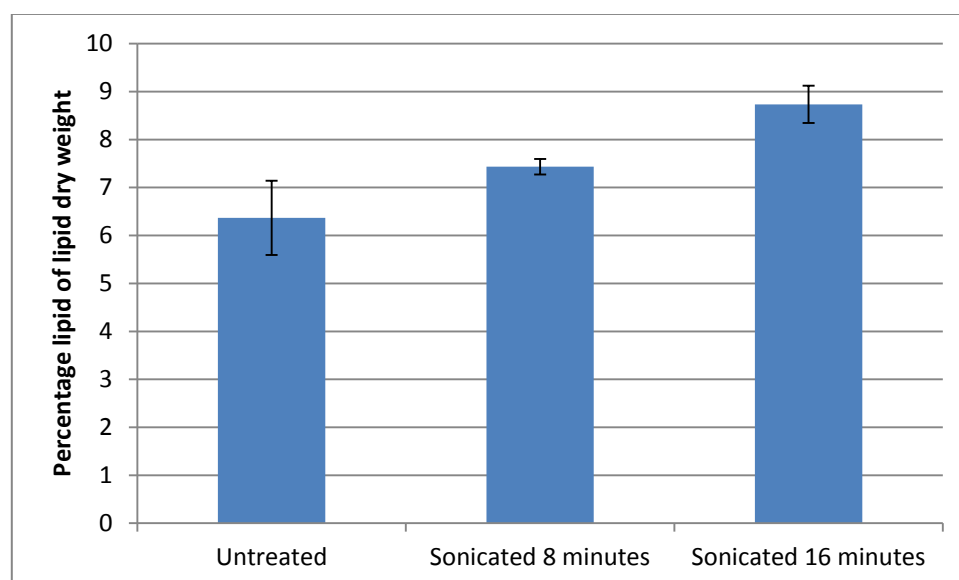


Figure 7.6.7 clearly demonstrates that sonication increases the amount of lipid recovered from *Chlorella Sp.* from ~6.3 - ~8.7% dry biomass. An 8 minute treatment time was included to determine if the Nile Red study was correct in that at least 16 minutes treatment time was need in order to cause a substantial increase in lipid recovery. The 8 minute time interval shows an increase from 6.3 - 7.4% dry biomass, this then increases to 8.7% dry biomass after 16 minutes. This indicated that as

stated with the Nile Red study at least 16 minutes of sonication is needed to improve lipid recovery. If any time interval higher than this was employed, the economical viability of this method will be brought into question due to the amount of power required to run the ultrasonic equipment for prolonged periods of time on large volumes of microalgae.

7.6.8 Summary of the effect of ultrasound on *Chlorella Sp.*

Table 7.6 summarises the effects of ultrasound on *Chlorella Sp.* (200 mL) when treated for 16 minutes with both ultrasonic systems employed. Results are expressed as a percentage.

Table 7.6 Effect of ultrasound on *Chlorella Sp.*

Test employed	20 kHz probe (0.097 W/cm ³)	40 kHz bath (0.07 W/cm ³)
% Reduction in cell population	70	22
% Reduction in OD	19	2
% Reduction in Chlorophyll peak	21	3
% Reduction in chlorophyll estimation	69	47
% Increase in Nile Red lipid peak	80	55
% Increase in lipids recovered from dry biomass using Bligh and Dyer	From 6.3 to 8.7%	N/A

The table above shows that both ultrasonic systems employed have a slightly destructive effect on *Chlorella Sp.* It appears that the 20 kHz probe had the strongest effect as it brought about the greatest reduction in all areas investigated and after 16 minute of treatment the greatest increase in the Nile Red lipid peak. The data suggests that 16 minutes of treatment time is sufficient to cause enough damage to *Chlorella Sp.* to bring about an increase in lipid recovery. This was confirmed by the chloroform:methanol (1:2) extraction, lipid recovery increased from 6.3 - 8.7% dry biomass.

The highest lipid recovery from *Chlorella Sp.* was 8.7% dry biomass. Previous studies from Araujo *et al.* (2012) have stated that the *Chlorella Sp.* species typically have a lipid content between 16 - 52% dry biomass. This indicates that a lipid recovery of 8.7% dry biomass could potentially be greatly improved upon. Section 7.7.4 will report on experiments that investigate stressing techniques to increase the lipid content of *Chlorella Sp.* The data from this section has determined that 16 minutes treatment with the 20 kHz probe (40% amplitude, 0.097 W/cm³) with chloroform: methanol as the extraction solvent should be employed as the lipid extraction method for stressed *Chlorella Sp.* in section 7.7.4.

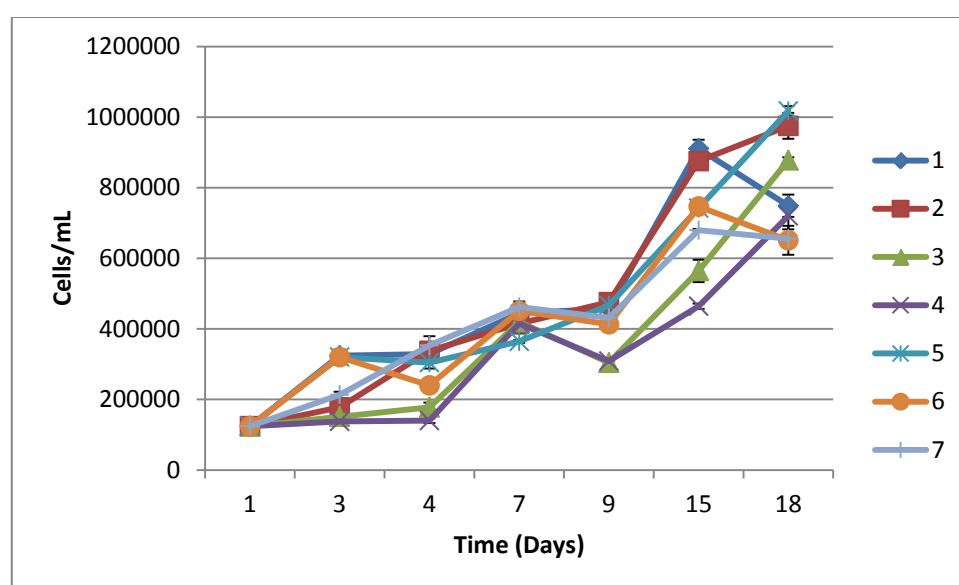
7.7 Optimisation of microalgal lipid content

Stressing methods were carried out on each microalgal species to induce greater lipid production. The following variables were investigated by manipulating growth media; high salinity, nitrogen deprivation and reducing trace metals. During growth haemocytometer readings and optical density measurements at 686 nm were carried out. Nile Red lipid analysis by spectro-fluorophotometer was employed to monitor lipid levels within the microalgal cells. When the optimum conditions for lipid induction in each microalgal species was determined, lipid extraction was undertaken in these same conditions and measured by gravimetric analysis and GC-MS.

7.7.1 Optimisation of the lipid content of *D. salina*

The effect of various stressing methods to promote lipid induction in *D. salina* was analysed on days 1, 3, 5, 7, 9, 15 and 18 growth. Figure 7.7.1 displays the effect of stressing on the cell population of *D. salina* over its growth period.

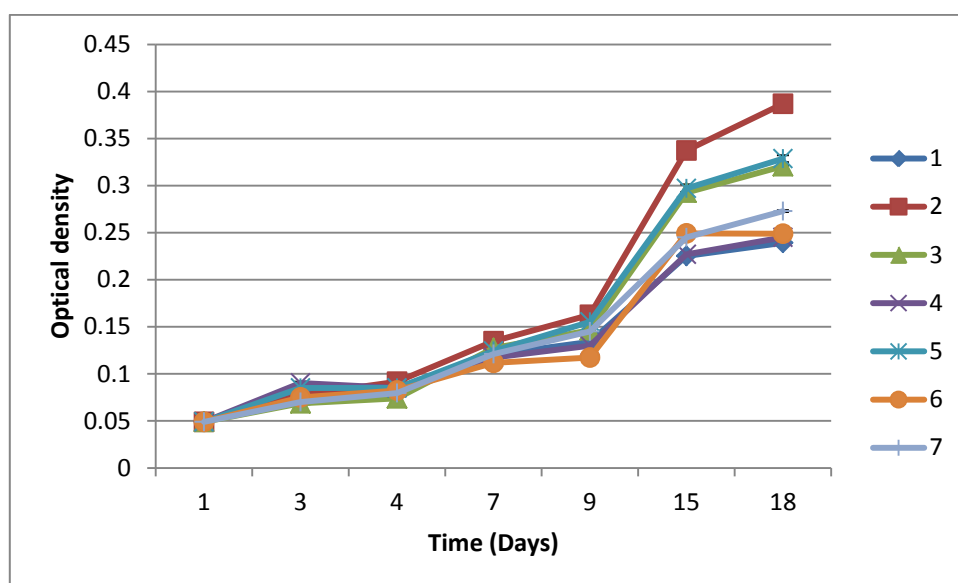
Figure: 7.7.1 Haemocytometer data for the growth of stressed *D. salina*



Key: 1. F/2, 2. F/2 + 30 g/l NaCl, 3. F/2 + 35 g/L NaCl, 4. F/2 media - 25% N, 5. F/2 - 50% N, 6. F/2 - 75% trace metal, 7. F/2 - 50% trace metal.

The above figure shows that all conditions caused similar growth trends in *D. salina*. After 18 days growth *D. salina* stressed with 30 g/L NaCl and 50% reduced Nitrogen concentration produced the highest cellular concentration. Optical density data for the cellular population of *D. salina* is illustrated in Figure 7.7.2.

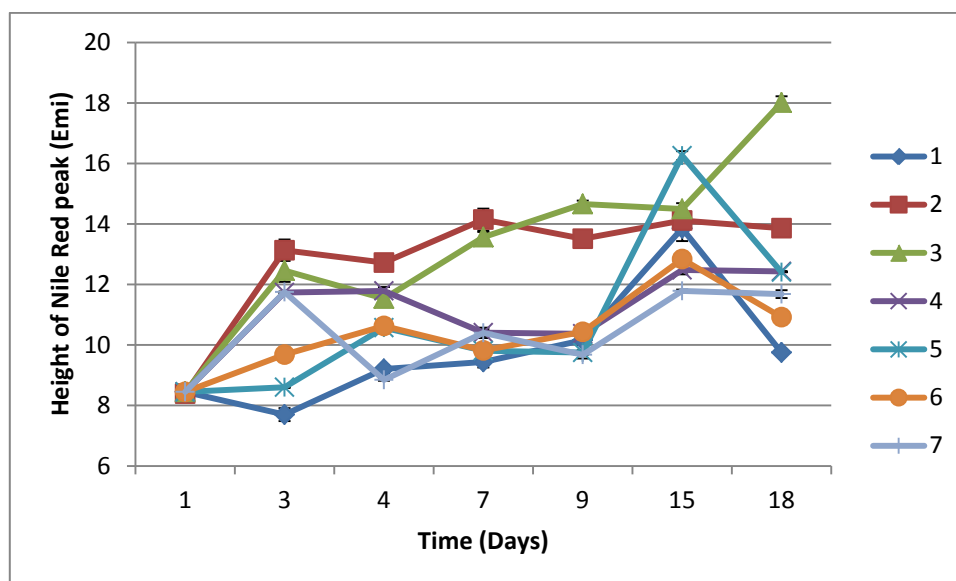
Figure 7.7.2 Optical density measurements (686 nm) for the growth of stressed *D. salina*



Key: 1. F/2, 2. F/2 + 30 g/l NaCl, 3. F/2 + 35 g/L NaCl, 4. F/2 media - 25% N, 5. F/2 - 50% N, 6. F/2 - 75% trace metal, 7. F/2 - 50% trace metal.

As illustrated by the haemocytometer data the above figure shows a steady increase in the optical density for each condition over time, indicating steady microalgal growth. Again as with Figure 7.7.1 F/2 media with 30 g/L NaCl produced the highest increase in optical density. Figure 7.7.3 displays the effect of stressing methods on the intracellular lipid levels of *D. salina* by Nile Red measurement.

Figure 7.7.3 Spectro-fluorophotometer data of Nile Red lipid peak during the growth of stressed *D. salina*

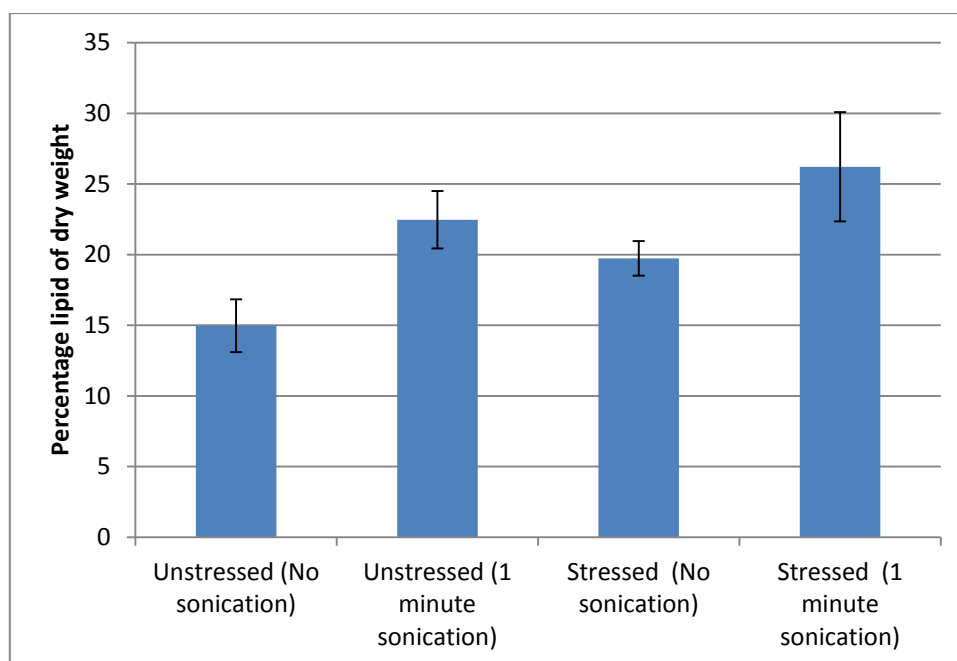


Key: 1. F/2, 2. F/2 + 30 g/l NaCl, 3. F/2 + 35 g/L NaCl, 4. F/2 media - 25% N, 5. F/2 - 50% N, 6. F/2 - 75% trace metal, 7. F/2 - 50% trace metal.

The above figure shows that after 18 days growth the lipid content of *D. salina* stressed with 35 g/L NaCl is significantly higher ($P = 0.001$), being ~95% higher than that of normal F/2 media. This information reveals that out of the conditions tested, for optimum lipid production in *D. salina* F/2 media with NaCl levels increased to 35 g/L should be employed as growth media and cells must be harvested on day 18 of growth. This was carried out and the extraction method previously described was employed to determine any increase in lipid levels. It is notable that microalgae growth and lipid production do not run in parallel, this is because during rapid growth (days 8-15) lipid production is primarily focused on structural lipids. When the most microalgal cells enter a stationary phase (day 15 onwards) lipid production focuses on storage lipids (Sharma *et al.* 2012). Figure 7.7.4 illustrates the lipid recovery yields of both stressed and unstressed *D. salina* when extracted with and

without 1 minute sonication with a 20 kHz probe. An additional Nile Red reading took place on day 25 of growth which depicted a drop in all Nile Red peaks.

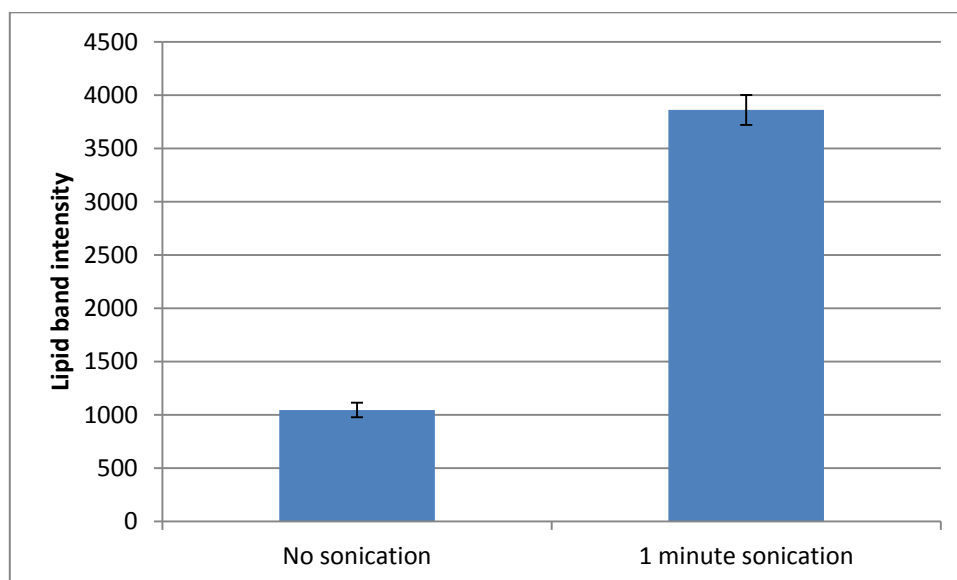
Figure 7.7.4 Gravimetric analysis of stressed *D. salina*



The above figure clearly shows that stressed *D. salina* has higher lipid content than unstressed. What is also obvious from this figure is that ultrasound increased the amount of lipid recovered from *D. salina*. Unstressed lipid recovery levels increased from ~15 - ~22.5% dry biomass when ultrasound was applied and stressed lipid recovery significantly increased from ~19 - ~26% dry biomass ($P = 0.04$). Ultrasound was applied using a 20 kHz probe (40% amplitude, 0.097 W/cm^3) for 1 minute. The first 2 data sets from figure 7.7.4 are taken from figure 7.3.9. Stressed samples were then transesterified and analysed using GC-MS in section 7.8.1.

TLC analysis of the stressed *D. salina* lipid extract was also employed, this provided a quick semi-quantitative measurement of how much lipid was extracted with and without sonication by analysis of the intensity of the lipid band by the ImageJ software. This is displayed in Figure 7.7.5.

Figure 7.7.5 TLC analysis of *D. salina* lipid extract



The data shows that there is a significantly higher lipid band intensity when ultrasound is employed ($P = 0.001$). This indicates a higher lipid concentration is present when ultrasound is employed in the extraction process which concurs with previous gravimetric data. Gouveia and Oliveira (2009) stated that *D. salina* usually has a lipid content between 16-20% dry biomass, 26% dry biomass lipid recovery is larger than 16-20% dry biomass lipid recovery previously reported for a UAE lipid extraction method on *D. salina*.

7.7.2 Optimisation of the lipid content of *N. oculata*

7.7.2.1 Effect of ultrasound combined with beating beads on *N. oculata*

As previously stated in chapter 7.5 none of the ultrasonic systems employed had a strong destructive effect on *N. oculata*. This section will investigate the effect of the 20 kHz probe with a variety of beating beads to see if a stronger disruptive effect is observed. The beads employed were either glass beads (425 - 600 nm) or Guyson Turbobeats (S070 or S110), which were spherical shaped carbon steel beads, the S070 beads were sized between 180 and 350 μ M and the S110 bead was sized between 300 and 500 μ M. Haemocytometer counts, optical density measurements and spectro-fluorophotometer analysis were employed to observe the effects of ultrasound combined with beating beads.

Haemocytometer measurements were employed to monitor changes in the cellular population of *N. oculata* as ultrasound was applied. Figure 7.7.6 displays the reduction in the cellular population for low density *N. oculata* cultures treated with the 20 kHz probe with beating beads.

Figure 7.7.6 Reduction in the cellular population of low density *N. oculata* treated with the 20 kHz probe with beating beads

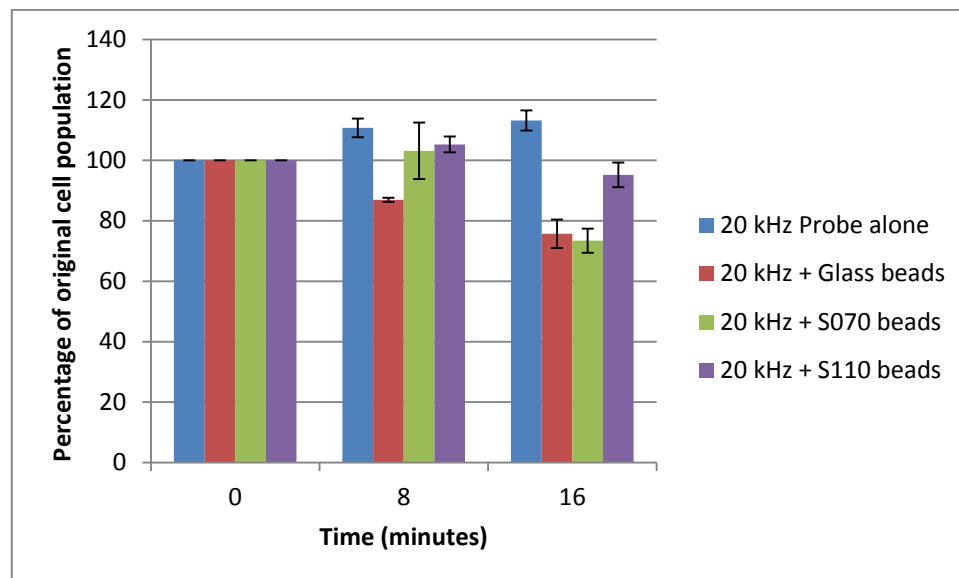
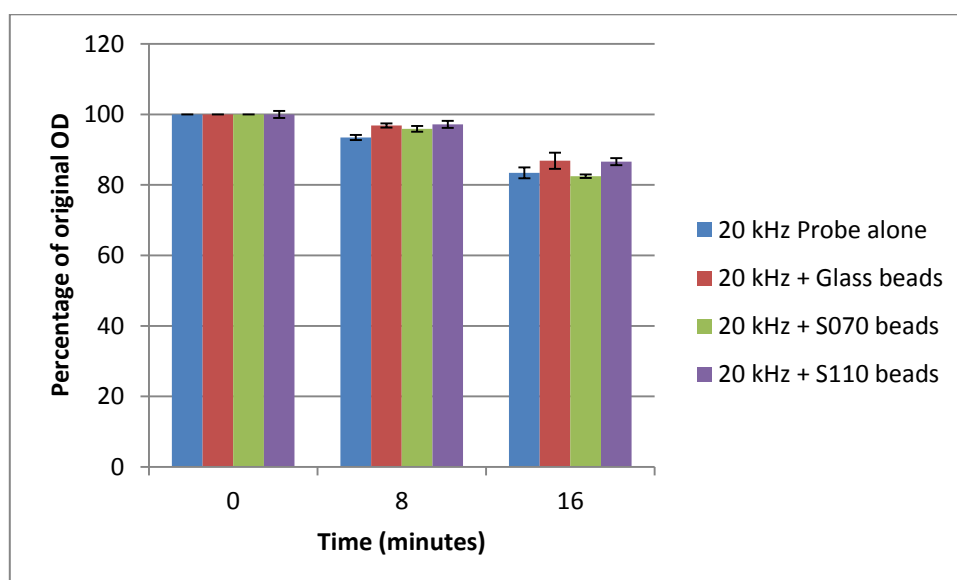


Figure 7.7.6 shows that ultrasound combined with bead beating causes a reduction in the cell population of *N. oculata*. The highest reduction was from ultrasound combined with the S070 beads which produced a 26% reduction in the cell population ($P = 0.03$). This data suggests that a 20 kHz probe combined with bead beating can cause greater cellular disruption to *N. oculata* than ultrasound alone. The starting concentration of *N. oculata* was $\sim 2.4 \times 10^6$ cells/mL.

Optical density measurements at 686 nm were taken to monitor changes in the cellular population. Figure 7.7.7 displays the optical density measurements for low density *N. oculata* samples treated with the 20 kHz probe with beating beads.

Figure 7.7.7 Percentage reduction in the optical density readings (686 nm) for low density *N. oculata* treated with the 20 kHz probe with beating beads



Optical density data has revealed that ultrasound combined with beating beads causes a drop in the optical density of *N. oculata*. The greatest drop (18%) resulted from the 20 kHz probe employed with S070 beating beads ($P = 1.6E^{-14}$), which agrees with the haemocytometer data and suggests that this system is the most aggressive in terms of cell disruption. The starting OD was ~0.74.

The spectro-fluorophotometer was employed to detect changes in the level of intracellular chlorophyll as ultrasound was applied. Figure 7.7.8 displays the percentage reduction in the chlorophyll emission peak for low density *N. oculata* cultures treated with the 20 kHz probe and beating beads.

Figure 7.7.8 Effect of ultrasound on the chlorophyll emission peak of *N. oculata* treated with the 20 kHz probe with beating beads

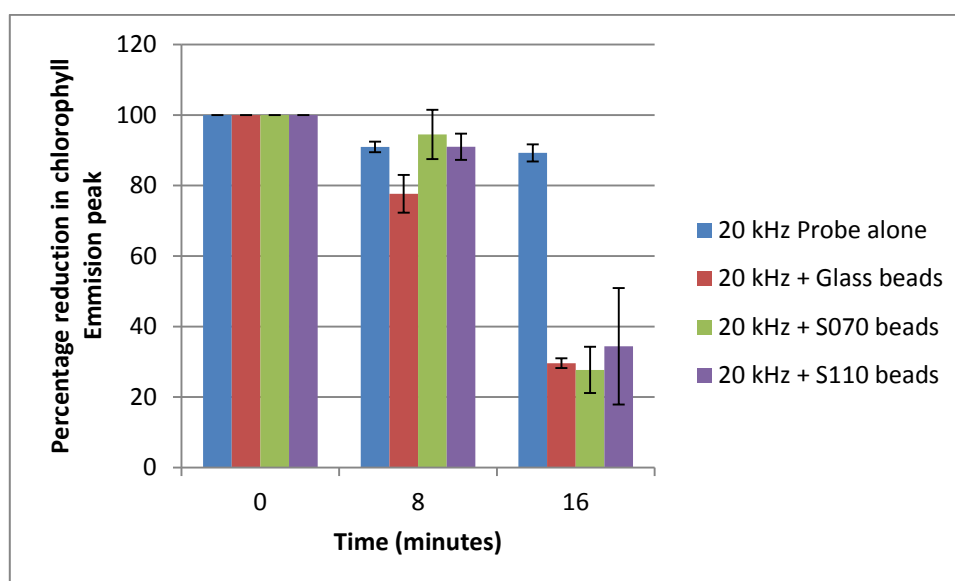


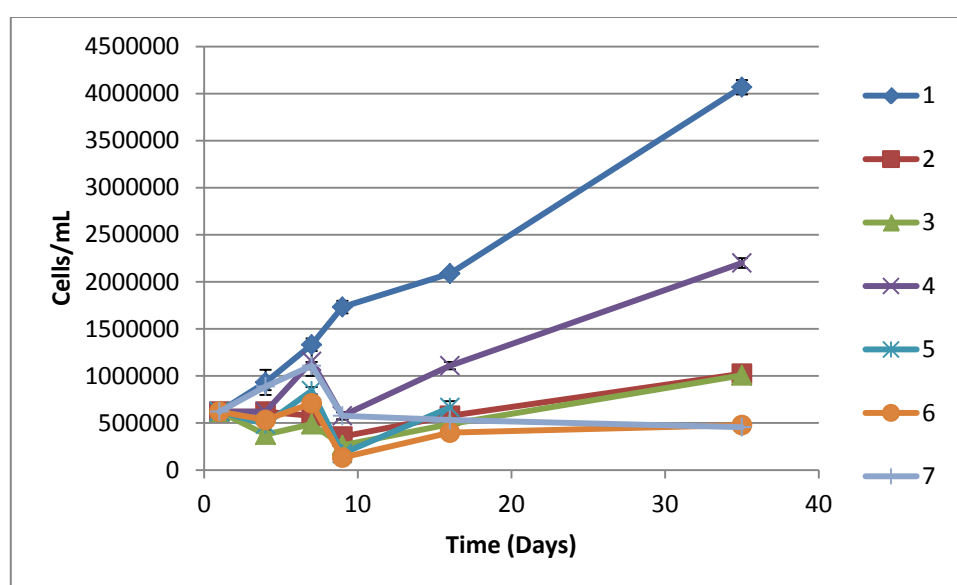
Figure 7.7.8 demonstrates that all beating beads cause a rapid reduction in the intracellular chlorophyll concentration of *N. oculata*. The largest reduction (72%) was again from the 20 kHz probe combined with S070 beads ($P = 0.001$). This agrees with previous data (from figures 7.7.6 and 7.7.7) which strongly suggests that this system causes the greatest cellular damage to *N. oculata*. The starting height of the chlorophyll emission peak was ~153.5.

The data gathered strongly suggests that of the treatments tested, ultrasound combined with the S070 beads has the greatest disruptive effect on *N. oculata*. This may be due to the fact that these beads were the smallest size employed out of the 3 beads (180-300 μM). The small size and low weight allowed more bead movement in the medium when exposed to ultrasound, increasing the chances of contact with the *N. oculata* cells and causing a disruptive effect. This system was employed on *N. oculata* when the optimum stressing conditions are established; this is described later in this section.

7.7.2.2 Stress induced lipid induction of *N. oculata*

The effect of various stressing methods to promote lipid induction in *N. oculata* was analysed on days 1, 3, 5, 7, 9, 16 and 35. Figure 7.7.9 displays the effect of stressing on the cell population of *N. oculata* over its growth period.

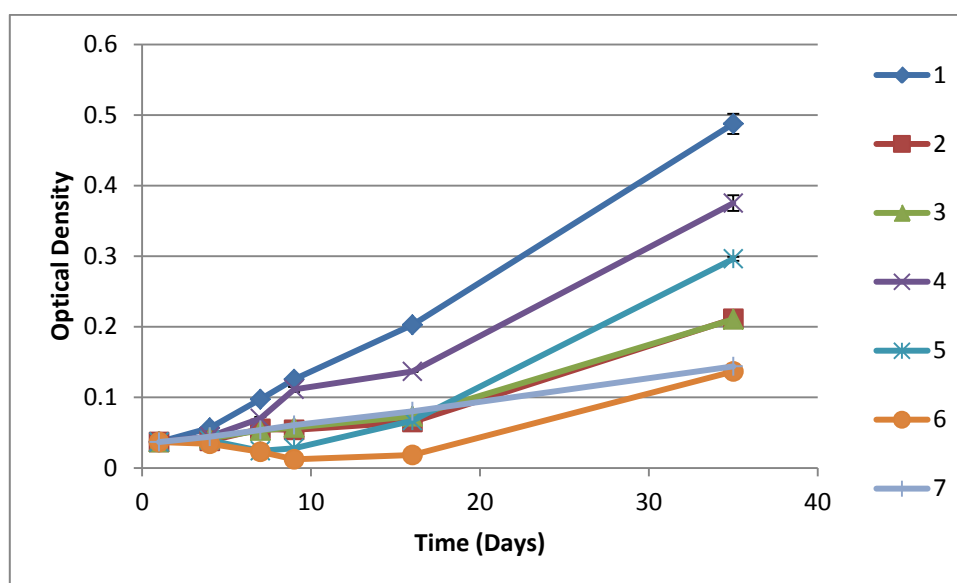
Figure 7.7.9 Haemocytometer data for the growth of stressed *N. oculata*



Key: 1. F/2, 2. F/2 + 30 g/l NaCl, 3. F/2 + 35 g/L NaCl, 4. F/2 media - 25% N, 5. F/2 - 50% N, 6. F/2 - 75% trace metal, 7. F/2 - 50% trace metal.

The above figure shows that most conditions caused similar growth trends in *N. oculata*. After 35 days growth the original F/2 growth media produced the highest cellular concentration, indicating that F/2 media is well suited for *N. oculata* growth. The data also shows that removing trace metals from F/2 induces a stationary phase of growth, highlighting its importance. Optical density data for the cellular population of *N. oculata* is provided in Figure 7.7.10.

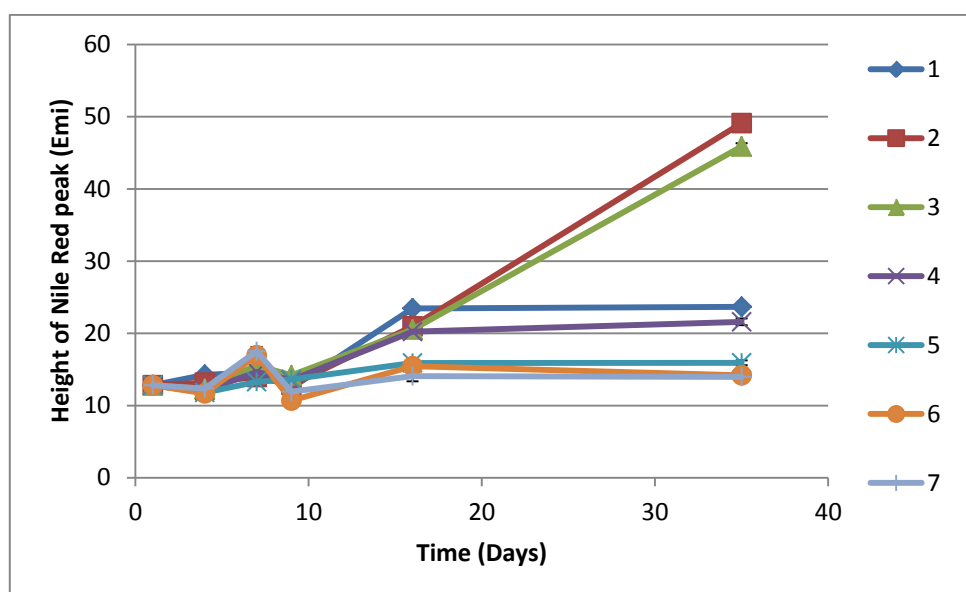
Figure 7.7.10 Optical density measurements (686 nm) for the growth of stressed *N. oculata*



Key: 1. F/2, 2. F/2 + 30 g/l NaCl, 3. F/2 + 35 g/L NaCl, 4. F/2 media - 25% N, 5. F/2 - 50% N, 6. F/2 - 75% trace metal, 7. F/2 - 50% trace metal.

As illustrated with the haemocytometer data the above figure shows a steady increase in the optical density for each stressing condition over time, indicating steady microalgal growth. Again as with Figure 7.7.9, F/2 media without any additional stress factors produced the greatest increase in optical density. Figure 7.7.11 displays the effect that stressing methods have on the intracellular lipid levels of *N. oculata* expressed as a percentage by Nile Red measurement.

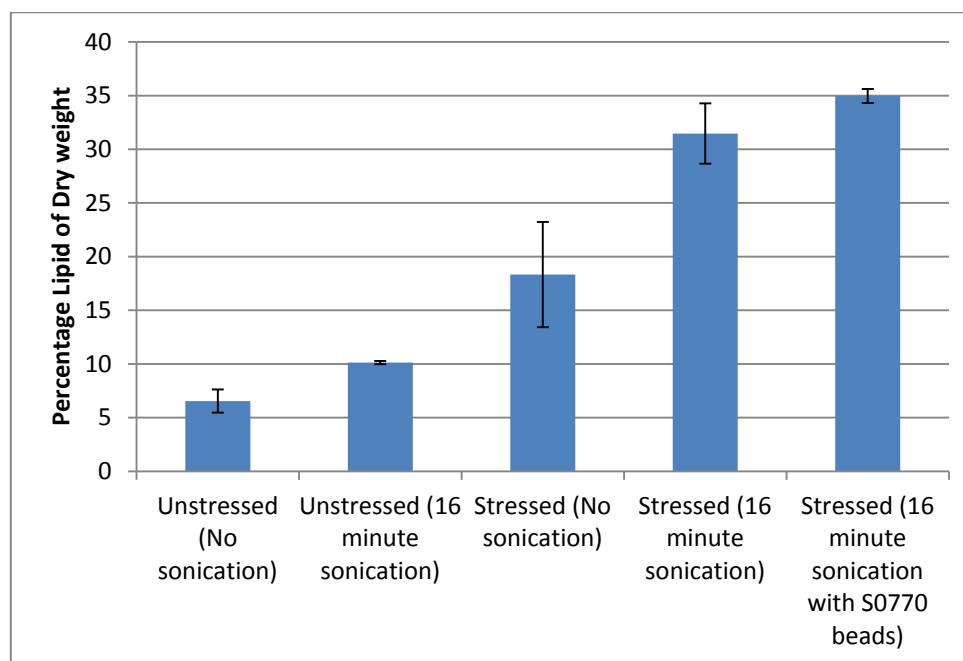
Figure 7.7.11 Spectro-fluorophotometer data of Nile Red lipid peak during the growth of stressed *N. oculata*



Key: 1. F/2, 2. F/2 + 30 g/l NaCl, 3. F/2 + 35 g/L NaCl, 4. F/2 media - 25% N, 5. F/2 - 50% N, 6. F/2 - 75% trace metal, 7. F/2 - 50% trace metal.

The above figure shows that after 35 days growth the lipid content of *N. oculata* stressed with 30 g/L NaCl is significantly greater ($P = 0.0004$), being ~200% higher than that of normal F/2 media. The obvious trend here is that increased salinity induces higher levels of intracellular lipids. This information reveals that for optimum lipid production in *N. oculata* F/2 media with an additional 30 g/L NaCl should be employed and cells must be harvested after 35 days of growth. This was carried out and the extraction method previously described was employed to determine any increase in lipid recovery levels. Figure 7.7.12 displays the original extractions with unstressed *N. oculata* and extractions with stressed *N. oculata*, both examples show values with and without sonication. Stressed samples were also sonicated with S070 beating beads.

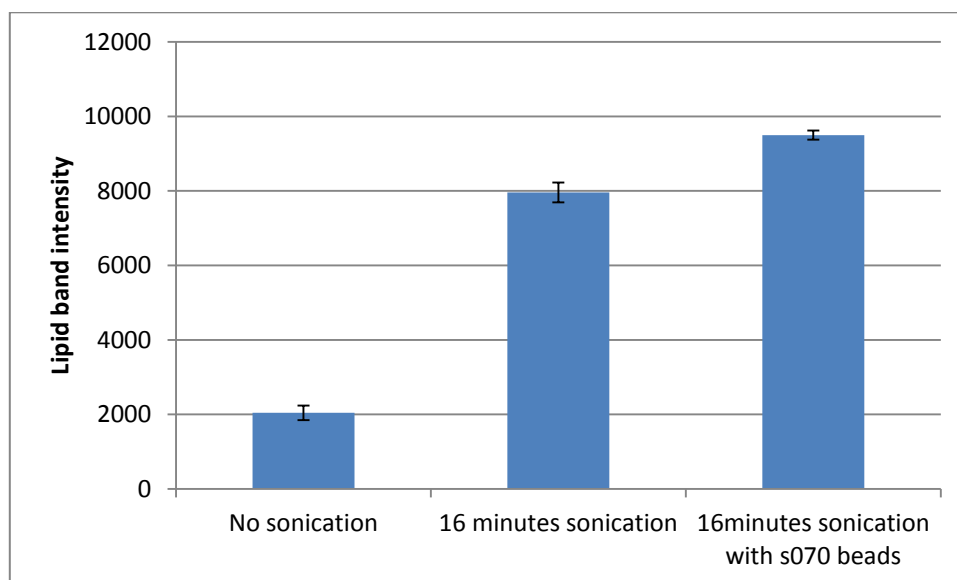
Figure 7.7.12 Gravimetric analysis of stressed *N. oculata*



The above figure shows that stressed *N. oculata* has a higher lipid content than when unstressed. What is also obvious from this figure is that ultrasound increases the amount of lipid recovered from *N. oculata*. Unstressed lipid recovery levels increased from 6.6 - 10% dry biomass when ultrasound was applied and when stressed lipid recovery significantly increased from 18 to 31.5% dry biomass ($P = 0.047$) when ultrasound was applied. When beating beads were applied in conjunction with ultrasound lipid recovery was significantly higher at 35% dry biomass ($P = 0.045$). Ultrasound was applied using a 20 kHz probe (40% amplitude, 0.097 W/cm^3) for 16 minutes. The first 2 data sets from figure 7.7.12 are taken from figure 7.4.9. Stressed samples were then transesterified and analysed using GC/MS outlined in section 7.8.2.

TLC analysis of the stressed *N. oculata* lipid extract was also employed. This provided a rapid semi-quantitative measurement of how much lipid was extracted with and without sonication by analysing of the intensity of the lipid band with the ImageJ software. This is displayed in Figure 7.7.13.

Figure 7.7.13 TLC analysis of *N. oculata* lipid extract

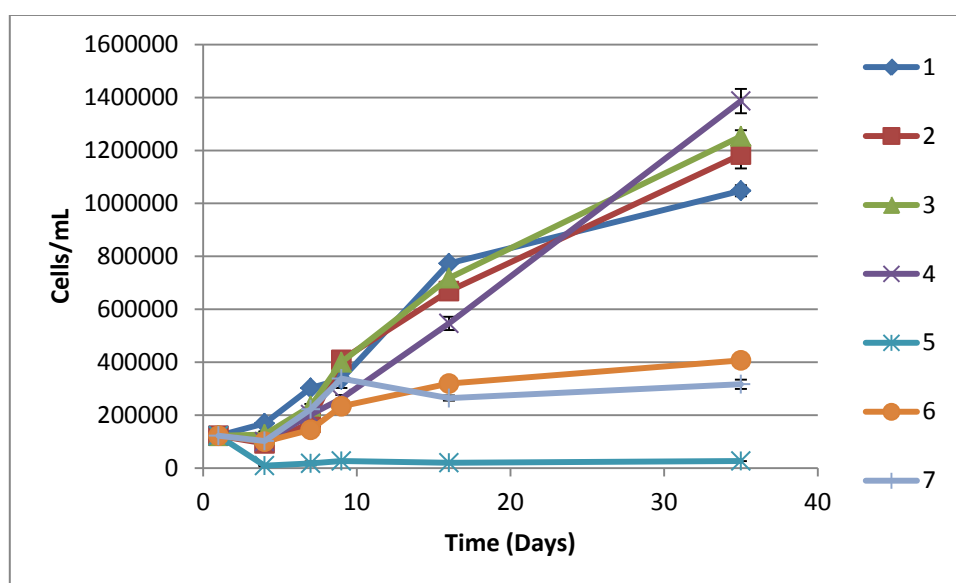


The data above shows a significantly higher lipid band intensity when ultrasound is employed ($P = 0.0001$) and a further increase is also observed when ultrasound is employed with the S070 beads ($P = 8.31E^{-5}$). This indicates a higher lipid concentration is recovered when ultrasound and beads are employed which concurs with previous gravimetric data. Gouveia and Oliveira (2009) indicated that *N. oculata* usually has a lipid content of around 23% dry biomass, however Araujo *et al.* (2011) stated that when stressed the lipid content of *N. oculata* can reach as high as 28.7% dry biomass. A 31% dry biomass lipid recovery with ultrasound is greater than this and the 35% dry biomass lipid recovery by employing the 20 kHz probe with S070 beads is larger still.

7.7.3 Optimisation of the lipid content of *C. concordia*

The effect of the various stressing methods to promote lipid induction in *C. concordia* were analysed on days 1, 3, 5, 7, 9, 16 and 35 of growth. Figure 7.7.14 displays the effect of stressing on a cell population of *C. concordia* over its growth period.

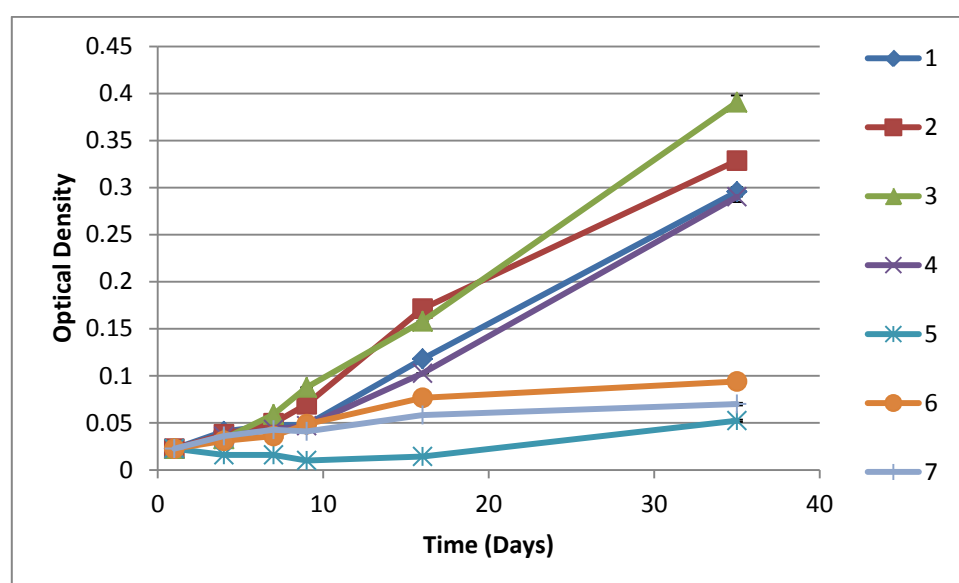
Figure 7.7.14 Haemocytometer data for the growth of stressed *C. concordia*



Key: 1. F/2, 2. F/2 + 30 g/l NaCl, 3. F/2 + 35 g/L NaCl, 4. F/2 media - 25% N, 5. F/2 - 50% N, 6. F/2 - 75% trace metal, 7. F/2 - 50% trace metal.

The above figure shows that most conditions caused similar growth trends in *C. concordia*. After 35 days growth the media containing 25% reduced nitrogen produced the highest cellular concentration, both sets F/2 media with increased salinity closely followed, data also showed that removing trace metals from F/2 and reducing the nitrogen concentration by 50% brings about a stationary phase of growth. Optical density data for the cellular population of *N. oculata* is provided in Figure 7.7.15.

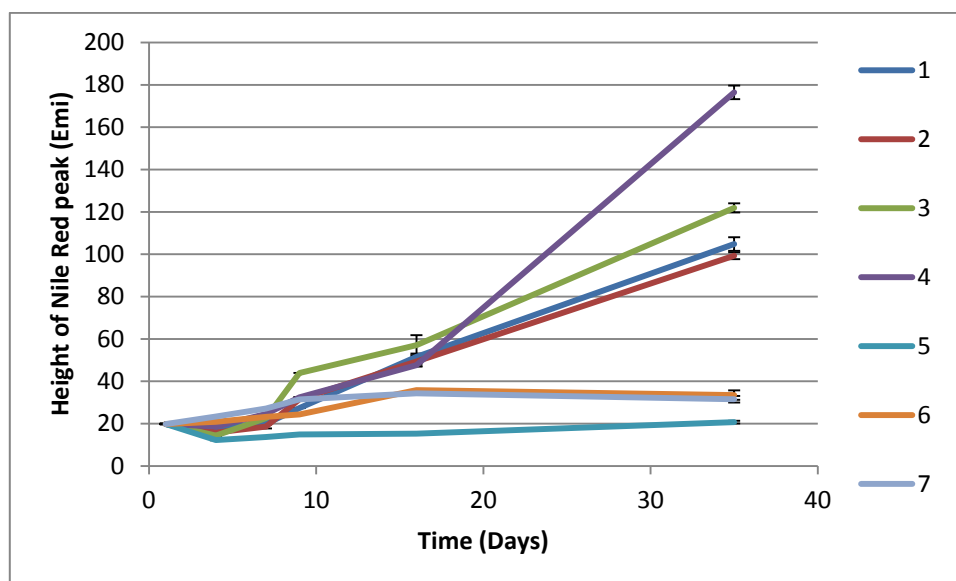
Figure 7.7.15 Optical density measurements (686 nm) for the growth of stressed *C. concordia*



Key: 1. F/2, 2. F/2 + 30 g/l NaCl, 3. F/2 + 35 g/L NaCl, 4. F/2 media - 25% N, 5. F/2 - 50% N, 6. F/2 - 75% trace metal, 7. F/2 - 50% trace metal.

The above optical density data mirrors Figure 7.7.14 which illustrates that removing trace metals from F/2 and reducing the nitrogen concentration by 50% brings about a stationary phase. The other 4 conditions show a rapid rise in optical density with F/2 with 35 g/L NaCl being the highest. Figure 7.7.16 displays the effect of stressing methods on intracellular lipid levels of *C. concordia* by Nile Red measurement.

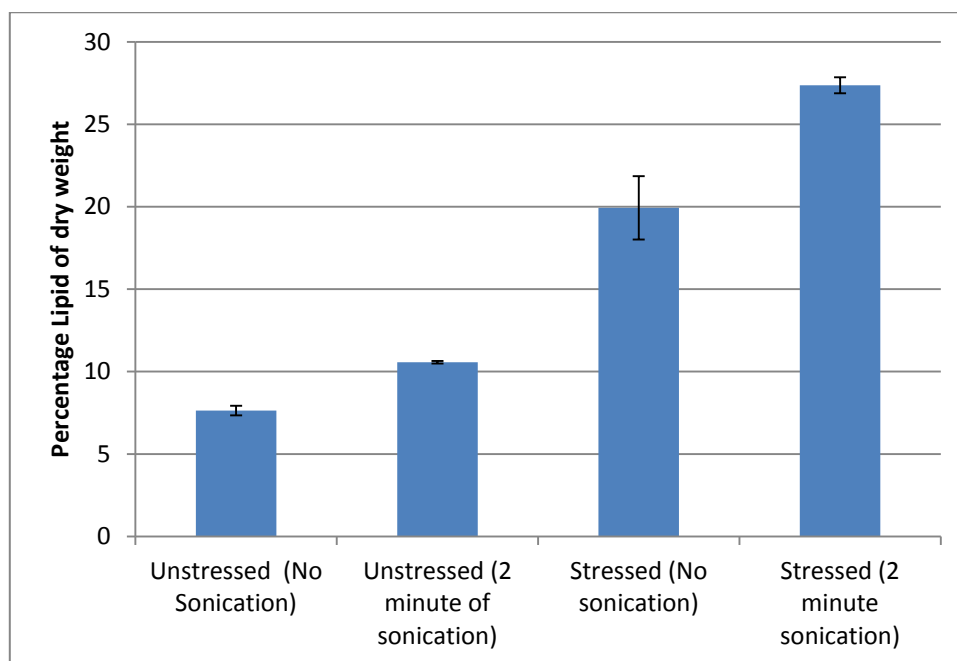
Figure 7.7.16 Spectro-fluorophotometer data of Nile Red lipid peak during the growth of stressed *C. concordia*



Key: 1. F/2, 2. F/2 + 30 g/l NaCl, 3. F/2 + 35 g/L NaCl, 4. F/2 media - 25% N, 5. F/2 - 50% N, 6. F/2 - 75% trace metal, 7. F/2 - 50% trace metal.

The above figure shows that after 35 days growth the lipid content of *C. concordia* stressed with a nitrogen concentration reduced by 25% is significantly higher ($P = 0.0002$), ~70% higher than that of normal F/2 media. This information reveals that for optimum lipid production in *C. concordia* F/2 media with nitrogen levels reduced by 25% should be employed as growth media and cells must be harvested on day 35 of growth. This was carried out and the extraction methods previously described was employed to determine any increase in lipid recovery levels. Figure 7.7.17 displays the original extractions with unstressed *C. concordia* and extractions with stressed *C. concordia*, both examples show values with and without sonication.

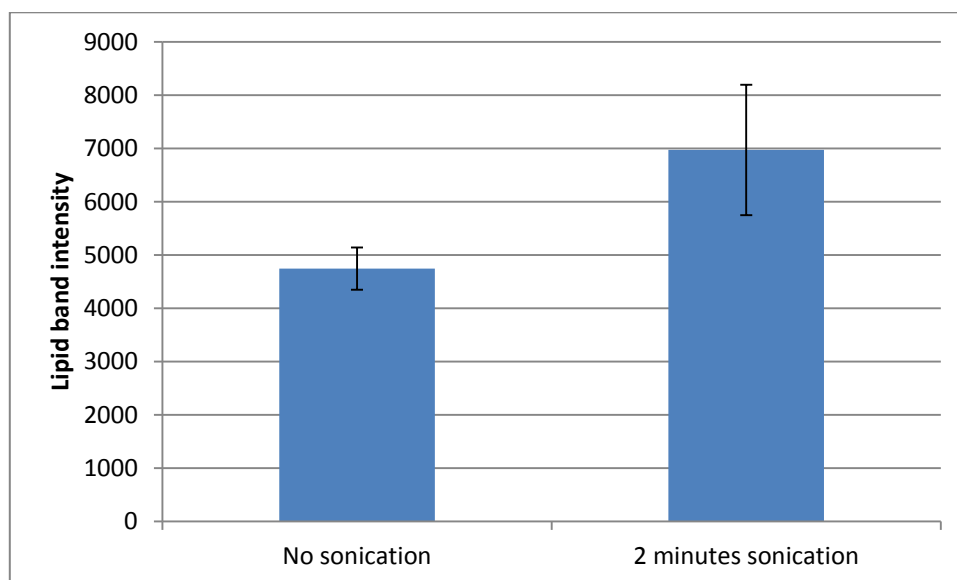
Figure 7.7.17 Gravimetric analysis of stressed *C. concordia*



The above figure clearly shows that the stressed *C. concordia* has a higher lipid content than when unstressed. What is also obvious from this figure is that ultrasound increases the amount of lipid recovered from *C. concordia*. Unstressed lipid recovery levels increased from 7 - 10% dry biomass when ultrasound was applied and stressed lipid recovery significantly increased from 20 - 27% dry biomass ($P = 0.037$). Ultrasound was applied using the 20 kHz probe (40% amplitude, 0.097 W/cm^3) for 2 minutes. The first 2 data sets from figure 7.7.17 were taken from figure 7.5.7. Stressed samples were then transesterified and analysed using GC/MS in section 7.8.3.

TLC analysis of the *C. concordia* lipid extract was also employed; providing a quick semi-quantitative measurement of how much lipid was extracted with and without sonication by analysis of the intensity of the lipid band by the ImageJ software, which is displayed in Figure 7.7.18.

Figure 7.7.18 TLC analysis of *C. concordia* lipid extract

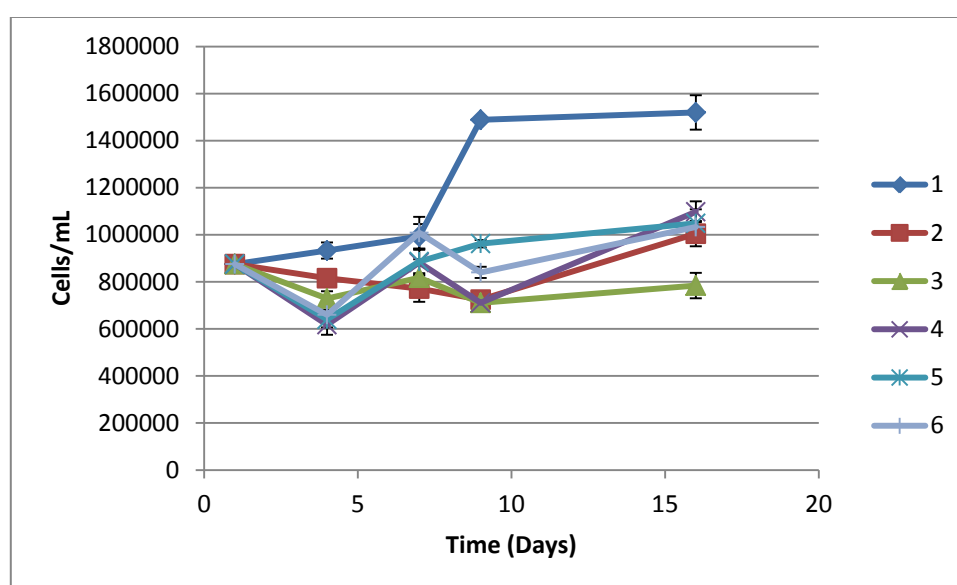


The data shows that there is a significantly higher lipid band intensity when ultrasound was employed. This indicates a higher lipid concentration is recovered when ultrasound is employed which agrees with previous gravimetric data. Currently there are no reported lipid extractions of *C. concordia* on record in literature, therefore the 27% dry biomass lipid recovery achieved here constitutes the highest recovery rate known. Yoo *et al.* (2012) stated that *C. reinhardtii* (a close relative of *C. concordia*) usually has a lipid content of 25-35% dry biomass. This suggest that either *C. concordia* may not be able to produce as high a lipid content as *C. reinhardtii* due to slight differences in physiology or secondly there may be room for potential improvements in the extraction or optimisation methods.

7.7.4 Optimisation of the lipid content of *Chlorella Sp.*

The effect of the various stressing methods to promote lipid induction in *Chlorella Sp.* were analysed on days 1, 3, 5, 7, 9, and 16 of growth. Figure 7.7.19 displays the effect of stressing on the cell population of *Chlorella Sp.* over its growth period.

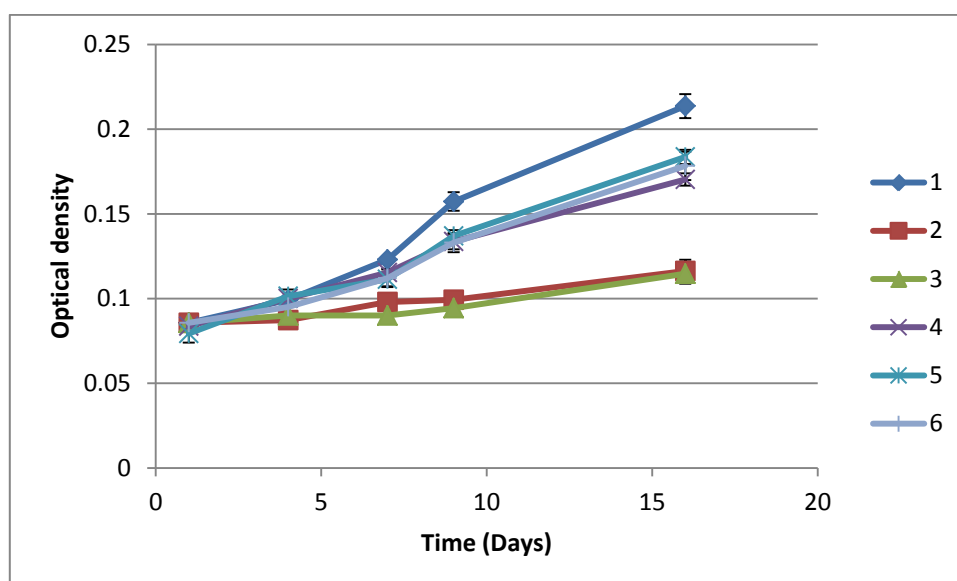
Figure 7.7.19 Haemocytometer data for the growth of stressed *Chlorella Sp.*



Key: 1. BBM +3 N, 2. BBM +3 N + 30 g/l NaCl, 3. BBM +3 N + 35 g/L NaCl, 4. BBM +3 N media - 25% N, 5. BBM +3 N - 50% N, 6. BBM +3 N - 50% trace metal.

The above figure shows that BBM +3N produced the highest cellular concentration for *Chlorella Sp.*, all other stressing conditions produced lower cellular concentrations after 18 days growth. Optical density data for the cellular population of *Chlorella Sp.* is illustrated in Figure 7.7.20.

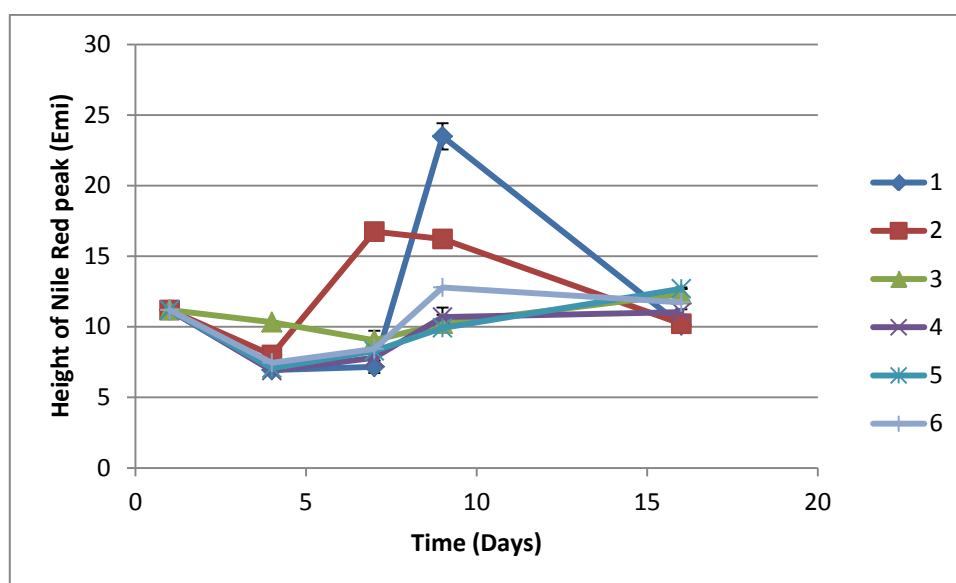
Figure 7.7.20 Optical density measurements (686 nm) of the growth of stressed *Chlorella Sp.*



Key: BBM +3 N, 2. BBM +3 N + 30 g/l NaCl, 3. BBM +3 N + 35 g/L NaCl, 4. BBM +3 N media - 25% N, 5. BBM +3 N - 50% N, 6. BBM +3 N - 50% trace metal.

The above figure concurs with Figure 7.7.19, which illustrated that BBM + 3N produced the highest optical density measurement over 18 days growth. This again indicates that BBM +3N is the correct media for the growth of *Chlorella Sp.*, its growth was not affected by the stressing methods employed. Figure 7.7.21 displays the effect of the stressing methods on the intracellular lipid levels of *Chlorella Sp.* by Nile Red measurement.

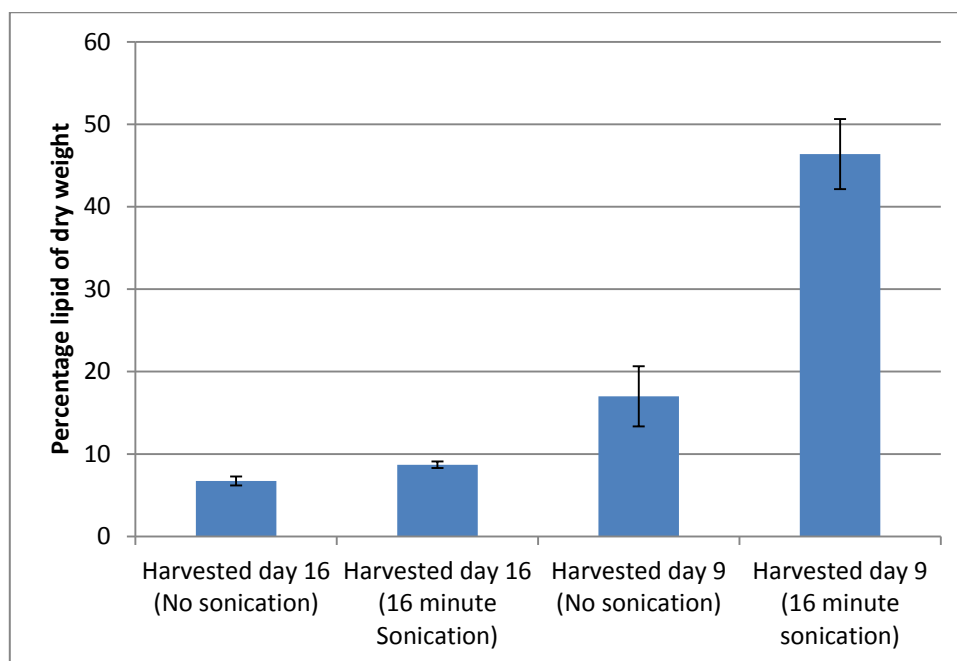
Figure 7.7.21 Spectro-fluorophotometer data of Nile Red lipid peak during the growth of stressed *Chlorella Sp.*



Key: BBM +3 N, 2. BBM +3 N + 30 g/l NaCl, 3. BBM +3 N + 35 g/L NaCl, 4. BBM +3 N media - 25% N, 5. BBM +3 N - 50% N, 6. BBM +3 N - 50% trace metal.

The above figure shows that after 9 days growth the lipid content of *Chlorella Sp.* using BBM +3N peaks at level which is at least ~25% higher than all of the stressed cultures ($P = 0.001$). This indicates that stressing is not necessary for lipid induction in *Chlorella Sp.*, BBM +3N should be employed as the growth media and cells must be harvested on day 9 of growth. A possible explanation for this is that there is more storage lipids present in *Chlorella Sp.* cells on day 9 as these cells are at the end of the log phase of their growth. After day 9 these storage lipids are used up as the cells are in the stationary growth phase. *Chlorella* was cultured as described and the extraction method previously described was employed to determine any increase in lipid recovery levels. Figure 7.7.22 displays the original extractions with unstressed *Chlorella Sp.* and extractions with stressed *Chlorella Sp.*, both examples show values with and without sonication.

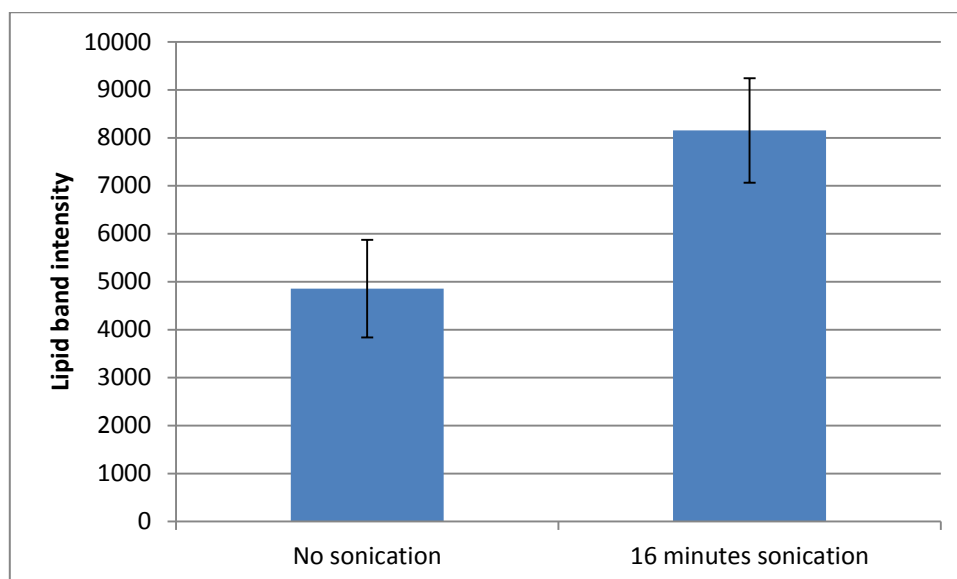
Figure 7.7.22 Gravimetric analysis of stressed *Chlorella Sp.*



The above figure shows that *Chlorella Sp.* which was harvested after 9 days has higher lipid content than when harvested on 16 days. What is also obvious from this figure is that ultrasound increases the amount of lipid recovered from *Chlorella Sp.* When harvested after 16 days lipid recovery levels increased from 6.3 – 8.7% dry biomass when ultrasound was applied and when harvested after 9 days lipid recovery significantly increased from 17 to 44% dry biomass ($P = 0.01$). Ultrasound was applied by the 20 kHz probe (40% amplitude, 0.097 W/cm^3) for 16 minutes. The first 2 data sets from figure 7.7.22 were taken from figure 7.6.7. Stressed samples were then transesterified and analysed using GC-MS outlined in section 7.8.4.

TLC analysis of the *Chlorella Sp.* lipid extract was also employed, providing a quick semi-quantitative measurement of how much lipid was recovered with and without sonication by analysis of the intensity of the lipid band by the ImageJ software. This is displayed in Figure 7.7.23.

Figure 7.7.23 TLC analysis of *Chlorella Sp.* lipid extract



The above data shows there is a significantly higher lipid band intensity when ultrasound is employed. This indicates a higher lipid concentration is recovered when ultrasound is employed which concurs with previous gravimetric data. Araujo *et al.* (2013) stated that *Chlorella Sp.* employed in their study achieved a lipid recovery of 52% dry biomass. This is higher than the 44% dry biomass lipid recovery from *Chlorella Sp.* in this study. Possible reasons for this may be that the strain of *Chlorella Sp.* employed in this study may not be able to produce a lipid content as high as the strain used in the Araujo study due to physiological differences. There also may be room for potential improvement in the extraction or optimisation methods. It is also worth noting that a total of 60 minutes sonication was employed in the method by Araujo *et al* which achieved this 52% dry biomass lipid recovery in comparison to the 16 minutes employed in this study for a 44% dry biomass lipid recovery. Long extraction times may not be acceptable in a carbon neutral method as the amount of power needed to sustain this length of sonication could potentially be large. It may be possible to reduce the ultrasonic treatment time from 16 minutes

by employing beating beads in conjunction with ultrasound as shown with *N. oculata* (see section 7.7.2.1). This may cause a similar level of cellular disruption in quicker time. The potential economic impacts of ultrasound assisted extraction methods are discussed further in chapter 8.

7.7.5 Summary of optimisation results

This section has determined the ideal culturing and harvesting conditions to bring about higher lipid yields for the four microalgal species employed.

- *D. salina* requires growth in F/2 medium enriched with 35 g/L additional NaCl. Harvesting must take place between day 15 and 18 and this will cause an increase in lipid induction resulting lipid recovery increasing from 22.5 - 26% dry biomass when ultrasound was employed in the extraction method.
- *N. oculata* requires growth in F/2 medium enriched with 30 g/L additional NaCl. Harvesting must take place between day 16 and 35 and this will cause an increase in lipid induction resulting in lipid recovery increasing from 18 - 31.5% dry biomass when ultrasound was applied in the extraction method. This section has also determined that S070 beating beads combined with ultrasound induces a strong disruptive effect and can increase ultrasonic lipid recovery to 35% dry biomass.
- *C. concordia* requires growth in F/2 medium with a 25% nitrogen reduction. Harvesting must take place between day 16 and 35 and this will cause an increase in lipid induction resulting in lipid recovery increasing from 20 - 27% dry biomass when ultrasound is employed in the extraction method.
- *Chlorella Sp.* requires growth in BBM + 3N. Harvesting must take place between day 7 and 9 and this will cause an increase in lipid induction resulting in lipid recovery increasing from 17 - 44% dry biomass when ultrasound is employed in the extraction method.

Table 7.7 displays the potential lipid recovery achieved from each species for each test with and without ultrasound and under optimised conditions. For reference

purposes the highest ultrasonic lipid recovery reported in the literature was also included as well as the potential hourly lipid recovery yield for each species.

Table 7.7 Summary of lipid recovery rates from dry biomass for each species

Species	Highest lipid recovery no sonication	Highest lipid recovery from UAE	Highest lipid recovery from UAE (optimised)	Highest UAE lipid recovery in literature
<i>D. salina</i>	15%	22.5%	26%	16-20% (Gouveia and Oliveira, 2009)
<i>N. oculata</i>	6.5%	10%	31.5% 35% (with S070 beads)	23% (Araujo <i>et al.</i> 2011)
<i>C. concordia</i>	7.5%	10.5%	27%	None found in literature
<i>Chlorella Sp.</i>	6.3%	8.7%	44%	52% (Araujo <i>et al.</i> 2012)

The above table reveals a number of important facts; firstly the use of ultrasound is capable of increasing lipid recovery yields in all 4 species. Secondly the optimisation methods employed, both with bead beating, stressing or a combination of both are capable of producing even higher lipid recovery yields. Most importantly the yields recovered are either close to or beyond the ultrasound assisted lipid recovery yields reported in literature for these species.

The only species that did not have a lipid recovery that surpassed that found in the literature was *Chlorella Sp.* This achieved a 44% dry biomass lipid recovery, whereas Araujo *et al.* achieved a 52% dry biomass lipid recovery. However it is important to note that their 52% dry biomass lipid recovery was achieved after 1 hour of ultrasonic treatment, whereas the UAE method employed in this study achieved a 44% dry biomass lipid recovery after 16 minutes. However in theory the potential hourly lipid recovery yield of the optimised UAE method would be higher than the Araujo (2013) method due to its shorter sonication time, this is discussed further in chapter 8.

It terms of improving lipid recovery yields with ultrasonic application the results prove positive. However there may be significant areas for improvement. It should be noted that close relatives of *D. salina*, *N. oculata* and *C. concordia* are capable of producing higher lipid recovery yields than that shown in Table 7.7. *Dunaliella Sp.* can achieve a lipid recovery of 30.12% dry biomass, this is 4.12% higher than the UAE method employed in this study (Araujo *et al*, 2011). Vyas *et al.* (2010) state that the close relative of *N. oculata*, *Nannochloropsis Sp.* can achieve a lipid content between 31 and 68% dry biomass indicting that lipid recovery rates from *N. oculata* in this study (35% dry biomass) may be improved. *C. reinhardtii* (a close relative of *C. concordia*) has been shown to produce a lipid recovery of 35% dry biomass, which is 8% higher than what has been achieved in this study. Possible explanations for this may be that better stressing methods were employed to bring about higher rates of lipid induction or simply *D. salina*, *N. oculata* and *C. concordia* are not capable of producing as high lipid contents as their close relatives due to physiological differences between them.

It is important to raise the point that this data was gathered at a laboratory level and further scale up must be considered for ultrasound assisted lipid extraction to move forward in microalgal biodiesel production. However the data gathered does strongly suggest that lipid recovery can be greatly improved by the use of ultrasound. A pilot scale up system with a modified DFR treating 800 mL of high density microalgae in a flow system is explored in section 7.10.

7.8 GC-MS analysis of lipid extracts

GC/MS analysis was employed on the transesterified lipid extracts of each microalgal species to identify and quantify the amount of FAMES extracted with and without sonication. The ultrasonic extraction method employed for each species is described in section 7.7. The major FAMES detected were compared with literature to determine if the lipid extracts from each species met the standards set for biodiesel production. A study from Demirbas and Demirbas (2011) stated that to be considered for biodiesel production any transesterified lipid extract needs to contain large amounts of saturated and monounsaturated fatty acids. Examples include palmitic, oleic, stearic and linoleic acid methyl esters. The reason these FAMES are considered high quality in terms of biodiesel is because during combustion fuel polymerisation would be less than that of fuel produced from polyunsaturated fatty acids (Sheehan *et al.*1998). Increased fuel polymerisation can lead to engine damage through the blockage of fuel filters which is why a high concentration of polyunsaturated fatty acids is not desirable (Sheehan *et al.*1998).

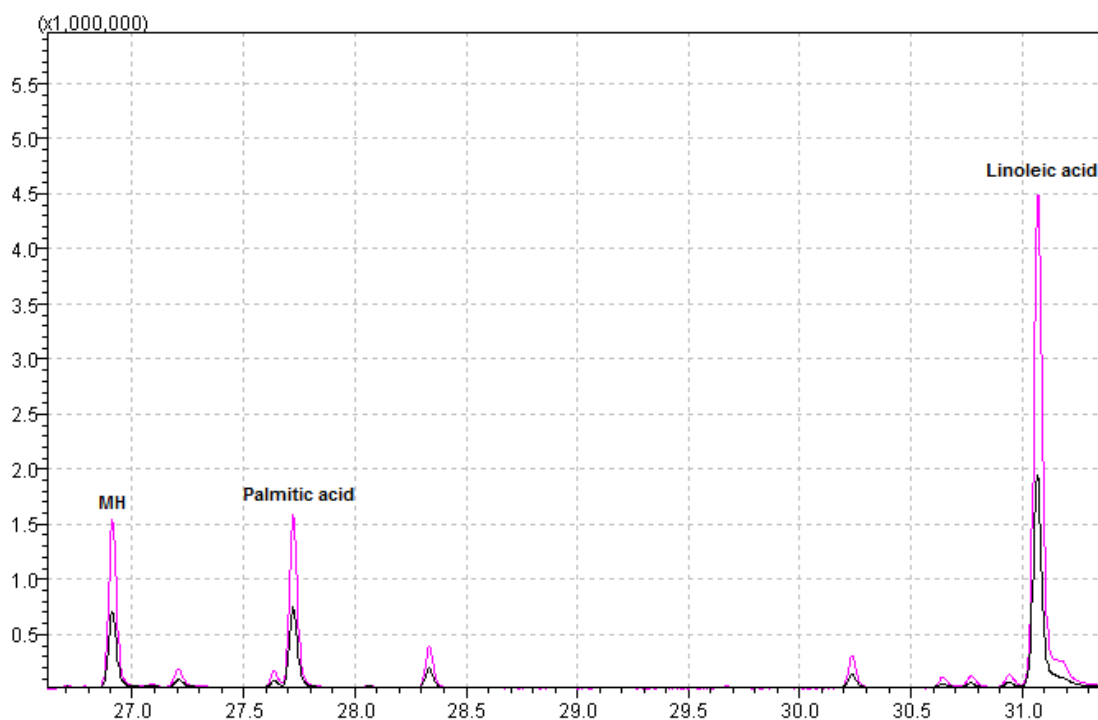
7.8.1 GC/MS analysis of the lipid extract of *D. salina*

The transesterified lipid extract of untreated and sonicated *D. salina* was analysed by GC-MS to identify and quantify the variety of FAMES extracted in each condition. The concentrations of the FAMES extracted from *D. salina* are shown in Table 7.8.1. The overlay GC-MS trace of *D. salina* with and without sonication is shown in Figure 7.8.1.

Table 7.8.1 Comparison of FAMES and other analytes detected from *D. salina* with and without ultrasound

Analyte	Concentration before sonication (mM)	Concentration after sonication with 20 kHz probe (mM)
3- Heptadecane (Z)	0	0.0435
7,10,13_ Eicosatrienoic	0	0.0672
Tridecanoic acid	0	0.022
3,7,11,15-Tetramethyl-2-hexadecen	0	0.0653
4,7,11,15-Hexadecatrienoic acid methyl ester	0	0.0437
Methyl 4,7,10,13-hexadecatetraenoate (MH)	0.4711	0.8193
7,10 Hexadecatetraenoate acid methyl ester	0.0692	0.0781
9,12,15-Octadecatrienoic methyl ester	0.0737	0.1084
7,10,13-Hexadecatrienoic acid methyl ester	0.0512	0.0684
Methyl hexane-9-enoate	0.0928	0.1268
Palmitic acid methyl ester	0.4947	0.8038
Valeric acid vadece 2-enyl ester	0.1547	0.2437
Linolenic acid methyl ester	0.0815	0.1124
Methyl 9,11,14,17-eicosetetraenoate	0.0872	0.1227
Linoleic acid methyl ester	1.0444	2.6214
Heptadecanoic acid methyl ester	0.465	0.0794

Figure 7.8.1 Overlay GC-MS trace of *D. salina* FAME content with and without ultrasound



Key: Black trace = No sonication Pink trace = Sonication with 20 kHz probe

The above table and figure shows that without sonication 12 different analytes were detected from the lipid extract, this increased to 17 different analytes when ultrasound was employed in the extraction method. This data suggests that a higher variety of lipid molecules are extracted when ultrasound is employed. This may be due to the fact that when solvent extraction is employed alone the majority of lipid transfer occurs through diffusion through the cell membrane of *D. salina*. Not all lipid molecules are capable of being extracted through diffusion; this was described by Ranjan *et al.* (2010) who noted this occurring with *Scenedesmus sp.* When the *D. salina* cells are disrupted the extraction solvents come into contact with a higher

variety of lipid molecules which in turn results in a higher variety of FAMES as observed in Table 7.8.1.

It is also notable that after sonication a higher concentration of all FAMES was observed. This is further highlighted in Figure 7.8.2 where the concentrations of the 3 most abundant FAME molecules are compared.

Figure 7.8.2 Comparison of major FAMES detected from *D. salina* with and without sonication

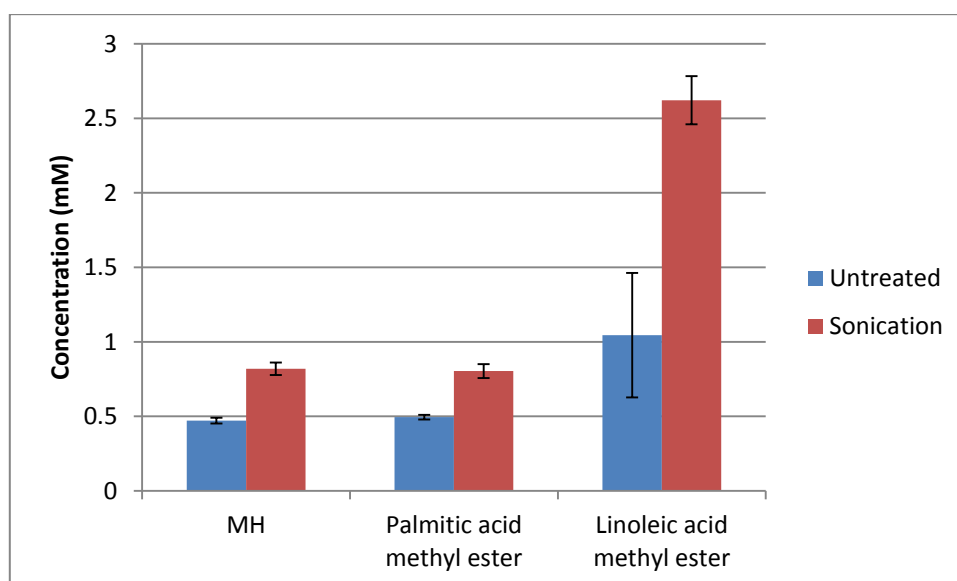


Figure 7.8.2 displays the main FAME molecules recovered from *D. salina*, which were Methyl 4,7,10,13-hexadecatetraenoate ($P = 0.02$), Palmitic acid methyl ester ($P = 0.023$) and Linoleic acid methyl ester ($P = 0.047$). This data coincides with what was stated by Sheehan *et al* (1998) who describe Palmitic and Linoleic acid methyl ester being two of the most prominent fatty acids present in *Dunaliella*. Figure 7.8.1 also shows that the concentration of each FAME molecule significantly increased when ultrasound was employed in the extraction method. This FAME extract from *D. salina* can be considered for biodiesel production as it contains high concentrations of palmitic and linoleic acid methyl esters (Demirbas and Demirbas, 2011).

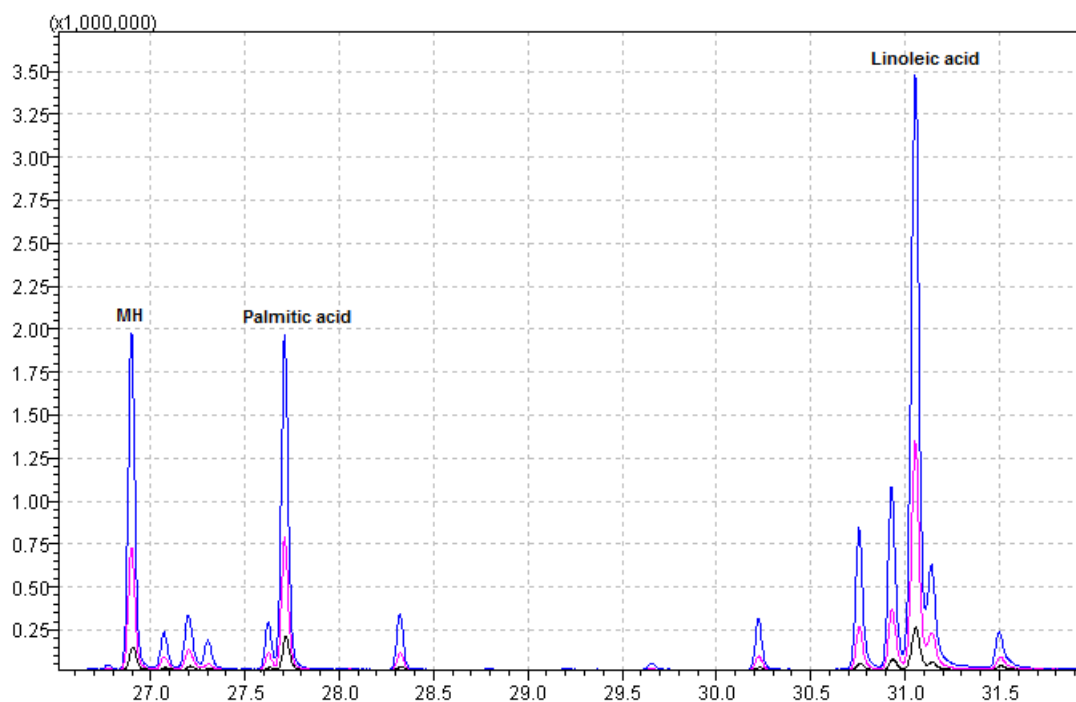
7.8.2 GC/MS analysis of the lipid extract of *N. oculata*

Transesterified lipid extracts of *N. oculata* from samples that were untreated, sonicated and sonicated with beads were analysed by GC-MS to identify and quantify the variety of analytes extracted under each condition. The concentration of the analyte extracted from *N. oculata* is shown in Table 7.8.2. The overlay GC-MS trace of *N. oculata* with and without sonication and S070 beads is shown in Figure 7.8.3.

Table 7.8.2 Comparison of FAMES and other analytes detected from *N. oculata* with and without ultrasound and in conjunction with S070 beads

Analyte	Concentration before sonication (mM)	Concentration after sonication with 20 kHz probe (mM)	Concentration after sonication with 20 kHz probe and S070 beads (mM)
3- Heptadecane (Z)	0	0.0221	0.27
Tridecanoic acid	0	0.0699	0.0894
4,7,11,15-Hexadecatrienoic acid methyl ester	0	0.0216	0.0759
Methyl 4,7,10,13-hexadecatetraenoate (MH)	0.1394	0.4711	1.0352
7,10 Hexadecatetraenoate acid methyl ester	0.0671	0.1065	0.2181
9,12,15-Octadecatrienoic methyl ester	0.0718	0.1391	0.2548
7,10,13-Hexadecatrienoic acid methyl ester	0	0.0776	0.1671
Methyl hexane-9-enoate	0.0447	0.112	0.1992
Palmitic acid methyl ester	0.1653	0.5142	1.1091
Valeric acid vadec 2-enyl ester	0.0677	0.1183	0.2229
Methyl 9,11,14,17-eicosetetraenoate	0.0818	0.2236	0.5088
Linoleic acid methyl ester	0.2239	0.9293	2.1867
Octadecenoic methyl ester	0.0894	0.2393	0.4972
Heptadecanoic acid methyl ester	0.0712	0.1268	0.1966

Figure 7.8.3 Overlay GC-MS trace of *N. oculata* FAME content with and without ultrasound and S070 beads



Key: Black trace = No sonication Pink trace = Sonication with 20 kHz probe Blue trace = Sonication with 20 kHz probe with S070 beads

Table 7.8.2 and Figure 7.8.3 shows that without sonication 14 different analytes were detected from the lipid extract, this increased to 18 different analytes with ultrasound alone and with ultrasound combined with S070 beads employed in the extraction method. This again suggests that when ultrasound is employed a higher variety of lipid molecules can be extracted. It is also important to note that when ultrasound is applied in the extraction method the concentration of the FAME molecules extracted increases and again increases further when S070 beads are also employed. This indicates that sonicating with beating beads causes significantly more cellular disruption to *N. oculata* than ultrasound alone as it allows the extraction solvent to interact with more lipid molecules and produce higher lipid recoveries. This increase

in FAME concentration is highlighted in Figure 7.8.4 where the concentrations of the 3 most abundant FAME molecules are compared in each extraction condition.

Figure 7.8.4 Comparison of major FAMES detected from *N. oculata* with and without ultrasound and in conjunction with beads

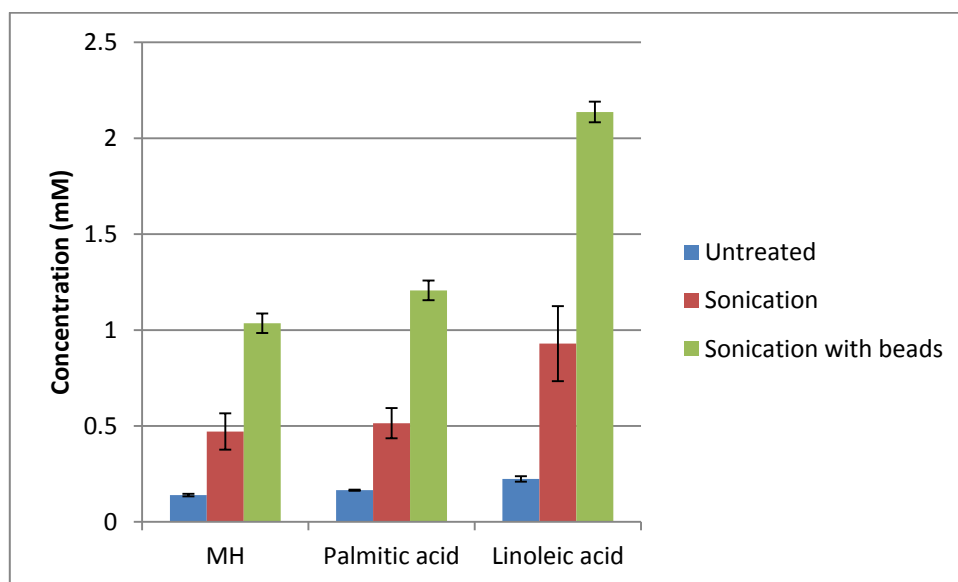


Figure 7.8.4 displays the main FAME molecules recovered from *N. oculata* which were Methyl 4,7,10,13-hexadecatetraenoate ($P = 0.038$, beads $P = 0.025$), palmitic acid methyl ester ($P = 0.03$, beads $P = 0.02$) and linoleic acid methyl ester ($P = 0.044$, beads $P = 0.01$) which was the most prominent. Studies by Tanzi *et al.* (2013) and Pieber *et al.* (2012) both agree with the data gathered in that palmitic and linoleic acid methyl esters are two of the most abundant fatty acids present in *N. oculata*. Figure 7.8.2 also shows that the concentration of each FAME molecule significantly increased when ultrasound was employed and then increased further when ultrasound with S070 beads was employed in the extraction method. The FAME extract from *N. oculata* can be considered for use in biodiesel production as it contains high concentrations of palmitic and linoleic acid methyl esters (Demirbas and Demirbas, 2011).

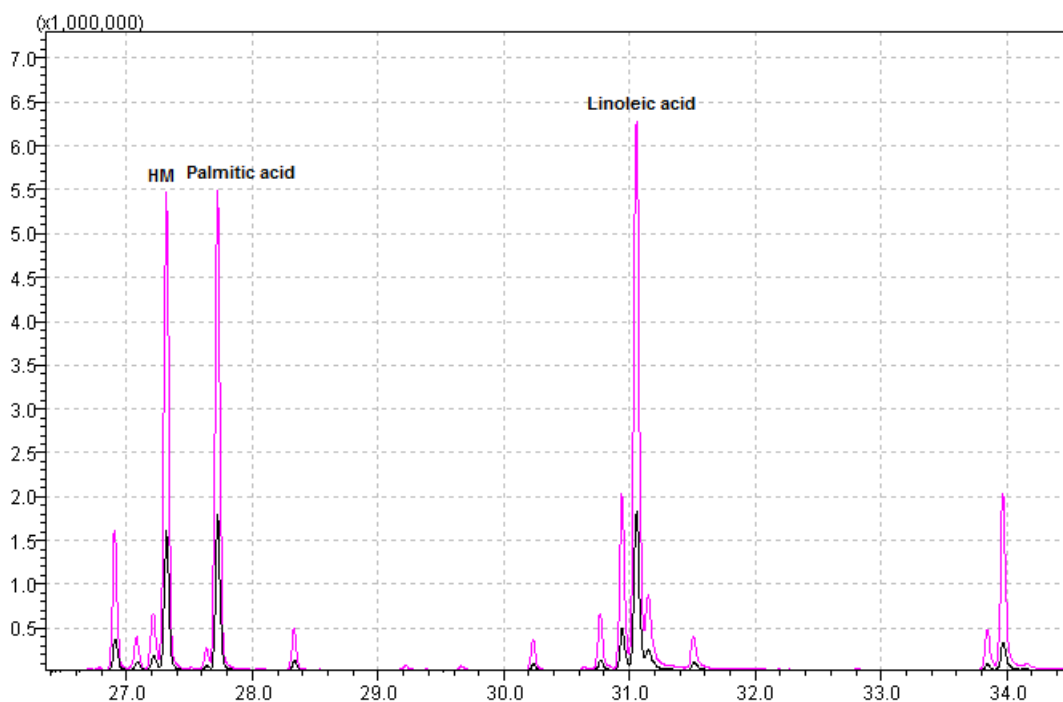
7.8.3 GC/MS analysis of the lipid extract of *C. concordia*

The transesterified lipid extract of untreated and sonicated *C. concordia* was analysed by GC-MS to identify and quantify the variety of FAMES extracted under each condition. The concentrations of the FAMES extracted from *C. concordia* are shown in Table 7.8.3. The overlay GC-MS trace of *C. concordia* with and without sonication is shown in Figure 7.8.5.

Table 7.8.3 Comparison of FAMES and other analytes detected from *C. concordia* with and without ultrasound

Analyte	Concentration before sonication (mM)	Concentration after sonication with 20 kHz probe (mM)
Lauric acid methyl ester	0	0.0686
3- Heptadecane (Z)	0	0.0224
Tridecanoic acid	0.1568	0.2868
Pentadecanoic acid methyl ester	0	0.0722
4,7,11,15-Hexadecatrienoic acid methyl ester	0	0.0463
Methyl 4,7,10,13-hexadecatetraenoate	0.3092	0.6735
7,10 Hexadecatetraenoate acid methyl ester	0.1319	0.2316
9,12,15-Octadecatrienoic methyl ester	0.1845	0.3509
7,10,13-Hexadecatrienoic acid methyl ester (HM)	1.1005	2.2402
Methyl hexane-9-enoate	0.0853	0.1143
Palmitic acid methyl ester	1.1475	2.2306
Valeric acid vadec 2-enyl ester	0.1288	0.223
Cis-10-Heptadecenoic acid methyl ester	0	0.0757
Linolenic acid methyl ester	0	0.0464
Methyl 9,11,14,17-eicosetetraenoate	0.1542	0.3232
Linoleic acid methyl ester	1.443	2.9102
Octadecenoic methyl ester	0.2898	0.572
Heptadecanoic acid methyl ester	0.1356	0.249
Arachidonic acid methyl ester	0.1107	0.2234
Cis-5,8,11,14,17- Eicosapentaenoic acid methyl ester	0.3219	0.8593
7,10,13-Eicosatrienoic acid methyl ester	0.0227	0.025
11,13-Eicosatrienoic acid methyl ester	0	0.022

Figure 7.8.5 Overlay GC-MS trace of *C. concordia* FAME content with and without ultrasound



Key: Black trace = No sonication Pink trace = Sonication with 20 kHz probe

Table 7.8.3 and Figure 7.8.5 show that without sonication 16 different analytes were detected from the lipid extract, this increased to 23 different analytes when ultrasound was employed in the extraction method. This again suggests that when ultrasound is employed a wider variety of lipid molecules can be extracted. It is also important to note that when ultrasound is applied in the extraction method the concentration of the FAME molecules in the extract increases. This indicates that sonication causes enough cellular disruption to *C. concordia* to allow the extraction solvent to interact with more lipid molecules through cracks in the cell wall and membrane and produce higher lipid recoveries (Ranjan *et al.* 2010). This increase in

FAME concentration is highlighted in Figure 7.8.6 where the concentrations of the 3 most abundant FAME molecules are compared in both extraction conditions.

Figure 7.8.6 Comparison of major FAMES detected from *C. concordia* with and without ultrasound

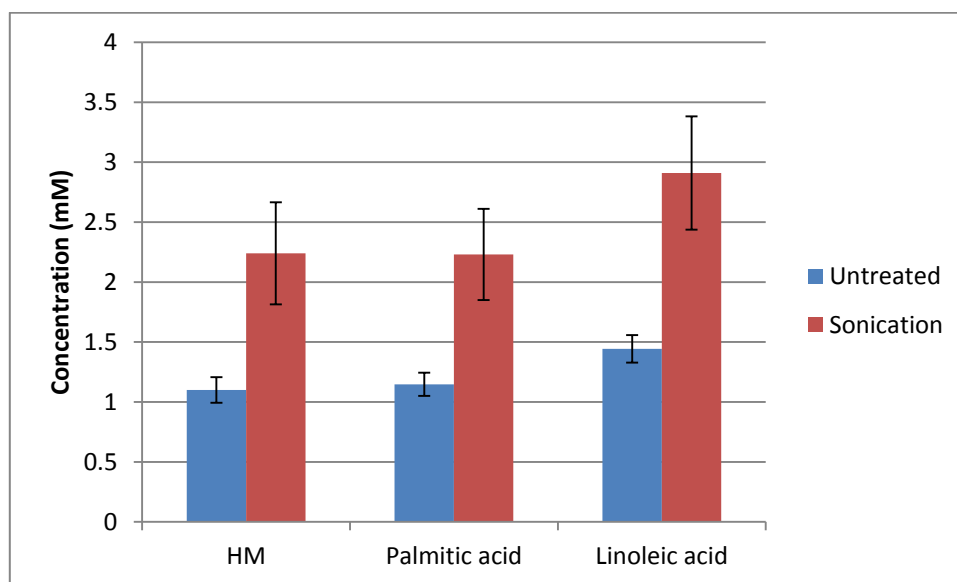


Figure 7.8.6 displays the main FAME molecules recovered from *C. concordia*, which were 7,10,13-hexadecatrienoic acid methyl ester, palmitic acid methyl ester and linoleic acid methyl ester which was the most prominent. Data gathered by Yoo *et al.* (2012) and Siaut *et al.* (2011) suggest that palmitic and linoleic acid methyl esters are two of the most commonly occurring fatty acids within *C. reinhardtii* (a close relative of *C. concordia*). It is therefore reasonable to conclude that this is also the case for *C. concordia* as this is reinforced by what is seen in table 7.8.3. Figure 7.8.6 also shows that the concentration of each FAME molecule significantly increased when ultrasound was employed in the extraction method. This FAME extract from *C. concordia* can be considered for biodiesel production as it contains high concentrations of Palmitic and Linoleic acid methyl esters (Demirbas and Demirbas, 2011).

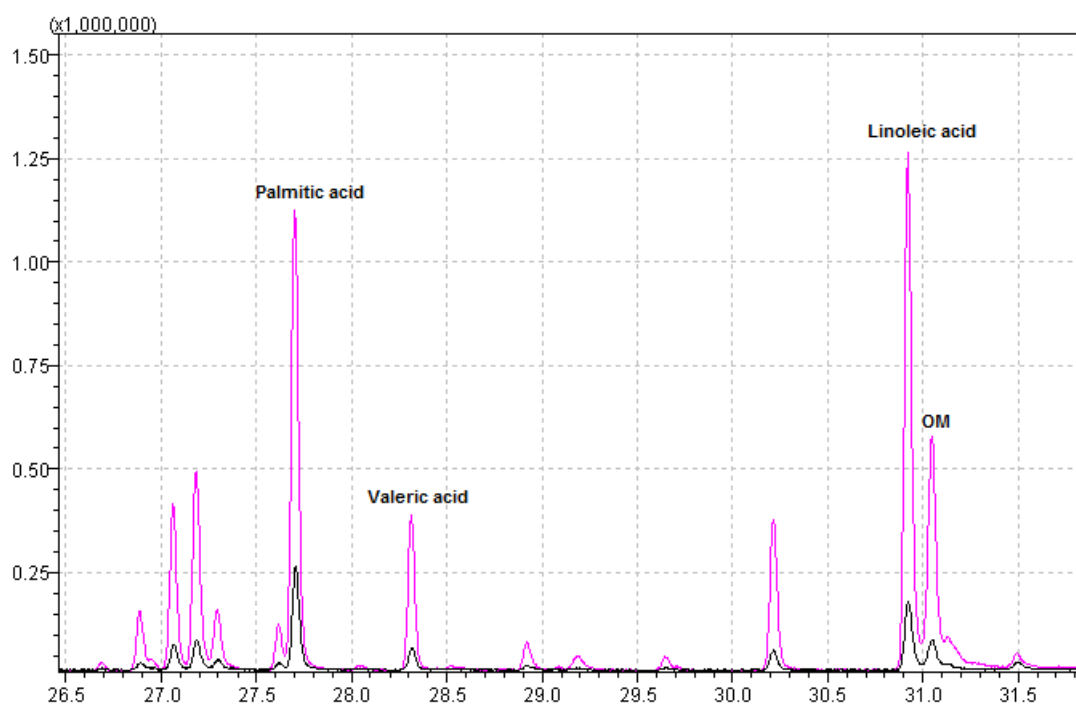
7.8.4 GC/MS analysis of the lipid extract of *Chlorella Sp.*

The transesterified lipid extract of untreated and sonicated *Chlorella Sp.* was analysed by GC-MS to identify and quantify the variety of FAMES extracted in each condition. The concentrations of the FAMES extracted from *Chlorella Sp.* are shown in Table 7.8.4. The overlay GC-MS trace of *C. concordia* with and without sonication is shown in Figure 7.8.7.

Table 7.8.4 Comparison of FAMES and other analytes detected from *Chlorella* Sp. with and without ultrasound

Analyte	Concentration before sonication (mM)	Concentration after sonication with 20 kHz probe (mM)
Pentadecanoic acid methyl ester	0	0.07144
4,7,11,15-Hexadecatrienoic acid methyl ester	0	0.0467
Methyl 4,7,10,13-hexadecatetraenoate	0.053	0.0998
7,10 Hexadecatetraenoate acid methyl ester	0.1169	0.1997
9,12,15-Octadecatrienoic methyl ester (OM)	0.1269	0.2842
7,10,13-Hexadecatrienoic acid methyl ester	0.0817	0.2077
Methyl hexane-9-enoate	0.049	0.1172
Palmitic acid methyl ester	0.2559	0.4118
Valeric acid vadec-2-enyl ester	0.1041	0.3841
Margaric acid methyl ester	0.0461	0.1499
Cis-10-Heptadecenoic acid methyl ester	0.0217	0.0877
Linolenic acid methyl ester	0	0.1525
Linoleic acid methyl ester	0.1402	0.2338
Octadecenoic methyl ester	0.0715	0.2345
Heptadecanoic acid methyl ester	0.025	0.0992
Arachidonic acid methyl ester	0	0.0308

Figure 7.8.7 Overlay GC-MS trace of *Chlorella* Sp. FAME content with and without ultrasound



Key: Black trace = No sonication Pink trace = Sonication with 20 kHz probe

Table 7.8.4 and Figure 7.8.7 show that without sonication 13 different analytes were detected from the lipid extract, this increased to 17 different analytes when ultrasound was employed in the extraction. This again suggests that when ultrasound is employed a higher variety of lipid molecules can be extracted. It is also important to note that when ultrasound is applied in the extraction the concentration of the FAME molecules in the extract increases. This indicates that sonication causes enough cellular disruption to *Chlorella* Sp. to allow the extraction solvent to interact with more lipid molecules and produce higher lipid recoveries. This increase in FAME concentration is highlighted in Figure 7.8.8 where the concentrations of the 4 most abundant FAME molecules are compared under both extraction conditions.

Figure 7.8.8 Comparison of major FAMES detected from *Chlorella Sp.* with and without sonication

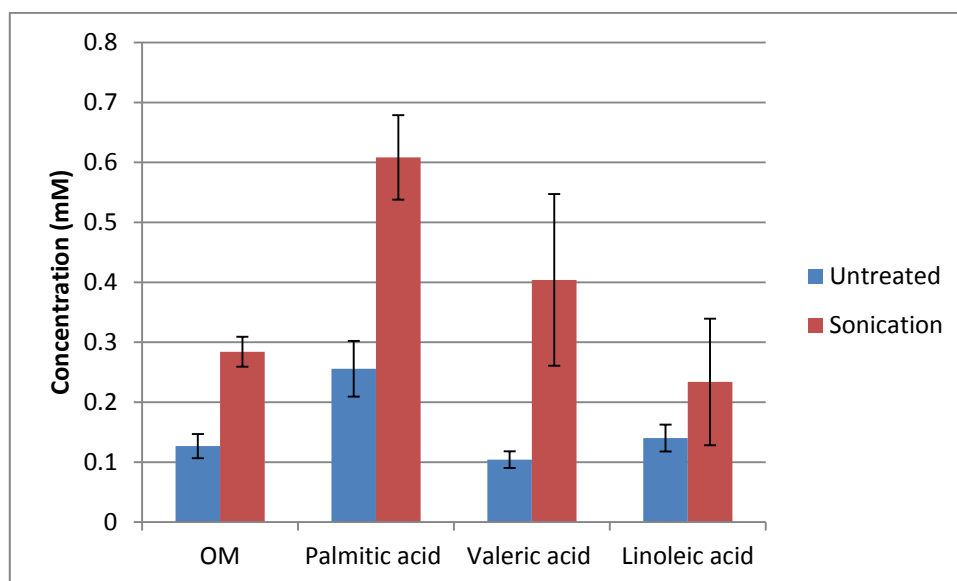


Figure 7.8.8 displays the main FAME molecules recovered from *Chlorella Sp.*; 9,12,15-octadecatrienoic methyl ester, valeric acid vade 2-enyl ester, linoleic acid methyl ester and palmitic acid methyl ester which was the most prominent. Data gathered by Kim *et al.* (2013) and Chen *et al.*(2013) both state that linoleic and palmitic acid methyl esters are two of the most commonly occurring fatty acids found within the *Chlorella* species. Figure 7.8.8 also shows that the concentration of each FAME molecule significantly increased when ultrasound was employed in the extraction method. The FAME extract from *Chlorella Sp.* can be considered for biodiesel production as it contains high concentrations of palmitic and linoleic acid methyl esters (Demirbas and Demirbas, 2011).

7.8.5 Conclusions

The GC-MS data gathered has shown that the transesterified lipid extracts of all four microalgal species have fatty acid profiles suitable for biodiesel production. Each microalgal species contains high concentrations of Palmitic and Linoleic acid methyl esters, both of which were stated by Demirbas and Demirbas (2011) as being suitable for biodiesel production as they are not polyunsaturated fatty acids. The data in this chapter has also confirmed what gravimetric data had previously suggested, that the amount of lipids (and FAMES) recovered from each microalgal species increases when ultrasound is employed in the extraction method.

7.9 Post sonication growth of microalgal species

The results from this section were used for the following publication:

- “The effect of ultrasound on the growth and viability of microalgal cells” (Joyce , King and Mason, 2014)

Microalgal species were sonicated with a 20 kHz probe for the following times: 60 minutes for *N. oculata*, 8 minutes for *D. salina* and 16 minutes for *C. concordia* respectively. Samples were taken at different time periods depending on the species (0, 15, 30, 45 and 60 minutes for *N. oculata*, 0, 1, 2, 4 and 8 minutes for *D. salina* and 0, 2, 4, 8 and 16 minutes for *C. concordia*). Post sonication growth studies were not carried out on *Chlorella Sp* due to time constraints. Samples were then treated in a number of ways in order to explore various effects sonication may have on microalgal growth rates.

- Effect of sonication on the growth of microalgal species. Sonicated microalgae were returned to the growth room and allowed to grow under normal conditions.
- Effect of sonication on the growth of microalgal species with additional F/2 media. Fresh F/2 media was added to sonicated microalgae which were then allowed to grow under normal conditions.
- Effect of adding sonicated microalgae supernatant to an established microalgal culture. The supernatant of sonicated microalgae was added to an established culture in a **1:4 ratio** and allowed to grow under normal conditions.
- Effect of adding sonicated microalgae supernatant to an established microalgal culture. The supernatant of sonicated microalgae was added to an

established culture in a **4:1 ratio** and allowed to grow under normal conditions.

Samples were analysed by haemocytometer counts on days 1, 3, 5, 10, 15, 20, 25, 30 and every 10 days thereafter. The growth rate for each culture was also determined using the following equation (Fogg and Thake, 1987):

$$\text{Growth rate} = \text{Ln} (N2/N1) / (t2 - t1)$$

[N1 is the starting time point and N2 is the ending time point, t1 is the starting cell count and t2 in the ending cell count.]

7.9.1 Post sonication growth of *D. salina*

As previously seen in Figures 7.3.1 and 7.3.2, when treated with a 20 kHz probe the entire culture of *D. salina* rapidly decreased and was completely destroyed after 4 minutes ultrasonic treatment. Table 7.9.1 displays the results for post sonication growth for *D. salina* with samples taken at 0, 1, 2, 4 and 8 minutes.

What is most noticeable from Table 7.9.1 is that after sonication *D. salina* remains viable after each time interval. Haemocytometer data shows 100% reductions in the cell counts for *D. salina* after sonication, but after a short lag phase (5 - 20 days) cell cultures resumed normal growth. A possible explanation for this is that although the cells do not appear to be intact after treatment some cells have shrunk and are not visible and some cells are able to repair themselves after a short period of regeneration and resume growth. The introduction of supernatant liquid from sonicated microalgae shows quite interesting results for *D. salina*. A 2.5 fold increase in *D. salina* cell concentration was observed in samples treated for 16 minutes (in comparison with the control samples) when 80% supernatant was added.

Table 7.9.1 Summary of results for *D. salina* post sonication growth

Treatment	Sonication time (mins)	Starting cell concentration (cell/mL)	Highest cell concentration (cells/mL)	Initial Lag phase (days)	Fastest growthrate (days ⁻¹)
Post sonication growth	Untreated	2.3×10^6	2.6×10^6	0	4.2×10^{-5}
	1	6600	1.6×10^6	3	5.4×10^{-5}
	2	<1	1.8×10^6	5	4×10^{-5}
	4	<1	1.7×10^6	15	3.5×10^{-5}
	8	<1	1.7×10^6	20	3.3×10^{-5}
Post sonication growth of re-suspended culture	Untreated	4.5×10^6	1.1×10^7	0	4.5×10^{-5}
	1	2.8×10^5	7.4×10^6	5	6.5×10^{-5}
	2	<1	6.9×10^6	10	5.1×10^{-5}
	4	<1	6.4×10^6	15	3.9×10^{-5}
	8	<1	5.5×10^6	15	4.4×10^{-5}
Growth of an established culture when introduced to the supernatant (20%) of a sonicated culture	Untreated	1.8×10^6	2.3×10^6	0	1×10^{-4}
	1	1.8×10^6	2.3×10^6	0	1.1×10^{-4}
	2	1.8×10^6	2.6×10^6	0	5.7×10^{-4}
	4	1.8×10^6	2.2×10^6	0	5.7×10^{-5}
	8	1.8×10^6	2.6×10^6	0	5.6×10^{-5}
	Untreated	2.3×10^5	5.2×10^6	0	8.8×10^{-5}
	1	1.5×10^5	7.3×10^6	0	1.8×10^{-5}

Growth of an established culture when introduced to the supernatant (80%) of a sonicated culture	2	2×10^5	8.4×10^6	5	3.2×10^{-5}
	4	2×10^5	1×10^7	5	2.5×10^{-5}
	8	1.9×10^5	1.3×10^7	5	1.9×10^{-5}

7.9.2 Post sonication growth of *N. oculata*

As previously seen in Figures 7.4.1 and 7.4.2 when treated with a 20 kHz probe the population of *N. oculata* cultures slightly increases after sonication due to de-clumping. Figure 7.4.5 shows chlorophyll is released from *N. oculata* as ultrasound was applied, indicating that some damage to the microalgal cell walls and membranes had occurred. Table 7.9.2 displays the results for post sonication growth for *N. oculata* with samples taken at 0, 15, 30, 45 and 60 minutes.

After each sonication time interval *N. oculata* remained viable. Under most conditions a lag phase was not observed, if one did occur it lasted ~3-5 days. Cells were able to grow immediately after 60 minutes sonication, though at a slower rate than untreated samples. Sonication did not seem to have a strong effect on the growth rates of *N. oculata* under most conditions.

Table 7.9.2 Summary of results for *N. oculata* post sonication growth

Treatment	Sonication time (mins)	Starting cell concentration (cells/mL)	Highest cell concentration (cells/mL)	Initial Lag phase (days)	Fastest growth rate (days ⁻¹)
Post sonication growth	Untreated	4.7×10^6	6.1×10^6	0	3.6×10^{-6}
	15	4.2×10^6	1×10^7	5	4.5×10^{-6}
	30	4.4×10^6	6.1×10^6	5	1.5×10^{-5}
	45	4.1×10^6	6.4×10^6	5	9×10^{-6}
	60	4×10^6	8.1×10^6	5	4.9×10^{-6}
Post sonication growth of re-suspended culture	Untreated	4.8×10^6	1.5×10^7	0	2.6×10^{-6}
	15	4.1×10^6	1.5×10^7	0	2.4×10^{-6}
	30	4.4×10^6	1.5×10^7	0	2.3×10^{-6}
	45	4.8×10^6	1.5×10^7	0	2.6×10^{-6}
	60	4.2×10^6	1.4×10^7	0	2.6×10^{-6}
Growth of an established culture when introduced to the supernatant (20%) of a sonicated culture	Untreated	9.8×10^6	1.4×10^7	0	9×10^{-6}
	15	9.3×10^6	1.4×10^7	0	6.3×10^{-6}
	30	1.1×10^7	1.4×10^7	0	1.1×10^{-5}
	45	9.8×10^6	1.4×10^7	0	8.6×10^{-6}
	60	9.8×10^6	1.4×10^7	0	6.6×10^{-6}
	Untreated	2.1×10^6	7.4×10^6	3	1.8×10^{-6}

Growth of an established culture when introduced to the supernatant (80%) of a sonicated culture	15	2.1×10^6	7.5×10^6	3	2.8×10^{-6}
	30	1.8×10^6	8.2×10^6	3	7.8×10^{-6}
	45	2×10^6	7.1×10^6	3	9.9×10^{-6}
	60	2×10^6	6.8×10^6	3	1.1×10^{-5}

7.9.3 Post sonication growth of *C. concordia*

As previously seen in Figure 7.5.1 when treated with a 20 kHz probe the entire population of *C. concordia* rapidly decreased and was completely destroyed after 8 minutes ultrasonic treatment. Table 7.9.3 displays the results for the post sonication growth for *C. concordia* with samples taken at 0, 2, 4, 8 and 16 minutes.

What is most noticeable from Table 7.9.3 is that after sonication *C. concordia* remains viable after each time interval. Haemocytometer data shows that 100% reductions in the cell population of *C. concordia* occurred after sonication, however after a short lag phase (5 - 25 days) it resumed normal growth. A possible explanation for this is that although the cells do not appear to be intact after treatment some cells have shrunk and are not visible and some cells are able to repair themselves after a short period of regeneration and resume growth. It is also noticeable that the introduction of supernatant liquid from sonicated microalgae shows quite interesting results for *C. concordia*. An over 2 fold increase in the highest *C. concordia* cell concentration was observed in samples treated for 16 minutes (when compared to control samples) when 80% supernatant was added.

Table 7.9.3 Summary of results for *C. concordia* post sonication growth

Treatment	Sonication time (mins)	Starting cell concentration (cells/mL)	Highest cell concentration (cells/mL)	Initial Lag phase (days)	Fastest growth rate (days ⁻¹)
Post sonication growth	Untreated	4.7×10^5	5.8×10^5	3	4.7×10^{-4}
	2	1.9×10^4	3×10^5	5	7.5×10^{-4}
	4	6×10^3	1.9×10^5	5	2.9×10^{-4}
	8	<1	2.4×10^5	15	3.8×10^{-4}
	16	<1	1.8×10^5	25	1.7×10^{-4}
Post sonication growth of re-suspended culture	Untreated	3.9×10^4	3.9×10^5	3	1×10^{-4}
	2	1.5×10^4	5.5×10^5	5	6×10^{-4}
	4	<1	4.9×10^5	5	1×10^{-4}
	8	<1	1.8×10^5	10	2×10^{-4}
	16	<1	4.6×10^5	10	1×10^{-4}
Growth of an established culture when introduced to the supernatant (20%) of a sonicated culture	Untreated	4.1×10^5	5.1×10^5	0	1.6×10^{-4}
	2	4.4×10^5	5.8×10^5	0	2×10^{-3}
	4	4.7×10^5	5.4×10^5	0	8×10^{-4}
	8	4.1×10^5	6×10^5	0	1.3×10^{-4}
	16	4.2×10^5	6.3×10^5	0	1.3×10^{-4}
	Untreated	8.2×10^4	1.7×10^5	0	3×10^{-4}

Growth of an established culture when introduced to the supernatant (80%) of a sonicated culture	2	1.2×10^5	1.8×10^5	0	9×10^{-4}
	4	9.5×10^4	1.8×10^5	0	6×10^{-4}
	8	7.9×10^4	2.9×10^5	0	4×10^{-4}
	16	8.6×10^4	3.7×10^5	0	3×10^{-4}

A possible explanation for the increase in growth rates observed for *D. salina* and *C. concordia* may be because nutrients released from disrupted cells of sonicated microalgae are present in the supernatant and fortify the growth medium when added to an established culture therefore enhancing the growth of microalgal cultures. A report has suggested that nitrogen and phosphorus derived from microalgal waste can be employed as a potential fertilizer for other microalgal cultures, which concurs with the data gathered (Oilgae, 2013). Results show that the supernatant medium which is removed after sonication of microalgae could also have potential uses in the microalgal biofuel industry in that such supernatants could be used as nutrient when added to culture, promoting the growth of microalgal biomass prior to harvesting.

Conclusions

Post sonication growth studies revealed that after ultrasonic treatment (8 minutes for *D. salina*, 16 minutes for *C. concordia* and 60 minutes for *N. oculata*) with the 20 kHz probe (40% amplitude, 0.097 W/cm³) all microalgal cultures remain viable. This suggests that cells have either shrunk and are not detectable or cells are able to regenerate following exposure to ultrasound at 20 kHz for the time periods stated for each species. Supernatants of sonicated *D. salina* and *C. concordia* have demonstrated the ability to boost the growth of established cultures. This indicates that the spent microalgal waste after extraction may show potential to be employed as a feedstock for future cultures.

7.10 Scale up extraction with improved DFR system on *N. oculata*

To highlight the potential of using ultrasound on a commercial level the DFR system was adjusted to provide greater intensity. In this scale-up the space in between the two internal ultrasonic plates of the DFR was reduced to create a more intense reaction chamber, this in turn reduced the volume of the reaction chamber from 1.1L to 100 mL. The DFR was employed in a flow system to demonstrate that ultrasonic steps can easily be inserted into a microalgal biodiesel production line. The size and scale of the DFR can be adapted to suit the needs of the user. The power density of the improved DFR was 6 W/cm^3 (this was measured by a power monitor plug (Wilkinsons)).

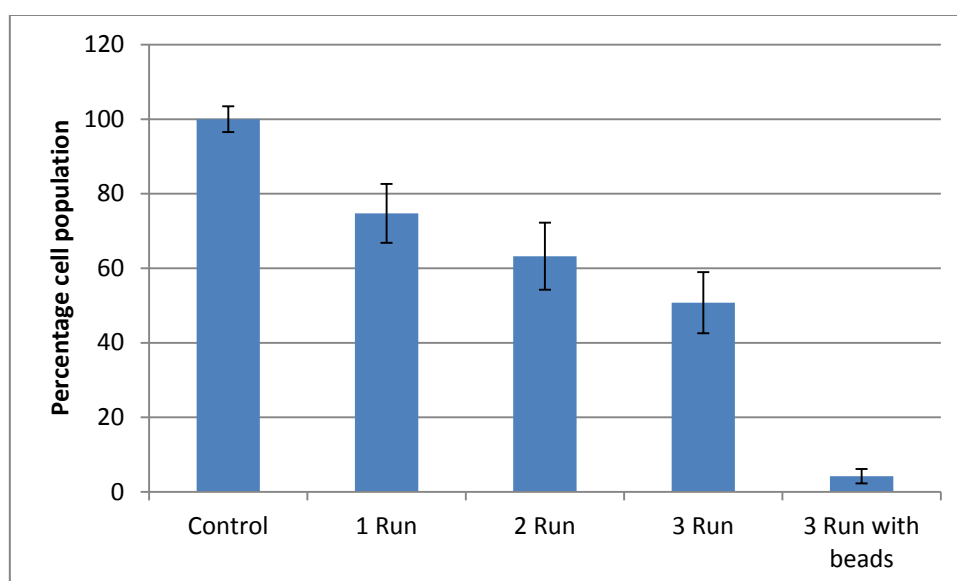
Due to restrictions in the time available *N. oculata* was the only microalgal species tested using the scaled-up DFR system. The high lipid content of *N. oculata* makes it a prime microalgal species for microalgae biodiesel production. It was also of interest to note if the improved DFR system was capable of disrupting *N. oculata* cells at rates higher than previously reported (the previous DFR system caused a 10% reduction in the cellular population of *N. oculata*, see chapters 7.4 and 7.7). If the system is capable of causing significant *N. oculata* disruption then it should be more than adequate to rupture the other microalgal species tested in this project. In this study 800 mL samples of high density stressed *N. oculata* were subjected to the DFR flow system (flow rate 0.5 L/minute) for 3 passes (triplicate). Samples were taken for analysis after each pass. A second test involved further optimisation by passing the microalgae and S070 beads through the system to see if a further disruptive effect was observed. The working time and actual sonication time in the reaction vessel for each pass is shown in table 7.10.1.

Table 7.10.1 Working time and actual sonication time for each pass through the modified DFR system

Number of passes through the system	Time (Seconds)	Actual time within reaction chamber (Seconds)
1	96	12
2	192	24
3	288	36

Samples were analysed by haemocytometer counts, optical density measurements at 686 nm, chlorophyll and lipid analysis by spectro-fluorophotometer analysis and lipids extracted through the adapted Bligh and Dyer method. Figure 7.10.1 displays the percentage cell reduction of *N. oculata* after each pass through the DFR.

Figure 7.10.1 Percentage reduction of *N. oculata* cells using the modified DFR system



The above figure shows that after each pass through the DFR the population of *N. oculata* drops considerably and after 3 runs the total population significantly drops by ~50% ($P = 0.013$). However by employing S070 beads with the DFR system a further reduction in cell population was observed, ~90% in total ($P = 7.81 \times 10^{-7}$). It is worth noting that during the haemocytometer analysis of *N. oculata* treated for 3 runs with beads; large clumps of cellular debris were visible with observable cell leakage present, which did not occur previously. This regularly occurred with *D. salina* (after 1 minute with the 20 kHz probe), *C. concordia* (after 2 minutes with the 20 kHz probe) and *Chlorella* (after 16 minutes with the 20 kHz probe) but this was the first time that this phenomena was observed in the project for *N. oculata*, this indicates that the DFR with beating beads caused the highest amount of cellular disruption to *N. oculata*. The starting concentration was 2.4×10^6 cells/mL.

Figure 7.10.2 displays the percentage reduction in the OD of *N. oculata* after each pass through the DFR system.

Figure 7.10.2 Percentage reduction of *N. oculata* OD (686 nm) using the modified DFR system

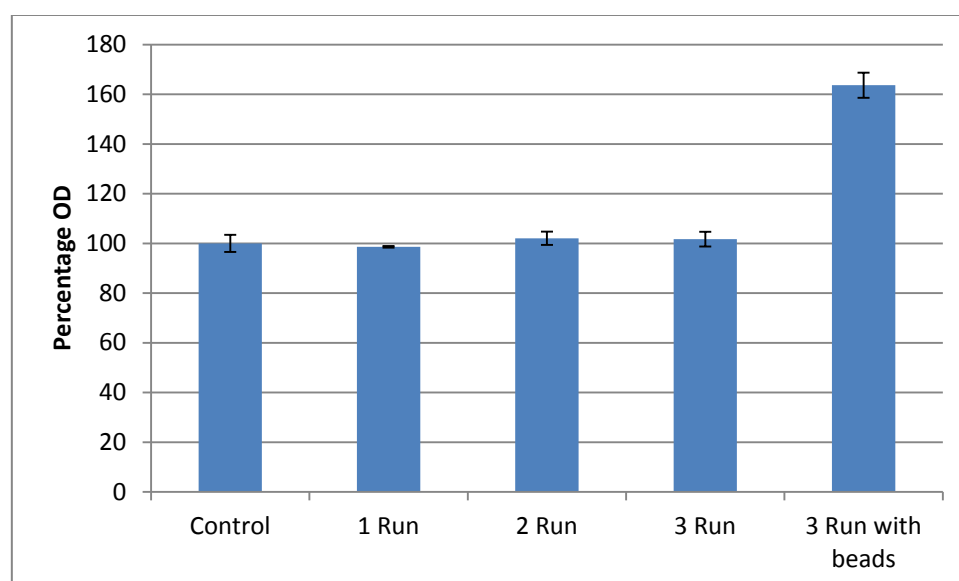
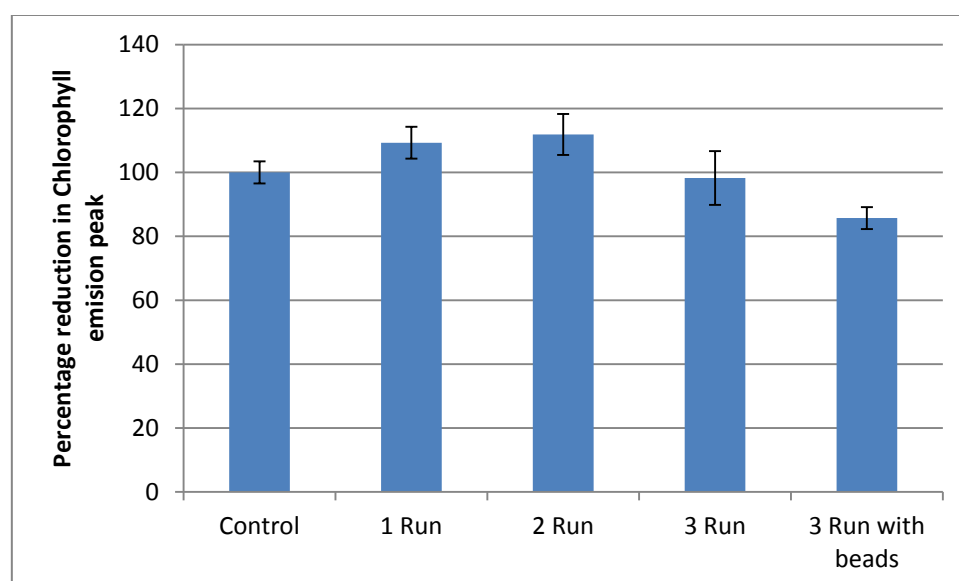


Figure 7.10.2 shows that the OD of *N. oculata* remains roughly stationary after each pass through the DFR. However after 3 runs through the system with S070 beads the OD rose sharply. This increase may be due to the increased cellular debris present within the sample interfering with the passage of light through the UV-Visible-spectrophotometer as previously reported by Wu *et al.* (2010), please refer to chapter 7.3 for further details. The starting OD was 0.4.

The chlorophyll emission peak of *N. oculata* measured by spectro-fluorophotometer after each run through the DFR is shown in Figure 7.10.3.

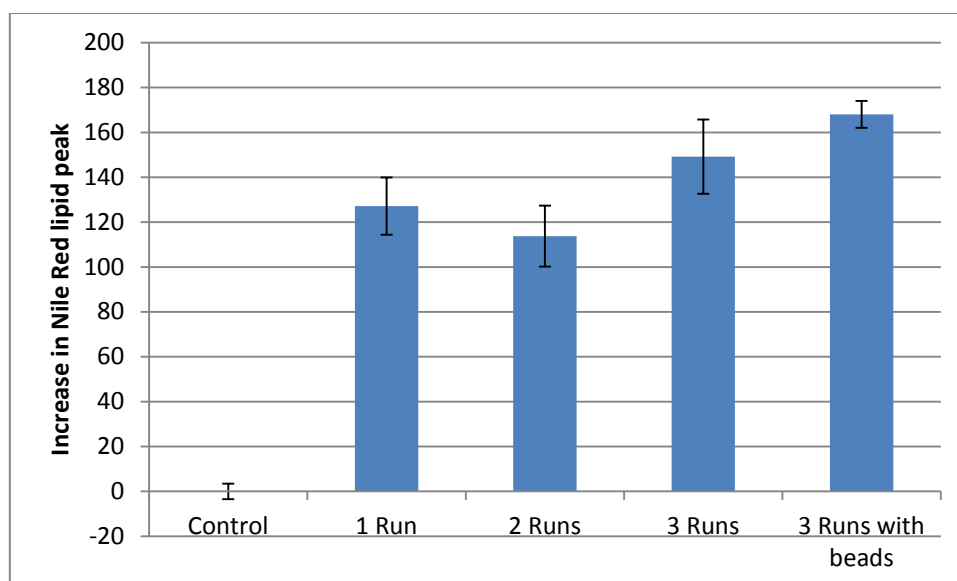
Figure 7.10.3 Percentage reduction of *N. oculata* Chlorophyll emission peak using the modified DFR system



The above figure shows that after 3 runs with the improved DFR system the chlorophyll emission peak drops by ~5%. This then drops by 19% when S070 beating beads were additionally employed ($P = 0.09$). This suggests that the optimised system caused damage to *N. oculata*. The starting height of the chlorophyll peak was 11.2.

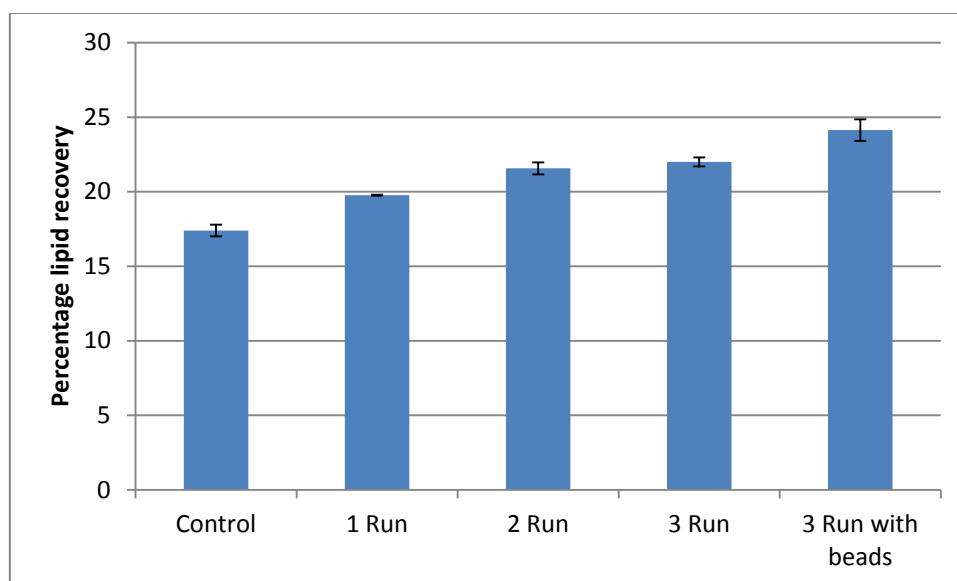
The effect of ultrasound on the increase of the Nile Red lipid emission peak is shown in Figure 7.10.4.

Figure 7.10.4 Percentage increase of Nile Red lipid emission peak using the modified DFR system



The above figure shows that the Nile Red lipid emission peak of *N. oculata* significantly increases when *N. oculata* is passed through the improved DFR system ($P = 2.66E^{-6}$). The lipid peak increases by ~150% after 3 passes through the system and further increases to ~170% after 3 runs through the system with S070 beads. This information concurs with the results from the haemocytometer, OD and chlorophyll emission peak data which suggests that significant cellular damage has occurred allowing increases transfer of materials in and out of cells. This data suggests that during extraction higher lipid recovery rates will occur. The gravimetric lipid recovery after each run is shown in figure 7.10.5. The starting Height of the Nile Red emission peak was 10.6.

Figure 7.10.5 Percentage lipid recovery from *N. oculata* using the modified DFR system



The above figure confirms that when ultrasound is applied lipid recovery yields significantly increase ($P = 8.25E^{-6}$). When ultrasound is not applied a 16.5% dry biomass lipid recovery is achieved, this increases to ~21.5% dry biomass after 3 passes through the improved DFR system and then increases further to ~24% dry biomass after 3 passes through the improved DFR with beads ($P = 0.04$). These 3 passes equate to just 36 seconds actual ultrasonic treatment in the reaction chamber.

This recovery rate observed is less than the 35% dry biomass lipid recovery that was achieved from *N. oculata* on a laboratory scale, however it is often the case that when moving from laboratory to pilot scale total yield is often less than what can be achieved on a laboratory scale. This is often this is due to the size of the production system allowing more margin for error. It is also worth noting that the two extraction techniques were not exactly the same. The laboratory scale system extracted lipids during the ultrasonic treatment, the pilot scale DFR system extracted lipids after

ultrasonic treatment. This was because it was inadvisable to run solvents through the DFR system as it could potentially corrode the internal seals of the system. This may or may not be responsible for the difference in lipid recovery yields for the two systems.

In the laboratory scale system 200 mL of *N. oculata* was treated for 16 minutes achieving a lipid recovery yield of 35% dry biomass, however in the pilot scale set up 800 mL of *N. oculata* was sonicated for 4:48 minutes (36 seconds in the reaction chamber) and achieved a 24% dry biomass lipid recovery. Due to the improved DFR system producing a relatively high lipid recovery from a large volume in less than 5 minutes its hourly theoretical lipid recovery yield could be potentially higher than the laboratory scale system. The potential costs and hourly theoretical yields of these systems are compared and discussed further in Chapter 8.

Conclusions

The pilot scale improved DFR system with a smaller (100 mL) reaction chamber was employed to create more aggressive ultrasonic conditions. When *N. oculata* was treated with the improved DFR for 4:48 minutes (288 seconds) a ~50% drop in the cellular population was observed which achieved a lipid recovery yield which increased from 16.5 to 21.5% dry biomass. When the DFR was employed in conjunction with S070 beating beads this system produced a 90% reduction in the cell population and a lipid recovery yield of 24% dry biomass. Despite this lipid recovery yield being less than that which was achieved on a laboratory scale this system should produce a higher hourly lipid extraction yield, this will be discussed further in Chapter 8.

8. Potential impact of data

Results gathered so far have determined that the application of ultrasound can increase lipid recovery yields from the 4 microalgal species employed in this study via cell disruption. This level of ultrasonic cell disruption is not only of great importance to the biofuel industry but could potentially have impacts in other microalgal fields such as extraction of compounds for the pharmaceutical/nutraceuticals industries, and microalgal bloom control. These impacts and potential future work for this project will be discussed in this chapter.

8.1 Potential economical impact of data

A study by Preiss and Kowalski (2010) stated that the average production cost of one litre of microalgal biodiesel is roughly £1.90. This is considerably higher than the production cost of a litre of petroleum which in the past 10 years has varied between £0.23 - £0.42 per litre (Preiss and Kowalski, 2010). It is clear that steps need to be taken to ensure that the cost of microalgal biodiesel production is close to or less than the cost of petroleum production. This section will explore the potential production values and costs of the laboratory based extraction system; a pilot-scale extraction system and other ultrasonic microalgal lipid extraction set-ups that have been reported in the literature.

8.1.1 *N. oculata*

The estimated production values and costs of lipid extraction from *N. oculata* are discussed here. This was the only species which was examined on both a laboratory (20 kHz) and a pilot-scale (improved DFR), this is because it was considered that if the DFR system could sufficiently damage *N. oculata*, it would also have a similar or greater effect on the other weaker celled species. It is important to note that the dry biomass of *N. oculata* was 50g per litre for the lab scale system and 100g per litre for the DFR system. The hourly crude lipid yield was calculated by employing the percentage recovery yield with the amount of biomass (kg) that can be processed in an hour. For example, the extraction yield of the pilot-scale (improved DFR) system in conjunction with S070 beads was 24% dry biomass and 1 kg of dried biomass could be processed in 1 hour. Therefore the hourly crude lipid yield is 0.24 L. The cost of electricity in the UK as of August 2013 was roughly £0.145 per kWh (BERR, 2013). This information is used to determine the cost of the energy needed to extract a litre of microalgal oil using the UAE method. Table 8.1 displays a comparison of the potential capacities, production yields and forecasted cost of lipid extraction for both the laboratory scale and the improved DFR pilot scale extraction systems on *N. oculata* (systems with and without ultrasonic treatment and beads are displayed).

Table 8.1 Comparison forecast of the capacity, production values and costs of the laboratory and pilot scale lipid extraction systems for *N. oculata*

System	200 mL Static extraction (no ultrasound)	200 mL 20 kHz probe extraction (0.097 W/cm³)	200 mL 20 kHz probe extraction beads (0.097 W/cm³)	800 mL Flow extraction (no ultrasound)	800 mL Improved DFR extraction (6 W/cm³)	800 mL Improved DFR extraction S070 beads (6 W/cm³)
Lipid recovery rate	18% dry biomass	31.5% dry biomass	35% dry biomass	16.5% dry biomass	21.5% dry biomass	24% dry biomass
Capacity (L of microalgae biomass/hour)	0.75	0.75	0.75	10	10	10
Capacity (kg of dried biomass/hour)	0.0375	0.0375	0.0375	1	1	1
Hourly crude lipid yield (L)	0.00675	0.012	0.013	0.165	0.215	0.24
Kilowatt hours (kWh)	N/A	0.005	0.005	N/A	0.048	0.048
Crude lipid yield (L) per kWh	N/A	2.4	2.6	N/A	4.479	5
Daily crude lipid production yield (L)	0.162	0.288	0.312	3.96	5.16 (30% increase)	5.76 (45% increase)
Cost of the production of 1 L lipid extract	£1.90	£1.96	£1.956	£1.90	£1.932	£1.929

Table 8.1 shows that the pilot-scale (improved DFR) system with beads has a higher theoretical production capacity, hourly lipid yield and higher yield per kWh than all other extraction systems despite the pilot-scale systems giving a lower percentage lipid recovery yield than the laboratory scale extraction system. The pilot-scale (improved DFR) system with beating beads could potentially produce 0.24 L of crude lipid extract per hour; the laboratory scale extraction system (20 kHz probe) with beads had almost a 20 fold reduction in this value with an hourly yield of 0.013 L. This information is based on the improved DFR system being configured as a flow system; if a batch configuration was employed an even greater hourly yield could possibly be achieved (although emptying and refilling times should be considered

The theoretical daily lipid extraction yield was also considerably higher in the pilot-scale system. The flow extraction system without ultrasound could potentially produce 3.96 L of crude lipid extract per day, the improved DFR system with ultrasound could produce 5.16 L, and the improved DFR system with ultrasound in conjunction with beating beads could produce an even higher 5.76 L per day. There is of course an additional cost of adding an ultrasonic step to the lipid extraction process which is roughly 3.2p per L for ultrasound alone and 2.9p per L ultrasound with beating beads. This small increase in production cost results in a significant increase in the daily lipid production yields (a 30% increase in lipid recovery from ultrasound alone and a 45% increase from ultrasound with beads) which may prove a worthwhile investment as the economic and environmental benefits outweigh the implementation cost.

The UAE method reported by Araujo *et al.* (2011) achieved a 23% dry biomass lipid recovery yield from *N. oculata* in 20 minutes using a 40 kHz bath (80 W). The exact volume of microalgae processed in this extraction method was not stated in their

study which means the production capacity of their system is not known. However, if it assumed that the volumes treated are the same as this study, comparisons can be drawn. Table 8.2 compares the potential production values, capacity and costs of the ultrasonic extraction employed in this study and by Araujo *et al.* (2011).

Table 8.2 Comparison of ultrasonic extraction with the UAE method employed by Araujo *et al.* (2011)

System	200 mL 20 kHz probe extraction beads (0.097 W/cm ³)	Araujo <i>et al.</i> (2011) UAE method (40 kHz 80 Watts*)
Lipid recovery rate	35% dry biomass	23% dry biomass
Capacity (L of microalgae biomass/hour)	0.75	0.6
Capacity (kg of dried biomass/hour)	0.0375	0.03
Hourly crude lipid yield (L)	0.013	0.007
Kilowatt hours (kWh)	0.005	0.026
Crude lipid yield (L) per kWh	2.6	0.27
Daily crude lipid production yield (L)	0.312	0.168
Cost of the production of 1 L lipid extract	£1.956	£2.437

* = Manufacturer quote, not measured.

Table 8.2 reveals that the method employed in this study resulted in more lipid extracted than the method employed by Araujo *et al.* (2011). The processing capacity, lipid recovery rate and hourly yield are all superior and the cost of production is cheaper by £0.48 per litre. A potential reason for this may be that the system employed by Araujo *et al.* (2011) was a 40 kHz bath, which provides less powerful ultrasound than the 20 kHz probe used in this study. Lower frequencies such as 20 kHz are known to produce greater shear forces which disrupt microalgal cell walls (Broekman *et al.* 2010).

8.1.2 *D. salina*

Table 8.3 shows the potential production capacity, lipid yields and costs of the laboratory scale *D. salina* lipid extraction systems with and without ultrasound (20 kHz) and also draws comparisons with the UAE developed by Araujo *et al.* (2011).

Table 8.3 Comparison forecast of the potential capacity, production values and costs of the laboratory scale lipid extraction of *D. salina*

System	200 mL Static extraction (no ultrasound)	200 mL 20 kHz probe extraction (0.097 W/cm ³)	Araujo et al. (2011) UAE method (40 kHz 80 Watts*)
Lipid recovery rate	19% dry biomass	26% dry biomass	30.12% dry biomass
Capacity (L of microalgae biomass/hour)	12	12	0.6
Capacity (kg of dried biomass/hour)	0.6	0.6	0.03
Hourly crude lipid yield (L)	0.114	0.156	0.009
Kilowatt hours (kWh)	N/A	0.0003	0.026
Crude lipid yield (L) per kWh	N/A	520	0.34
Daily crude lipid production yield (L)	2.74	3.744	0.216
Cost of the production of 1 L lipid extract	£1.90	£1.9002	£2.32

* = Manufacturer quote, not measured.

Table 8.3 shows that the hourly and daily lipid production yields of *D. salina* were higher when ultrasound is employed in extraction, at an additional production cost of 0.02p per litre. From a production point of view this minimal extra cost (0.01% cost increase) is a worthwhile investment considering the return in lipid yields. No UAE of *D. salina* was available from the literature however one study involved UAE using *Dunaliella Sp* was available for comparison. The UAE method employed by Araujo *et al.* (2011) achieved a 30.12% dry biomass lipid recovery yield from *Dunaliella Sp.* in 20 minutes using a 40 kHz bath (80 W). The exact volume of microalgal processed

in this extraction method was not stated. However, if we make the assumption that the volumes treated are the same as those employed in this study, comparisons can be drawn.

Table 8.3 demonstrates the method employed by Araujo *et al.* (2011) resulted in higher lipid recovery rates in terms of percentage lipid extracted from the biomass. The UAE method employed in this study gave higher hourly and daily lipid recovery yields, required less power to operate and is cheaper by 42.6p per litre. The difference between these two extraction systems is that 20 minutes sonication of *Dunaliella* at 40 kHz may actually be more sonication than that required to rupture cells. Data in chapter 7.3 shows that 8 minutes sonication with 40 kHz was sufficient to completely disrupt the cellular population of *D. salina* and bring about a 25% increase in its Nile Red emission peak.

8.1.3 *C. concordia*

Table 8.4 shows the potential production capacity, lipid yields and production costs of the laboratory scale *C. concordia* lipid extraction systems with and without ultrasound (20 kHz).

Table 8.4 Comparison forecast of the capacity, production values and costs of the laboratory scale lipid extraction of *C. concordia*

System	200 mL Static extraction (no ultrasound)	200 mL 20 kHz probe extraction (0.097 W/cm ³)
Lipid recovery rate	20% dry biomass	27% dry biomass
Capacity (L of microalgae biomass/hour)	6	6
Capacity (kg of dried biomass/hour)	0.3	0.3
Hourly crude lipid yield (L)	0.06	0.081
Kilowatt hours (kWh)	N/A	0.001
Crude lipid yield (L) per kWh	N/A	81
Daily crude lipid production yield (L)	1.44	1.944
Cost of the production of 1 L lipid extract	£1.90	£1.9018

Table 8.4 shows that the hourly and daily lipid production yields of *C. concordia* are significantly higher when ultrasound is employed in the extraction system. These improvements come at the additional production costs of 0.18p per litre. From a production point of view this minimal extra cost (0.1% cost increase) is a worthwhile investment when considering the return in lipid yield rates. As of March 2014 no UAE of *C. concordia* was reported in the literature.

8.1.4 *Chlorella Sp.*

Table 8.5 shows the potential production capacity, lipid yields and production costs of the laboratory scale *Chlorella Sp.* lipid extraction systems with and without ultrasound (20 kHz).

Table 8.5 Comparison forecast of the capacity, production values and costs of the laboratory scale lipid extraction of *Chlorella Sp.*

System	200 mL Static extraction (no ultrasound)	200 mL 20 kHz probe extraction (0.097 W/cm ³)	Araujo et al. (2013) UAE method (40 kHz, 80 Watts)
Lipid recovery rate	17% dry biomass	44% dry biomass	52.5% dry biomass
Capacity (L of microalgae biomass/hour)	0.75	0.75	0.068
Capacity (kg of dried biomass/hour)	0.0375	0.0375	0.005
Hourly crude lipid yield (L)	0.006	0.0165	0.003
Kilowatt hours (kWh)	N/A	0.005	0.08
Crude lipid yield (L) per kWh	N/A	3.3	0.033
Daily crude lipid production yield (L)	0.144	0.396	0.062
Cost of the production of 1 L lipid extract	£1.90	£1.944	£6.362

Table 8.5 shows that the hourly and daily lipid production yields of *Chlorella Sp.* are higher when ultrasound is employed in the extraction system. These improvements come at an additional production cost of 4.4p per litre. From a production point of view this minimal extra cost (2.3% cost increase) is worthwhile when considering the return in lipid production rates. The UAE method developed by Araujo *et al.* (2013) achieved a 52.5% dry biomass lipid recovery yield from a strain of *Chlorella Sp.* in 60 minutes using a 40 kHz bath (80 W). The experimental conditions were slightly different in that Araujo *et al.* (2013) employed 5g of dried *Chlorella Sp.* in 67.5mL of solvent.

Table 8.5 also shows that despite the fact that the UAE method employed by Araujo *et al.* (2013) produced a higher lipid recovery rate than the UAE developed in this study, the extraction method developed in this study could produce a higher hourly and daily lipid yield, using less energy at almost a quarter of the cost per litre. A possible reason for these differences is perhaps that 60 minutes is an unnecessarily long sonication time, table 7.6.1. shows only 16 minutes sonication was required to cause a 70% decrease in the cellular population of *Chlorella Sp.* This highlights the need to employ Nile Red lipid estimation at different times of sonication to determine the optimum time required to increase membrane permeability.

For all 4 species investigated, adding an ultrasonic treatment step to a lipid extraction method will result in higher daily lipid production yield. However this process will add a small increment to the production cost (0.01 – 4.4 p/litre).

Conclusions

This section has highlighted that ultrasound improves the potential lipid daily extraction yields from all 4 microalgal species studied at only a small increase to the production costs. The pilot-scale system was also able to produce higher daily lipid yields than the laboratory scale UAE system at only a fractionally higher cost. The UAE methods developed in this study did not always have as high a lipid recovery rate as what that reported in the literature (in this study *Chlorella Sp.* achieved a 44% dry biomass recovery and in literature a 52.5% dry biomass recovery was achieved from a related species). However the daily lipid production rates were greater, used less energy and had smaller costs per litre of microalgal lipid extracted. An ultrasonic treatment step will add a small cost to the production process; resulting in large returns in terms of increased production. Further advances in ultrasonic lipid

extraction and microalgal biofuel production may reduce production costs closer to the level of those achieved with petroleum based fuel.

The improved DFR system has shown the potential for scale-up in UAE methods. The DFR system could be further optimised. The amplitude could be increased to above 50% of maximum or longer ultrasonic plates could be introduced providing a larger reaction area to increase production capacity. All these factors could potentially improve results. It might be argued that the employment of beating beads adds a complication to the extraction process in terms of their removal. However, removal can be facilitated by using beads made from magnetic materials that could easily be removed or using an appropriate filter system on the outlet to retain the beads. The beads would then be recycled in the process.

8.2 Impact of data outside the biofuels industry

The data gathered in this study is not limited to the biofuel industry. It may have similar impacts in ultrasonic microalgal bloom control and in the extraction of valuable co-products from microalgae for the pharmaceutical or nutraceutical industries.

8.2.1 Ultrasonic treatment of microalgal blooms

It is estimated that the annual cost of excessive microalgal bloom growth in England and Wales is £75 - 114.3 million. This includes the cost of removing excess nitrogen, microalgal toxins and the microalgal biomass from water supplies as well as the negative impacts to waterfront properties and the tourist industry (Pretty *et al.* 2002). Ultrasound has shown great potential for removing harmful microalgal blooms from water systems (Rajaekhar *et al.* 2012). Most research has concentrated on the effects of ultrasound on toxin producing cyanobacteria such as *Microcystis aeruginosa* (Wu *et al.* 2011, 2012) and very little on bloom forming microalgal species such as *Chlorella* or *Dunaliella*. The studies by Wu *et al.* (2012) show that ultrasound has a strong disruptive effect on *M. aeruginosa*, however a report involving 200 mL *Chlorella Sp.* treated with ultrasound at a frequency of 20 kHz for 20 minutes showed little impact on the culture and its ability to grow after treatment (Rajasekhar *et al.* 2012). This difference in behavior between species seems to highlight the need to investigate the effect of sonication on a range of microalgae cells in terms of viability not only immediately after sonication but also the longer term effects on its ability to grow again after treatment. A possible factor in the period after sonication could be the onset of programmed cell death (PCD) which involves the release of messenger chemicals from cells in response to external stresses that will effectively shut down other live

cells that come in contact with these chemicals (Zuo *et al.* 2011). Such is the case with the microalgae *Chlamydomonas reinhardtii* where volatile organic compounds (VOC) are released as the messengers to interact with other cells, instructing them to slow down metabolic rates or shut down completely (Zuo *et al.* 2012). Ultrasound has also been shown to be capable of inducing PCD in some bacteria and other algae species (Broekman *et al.* 2011).

This study has determined that after 8 minutes treatment with 20 or 40 kHz systems both low and high density cultures of *D. salina* were completely destroyed. In the case of *Chlorella Sp.*, after a 16 minutes treatment with the 20 kHz probe system a 65% reduction in the cellular population was observed, which is more positive than the study by Rajasekhar *et al.* (2012) who reported that 20 minutes treatment with a 20 kHz system (0.085 W/mL) had little effect on 200 mL *Chlorella Sp.* The differences in these results may be due to physiological differences between *Chlorella Sp.* and the strain of *Chlorella Sp.* employed in this study. The post sonication studies in chapter 7.9 have also demonstrated that cultures of *D. salina* remain viable after 8 minutes treatment with the 20 kHz probe. This was also observed by Rajasekhar *et al.* (2012) for *Chlorella Sp.* after 20 minutes treatment with a 20 kHz probe (0.085 W/mL) and therefore may also be true for the *Chlorella Sp.* employed in this study, a similar effect was observed with *N. oculata*; which also has a thick cell wall. This data suggests that in terms of microalgal bloom control after a period of 16 minutes treatment with the 20 kHz probe the majority if not all of the population of *D. salina* and *Chlorella Sp.* will be disrupted, however after some time (20 days for *D. salina*) cellular regeneration occurs and normal growth resumes (Rajasekhar *et al.* 2012). This would suggest that if ultrasound was used to treat/control microalgal blooms it would be

advisable to carry out further treatments to prevent cellular regeneration and the bloom returning, though significant research of the effect of repeated ultrasonic treatment on microalgae would have to be undertaken first. The introduction of sonicated microalgae to established cultures does not induce any negative effects in *D. salina*. This indicates that ultrasound (20 kHz) did not induce PCD. If PCD had been observed it would have been advantageous in terms of microalgal bloom control.

8.2.2 Extraction of other valuable co-products from microalgae

Microalgae are employed in other industries (pharmaceutical/nutraceutical) for the extraction of many natural products for example carotenoids, enzymes, antioxidants and vitamins for industrial use (Tafreshi and Shariati, 2009). This study has already demonstrated that treatment with the 20 kHz probe for 16 minutes increases the amount of carotenoid removed from the solid biomass of all 4 species. This suggests that sonication could greatly assist carotenoid extraction. Carotenoid recovery from the biomass of *D. salina* dropped by ~60%, for *N. oculata* by 6%, for *C. concordia* by ~80%, and for *Chlorella Sp.* by ~65% after 16 minutes treatment with the 20 kHz probe. This strongly indicates that if ultrasound was employed for carotenoid extraction for these 4 species the recovery yield would rapidly increase. Evidence from Zhao *et al.* (2006) has suggested that prolonged ultrasonic treatment can cause the degradation of carotenoids, therefore significant care should be taken if this area is to be explored.

β-carotene is a compound that is commonly extracted from *Dunaliella* and is used as a health supplement (Tafreshi and Shariati, 2009). Numerous methods can be employed to extract β-carotene from microalgal biomass; however employing

acetone as an extraction solvent is most commonly used (Abu-Rezq *et al.* 2010). This study determined that after 1 minute ultrasonic treatment with the 20 kHz probe the cellular permeability of *D. salina* increased by ~37%. This suggests that in theory if an ultrasonic step was employed in the extraction method for the recovery of β -carotene from *Dunaliella* potential increases in its recovery yields may be observed. Data in this project has demonstrated that 16 minutes ultrasonic treatment with 20 kHz achieves an increase in membrane permeability in *N. oculata* by 260%, 2 minutes at 20 kHz increases the membrane permeability of *C. concordia* by 250% and 16 minutes at 20 kHz increases the membrane permeability of *Chlorella Sp.* by 80%. These treatment regimes can be inserted into potentially any microalgal extraction process and the increase in membrane permeability caused by the application of ultrasound should increase extraction yields.

Omega 3 fatty acids such as Eicosapentaenoic acid (EPA) and Eicosatrienoic Acid (ETA) are often extracted from a number of microalgal species. They are considered very important for human health and are commonly used as dietary supplements (Hoshida *et al.* 2005). GC-MS analysis in this study has shown that Methyl 9,11,14,17-eicosetetraenoate a variant of ETA was present in the crude extract of *D. salina*, *N. oculata* and *C. concordia*. The data also shows that the concentration of Methyl 9,11,14,17-eicosetetraenoate in the extract increases after ultrasonic treatment in all 3 species; 41% with *D. salina*, 173% with *N. oculata* (522% with ultrasonic treatment in the presence of S070 beads) and 110% with *C. concordia* respectively. This data is of great interest if a secondary sequential extraction of Methyl 9,11,14,17-eicosetetraenoate from the crude extract could be carried out, this would result in a potential second revenue

stream from the extraction of microalgae. For all extraction systems described in this chapter it is possible for these products to be recovered together with lipids.

8.3 Future work

This study has explored ultrasound assisted lipid extraction from microalgae. In the course of this project a number of questions about the improvements possible with ultrasound have been answered and areas that may need to be further explored have been identified. Stressing microalgae to bring about lipid induction is a very important enhancement step in the production of microalgal biofuels. In this study only three factors were investigated to trigger lipid induction (increased salinity or the depletion of nitrogen and trace metals). There are many other factors that could be investigated including different intensities, sources and photoperiods of lighting. Investigating additional stress factors is especially important for *Chlorella Sp.* as none of the factors investigated in this study had a strong effect. A study by Ding *et al.* 2011 has highlighted that variation in light intensity can influence growth and lipid induction in *Chlorella Sp.*, therefore this may be considered for further investigation. These were not included in this study but could play a crucial role in increasing lipid induction. The introduction of bubbled gases and varying concentrations of carbonate in the growth media may also have a strong impact on lipid induction (Perez-Pazos and Fernandez-Izquierdo, 2011). Finally, exploring combined stressing techniques such as increased salinity coupled with nitrogen deprivation may bring about a further increase in lipid induction.

It is advisable that in further work a wider range of microalgal species should be considered for ultrasonic lipid extraction. This study attempted to represent a diverse

group of microalgae by exploring the effect of ultrasound on species with differing cell wall strengths and lipid contents. In doing so an indication of how ultrasound may effect similar species was achieved. Species that may be worth considering in the future include the filamentous *Botryococcus braunii* and the elliptical *Chaetoceros gracilis* whose lipid contents have both been estimated to exceed 60%.

Further exploration into the genetic and metabolic manipulation of microalgae could have a number of benefits for the biofuels industry. A study by Chisti (2013) discusses a number of areas where genetic and metabolic manipulation could be employed to increase lipid production efficiency. These areas include improving photosynthetic ability, inducing microalgal oil secretion, inducing cell flocculation and many more. A result of these manipulations would be a microalgal species with an extremely high lipid content that either has the ability to secrete the oil it produces at a certain stage of metabolism or has developed a thinner cell wall and membranes to ease lipid extraction. Some microalgae can be manipulated into flocculating when triggered by exposure to certain trace elements, this will improve the harvesting stage of production as flocculated cultures can be more easily dewatered (Eldridge et al. 2012).

Zhang *et al.* (2011) developed a method of “milking” lipids from *Botryococcus braunii* by exposing it to 10% tetradecane in a growth reactor. The tetradecane was removed, lipids were recovered and the microalgal biomass continued to grow. This method encouraged the translocation of lipid bodies across the cell wall and membrane which were made considerably more permeable by the 10% tetradecane. If ultrasound was employed with tetradecane this milking process may potentially be improved upon and applied to additional species to improve lipid translocation.

The use of ionic liquids or “green solvents” in the extraction of microalgal lipids instead of solvents such as chloroform, methanol and hexane should be explored. Many ionic liquids are organic salts that can have strong affinities for both polar and non polar compounds (Kim *et al.* 2013). These liquids are usually custom developed for the target extractant in mind, which makes them very specific (Freemantle, 1998). They are non volatile and thermally stable which makes them an environmentally friendly alternative to the current organic compounds employed. Recently studies have shown that the use of the ionic liquid [Bmim][MeSO₄] combined with ultrasound (frequency and power not reported) had a lipid recovery rate that was 61% higher than the Bligh and Dyer extraction method for *C. vulgaris* (Kim *et al.* 2013). This is definitely an area that should be explored further and on other species using a range of ultrasonic equipment and frequencies and perhaps employing beating beads for species with thicker cell walls. However, there is a drawback because the production of these ionic liquids can be costly due to their specificity (Kim *et al.* 2013).

Finally, an area which deserves significant future study is the use of spent microalgal biomass as a feedstock for future cultures. After lipid extraction, instead of discarding the spent microalgal biomass as waste some studies have shown that this biomass can be used as a source of nitrogen and phosphorus acting as a “fertiliser” to promote the growth of future microalgal cultures (Oilgae, 2009). This will ensure that no microalgae biomass goes to waste, boosting the appeal of this already green technology.

Wijffells and Barbosa (2010), Brennan and Owende (2010), and Lee *et al.* (2010) and many others have all emphasised how important a cell disruption step is in the extraction of microalgal lipids. It was reported that traditional extraction methods were not sufficient to achieve good lipid recovery yields from species such as

Nannochloropsis due to its thick cell wall; therefore a cell disruption step is needed. This project has demonstrated that ultrasound can be employed as a cell disruption step to increase lipid recovery yields from a wide range of microalgal species. The work carried out with the Nile Red stain has helped to optimise ultrasound assisted lipid recovery by ensuring that the treatment time and frequency which causes cells to rupture is known for each species. It is this optimisation which makes this project stand out, other studies (Araujo *et al.* 2011 and 2013, Lee *et al.* 2010, and Ranjan *et al.* 2010 for example) have used seemingly arbitrary frequencies and treatment times which have not always proved effective. This highlights the importance of employing the correct ultrasonic frequency and treatment time to disrupt microalgal cells.

9. Conclusions

Each ultrasonic system invested (20 kHz probe, 40 kHz bath, DFR (1.1L) and Hielscher unit (1.1L)) displayed a strong disruptive effect on *D. salina*. However, it appears that the 20 kHz probe (40% amplitude, 0.097 W/cm^3) had the greatest effect; with the highest reduction in optical density, chlorophyll and after 1 minute of sonication visible cellular destruction and the highest increase in Nile Red lipid peak. This data suggests that 1 minute sonication with the 20 kHz probe is the optimum time required to cause enough damage to *D. salina* to bring about an increase in lipid recovery. This was confirmed by both extraction techniques employed as the lipid recovery increased from 15 - 22% dry biomass with chloroform:methanol (1:2) and from 4.5 - 9% dry biomass with hexane. Stressing studies were carried out to further increase the lipid content of *D. salina*. Results determined that F/2 media enriched with 35 g/L additional NaCl should be employed as growth media as this will induce increased lipid production, cell harvesting should take place between day 15 and 18. Ultrasonic extraction (20 kHz probe, 40% amplitude, 0.097 W/cm^3) carried out on stressed cultures caused an increase from 22.5 - 26% dry biomass in lipid recovery from the microalgal biomass.

None of the ultrasonic systems initially used in this study (20 kHz probe, 40 kHz bath, DFR (1.1L) and Hielscher unit (1.1L)) had a strong destructive effect on *N. oculata*. All systems caused the de-aggregation of clumps of *N. oculata* cells into individual cells. Haemocytometer and chlorophyll analysis showed that the DFR system had the strongest destructive effect; however this system was not available for Nile Red lipid determination and gravimetric analysis because for a period of time it was out of commission while it was being modified by the manufacturers. The 20 kHz probe (40% amplitude, 0.097 W/cm^3) caused a 260% increase in the Nile Red

lipid peak after 16 minutes; the corresponding increase for the 40 kHz bath was only 30%. The data suggests that 16 minutes treatment with the 20 kHz probe is sufficient to cause enough damage to *N. oculata* to bring about an increase in lipid recovery. This was confirmed by both extraction techniques employed, lipid recovery increased from 6.5 - 10% dry biomass with chloroform:methanol (1:2) and from 6 - 9% dry biomass with hexane. Optimisation was carried out to further increase lipid recovery by employing S070 beating beads in conjunction with ultrasonic treatment (20 kHz probe, 40% amplitude, 0.097 W/cm^3), this produced the strongest disruptive effect on *N. oculata* (26%). Stressing studies were then carried out to further increase the lipid content of *N. oculata*. Results determined that F/2 media enriched with 30 g/L additional NaCl should be employed as growth media to induce increased lipid induction and under these conditions cell harvesting should take place between day 16 and 35. Ultrasonic extraction (20 kHz probe, 40% amplitude, 0.097 W/cm^3) on stressed cultures caused an increase from 18 – 31.5% dry biomass in lipid recovery. Additionally ultrasonic treatment (20 kHz probe, 40% amplitude, 0.097 W/cm^3) in conjunction with S070 beating beads increased lipid recovery from 31.5 - 35% dry biomass.

All ultrasonic systems (20 kHz probe, 40 kHz bath, DFR (1.1L) produced a destructive effect on *C. concordia*. It appears that the 20 kHz probe (40% amplitude, 0.097 W/cm^3) had the greatest effect as it brought about the highest reduction in cell population, internal chlorophyll estimation and after 2 minutes treatment the highest increase in Nile Red lipid peak. This data suggests that 2 minutes treatment is sufficient to cause enough damage to *C. concordia* to bring about an increase in lipid recovery. This was confirmed by both extraction techniques employed, lipid recovery increased from 7.55 - 10.5% dry biomass with chloroform:methanol (1:2) and from

0.6 - 1.1% dry biomass with hexane. Stressing studies were carried out to further increase the lipid content of *C. concordia*. Results determined that F/2 media with a 25% nitrogen reduction should be employed as growth media to produce increased lipid induction and under these conditions cell harvesting should take place between day 16 and 35. Ultrasonic extraction (20 kHz probe, 40% amplitude, 0.097 W/cm³) carried out on stressed cultures resulted in an increase from 20 - 27% dry biomass in lipid recovery.

The 20 kHz probe (40% amplitude, 0.097 W/cm³) and the 40 kHz bath (0.002 W/cm³) had some destructive effect on *Chlorella Sp.* As with the other species the 20 kHz probe had the greatest effect resulting in the largest reduction in all areas investigated and after 16 minutes treatment the greatest increase in the Nile Red lipid peak was observed. The data suggests that 16 minutes sonication is sufficient to cause enough damage to *Chlorella Sp.* to bring about an increase in lipid recovery. This was confirmed by the chloroform:methanol (1:2) extraction, lipid recovery increased from 6.3 - 8.7% dry biomass. A hexane extraction was not carried out due to time constraints and poor lipid recovery yields for the other three species. Stressing studies were carried out to further increase the lipid content of *Chlorella Sp.* Results suggested that Bolds Basel Medium with 3 fold nitrogen and vitamins should be employed as growth media, however harvesting should occur between day 7 and 9 as internal lipid storage is highest at this stage of its growth. Ultrasonic extraction (20 kHz probe, 40% amplitude, 0.097 W/cm³) carried out on stressed cultures caused an increase from 17 - 44% dry biomass in lipid recovery.

GC-MS data has shown that the transesterified lipid extracts of all four microalgal species have fatty acid profiles suitable for biodiesel production. Each microalgal species contains high concentrations of palmitic and linoleic acid methyl esters, both

of which were considered suitable for biodiesel production as they are not polyunsaturated fatty acids (Demirbas and Demirbas, 2011). The data obtained in this study confirmed what gravimetric data had previously reported, that the amount of lipids (and FAMES) recovered from each microalgal species increased when ultrasound is employed in the extraction.

Post sonication growth studies revealed that after ultrasonic treatment (8 minutes for *D. salina*, 16 minutes for *C. concordia* and 60 minutes for *N. oculata*) with the 20 kHz probe (40% amplitude, 0.097 W/cm³) all microalgal cultures remain viable. The post sonication growth rates for *N. oculata* were unaffected, however for *D. salina* and *C. concordia* there was a lag phase of up to 20 days before growth resumed. This suggests that the microalgal cultures are viable following exposure to ultrasound. The supernatant liquids from sonicated *D. salina* and *C. concordia* when introduced into growing systems have demonstrated the ability to enhance the growth of established cultures. This indicates that the spent microalgal waste after ultrasonic extraction may be employed as a feedstock for future cultures. Post sonication growth studies were not carried out on *Chlorella Sp.* due to time constraints.

A pilot-scale improved DFR system with a smaller reaction chamber (100 mL) was employed providing more aggressive ultrasonic conditions for the disruption of *N. oculata*. When the improved DFR was employed for 4 minutes and 48 seconds a ~50% reduction in the cellular population was achieved resulting in a lipid recovery yield which increased from 16.5 - 21.5% dry biomass. When the improved DFR was employed in conjunction with S070 beating beads this system produced a 90% reduction in the cell population and a lipid recovery yield which increased from 16.5 - 24% dry biomass. Despite having a lower lipid recovery rate than the laboratory scale extraction system (35% dry biomass) the pilot scale system was able to

produce higher daily lipid extraction yields at only a fractionally higher cost (3.2p/ L) due to the shorter treatment time required (4:48 minutes compared to 16 minutes).

This study has highlighted that ultrasound in theory can improve the potential daily lipid extraction yields from all 4 microalgal species studied at only a small increase (0.01 to 3p per litre of extract) to the production costs. The improved/pilot-scale DFR system was able to produce higher daily lipid extraction yields than the laboratory scale UAE system at only a fractionally higher cost (3.2p per litre extract). The UAE methods developed in this study did not always achieve the same lipid recovery rates to those reported in the literature (in this study a 44% dry biomass lipid recovery was obtained for *Chlorella Sp.* and in literature a 52% dry biomass recovery was reported from another strain of *Chlorella Sp.*) but in this study the theoretical daily lipid production rates were greater, using less energy and at lower costs per litre of extracted microalgal lipid. An ultrasonic treatment step will add a small cost to the production process; however there will great benefits in terms of increased production. This conclusion is based on the results obtained from the improved DFR system. Daily crude lipid extract yields using this system would increase from 3.96 - 5.16 L/day with the ultrasonic step in place. Advances in ultrasonic lipid extraction and microalgal biofuel production may ultimately reduce production costs to levels that are closer to those for petroleum based fuel.

References

- Abu-Rezq, T.S., Al-Hooti, S., Jacob, D., Al-Shamali, M., Ahmed, A., and Ahmed, N. (2010) *Induction and extraction of β -carotene from the locally isolated Dunaliella salina*. Journal of Algal Biomass Utilization. 1. 58-83.
- Al-Humaidan, F., Hauser, A., Al-Rabiah, H., Lababidi, H., Bouresli, R. (2013) *Studies on thermal cracking behaviour of vacuum residues in Eureka process*. Fuel. 109. 635-646.
- Aranda-Burgos, J.A., da Costa, F., Novoa, S., Ojea, J., and Martinez-Patino, D. (2014) *Effects of microalgal diet on growth, survival, biochemical and fatty acid composition of Ruditapes decussatus larvae*. Aquaculture. 420. 38-48.
- Araujo, G.S., Matos, J.J.B.L., Goncalves, R.B., Fernandes, F.A.N., and Farias, W.R.I. (2011) *Bioprocessing for oil producing microalgal strains: Evaluation of oil and biomass production for ten microalgal strains*. Bioresource Technology. 102. 5248-5250.
- Araujo, G.S., Matos, J.J.B.L., Fernandes, J.O., Cartaxo, S.J.M., Goncalves, L.R.B., Fernandes, F.A.N., and Farias, W.R.L. (2013) *Extraction of lipids from microalgae by ultrasound application: Prospection of the optimal extraction method*. Ultrasonics Sonochemistry. 20. 95-98. DOI: 10.1016/j.ultsonch.2012.07.027.
- Aravantinou, A.F., Theodorakopolous, M.A., and Manariotis, I.D. (2013) *Selection of algae for wastewater treatment and potential lipids extraction*. Bioresource Technology. 147. 130-134.
- Becker, E.W. (1994) *Microalgae biotechnology and microbiology*. Cambridge University Press.

- Behrend, O., Schubert, K.A.H. (2000) *Influence of continuous phase viscosity on emulsification by ultrasound*. Ultrasonics Sonochemistry. 7. 77-85.
- Ben-Amotz, A., Polle, J.E.W., Rao, D.V.S., (2009) *The Alga Dunaliella: Biodiversity, Physiology, Genomics and Biotechnology*. Science Publications.
- Berlan, J. and Mason, T.J. (1996) *Dosimetry for power ultrasound and sonochemistry*. Advances in Sonochemistry. 4. 1-73.
- Bligh, E.G., and Dyer, W.J. (1959) *A rapid method of total lipid extraction and purification*. Canadian Journal of Biochemistry and Physiology. 37. 911-917.
- Bonrath, W. (2003) *Industrial applications of sonochemistry in the syntheses of vitamin-building blocks*. Ultrasonics Sonochemistry. 10. 55-59.
- Borenstein, S., Cameron, A.C., and Gilbert, R. (1997) *Do gasoline prices respond asymmetrically to crude oil price changes*. The quarterly journal of Economics. February 1997 Edition. 305-339.
- Brennan, L., and Owende, P. (2010) *Biofuels from microalgae – A review of technologies for production, processing and extraction of biofuels and co-products*. Renewable and Sustainable Energy Reviews. 14. 557-577.
- Broekman, S., Pohlmann, O., Beardwood, E.S., and Cordmans de Meulenaer, E. (2011) *Ultrasonic treatment for microbiological control of water systems*. Ultrasonic Sonochemistry. 17. 1041-1048.
- Chen, C., Chang, J., Chang, H., Chen, T., Wu, J., and Lee, W. (2013) *Enhancing microalgal oil/lipid production from Chlorella sorokiniana CY1 using deep-sea water supplemented cultivation medium*. Biochemical and Engineering Journal. 77. 74-81.

- Chen, W., Zhang, C., Song, L., Sommerfeld, M., and Hu, Q. (2009) *A high throughput Nile red method for quantitative measurement of neutral lipids in microalgae*. Journal of Microbiological Methods. 77. 41-47.
- Cheng, C., Du, T., Pi, H., Jang, S., Lin, Y., and Lee, H. (2011) *Comparative study of lipid extraction from microalgae by organic solvent and supercritical CO₂*. Bioresource Technology. 102. 10151-10153.
- Chisti, Y. (2013) *Constraints to commercialization of algal fuels*. Journal of Biotechnology. 167. 201-214.
- Converti, A., Casazza, A.A., Ortiz, E.Y., Perego, P., and Del Borghi, M. (2009) *Effect of temperature and nitrogen concentration on the growth and lipid content of Nannochloropsis oculata and Chlorella vulgaris for biodiesel production*. Chemical Engineering and Processing: Process Intensification. 48. 1146-1151.
- Cooksey, K.E., Guckert, J.B., Williams, S.A., and Callis, P.R. (1987) *Fluorometric determination of the neutral lipid content of microalgal cells using Nile Red*. Journal of Microbiological Methods. 6. 333-345.
- Cooney, M.J., Young, G., and Pate, R. (2011) *Bio-oil from photosynthetic microalgae: Case study*. Bioresource Technology. 102. 166-172.
- Cravotto, G., Boffa, L., Mantegna, S., Perego, P., Avogadro, M., and Cintas, P. (2008) *Improved extraction of vegetable oils under high-intensity ultrasound and/or microwaves*. Ultrasonics Sonochemistry. 15. 898-902.
- Demirbas, A. and Demirbas, M.F. (2011) *Importance of algae oil as a source of biodiesel*. Energy Conservation and Management. 52. 163-170.
- Ding, Y., Gao, Q., Liu, J., Yi, Y., Liu, J., and Lin, W. (2011) *Effect of environmental factors on growth of Chlorella sp. and optimization of culture*

conditions for high oil production. Shentai Xuebao/ Acta Ecologica Sinica. 31. 5307-5315.

- Eldridge, R.J., Hill, D. R. A., and Gladman, B.R. (2012) *A comparative study of the coagulation behavior of marine microalgae*. Journal of Applied Phycology. 24. 1667-1679.
- Fawley, K.P., Elias., M., and Fawley, M.W. (2014) *The diversity and phylogeny of the commercially important algal class Eustigmatophyceae, including the new clade Goniochloridales*. Journal of Applied Phycology. 26. 1773-1782.
- Fogg, G.E., and Thake, B. (1987) *Algal cultures and phytoplankton ecology*. University of Wisconsin Press.
- Folch, J., Lees, M., and Slone Stanley, G.H. (1957) *A simple method for the isolation and purification of total lipids from animal tissues*. The Journal of Biological Chemistry. 226. 497-509.
- Freemantle, M. (1998) *Designer solvents. Ionic liquids may boost clean technology development*. Chemical Engineering News. 76. 32-37.
- Gallagher, B.J. (2011) *The economics of producing biodiesel from algae*. Renewable energy. 36. 158-162.
- Gong, Y. and Jiang, M. (2011) *Biodiesel production with microalgae as feedstocks: from strains to biodiesel*. Biotechnology Letters. 33. 1269-1284.
- Gouveia, L., and Oliveira, A.C., (2009) *Microalgae as a raw material for biofuels production*. Journal of Industrial Microbiology and Biotechnology. 36. 269-274.
- Graham, L.E., and Wilcox, L.W. (2000) *Algae*. Prentice-Hall Inc.

- Green, J.C., Neuville, D., and Daste, P.H. (1978) *Chlamydomonas Concordia* sp. Nov (Chlorophyceae) from oyster ponds on the Ile D'oleron, France. Journal of Marine Biology. 58. 503-509.
- Grubauer, G., Feingold, K.R., Harris, R.M., and Elias, P.M. (1989) *Lipid content and lipid type as determinants of the epidermal permeability barrier.* Journal of Lipid Research. 30. 89-96.
- Guillard, R.R.L., and Ryther, J.H. (1962) *Studies of marine planktonic diatoms. I. Cyclotella nana Hustdtand, Detonula confervacea Cleve.* Canadian Journal of Microbiology. 8. 229-239.
- Hoshida, H., Ohira, T., Minematsi, A., Akada, R., and Nishizawa, Y. (2005) *Accumulation of eicosapentaenoic acid in Nannochloropsis sp. in response to elevated CO₂ concentrations.* Journal of Applied Phycology. 17. 29-34.
- Hu, Q., Sommerfeld, M., Jarvis, E., Ghirardi, M., Posewitz, M., Seibert, M., and Darzins, L. (2008) *Microalgal triacylglycerols as feedstocks for biofuel production: perspectives and advances.* The Plant Journal. 54. 621-639.
- Iqbal, J., and Theegala, C. (2013) *Microwave assisted lipid extraction from microalgae using biodiesel as co-solvent.* Algal Research. 2. 34-42.
- International Energy Outlook (2013) U.S. Energy Information Administration.
- Jambrak, A.R., Lelas, V., Herceg, Z., Badanjak, M., Bafur, V., and Muža, M. (2009) *Advantages and disadvantages of high power ultrasound application in the dairy industry.* Mljekarstvo. 59. 267-281.
- James, G.O., Hocart, C.H., Hillier, W., Chen, H., Kordbacheh, F., Price, G.D., and Djordjevic, M.A. (2011) *Fatty acid profiling of Chlamydomonas reinhardtii under nitrogen deprivation.* Bioresource Technology. 102. 3343-3351.

- Joyce, E., Al-Hashimi, A., and Mason, T.J. (2011) *Assessing the effect of different ultrasonic frequencies on bacterial viability using flow cytometry*. Journal of Applied Microbiology. 110. 862-870.
- Joyce, E., King, P.M., Mason, T.J. (2014) *The effect of ultrasound on the growth and viability of microalgae cells*. Journal of Applied Phycology. 26. 1741-1748.
- Joyce E., Phull S.S., Lorimer J.P., and Mason T.J. (2003) *The development and evaluation of ultrasound for the treatment of bacterial suspensions. A study of frequency, power and sonication time on cultured Bacillus species*. Ultrasonics Sonochemistry. 6. 315-318.
- Kamari, P., Kumar, M., Gupta, V., Reddy, C.R.K., and Jha, B. (2010) *Tropical marine macroalgae as potential sources of nutritionally important PUFAs*. Food Chemistry. 120. 749-757.
- Kamari, P., Reddy, C.R.K., and Jha, B. (2011) *Comparative evaluation and selection of a method for lipid and fatty acid extraction from macroalgae*. Analytical Biochemistry. 415. 134-144.
- Kim, Y., Park, S., Kim, M.H., Choi, Y., Yang, Y., Kim, H.J., Kim, H., Kim, H., Song, K., and Lee, S. (2013) *Ultrasound-assisted extraction of lipids from Chlorella vulgaris using [Bmim][MeSO₄]*. Biomass and Bioenergy. 56. 99-103.
- Koberg, M., Cohen, M., Ben-Amotz, A., and Gedanken, A. (2011) *Bio-diesel production directly from the microalgal biomass of Nannochloropsis by microwave and ultrasound radiation*. Bioresource Technology. 102. 4265-4269.
- Korres, D.M., Karonis, D., Lois, E., Linck, M.B., and Gupta, A.K. (2008) *Aviation fuel JP-5 and biodiesel on a diesel engine*. Fuel. 87. 70-78.

- Krienitz, L., and Wirth, M., (2006) *The high content of polyunsaturated fatty acids in Nannochloropsis limnetica (Eustigmatophyceae) and its implication for food web interactions, freshwater aquaculture and biotechnology.* Limnologia. 36. 204-210.
- Kuijpers, M.W.A., Kemmere, M.F., and Keurentjes, J.T.F. (2002) *Calorimetric study of the energy efficiency for ultrasound-induced radical formation.* Ultrasonics. 40. 675-678.
- Kumar, P., Suseela, M.R., and Toppo, K. (2011) *Physio-Chemical characterization of algal oil: a potential biofuel.* Asian Journal of Experimental Biological Science. 2. 493-497.
- Kumari, P, Reddy, C.R.K and Jha, B. (2011) *Comparative evaluation and selection of a method for lipid and fatty acid extraction from macroalgae.* Analytical Biochemistry. 415. 134-144.
- Lee, Y., Yoo, C., Jun, S., Ahn, C., and Oh, H. (2010) *Comparison of several methods for effective lipid extraction from microalgae.* Bioresource Technology. 101. 575-577.
- Lee, R.E. (1999) *Phycology 3rd Edition.* Cambridge University Press.
- Li, S., Luo, S. and Guo, R. (2013) *Efficiency of CO₂ fixation by microalgae in a closed raceway pond.* Bioresource Technology. 136. 267-272.
- Liu, J., Huang, J., Sun, Z., Zhong, Y., Jiang, Y., and Chen, F. (2011) *Differential lipid and fatty acid profiles of photoautotrophic and heterotrophic Chlorella zofingiensis: Assessment of algal oils for biodiesel production.* Bioresource Technology. 102. 106-110.

- Liu, Q., Su, X.R., Li, T.W, and Yang, F.X. (2003) *Effects of salinity on growth rate, chlorophyll content and cell cycle of Dunafiella viridi*. Journal of Danlian Fisheries University. 18. 90-94.
- Lou, Z., Wang, H., Zhang, M., and Wang, Z. (2010) *Improved extraction of oil from chickpea under ultrasound in a dynamic system*. Journal of Food Engineering. 98. 13-18.
- Lv, H., Qu, G., Qi, X., Lu, L., Tian, C., and Ma, Y. (2013) *Transcriptome analysis of Chlamydomonas reinhardtii during the process of lipid accumulation*. Genome. 101. 229-237.
- Maimoun, M.A., Reinhart, D.R., Gammoh, F.T. and Bush, P.M. (2013) *Emissions from US waste collection vehicles*. Waste Management. 33. 1079-1089.
- Mason, T.J. (1990) *Critical Reports on Applied Chemistry 28: Chemistry with Ultrasound*.1. 2-4.
- Mason, T.J. (1991) *Practical Sonochemistry*.1. 22-24.
- Mason, T.J. and Lorimer, J.P. (2002) *Applied Sonochemistry. The uses of power ultrasound in Chemistry and processing*. 1. 4-5.
- Mason, T.J., and Peters, D. (2002) *Practical sonochemistry. Power ultrasound and its uses and applications*. 2nd edition. Horwood Publishing Series in Chemical Science. 1. 12-15.
- Mohalkar, V.S., Kumar, P.S., and Pandit, A.B. (1999) *Hydrodynamic cavitation for sonochemical effects*. Ultrasonics Sonochemistry. 6. 53-65.
- Mohammadi, M., Najafpour, G.D., Younesi, H., Lahijani, P., Uzir., M.H and Mohamed, A.R. (2011) *Bioconversion of synthesis gas to second generation biofuels: Renewable and Sustainable Energy reviews*. 15. 4255-4273.

- Neto, A.M P., de Souza, R A.S., Leon-Nino, A.D., de Costa, J.D.A., Tiburcio, R.S., Nunes, T.A., Mello, T.C.S., Kanemoto, F.T., Saklanha-Correa, F.M.P., Giancesella, S.M.F. (2013) *Improvement in microalgae lipid extraction using a sonication-assisted method*. Renewable energy. 55. 525-531.
- O'Rourke, D. and Connolly, S. (2003) *Just oil? The distribution of environmental and social impacts of oil production and consumption*. Annual Review of Environment and Resources. 28. 587-617.
- Paniwnyk, L., Cai, H., Albu, S., Mason, T.J., and Cole, R. (2009) *The enhancement and scale up of the extraction of anti-oxidants from Rosmarinus officinalis using ultrasound*. Ultrasonics Sonochemistry. 16. 287-292.
- Perez-Pazos, J., and Fernandez-Izquierdo, P. (2011) *Synthesis of neutral lipids in Chlorella Sp. under different light and carbonate conditions*. Ciencia, Tecnologia Y Futuro. 4. 47-57.
- Pernet, F., and Tremblay, R. (2003) *Effect of ultrasonication and grinding on the determination of lipid class content of microalgae harvested on filters*. Lipids. 38. 1191-1195.
- Phull, S.S., and Mason, T.J. (1999). *The use of ultrasound in microbiology*. Advances in Sonochemistry. 5. 175-207.
- Pieber, S., Schober, S., and Mittelbach, M. (2012) *Pressurized fluid extraction of polyunsaturated fatty acids from the microalga Nannochloropsis oculata*. Biomass and Bioenergy. 47. 474-482.
- Potts, T., Du, J., Paul, M., May, P., Beittle, R., and Hestekin, J. (2012) *The production of butanol from Jamaica Bay macroalgae*. Environmental Progress and Sustainable Energy. 31. 29-36.

- Pradakaran, P., and Ravindran, A.D. (2011) *A comparative study on effective cell disruption methods for lipid extraction from microalgae*. Letters in Applied Microbiology. 53. 150-154.
- Preiss, M.R., and Kowalski, S.P. (2010) *Algae and Biodiesel: Patenting energized as green goes commercial*. Journal of Commercial Biotechnology. 16. 293-312.
- Pretty, J.N., Mason, C.F., Nedwell, D.B., and Hine, R.E. (2002) *A Preliminary assessment of the environmental costs of the eutrophication of fresh waters in England and Wales*. Commissioned by the Environmental agency. University of Essex.
- Radakovits, R., Jinkerson, R.E., Darzins, A., and Posewitz, M.C. (2010) *Genetic engineering of algae for enhanced biofuel production*. Eukaryotic cell. 9. 486-501.
- Rajasekhar, P., Fan, L., Nguyen, T., and Roddick, F.A. (2012) *A review of the use of sonication to control cyanobacterial blooms*. Water Research. 46. 4319-4329.
- Rajasekhar, P., Fan, L., Nguyen, T., and Roddick, F.A. (2012) *Impact of sonication at 20 kHz on Microcystis aeruginosa Anabaena circinalis and Chlorella Sp.* Water research. 46. 1473-1481.
- Ranjan, A., Patil, C., and Moholkar, V.S. (2010) *Mechanistic Assessment of Microalgal Lipid extraction*. Industrial and Engineering Chemistry Research. 49. 2979-2985.
- Roessler, P.G., Brown, L.M., Dunahay, T.G., Heacox, D.A., Jarvis, E.E., Schneider, J.C., Talbot, S.G., and Zeiler, K.G. (1994) *Genetic engineering*

approaches for enhanced production of biodiesel fuel from microalgae. American Chemical Society. 256-270.

- Rombaut, R., De Clercq, N., Foubert, I., and Dewettinck, K. (2009) *Triacylglycerol analysis of fats and oils by Evaporative Light Scattering Detection.* Journal of the American Chemistry Society. 86. 19-25.
- Schuhmann, H., Lim, D.K.Y, and Schenk, P.M. (2012) *Perspectives on metabolic engineering for increased lipid contents in microalgae.* Biofuels. 3. 71-86.
- Sharma, K.K., Schuhuman, H., and Schenk, P.M. (2012) *High Lipid Induction in Microalgae for Biodiesel Production.* Energies. 5. 1532-1553.
- Sheehan, J., Dunahay, T., Benemann, J. and Roessler, P. (1998) *A look back at the US. Department of Energy's Aquatic Species Program—biodiesel from algae.* National Renewable Energy Laboratory Report: NREL/TP-580-24190.
- Siaut, M., Cuine, S., Cagnon, C., Fessler, B., Nguyen, M., Carrier, P., Beyly, A., Beisson, F., Triantaphylides, C., Li-Beisson, Y., and Parker, G. (2011) *Oil accumulation in the model green alga Chlamydomonas reinhardtii: characterization, variability between common laboratory strains and relationship with starch reserves.* BMC Biotechnology. 11. 1-15.
- Sivakumar, V., and Rao, P.G. (2003) *Studies on the use of power ultrasound in leather dyeing.* Ultrasonic's Sonochemistry. 2. 85-94.
- Soxlet, F. (1879) *The weight analytic determination of milk fat.* Polytechnisches J. 232. 461.
- Su, C., Chien, L., Gomes, J., Lin, Y., Yu, Y., Liou, J., and Syu, R. (2008) *Factors affecting lipid accumulation by Nannochloropsis oculata in a two-stage cultivation process.* Journal of Applied Phycology.

- Sukenik, A., Carmeli, Y., and Berner, T. (1989). *Regulation of fatty acid composition by irradiance level in the eustigmatophyte Nannochloropsis sp.* Journal of Phycology. 25. 686-692.
- Tafreshi, A.H., and Shariati, M. (2009) *Dunaliella biotechnology: methods and applications.* Journal of Applied Microbiology. 107. 14-35.
- Tang, H., Abunasser, N., Garcia, M.E.D., Chen, M., Simon Ng, K.Y., and Salley, S.O. (2010) *Potential of microalgae oil from Dunaliella tertiiella as a feedstock for biodiesel.* Applied Energy. 88. 3324-3330.
- Tanzi, C.D., Vian, M.A., and Chemat, F. (2013) *New procedure for extraction of algal lipids from wet biomass: A green_clean and scalable process.* Bioresource technology. 134. 271-275.
- Vieler, A., Wilhelm, C., Goss, R., Süß, R., and Schiller, J. (2007) *The lipid composition of the unicellular green alga Chlamydomonas reinhardtii and the diatom Cyclotella meneghiniana investigated by MALDI-TOF MS and TLC.* Chemistry and physics of lipids. 150. 143-155.
- Vyas, A.P, Verma, J.L, and Subrahmanyam, N. (2010) *A review on FAME production processes.* Fuel. 89. 1-9.
- Wei, N., Quarterman, J., and Jin, Y. (2013) *Marine macroalgae: an untapped source for producing fuels and chemicals.* Trends in biotechnology. 31. 70-77.
- Wijffels, R.H., and Barbosa, M.J. (2010) *An Outlook on Microalgal Biofuels.* Science. 329. 796-799.
- Williams, P.J., and Laurens, L.M.L. (2010) *Microalgae as biodiesel and biomass feedstocks: Review & analysis of the biochemistry, energetic and economics.* Energy and Environmental Science. 3. 554 – 590.
- World Key Energy Statistics (2012) International Energy Agency.

- Wu, X. (2010) *The effects of ultrasonic treatment on cyanobacterial in surface waters*. PhD Thesis. Coventry University.
- Wu, X., Joyce, E.M., and Mason, T.J. (2011) *The effects of ultrasound on cyanobacteria*. Harmful Algae. 10. 738-743.
- Wu, X., Joyce, E.M., and Mason, T.J. (2012) *Evaluation of the mechanisms of the effect of ultrasound on Microcystis aeruginosa at different ultrasonic frequencies*. Water Research. 46. 2851–2858.
- Yoo, G., Park, W., Kim, C.W., Choi, Y., and Yang, J. (2012) *Direct lipid extraction from wet Chlamydomonas reinhardtii biomass using osmotic shock*. Bioresource Technology. 123. 717-722.
- Zhang, F., Cheng, L.H., Gao, W.L., Xu, X.H., Zhang, L., and Chen, H.L. (2011) *Mechanism of lipid extraction from Botryococcus brauni FACHB 357 in a biphasic bioreactor*. Journal of Biotechnology. 154. 281-284.
- Zhang, G., Wen, X., Liang, F., Ouyang, Z., Geng, Y., Mei, H., and Li, Y. (2011) *The effects of physical and chemical factors on the growth and lipid production of Chlorella*. Acta Ecologica Sinica. 31. 2076-2085.
- Zhao, L., Zhao, G., Chen, F., Wang, Z., Wu, J., and Hu, X. (2006) *Different effects of microwave and ultrasound on the stability of (all-E)-astaxanthin*. Journal of Agricultural Food Chemistry. 18. 8346-51.
- Zimmerman, W.B., Zandi, M., Bandulasena, H.C.H., Tesar, V., Gilmour, D.J., and Ying, K. (2011) *Design of an airlift loop bioreactor and pilot scales studies with fluidic oscillator induced microbubbles for growth of a microalgae Dunaliella salina*. Applied Energy. 88. 2257-3369.

- Zuo, Z., Zhu, Y., Bai, Y., and Wang, Y. (2012) *Acetic acid induced programmed cell death and release of volatile organic compounds in Chlamydomonas reinhardtii*. Plant Physiology and Biochemistry. 51. 175-184.

Web References

- 77 Ingredients URL: <http://www.77ingredients.com> – Accessed August 2013.
- Algae Industry Magazine. URL: <http://www.algaeindustrymagazine.com> – Accessed August 2013.
- BERR (Department of Business, Enterprise and Regulatory reform) URL: <http://www.berr.gov.uk> Accessed August 2013.
- *Culture Collection of Algae and Protozoa*. URL: <http://www.ccap.org> – Accessed August 2013.
- Department for Business, Enterprise and Regulatory Reform. URL: <http://www.confusedaboutenergy.co.uk> - Accessed August 2013.
- Nation Master URL: <http://www.nationmaster.com> - Accessed August 2013.
- Oilgae. URL: <http://www.oilgae.com> – Accessed August 2013.
- Oilgae. *Reuse of Algal Biomass Waste as Fertilizer for Algae Cultivation*. URL: <http://www.oilgae.com/blog/2009/05/reuse-of-algal-biomass-waste-as.html> - Accessed August 2013.
- Polar Bear Specialist Group. URL: <http://pbsg.npolar.no> – Accessed August 2013.
- Rapoza, K. (2013) Within Four Years, China To Consume More Oil Than U.S. (Forbes) URL: <http://www.forbes.com/sites/kenrapoza/2013/08/25/within-four-years-china-to-consume-more-oil-than-u-s/> - Accessed December 2013
- Really Big Oil (The Economist) URL: <http://www.economist.com/node/7276986> - Accessed August 2013
- San Diego Centre for Algae Biotechnology. URL: <http://algae.ucsd.edu> – Accessed August 2013.

- San Fransico State University. URL: <http://sfsu.edu> – Accessed August 2014.
- Solix Biofuels. URL: <http://www.solixbiofuels.com> – Accessed August 2013.
- The Pherobase. URL: <http://www.pherobase.com> - Accessed August 2013.
- Triacylglycerol Wikipedia. URL: <http://wikipedia.org> Accessed August 2013.